The Development of Photo-activated Antimicrobial Dyes Against Opportunistic Infections

by

Murhaf Jalab

A thesis submitted in partial fulfilment for the requirements for the degree of Doctor of Philosophy at the University of Central Lancashire

June 2020

Student declaration form

Concurrent registration for two or more academic awards

*I declare that while registered as a candidate for the research degree, I have not been a registered candidate or enrolled student for another award of the University or other academic or professional institution.

Material submitted for another award

*I declare that no material contained in the thesis has been used in any other submission award and is solely my own work.

Collaboration

Where a candidate's research programme is part of a collaboration project, the thesis must indicate in addition clearly the candidate's individual contribution and the extent of the collaboration. Please state below: N/A.

Signature of candidate ------------   ----------

Type of award: Doctor of Philosophy (PhD)

School: Pharmacy and Biomedical Sciences

Abstract

Microbial infections cause a major health threat and the growing incidence of invasive and opportunistic infections is usually associated with high rates of morbidity and mortality. Approximately 300,000 patients a year in England are affected by a healthcare-associated infection as a result of care within the NHS and the NHS cost is estimated at approximately £1 billion a year. The treatment of infectious diseases is one of the most challenging problems in medicine due to the emergence of microbial resistance, side effects and spectrum of activity. Therefore, there is an obvious and urgent need to develop new and effective antimicrobial strategies. A possible alternative to traditional antimicrobial drugs is photodynamic therapy (aPDT), which depends on the activation of a photosensitiser (PS) by a visible light source to produce reactive oxygen species (ROS) and singlet oxygen, which can inactivate and kill microbial cells.

A library of novel photoactivatable compounds, based on acridine, flavin, acridine-isoalloxazine and anthraquinone dyes, has been characterised to quantify singlet oxygen release following activation by blue light for 10 and 20 minutes. Candidate compounds were then screened, using the European Committee for Antimicrobial Susceptibility Testing (EUCAST) microbroth dilution method, for antimicrobial activity against a range of clinically important fungi, including *Candida albicans* (*C. albicans*)*, Saccharomyces cerevisiae* (*S. cerevisiae*) and *Aspergillus* spp., and medically important bacteria, including *Escherichia coli* (*E. coli*) and *Staphylococcus aureus (S. aureus*).

The chemical results demonstrated the ability of the studied compounds to generate singlet oxygen upon exposure to blue light. Determination of the minimum inhibitory concentration (MIC) has identified a number of novel candidate compounds with activity against fungi and bacteria. These compounds were further investigated to determine their mechanism of action using a *hog1* and *msn2/4* genomic deletion strain of *S. cerevisiae.* The findings suggest that the general stress HOG pathway (High-osmolarity glycerol) has a limited role in the cellular response to the compounds. However, *msn2/4* deletion strains, which encode key transcription factors for the oxidative stress response, showed an increase in sensitivity suggesting these compounds are inhibiting microbial cell growth via oxidative stress. Further characterisation of the compounds indicates

that these photo-activated compounds do not develop resistance in fungal and bacterial species following three repeated exposures. Additionally, a significant effect against *Candida albicans* biofilm was shown for three tested PDT compounds. Finally, the tested compounds showed toxicity against HeLa cells in the absence and presence of light. This suggests that, in their current form, they are not ideal compounds for clinical use.

The results from this project support ongoing work in this field which may help in the development of a new arsenal of antimicrobial drugs.

Contents

List of Figures

List of Tables

Acknowledgments

I would like to take this opportunity to thank all that have provided me with the support needed allowing me to complete this project.

Firstly, I would like to thank the school of Pharmacy and Biomedical Sciences and cara organisation to provide funding for my PhD. Also I really thank Dr. Clare Lawrence, for giving me the opportunity to work on such an interesting and challenging project. Your assistance, support, guidance and above of all patience, helped me a lot during my PhD journey.

I would also like to thank my secondary supervisors.

Finally, I extend special thanks to my family and friends, especially my lovely wife Joud for their continual support, encouragement and advice, without which I undoubtedly would not have been able to reach where I am today.

Abbreviations

5-FC	Flucytosine
AMB	amphotericin B
FLU	Fluconazole
VRE	vancomycin-resistant enterococcal
MSRA	methicillin-resistant *S. aureus*
PBP	penicillin binding protein
EPS	extracellular polysaccharide
PDT	photodynamic therapy
aPDT	Antimicrobial photodynamic therapy
PS	Photosensitiser
ROS	Reactive oxygen species
$^1O_2$	Singlet oxygen
H_2O_2	Hydrogen peroxide
·OH	Hydroxyl radical
ALA	5-aminolevulinic acid
BPD	benzoporphyrin derivative
(SnET2	Tinethyletiopurpurin
LED	light-emitting diodes
MIC	Minimum inhibitory concentration
DMSO	dimethyl sulfoxide
DPPH	2,2-Diphenyl-1-picrylhydrazyl
ABTS	2,2′-Azino-bis (3-ethylbenzothiazoline-6-sulfonic acid)
PBS	phosphate buffered saline
SDA	Sabouraud dextrose agar
OD	optical density
MOPS	3-(N-morpholino) propanesulfonic acid
EUCAST	European Committee for Antimicrobial Susceptibility Testing
EDTA	Ethylenediaminetetraacetic acid
XTT	[2,3bis(2-methoxy-4-nitro-5-sulfo-phenyl)-2H-tetra-zolium-5-carboxanilide]
SMG	Supra-MIC growth
FBS	Foetal Bovine Serum

EMEM	Eagles Minimum Essential Media
NEAA	Non-Essential Amino Acids
TPCPD	2,3,4,5-tetraphenylcyclopentadienone
AF	Acriflavine
PF	Proflavine
AO	Acridine orange
AA	9-aminoacridine
UV	Ultraviolet
CFU	Colony forming unit
CLSI	Clinical Laboratory Standards Institute
ISC	increasing intersystem crossing
FMN	Flavin mononucleotide
NADPH	β-nicotinamide adenine dinucleotide phosphate
EEHEC	Enterohemorrhagic *Escherichia coli*
FAD	Flavin adenine dinucleotide
NBT	Nitro blue tetrazolium
RoF	Roseoflavin
ERG	Erythroglaucin
TEL	Teloschistin
HYQ	1-hydroxy-2-methylanthraquinone
NEQ	Hydroxyanthraquinone
RFU	Relative Fluorescence Unit
VVC	Vulvovaginal candidiasis
HPF	Fluorescence probes, 3'-(p-hydroxyphenyl)-fluorescein

1. Introduction

An infection is defined as the pathological state resulting from the invasion of the body by pathogenic microorganisms, such as bacteria, fungi and viruses. Infectious diseases can be mild or develop into more serious diseases which may result in long-term consequences or death (Admassie, 2018).

Infectious diseases are a significant health and financial burden in the UK, causing a mortality rate of 7% and annual costs of £30bn (Fisher *et al.*, 2018). There is still a rise in infectious pathogens due to the increasing number of immunocompromised patients, older people, and diabetics. Despite the introduction of vaccination programmes and antimicrobial agents, infections remain a primary cause of high rates of morbidity and mortality worldwide (Peleg *et al.*, 2010). Treatment of infectious diseases is one of the most challenging problems in medicine due to the increased capability of infectious agents to develop resistance to existing antimicrobial agents and those agents' side-effects and spectrum of activity. Thus, there is a need to develop new and effective antimicrobial strategies (Denning *et al.*, 2015; Fisher *et al.*, 2018).

A possible alternative to traditional antimicrobial drugs is photodynamic therapy (aPDT), which depends on the activation of a photosensitiser (PS) by a visible light source, to produce reactive oxygen species (ROS) and singlet oxygen, which can inactivate and kill microbial cells. The main advantages associated with PDT are: activity against drug-resistant microorganisms and wide spectrum of activity (Macdonald *et al.*, 2001; Hamblin *et al.*, 2004). A library of novel photoactivated compounds based on acridine, flavin, acridine-isoalloxazine and anthraquinone has been characterised photochemically and subsequently screened for antimicrobial activity against a range of fungi, including: *Saccharomyces cerevisiae* (*S. cerevisiae*) *Candida albicans* (*C. albicans*) and *Aspergillus fumigatus (A. fumigatus)* and bacteria, including: *Staphylococcus aureus* (*S. aureus)* and *Escherichia coli (E. coli).*

1.1   Fungi

Fungi are eukaryotic, which means that they contain a membrane-bound nucleus and several types of organelles that are common to animal cells. There is a wide variety of fungi ranging from the smallest unicellular fungi such as yeast, to large multicellular fungi capable of forming hyphal threads. The majority of fungal infections affect the skin or mucosa, and can be treated readily, however substantial minority are invasive or chronic, and can be difficult to treat (Denning *et al.*, 2015). An estimated 1.5 to 2 million people die of fungal infections every year, mainly caused by species belonging to four genera of fungi: *Aspergillus*, *Candida*, *Cryptococcus* and *Pneumocystis* (Denning *et al.*, 2015).

The fungal cell wall fulfils important functions: it offers a rigid and mechanical barrier, plays a pivotal role in cell recognition and acts as a site for several extracellular enzymes (Vandeputte *et al.*, 2012).

1.1.1 Fungal cell structure

1.1.1.1   Fungal cell wall

Fungal cell wall is a dynamic structure, which is fundamental for cell viability, morphogenesis and pathogenesis (Gow *et al.*, 2017). It is unique and considered a key target for antifungal drugs. It is typically a mutilayered structure comprised of glucans, the predominant glucan component being β-1,3-glucan, which forms around 50-60% of the total cell wall. A minor, but important, component is chitin (1-2%), while mannans (phosphopeptidomannan) are composed of mannoproteins and account for 35-40% of the cell wall structure (Figure 1.1; Bowman *et al.*, 2006). The β-1,3-glucan and chitin components are largely responsible for offering the cell wall strength and can be oserved as an inner layer. The outer cell wall layer is composed of mannoproteins and is predominantly responsible for determining the porosity of the cell wall (Georgopapadakou *et al.*, 1995; Ruiz-Herrera, 2016).
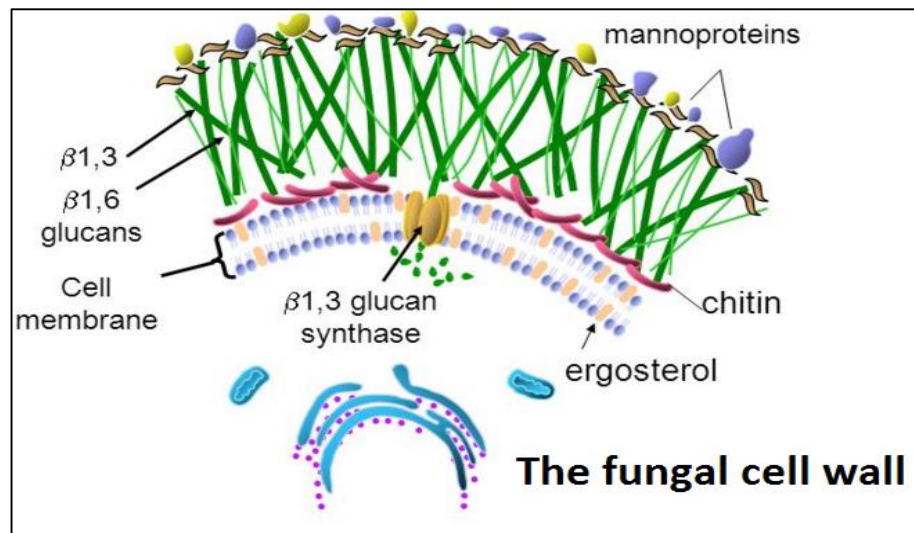
Figure 1.1 Structure of the fungal cell wall (Klepser, 2001).

1.1.1.2 Fungal cell membrane

The fungal cell membrane is predominantly composed of sterols and lipids. The mains sterol in fungi is ergosterol, which possesses a rigid and compact structure, in contrast to cholesterol found in mammalian cells (Rella *et al.*, 2016). Ergosterol is biosynthesised by lanosterol 14 alpha-demethylase, and is considered an attractive target for antifungal treatment, which can affect cell membrane integrity (Maertens *et al.*, 2000; Sant *et al.*, 2016).

1.1.2 Medically important fungi

Opportunistic fungal pathogens are an increasing problem in human health, leading to superficial or serious invasive infections. As described previously, the main reasons behind mortality associated with fungal infections are four genera of fungi: *Aspergillus*, *Candida*, *Cryptococcus* and *Pneumocystis*.

The most common fungal infections are caused by *C. albicans* and *A. fumigatus*; major burdens in terms of mortality and morbidity in critical care settings and leading causes of nosocomial and opportunistic infections.

Candida is normally present on the skin, intestinal tract and in the genital area (Mayer *et al.*, 2013). They can cause skin and mouth infections in healthy people; however it is are more common or persistent in people with diabetes, cancer or AIDS. A few forms of candidiasis can be serious:

- Invasive candidiasis: can spread to other body organs, such as brain, kidneys and eyes. It is one of the most common infections acquired in hospital (Reboli *et al.*, 2007).
- Candidemia: a serious infection of the bloodstream; often causing death if not promptly treated (Pappas *et al.*, 2004).

The most common species is *C. albicans* (Figure 1.2), a yeast like fungi responsible mainly for candidemia which cause a high mortality rate in the UK (approximately 50%) (Miceli *et al.*, 2011; Denning *et al.*, 2015). There are other important *Candida* species such as *C. glabrata and C. krusei*, which are responsible for around 14% and 2% of candidemia infections, respectively (Sardi *et al.*, 2013). Both *C. glabrata* and *C. krusei* are intrinsically resistant to azole compounds.

Fungal biofilm is frequently found on artificial surfaces. Infections related to biofilm are difficult to eliminate; particularly with the conventional antifungal treatment (Ramage *et al.*, 2001). The biofilm-forming ability of *C. albicans* contributes to the high resistance of biofilms to antimicrobials and to high rates of nosocomial infections (Casalinuovo *et al.*, 2017).
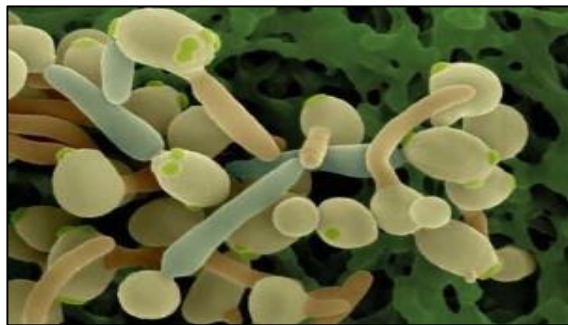
Figure 1.2 *C. albicans* (Klepser, 2001).

The Aspergillus mould genus comprises spore-bearing fungi; some of the mould of this genus are pathogenic to humans, such as *A. fumigatus* and *A. nidulams*. They can cause diseases, such as pulmonary aspergilloma, Aspergillus pneumonia, or development of bronchial asthma. The most common fungus among them is *A. fumigatus* (Figure 1.3), a life-threatening pathogenic fungus, whose conidium is the infectious agent of aspergillosis (Fuller *et al.*, 2013). This fungus can grow in conidial and hyphal forms, however hyphae are the morphological form observed in tissue during invasive *A. fumigtatus* infections

(Rhodes, 2006). The most common infection route is inhalation of the conidia, as inhaled conidia survive and infect the lungs of immunocompromised patients, however they are treated in the healthy host's lung by phagocytes (Liu *et al.*, 2013). Unfortunately, 30-50% of invasive aspergillosis patients usually die, due to late diagnosis, and infections of parts of body such as brain that are left untreated with drugs (Denning *et al.*, 2015).

Figure 1.3 *A. fumigatus* (Klepser, 2001).

In recent years, there has also been an increase in the number of fungal infections in immunocompromised patients related to the budding yeast, *Saccharomyces cerevisiae (S. cerevisiae;* Figure 1.4; Petrikkos *et al.*, 2007). This yeast can be found naturally in many niches in the environment, however recently the number of cases of diagnosed infections has increased, probably as a result of the increased numbers of immunocompromised patients. *S. cerevisiae* has been related to a wide variety of infections, which range from vaginitis and cutaneous infections, to systemic bloodstream infections and infections of essential organs in immunocompromised and critically ill patients (Pérez-Torrado *et al.*, 2016).
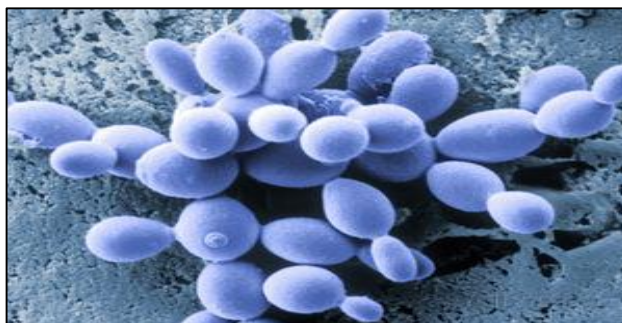
Figure 1.4 *S. cerevisiae* (Klepser, 2001)*.*

1.1.3 Antifungal therapy

The increasing rates of morbidity and mortality caused by fungal infections are also associated with the current limited antifungal drugs and their associated elevated toxicity. Furthermore, searching for novel antifungal drugs is a difficult task, due to the similarities between fungi and human cells (Sucher *et al.*, 2009). Currently there are only four groups of antifungal drugs that are used for treatment of fungal infections and their antifungal targets, which include fungal RNA synthesis and cell wall and cell membrane (Figure 1.5; Odds *et al.*, 2003).
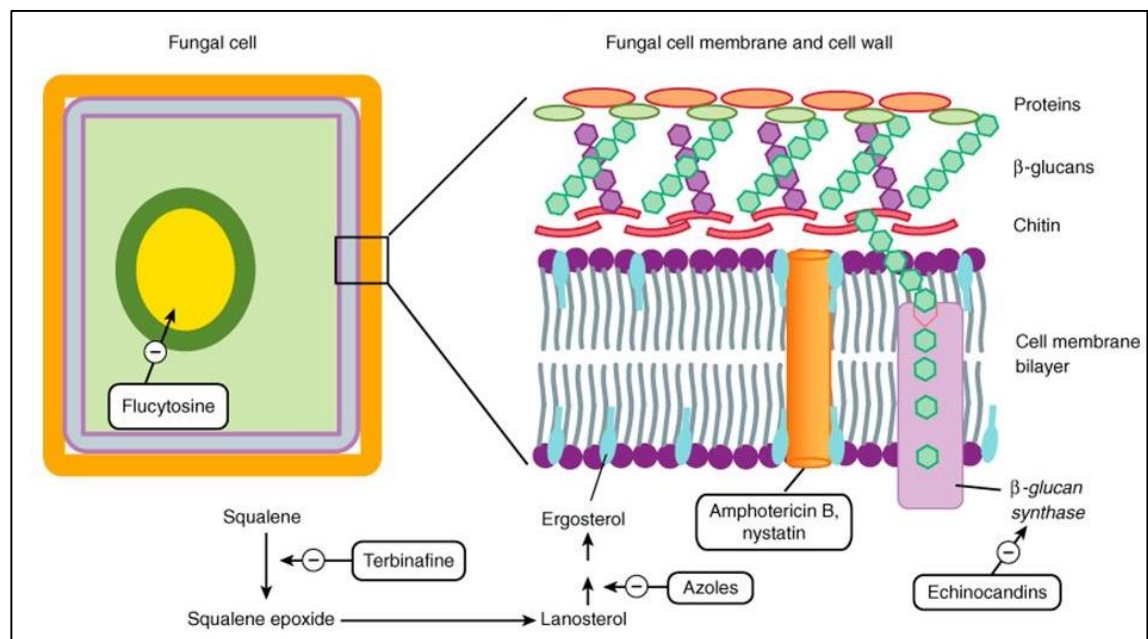
Figure 1.5 Antifungal targets (Odds *et al.*, 2003).

1.1.3.1 Flucytosine (5-FC)

5-FC was synthesised in 1957, however its antifungal activity was not discovered until 1964. Its mechanism of action is related to the inhibition of nucleic acid synthesis. 5-FC is rapidly taken up by fungal cells through specific cellular transporters, such as cytosine permease (Andriole, 1999). 5-FC (Figure 1.6) is converted to 5-fluorouracil (5-FU) by the enzyme cytosine deaminase, which is unique to fungal cells (Vermes *et al.*, 2000). 5-FU is utilised to produce 5-fluorouracil monophosphate (5-FUMP) which is either converted into 5-fluorouracil triphosphate, which combines into RNA instead of uridylic acid and disrupts protein synthesis, or is converted into 5-fluorodeoxyuridine monophosphate, which inhibits thymidylate synthase, a key enzyme of DNA

synthesis. 5-FC possesses potent activity, mainly against fungi, particularly *Candida* and *Cryptococcus* species (Sobel *et al.*, 2003).

Figure 1.6 Structure of 5-FC (Vermes *et al.*, 2000).

1.1.3.2 Polyenes

Polyenes are a large family of compounds, most of which were derived from *Streptomyces* bacteria. Only three compounds are known to possess clinical antifungal activity: amphotericin B (AmB), nystatin and natamycine. All polyenes target the fungal cell membrane by binding to the major sterol, ergosterol. This, in turn, results in formation of pores in the plasma membrane, which induces membrane destabilisation, destroying the fungal cell (Carrillo-Munoz *et al.*, 2006). AmB was discovered in 1956 and is considered the gold standard due to its broad-spectrum activity against the majority of medically important mould and yeast. AmB (Figure 1.7) is widely used in systemic infections therapy for *Candida* and *Aspergillus* (Vandeputte *et al.*, 2012).

Figure 1.7 Structure of amphotericin B (Zotchev, 2003).

7

1.1.3.3   Azoles

All azole derivatives prevent formation of the fungal membrane sterol ergosterol, by inhibition of a key enzyme, lanosterol 14 alpha-demethylase (Carrillo-Munoz *et al.*, 2006). This causes a block in the production of ergosterol, leading to the accumulation of a toxic sterol. This toxic sterol exerts a severe membrane stress causing cell death (Maertens, 2004). There are two classes of azoles, imidazoles and triazoles. Imidazoles, which have two nitrogen atoms, were synthesised first, however their use remained limited to superficial use due to their high toxicity (Maertens, 2004). The first imidazole antifungal, ketoconazole, was used in 1981 but then banned from clinical use for systemic fungal infections due to the risk of hepatic damage and risk of decreased human steroid synthesis. Further research led to the development of triazoles, having three nitrogen atoms, such as fluconazole (Figure 1.8), itraconazole and voriconazole. Triazoles bind more specifically to the fungal membrane compared to imidazoles. However, due to issues related to drug resistance, a second-generation of triazoles has been developed (Vandeputte *et al.*, 2012). Fluconazole is known to have activity against *Candida* species including *C. albicans*. However, development of resistance to fluconazole has become an issue. Additionally, fluconazole lacks activity against *Aspergillus*, while itraconazole and voriconazole are still being used in this infection setting (Dudley *et al.,* 2018).
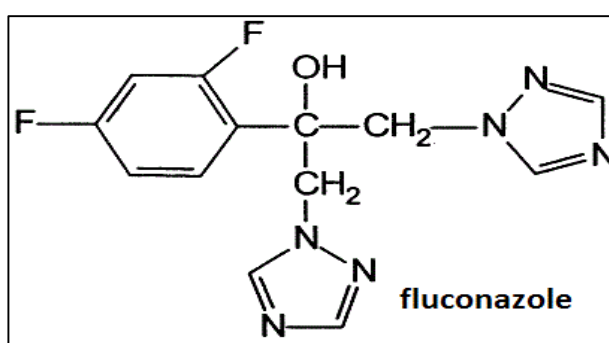
Figure 1.8 Structure of fluconazole (Maertens, 2004).

1.1.3.4   Echinocandins

Echinocandins were discovered in 1974 and were considered to be a significant addition to clinical use. Echinocandins are synthetic lipopetide compounds, which

target the fungal cell wall, these compounds have no equivalent in humans. This property reduces the possibility of attacking the host tissues (Sucher *et al.*, 2009). These agents inhibit β(1-3)-glucan synthase, the enzyme responsible for production of β(1-3)-glucan, one of the key elements responsible for fungal cell wall rigidity. Therefore, inhibition of β(1-3)-glucan synthase causes cell wall destabilisation, resulting in cell rupture (Carrillo-Munoz *et al.*, 2006). Echinocandins, such as caspofungin (Figure 1.9), are used to treat candidemia, invasive candidiasis and aspergillosis and are usually recommended following unsuccessful fungal treatment with azoles or AmB (Vandeputte *et al.*, 2012).
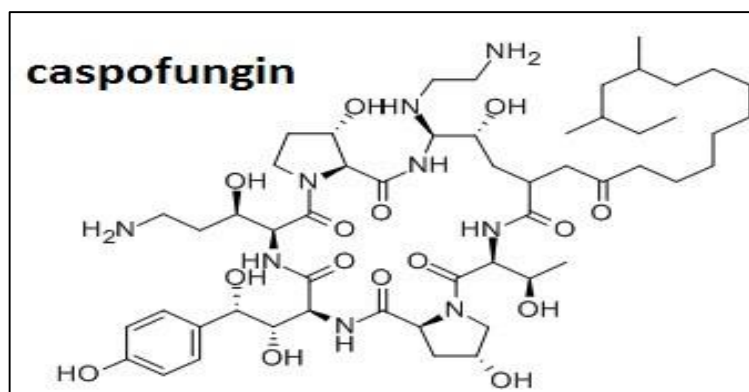
Figure 1.9 Structure of caspofungin, an example of an echinocandin (Carrillo-Munoz *et al.*, 2006).

1.1.4 Problems with current antifungals

There are several limitations associated with current antifungal agents including their resistance, side effects and spectrum of activity, which warrant an intensive search for more effective and safer drugs.

All invasive fungal infections need appropriate antifungal treatment to achieve successful clinical outcomes. Since only a few classes of antifungal agents are available, the development of resistance to single drug classes and, recently, multidrug resistance mainly affect patient management. One of the greatest difficulties in achieving clinical success is azole resistance amongst *Candida* and *Aspergillus* species, followed resistance to echinocandins and multidrug resistance amongst *Candida* species (Perlin *et al.*, 2017). Treatment failure occurs when a patient either fails to respond, or no longer responds to antifungal agent administered at standard doses. Many hosts and drugs lead to such

failures; for example, immunocompromised patients are more likely to fail to respond to treatment because the antifungal agents do not combine with the assistance of a robust immune system in the fight against fungal infection. Additionally, long-term treatment is often associated with the development of resistance. Primary drug resistance has emerged naturally among various fungi without previous treatment (Fuentefria *et al.*, 2018).

There are four major mechanisms contributing to development of fungal resistance to antifungal drugs. Firstly, the induction of the efflux pump, which decreases drug concentration inside the cell, is the most common mechanism of drug resistance. In fungi, two different drug efflux systems modulate azole resistance, the ATP-binding cassette (ABC) superfamily and the major facilitator superfamily (MFS) (Prasad *et al.*, 2014). Frequently, increased number of drug efflux pumps reduces the intracellular accumulation of azoles. This mechanism is based on overexpression of the *Candida drug resistance CDR1* and *CDR2* genes, which encode transporters, Cdr1p and Cdr2p, of the ATP-binding cassette (ABC) family. Upregulation of both *CDR1* and *CDR2* mediates azole resistance by enhanced drug efflux and reduced azole accumulation (Vandeputte *et al.*, 2012; Holmes *et al.*, 2016). The *multidrug resistance MDR1* gene, which encodes for a major facilitator transporter, Mdr1p, is also crucial in the regulation of transporter-mediated efflux pump to confer resistance to azoles.

Gain-of-function mutations in the transcription factors *TAC1* and *CgPDR1* can result in greater gene expression of drug efflux pumps (Spettel *et al.*, 2019). *TAC1*, a *Candida albicans* transcription factor, is necessary for the upregulation of the ABC-transporter genes *CDR1* and *CDR2*, which mediate azole resistance. Since the *CgPDR1* gene is one of the major regulators of efflux pump genes, deletion of *CgPDR1* results in a loss of transcriptional control of the major transporters involved in azole resistance and, consequently, decreased resistance to these antifungals (Prasad *et al.*, 2014). Expression of ABC genes is often associated with azole resistance in *S. cerevisiae* and *C. neoformans* (Holmes *et al.*, 2016). Secondly, target alteration such as a point mutation in *FUR1*, a gene which encodes an enzyme responsible for 5FU metabolism, results in an entire resistance to both 5FC and 5FU in fungal cells (Perlin *et al.*, 2017). Thirdly, through a metabolism modification mechanism, some yeasts have the ability to grow in high echinocandin concentrations (i.e. greater than the MICs).

This phenomenon, called the echinocandins paradoxical effect, is due to the metabolic adaptation of the microorganism and is mediated by the cell wall integrity signalisation pathway (Vandeputte *et al.*, 2012). This response is the direct consequence of the *β*(1-3)-glucan synthesis inhibition and the subsequent cell wall composition modifications, upon echinocandin administration (Vandeputte *et al.*, 2012). Finally, both yeast and filamentous fungi can form biofilm structures which ensure fungal cell integrity, survival and resistance to most available antifungals. Biofilms are sessile cells, which strongly adhere to surfaces and to each other, offering protection by a polymetric extracellular matrix (ECM) composed primarily of polysaccharides. Pathogenic fungi can also adhere to abiotic surfaces such as catheters; in particular, yeasts take advantage of this property to gain access to blood circulation, reaching internal organs of patients (Desai *et al.*, 2014; Costa-Orlandi *et al.*, 2017).

With regard to side effects, some antifungal drugs exhibit various side effects, which limit their clinical use; 5-FC for example, may cause hepatotoxicity or bone marrow injury. The most serious side effect of amphotericin B therapy is nephrotoxicity; in this the patient develops some abnormalities in renal function. Ketoconazole possesses hepatotoxic properties and does produce an endocrine abnormality by suppression of testosterone and ACTH-stimulated cortisol synthesis (Roemer *et al.*, 2014; Vermes *et al.*, 2000). It should be noted that resistance to one antifungal often causes cross-resistance to others within the same class due to various pathways influencing multidrug resistance (Gulshan *et al.*, 2007).

Another example of a medically important fungus is *Cryptococcus neoformans,* which is a major cause of infection in immunocompromised patients and can cause a severe form of meningitis in patients with AIDS. Infections by *Cryptococcus neoformans* are common in the lungs and can lead to clinical manifestations in the skin, soft tissue and bones. *Pneumocystis jirovecii* is another example of fungus responsible for *Pneumocystis* pneumonia. It can infect patients with AIDS or who take ant immunity drugs (Catherinot *et al.*, 2010).

1.2 Bacteria

Bacteria are prokaryotes consisting of a single cell with a simple internal structure. Unlike eukaryotic DNA, which is included inside the nucleus. Bacterial DNA is free within the cytoplasm, in a twisted thread-like mass referred to as the nucleoid. Bacterial cells also contain separate, circular pieces of DNA called plasmids. Bacteria lack membrane-bound organelles, which are designed to execute a range of cellular functions from energy production to the transport of proteins (Huang *et al.*, 2008). However, both bacteria and eukaryotic cells contain ribosomes where proteins are assembled. In regard to bacteria, they are termed 70S ribosomes, composed of a small 30S subunit and large 50S subunit. On the external surface, bacterial cells are generally surrounded by two protective coverings: an outer cell wall and an inner cell membrane. However, certain bacteria, such as mycoplasmas do not have a cell wall at all (Hacker *et al.*, 1997).

Bacteria are often classified into two groups, as Gram-negative or Gram-positive bacteria. This classification is based on the work of Hans Christian Gram, who in 1884 discovered that there was a difference between some bacteria. Some of the bacteria would stain and exhibit a blue-violet colour when he added crystal violet complexed with iodine to the bacteria and then washed them with alcohol; these bacteria he called Gram-positive bacteria. Other bacteria would not stain but were counterstained with safranin or carbolfuchsin to gain a pink colour, these bacteria were called Gram-negative bacteria (Yazdankhah *et al.*, 2001). The difference between these bacteria is their cell wall and the arrangement of the wall (Figure 1.6).

1.2.1 Bacterial cell structure

The spectrum of activity is highly reliant on the sructural difference of the bacterial membrane between Gram-negative and Gram-positive bacteria (Figure 1.10). Despite antimicrobials passing through the bacterial membrane via passive transport through porin or other transporters, it is generally accepted that Gram-negative bacteria are more difficult to kill using antimicrobials because of their outer membrane. The bacterial cell membrane is a bilayer made up of phospholipids such as phosphatidylglycerol (Tommasi *et al.*, 2015). Gram-negative bacteria possess both an inner and an outer membrane, in periplasmic

space a thin layer of peptidoglycan (cell wall) is connected to the outer membrane via lipoproteins (murein lipoprotein) (Silhavy *et al.*, 2010). Peptidoglycan is a polymer consisting of disaccharides and short peptide chains and is synthesised via a series of enzymatic steps including the key biosynthetic enzyme, DD-transpeptidase (Scheffers *et al.,* 2005; Vollmer *et al.,* 2008). DD-transpeptidase is a penicillin-binding protein (PBP), responsible for the final stages of bacterial cell wall assembly and is a target of β-lactam antibiotics.This enzyme carries out the cross-linking of the cell wall, which gives the structural rigidity to the cell wall (Silhavy *et al.*, 2010; Malanovic *et al.*, 2016). The outer membrane of the Gram-negative bacteria is on the inward facing side composed of phospholipids similar to the inner membrane, whereas the outer facing side contains lipopolysaccharide (LPS) (Sarkar *et al.*, 2017). On the other hand, Gram-positive bacteria do not contain an outer membrane, however, they do have a thick cell wall (peptidoglycan), through which lipoteichoic acids and wall teichoic acids traverse (Malanovic *et al.*, 2016).
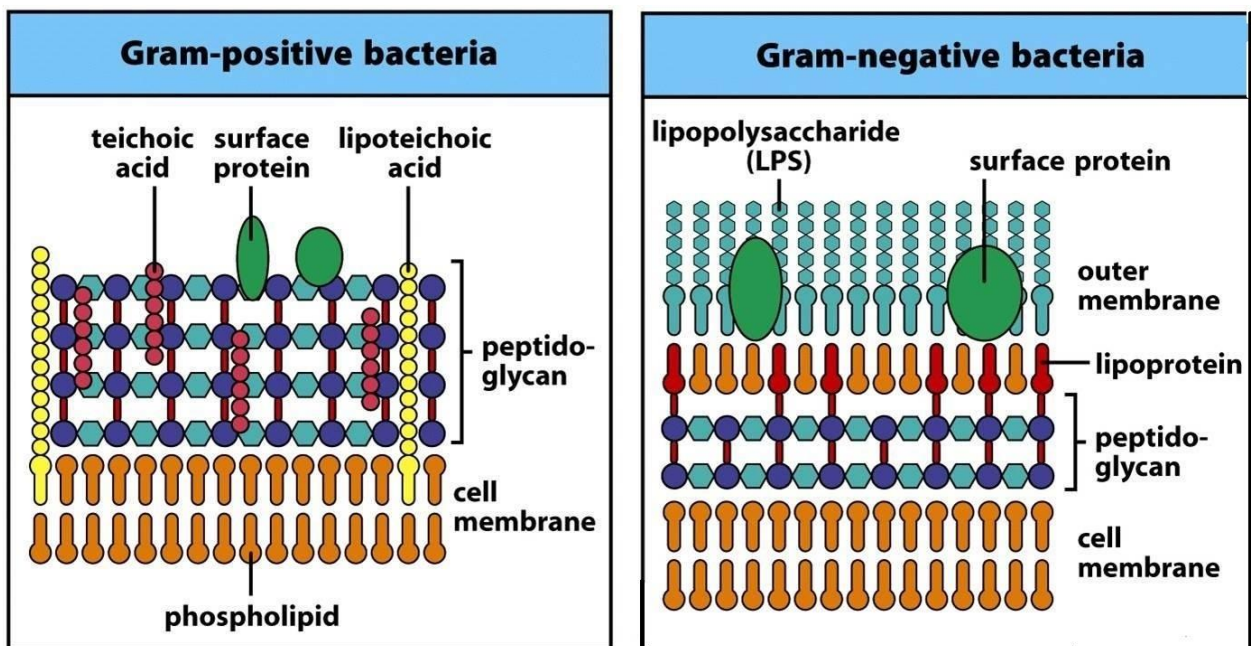
Figure 1.10 A comparison of the cell walls of Gram-negative and Gram-positive bacteria (Van Belkum, 2003).

1.2.2 Medically important bacteria

Bacterial pathogens cause a high rate of mortality around the world, particularly in developing countries due to unavailability of antibiotic therapy for resistant bacteria (Devasahayam *et al.*, 2010). Most bacterial infections are caused by particular microorganisms; *Staphylococcus aureus* and *Escherichia coli* (Bannerman *et al.*, 2004).

S. aureus (Figure 1.11) is a Gram-positive bacterium, present in the nose of about 30% of healthy people and on the skin of about 20% of them. The percentages are higher for people who are patients in a hospital or even work there. Bacteria can spread from person to person through direct contact with contaminated items or by inhalation of infected droplets dispersed by sneezing or coughing (Malachowa *et al.*, 2018). The most common *S. aureus* infections on the skin, can however travel through bloodstream (a bacteraemia) and infect any part of the body, particularly heart valves (endocarditis) and bones (osteomyelitis) (Tong *et al.,* 2015). These bacteria also tend to accumulate on medical devices in the body, such as artificial heart valves or joints, and catheters inserted through skin into blood vessels. Various strains of *S. aureus* produce toxins, which can cause food poisoning and toxic shock syndrome. In recent years, the development of methicillin-resistant *S. aureus* (MRSA) has caused a number of medical issues, especially in hospitals. (Nixon *et al.*, 2006). In the UK the estimated cost of treating MRSA is £13,972 per patient (Nixon *et al.*, 2006).
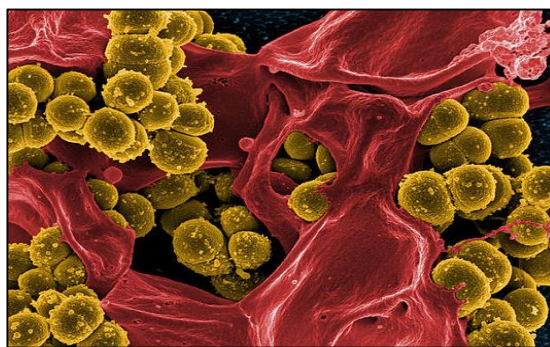
Figure 1.11 *S. aureus* (van Belkum, 2003).

E. coli (Figure 1.12) is a Gram-negative bacterium and is one of the most common microorganisms isolated in clinical laboratories (Russo *et al.*, 2000; Van Belkum, 2003). This bacterium is commonly found in the gut of humans and warm-blooded animals. This bacterium can be spread from one person to another by hand-to-

mouth contact. *E. coli* causes many infections, including cholangitis, neonatal meningitis and pneumonia. *E. coli*, particularly species of extended-spectrum β-lactamase (ESBL)-producing *E. coli*, cause many infections such as blood stream and urinary tract infections (Rodriguez-Bano *et al.*, 2006).

Figure 1.12 *E. coli*. (Van Belkum, 2003).

1.2.3 Bacterial therapy

The majority of the known antibiotics inhibit relatively few pathways in the bacterial cell including folic acid synthesis, transcription, DNA replication, protein synthesis and cell wall synthesis (Figure 1.13; Lange *et al.*, 2007)..
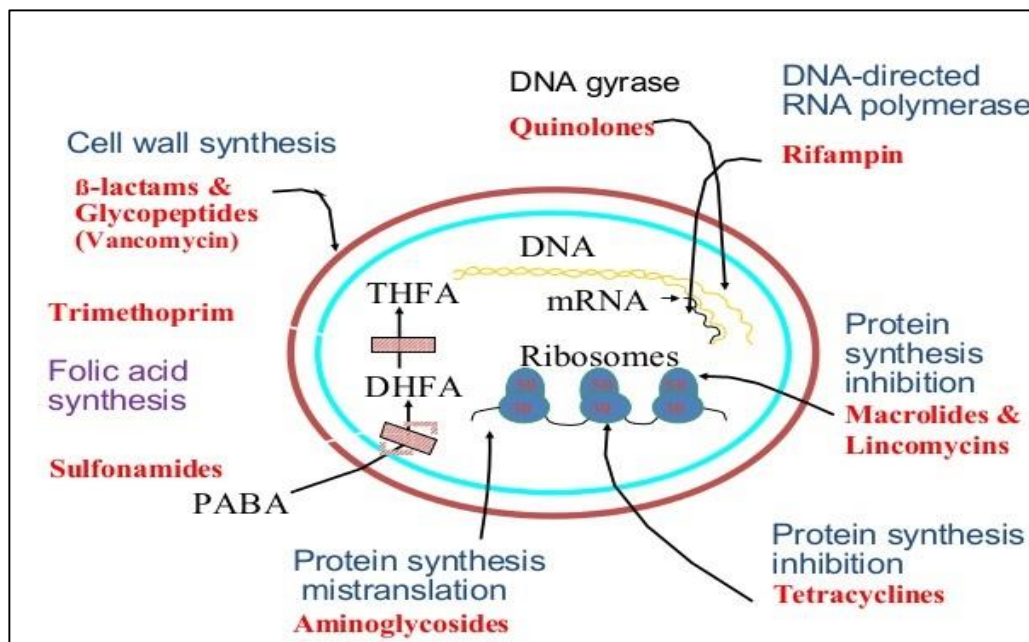
Figure 1.13 Antibacterial targets (Lange *et al.*, 2007).

Current bacterial therapy depends on a number of broad classes of antibiotics:

1.2.3.1 Penicillin

Penicillin (Figure 1.14) was isolated from the *Penicillium* fungi and was the first bacteriocidal antibiotic identified. Penicillin binds to the enzyme transpeptidase, which is required for the development of the bacterial cell wall. By inhibiting the cross-linking activity of the enzyme, peptidoglycan chains are no longer linked, preventing new cell wall formation. This causes cell lysis and results in cell death (Miller, 2002). Penicillin is mainly effective against Gram-positive bacteria, such as *Streptococci*, *Enterococci* and some *Staphylococci.*
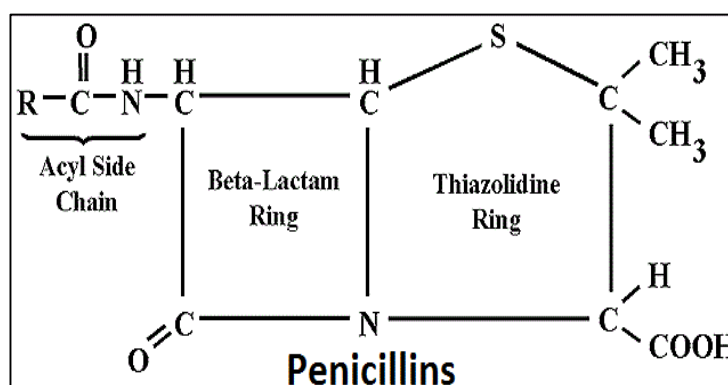
Figure 1.14 Structure of penicillin (Antunez *et al.*, 2006).

1.2.3.2 Cephalosporins

Cephalosporins are a set of bacteriocidal antibiotics originally derived from the fungus *Acremonium* and are structurally similar to penicillin (Figure 1.15). As such, these compounds have the same mode of action as penicillin. Cephalosporins possess greater efficacy than penicillin against Gram-negative bacteria and resistant bacterial strains because they are less susceptible to inhibition by β-lactamase (Demain *et al.*, 1999).
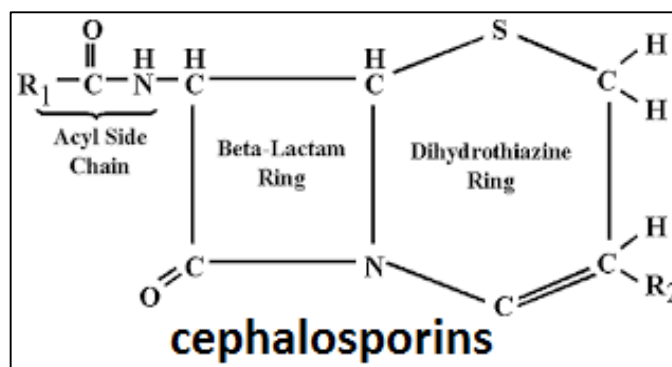
Figure 1.15 Structure of cephalosporins (Antunez *et al.*, 2006).

1.2.3.3   Aminoglycosides

The aminoglycoside family (Figure 1.16) are bactericidal, wide-spectrum compounds with activity against a number of infectious pathogens, particularly Gram-negative bacteria such as *E. coli*, *Pseudomonas* and *Salmonella* species. Aminoglycosides bind to the prokaryotic 30S small ribosomal subunits, resulting in inhibition of ribosome translocation and therefore protein synthesis (Mingeot-Leclercq *et al.*, 1999). There are a number of issues associated with using aminoglycosides including the toxicity profile, due to unspecific binding to mammalian ribosomes, and resistance (Hermann, 2007).

Figure 1.16 Structure of amikacin (Kotra *et al.*, 2000).

1.2.3.4   Fluoroquinolones

Fluoroquinolones, such as ofloxacin (Figure 1.17), are synthetic bactericidal agents, possessing outstanding activity against various species of Gram-negative and positive bacteria including gastrointestinal, urinary and respiratory bacterial pathogens (Scheld, 2003). Fluoroquinolones inhibit bacterial DNA gyrase, which is necessary for initiation of DNA synthesis, thereby preventing normal DNA replication and leading to bacterial cell death (Blondeau, 2004).

Figure 1.17 Structure of ofloxacin, an example of a fluoroquinolone (Blondeau, 2004).

1.2.3.5 Tetracyclines

Tetracyclines (Figure 1.18) are bacteriostatic compounds, which prevent bacterial protein synthesis by blocking the attachment of aminoacyl-tRNA with the ribosomal acceptor (A) site of the large ribosomal subunit. Consequently, this leads to disruption of protein synthesis. These agents display activity against both Gram-negative and Gram-positive bacteria (Chopra *et al.*, 2001) .
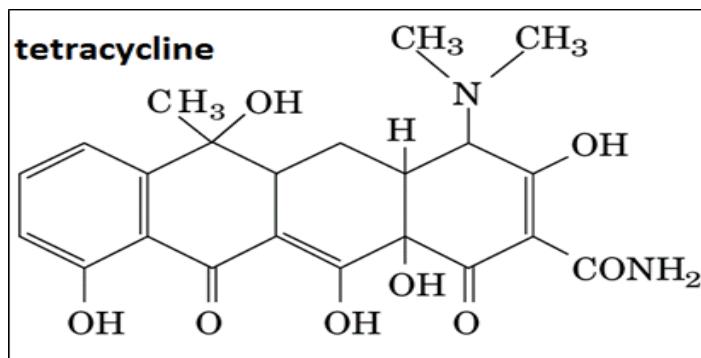
Figure 1.18 Structure of tetracycline (Chopra *et al.*, 2001).

1.2.3.6 Macrolides

Macrolides (Figure 1.19) are an important group of naturally occurring antibiotics, used mainly to treat lower respiratory infection. These agents bind reversibly to the 50S large subunit of the bacterial ribosome, stopping peptide bond formation by inhibiting peptidyltransferase activity. This leads to inhibition of bacterial protein synthesis (Zotchev, 2003).
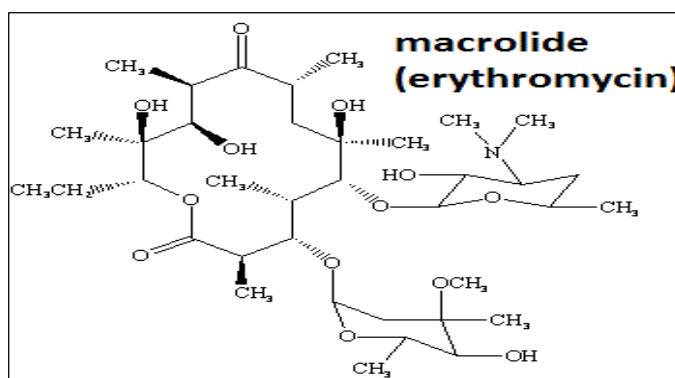
Figure 1.19 Structure of macrolide (erythromycin) (Zotchev, 2003).

1.2.4 Problems with antibiotics

Bacteria have a natural process that encourages resistance to antibiotics. The resistance process occurs via gene level mutations. Antibiotics induce selective pressure, and genes act in association with the induced pressure (Admassie, 2018). Bacteria have the ability to directly transfer genetic material between each other by transferring plasmids, which signifies that natural selection is not the only mechanism by which resistance evolves. Broad-spectrum antibiotics are prescribed in hospitals as a solution for nosocomial infections, however they increase emergence of resistance (Zaman *et al.*, 2017). The emergence of bacterial resistance has instigated researchers to look for effective alternative treatments. These resistant bacterial strains, such as MRSA and vancomycin-resistant enterococci (VRE), are important causative agents of nosocomial infections (Cosgrove *et al.*, 2003; Hurley, 2005).

Bacterial resistance can develop through three main mechanisms:

I.   Inactivation of the antibiotic by secretion of bacterial hydrolytic enzymes, as seen in resistance to β-lactam antibiotics (Walsh *et al.*, 2005).

II.   Bacterial modification of the antibiotic target so that it is no longer recognised. In methicillin-resistant *S. aureus* (MRSA) the mobile genetic element SCCmec (staphylococcal cassette chromosome mec) harbouring the *mecA* gene that encodes an alternative penicillin-binding protein (PBP2a) induced by β-lactams and with low affinity for β-lactams antibiotics (Walsh *et al.*, 2005; Munita *et al.*, 2016).

III. Upregulation of cellular efflux pumps to limit antibiotic accumulation inside the bacterial cell. This is the most frequent mechanism of the development of antibiotic resistance (Blair *et al.*, 2015).

Additionally, as resistance has evolved into multidrug resistance, this has resulted in increased global morbidity and mortality. Bacterial pathogens belonging to the ESKAPE group (*Enterococcus faecium, Staphylococcus aureus, Klebsiella pneumoniae, Acinetobacter, Pseudomonas aeruginosa and Enterobacter*) often carry MDR determining genes.

In addition, many bacterial species are able to form biofilms by adhering both to each other and surrounding themselves with an extracellular polymeric substances (EPC). This in turn protects the bacterial cells from the effects of the

antibiotic. The formation of biofilms occurs in many steps. It requires a special type of signalling, known as quorum sensing between bacterial cells (Wu *et al.*, 2015). Also, it requires transcription of different set of genes compared to those planktonic forms of the organisms. In addition, there are channels in the biofilm that separate the microcolonies. Mechanical stability of a biofilm is related to the viscoelastic features of the EPS matrix (Jamal *et al.*, 2018).

Further issues associated with antibiotics include host toxicity. For example, penicillin and cephalosporin may cause allergic reactions leading to allergic symptoms or serious anaphylaxis in rare situations (Antunez *et al.*, 2006). In general, the most common side effects affect the digestive system and cause vomiting, nausea and abdominal pain.

1.2.5 Tackling antimicrobial resistance issue

Considering the increasing number of pathogens resistant towards commonly used antimicrobial drugs and the rise in opportunistic microbial infections in immunocompromised patients, there is a pressing need for antimicrobial approaches that are capable of inactivating pathogens efficiently without the risk of developing resistance.

In a report on antimicrobial resistance published on 22 October 2018, the UK Parliament Health and Social Care Committee said that the Government must make this issue a "top five policy priority" and must urgently improve the market for drug companies to focus on developing and introducing new antibiotics. Without effective antimicrobial treatments, the risk of death from infectious disease would become substantially higher. In 2050 it is estimated that antimicrobial resistance will kill 10 million people per year, more than cancer and diabetes combined. Therefore, a dedicated budget should be made available to enable work and research to find alternative antimicrobial therapies and photodynamic therapy could be one of these promising tools to combat microbial infections (Rios *et al.*, 2016).

1.3   Photodynamic therapy

The basis of photodynamic therapy (PDT) is the initiation of toxic photochemistry in the target tissue. This involves a combination of two steps, the first being the injection of a photosensitiser followed by light illumination of the sensitised target tissue at a specific wavelength which is appropriate for absorbance by the photosensitiser (Abrahamse *et al.*, 2016). Although the exact biological mechanisms underlying PDT may vary with the nature of photosensitiser, its distribution in the tissue, the intracellular localisation sites and other parameters, the primary photochemistry involved in PDT-induced damage is similar for all photosensitisers.

1.3.1 Historical overview

In 1801 ultraviolet (UV) rays were discovered and scientists began to understand the therapeutic effect of the sunlight. Later, during the 19th century, the use of therapy with sunlight increased in the scientific community to treat a variety of diseases including rachitis, peritoneal tuberculosis and lupus vulgaris (Weishaupt *et al.*, 1976).

Towards the end of the 19th century, Lahmann constructed and used the first artificial light sources in Germany. His construction was made from a carbon arc lamp in combination with a parabolic mirror. He successfully treated a patient with lupus vulgaris of the nose and recorded an improvement in another patient that had the same condition. At the beginning of the 20th century, Niels Finsen received the Nobel Prize for his therapeutic results in treating lupus vulgaris with concentrated doses of UV radiation from a carbon arc lamp. This was regarded as the beginning of modern phototherapy (Roelandts, 2002).

In the mid-20th century scientists and doctors started using artificial light sources for treating neonatal jaundice, psoriasis, and several different skin conditions (Macdonald *et al.*, 2001). It was not until the 1990s when the first photosensitisers were approved for clinical use (Macdonald *et al.*, 2001; Konopka *et al.*, 2007; Ormond *et al.*, 2013). Nowadays, phototherapy can be used with or without the use of a photosensitiser. When used together with a photosensitiser, phototherapy is known as photochemotherapy (Ormond *et al.*, 2013).

Photodynamic therapy (PDT) is a type of photochemotherapy, which involves three components: light, a photosensitiser and oxygen.

Currently photodynamic therapy is mostly used in the treatment of cancers, as reviewed by (Allison *et al.*, 2005; Allison *et al.*, 2010), however, there are numerous recent studies that have shown that photodynamic therapy also has an antimicrobial effect (Cieplik *et al.*, 2014; Cieplik *et al.*, 2018).

1.3.2 General photochemistry of photodynamic therapy

The PSs are activated by a UV/visible light source of a specific wavelength to produce reactive oxygen species (ROS) (Maisch, 2007). During PDT the irradiation process transfers electrons of the PS to another orbital, changing the ground state of a PS (S0) to an unstable form (excited singlet state, S1). The phosphorescence emission, via intersystem crossing that involves a change in the spin rotation of an electron, allows S1 to convert to an excited triplet state, which is the major factor in the photodynamic treatment (Figure 1.20) (Baltazar *et al.*, 2015).

Photodynamic treatment includes two types of reactions. In the Type 1 photochemical mechanism, the excited triplet form of PS depends on direct electrons or hydrogen transference to a biomolecule (Castano *et al.*, 2004). This yields free radicals, which will readily react with oxygen to form cytotoxic species, such as; hydroxyl radicals, superoxide O_2^- and peroxide. The availability of oxygen is not necessary in Type 1 as free radicals can induce direct cell death. Conversely, Type 2 reactions require transfer of energy from the triplet form of PS to the ambient molecular oxygen (Dai *et al.*, 2012; Cieplik *et al.*, 2018). This produces singlet oxygen $^1O_2$ by shifting the external O_2 electron into the orbital with the other electron (Figure 1.20). This resulting singlet oxygen is powerful, short-lived and difficult to destroy by enzymes. Consequently, the resultant reactive species leads to cell death by apoptosis, necrosis and autophagy (Dougherty *et al.*, 1998; Cieplik *et al.*, 2018).
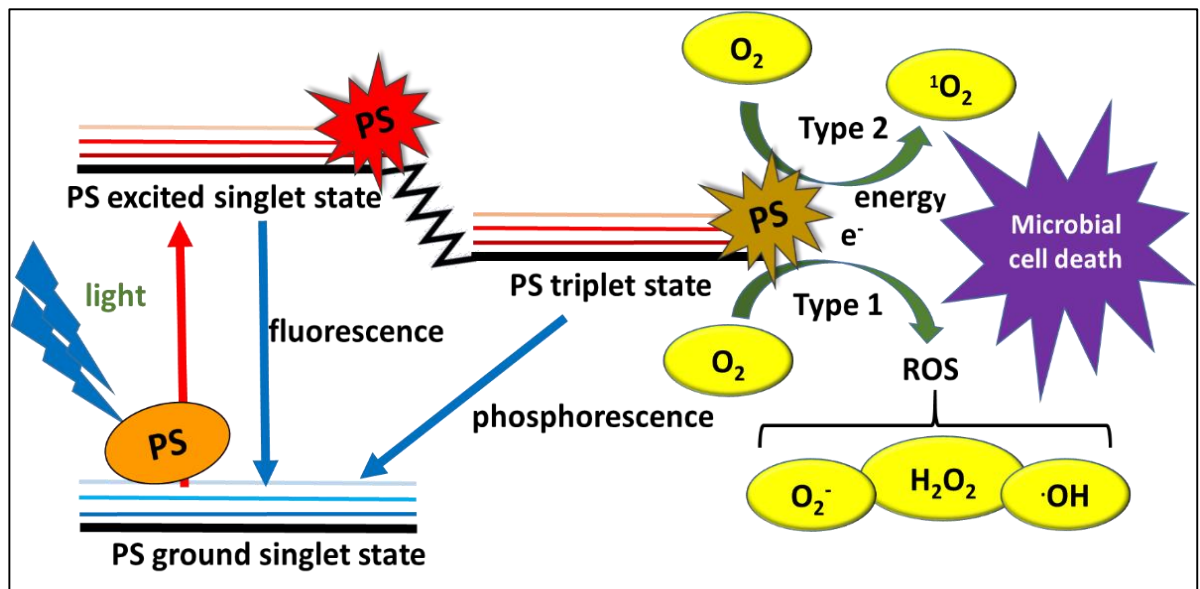
Figure 1.20 Schematic illustration of photodynamic therapy including the Jablonski diagram. The PS firstly absorbs photons that excite it to unstable excited singlet state, then this is converted to an excited triplet state. This triplet PS can act in two pathways, Type 1 and Type 2, resulting in formation of reactive oxygen species (ROS) and singlet oxygen respectively, adapted from (Dai *et al.*, 2012).

1.3.3 Oxygen in photodynamic therapy

The ground state of oxygen has two unpaired electrons, which are positioned on the outermost orbitals. Depending on the presence or absence of a magnetic field, these electrons can have three different configurations: both spins aligned up, both spins aligned down, or in opposite directions. Because of these three possible configurations, the ground state of oxygen is also called a triplet state (Macdonald *et al.*, 2001).

The predominant agents produced from photodynamic therapy are $\cdot OH$ and $^1O_2$. They are highly reactive forms that happen as a result of the photosensitising process. The lifetime of both species is very short due to their reactiveness, and as a result of this short lifetime the energy created and the oxidative damage induced by PDT is highly localised (Ormond *et al.*, 2013; Jiang *et al.*, 2018).

1.3.4 Photosensitisers in photodynamic therapy

The first photosensitisers used for photodynamic therapy were porphyrins, chlorins and bacteriochlorins. These dyes have the strongest light absorption in the red portion of the electromagnetic spectrum. They differ in the absorption

spectra ranging from around 400 nm to around 800 nm (Macdonald *et al.*, 2001). These photosensitisers are highly efficient singlet oxygen generators. The production efficiency of singlet oxygen is called singlet oxygen quantum yield (Φ) (Mathai *et al.*, 2007; Konopka *et al.*, 2007).

The first commercial photosensitiser was Photofrin®. It belongs to the porphyrin group of photosensitisers and absorbs at 630 nm. Initially, it was approved only for treating bladder cancer, but later was approved for treating many other cancers, including oesophageal, lung, head, neck and abdominal cancers (Pushpan *et al.*, 2002). In an attempt to create a better photosensitiser, many new compounds have been synthesised such as 5-aminolevulinic acid (ALA), benzoporphyrin derivative (BPD), lutetium texaphyrin, temoporfin (mTHPC), tinethyletiopurpurin (SnET2) and talaporfin sodium (LS11). These compounds are more potent than the first-generation compounds by releasing more ROS. As a result of their potency they can cause pain and lead to severe skin photosensitivity (Macdonald *et al.*, 2001; Ormond *et al.*, 2013).

Additionally, there are also several non-porphyrin photosensitisers, which are organic dyes and aromatic hydrocarbons. These compounds are effective photosensitisers as they possess a triplet state of appropriate energies for sensitisation of oxygen including acridines, flavines, antharquinones, phenothiazines, xanthenes and cyanines (DeRosa *et al.*, 2002; Babanzadeh *et al.*, 2018).

1.3.5 Light sources

The first light sources used for PDT were argon-pumped dye lasers, potassium titanyl phosphate (KTP)- or neodymium:yttrium aluminium garnet (Nd:YAG)-pumped dye lasers, and gold vapour or copper vapour-pumped dye lasers. All these devices are expensive and complex, which is why diode laser systems are now predominantly used. Diode lasers are easy to handle, portable and less expensive compared to previously used devices (Kübler, 2005; Zhu *et al.*, 2005). Recently, non-laser light sources, such as light-emitting diodes (LED), have also been applied in PDT procedures. These light sources are much less expensive and are small, lightweight, and highly flexible (Haas *et al.*, 1997; Steiner, 2006).

For an effective PDT treatment, the light source should be capable of activating the photosensitiser at a specific wavelength. The penetration of light within skin relies on its wavelength, which means that depending on the pathology treated, the PDT can be applied superficially, interstitially, intra-operatively, and intracavitary (Figure 1.21; Hill *et al.*, 2014). The shorter the wavelength the more skin absorption and the less tissue penetration (Tanzi *et al.*, 2003; Jin *et al.*, 2010).
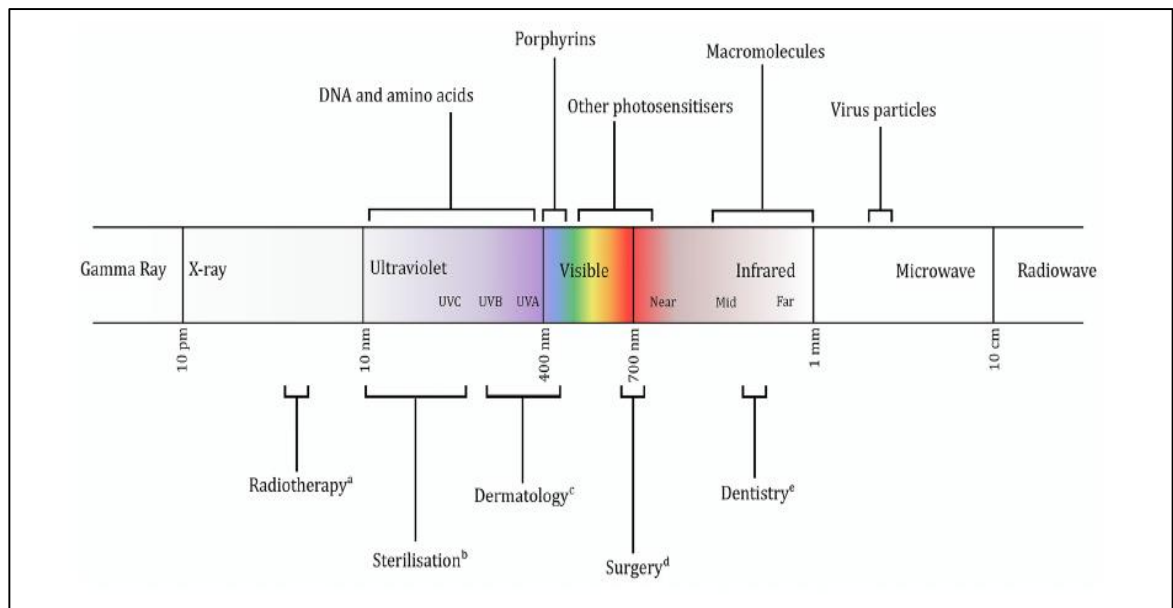
Figure 1.21 Representation of the electromagnetic spectrum, with regions of interest discussed in the text above. Current applications of certain wavebands also shown (Gwynne *et al.*, 2018).

1.3.6 Antimicrobial photodynamic therapy (aPDT)

The antimicrobial potential of PDT has been known since the beginning of the last century. However, it was not until the emergence of antibiotic-resistant strains of bacteria that scientists were motivated to look for alternative treatments, especially for localised infections of the skin and oral cavity (Konopka *et al.*, 2007; Davies *et al.*, 2010; Malik *et al.*, 2010).

It has been illustrated that PDT is effective against a number of microorganisms including Gram-positive and negative bacteria including multidrug-resistant (MDR) *Pseudomonas aeruginosa* (Tseng *et al.*, 2009), *Staphylococcus aureus* (Rosa *et al.*, 2014)*, Listeria monocytogenes* and *Bacillus subtilis* (Yin *et al.*, 2013). In addition, it has shown activity against a number of fungal species including C*andida* species, dermatophytes (Lyon *et al.*, 2011) and *A. fumigatus* (Friedberg

et al., 2001). It is unlikely that these microorganisms can develop resistance to aPDT. This is due to the fact that singlet oxygen and the free radicals interact with several cell structures and different metabolic pathways at the cellular level (Wainwright, 2004). As such, antimicrobial photodynamic therapy (aPDT) is a possible substitute for traditional antimicrobial drugs**.**

The products of photodynamic therapy cause damage to various components of the microbial cells or they can alter the metabolic activity irreversibly. This results in microbial elimination. This mechanism of action is based on the energy absorbed through intracellular photosensitisation which is transferred to the oxygen molecule in order to damage the oxidative reaction pathways in the plasma membrane and the genetic material of the microbial cells (Munin *et al.*, 2007; Hamblin *et al.*, 2002).

With regards to the uptake pathways of anionic and cationic photosensitisers, it has been reported that the uptake of anionic PSs by microbial cells may be mediated through a combination of electrostatic charge interaction, while the uptake of cationic PSs is mediated by electrostatic interactions and self-promoted uptake pathways (George *et al.*, 2009).

The localised action of radicals and $^1O_2$ produced during PDT, implies that the PS is more effective if it is taken up into its target cell before light is delivered (George *et al.*, 2009). Subsequently, these released species are better able to oxidise important cellular targets such as membrane, enzymes and lipids which leads to microbial killing. However, membrane barriers of the microbial cells limit the penetration of PSs into the microbial cell.

In relation to the mechanism of photodynamic inactivation, two pathways - Type 1 and Type 2 - can be involved in antimicrobial PDT, however one reaction may occur to a greater degree than the another due to PS structure and groups substituted on it. Some studies investigated the action of a set of acridine, thiazine, xanthene and phenazine dyes towards *E. coli* (Martin *et al.*, 1987), concluding that radicals were primarily responsible for the oxygen-dependent toxicity of the dyes examined.

On the other hand, other studies have implicated the Type 2 reaction (via energy transfer and $^1O_2$) in the inactivation mechanism of several cationic porphyrins against different *S. aureus* and *E. coli* species, concluding that the killing was

mediated predominantly by $^1O_2$ (Maisch, 2007). Although the microbial inactivation by aPDT mainly involves either Type 1 or 2 reactions, participation of the another reaction type could not be neglected (Ergaieg *et al.*, 2008).

With respect to the cytotoxic damage, two basic mechanisms have been studied in both bacteria and fungi to explain the lethal effect of radical species (Type 1) and singlet oxygen (Type 2) caused to microbial cells after PDT treatment (Hamblin *et al.*, 2004; Castano *et al.*, 2004):

1- Damage to DNA. DNA modification, breaks in both single- and double-stranded DNA and photomodification or disappearance of the plasmid supercoiled fraction of cytoplasm have been detected in both kinds of bacteria upon PDT using structurally different types of photosensitisers (Nitzan *et al.*, 1992; Malik *et al.*, 1990; Bertoloni *et al.*, 2000). Guanine residues were found to be the most easily oxidised.

2- Damage to the cytoplasmic membrane followed by a leakage of cellular contents or inactivation of membrane transport systems and enzymes (Valduga *et al.*, 1993).

These mechanisms achieve the cellular damage necessary for the success of aPDT, leading to cell lysis and, consequently, to its death.

Furthermore, the type of microorganisms determines difference in response to a PDT. Gram-positive bacteria, for example, can easily take up molecules such as neutral or anionic PS used for PDT and can be easily photoinactivated by them, especially when compared to Gram-negative which have a unique LPS-containing outer membrane, that excludes compounds from penetrating into the cell (Hamblin *et al.*, 2004; Zgurskaya *et al.*, 2015). Regarding Gram-negative bacteria, photoinactivation is not so easy since they are relatively impermeable to neutral or anionic drugs due to their highly negatively charged surface and when compared to Gram-positive (Zgurskaya *et al.*, 2015). Positively charged photosensitisershave been shown to be active against both Gram-positive and negative bacteria and fungi.

Due to the continuous need for new alternatives to antimicrobial therapy, narrow-wavelength light has been used alone as antimicrobial treatment (Gwynne *et al.*,

2018). This wavelength (blue light 400-450 nm) has the ability to activate intracellular photosensitisers such as porphyrins, and thus cause cell death by the production of toxic reactive oxygen species (Halstead *et al.*, 2016; Zhang *et al.*, 2016).

1.3.7 Advantages and disadvantages of photodynamic therapy

1.3.7.1 Advantages of aPDT

Antimicrobial photodynamic therapy has shown a reduction of emergence of photoresistant strains due to the absence of a specific target (Jori *et al.*, 2006), as the short-lived species related to the photodynamic effect have a multi-target impact property affecting different components of microbial cells (Giuliani *et al.*, 2010; Tavares *et al.*, 2010). Additionally, many possible PS compounds have been shown to possess aPDT action against bacterial and fungal biofilms, which are often untreated by traditional antimicrobial drugs (Yin *et al.*, 2013; Chabrier-Rosello *et al.*, 2005). The produced ROS species relating to PDT usually have irreversible effects on bacterial and fungal cells which hinder the microbial recovery after application (Jori *et al.*, 2006; Tavares *et al.*, 2010).

There are also many different applications of aPDT against a wide range of pathogenic microorganisms. As aPDT has a broader therapeutic window than other traditional antimicrobial agents, and thus it can be applied to several different localised infectious diseases (Donnelly *et al.*, 2008). An important observation about cationic antimicrobial PSs concerns their selectivity for microbial cells compared to host mammalian cells. It is thought that these PSs, such as porphyrin-based compounds, are only slowly taken up by host cells by the process of endocytosis, while their uptake into bacteria is relatively rapid (Demidova *et al.*, 2004).

1.3.7.2 Disadvantages of aPDT

In order for PDT to be effective, it requires the light to be directed to the appropriate site and tissue depth. Optimal light delivery with lasers and the coordination between different clinicians is complex, and sometimes the availability of the light sources is a major issue. Currently there are portable light sources, which have simplified the process. PDT in general is an ablative procedure and the treatments do not provide material for histopathological

diagnosis. That is why prior to the application of PDT, a treatment diagnosis should be made by other methods. Another limitation of PDT is the inability of the light to penetrate deeply, which reduces treatment effectiveness (Jin *et al.*, 2010). The extent of light penetration relies on the wavelength and the higher the wavelength the more penetration depth. If the target site of action is the skin, it is preferred to use shorter wavelengths which are absorbed mainly in the skin (Hill *et al.*, 2014; Gwynne *et al.*, 2018).

Photosensitivity is another issue that can last for some time after the application of certain photosensitisers. It is dependent on the method of application of the photosensitiser. When administered systemically, skin photosensitivity may last for several days or weeks. Patients are instructed to avoid exposure to sunlight, to protect the skin and the eyes until the drug is completely eliminated (Konopka *et al.*, 2007).

1.4 Aims

In the last decade, the rise in opportunistic microbial infections in immunocompromised patients and the reduction in efficiency of currently available treatments has resulted in an unmet medical need, which requires focus. Antimicrobial photodynamic therapy has already been identified as a promising treatment for microbial infections including resistant species.

The main aim of this thesis is to identify novel effective photoactivated antimicrobial compounds that may target clinically important fungi including *S. cerevisiae* and *C. albicans* and *A. fumigatus* and the bacteria *S. aureus* and *E. coli*. Due to the fact that acridine, flavine and anthraquinone compounds have photosensitising activity, it is hoped that synthesised photoactivated compounds based on their structures will show activity against several medically important microorganisms. Chapters 3, 4, 5, and 6 measure the amount of reactive oxygen species released *in vitro* from acridine, flavine, acridine-isoalloxazine and anthraquinone compounds under blue light illumination and determine the antimicrobial activity. A further aim was to identify a shortlist of compounds based on their antimicrobial activity.

Chapter 7 investigates the development of resistance by the microbial species to the shortlisted photoactivated compounds. Additionally, Chapter 7 examines the effect of pH and EDTA on growth inhibition activity of these shortlisted compounds.

Data within this thesis investigates the mechanism of action of the shortlisted photoactivated antimicrobial compounds and assesses their effects against microbial biofilms. Another important aim was to determine whether the novel photoactivated antimicrobial candidate compounds are cytotoxic to host mammalian cells. Finally, it is hoped that this work will suggest methods to improve the efficacy of these photosensitising compounds.

2. Materials and methods

2.1　Photosensitiser characterisation

A library of novel photosensitisers, based on acridine, acridine-isoalloxazine, flavine and anthraquinone structures, has been previously synthesised by Dr Robert Smith, School of Physical Sciences and Computing, University of Central Lancashire, Preston, UK (UCLan).

2.1.1 Determination of wavelength of maximum absorbance λ_{max}

The compounds were dissolved in dimethyl sulfoxide (DMSO), at a concentration of 0.5 mg/ml, and the absorption spectrum between the wavelengths 250-800 nm was taken using a UV-Visible spectrophotometer (Shimadzu-UV-3600). The wavelength of maximum absorbance, λmax, was determined for each of the compounds tested.

The blue light source used in this study was blue light LED (light-emitting diode) bulbs giving a peak wavelength of 470 nm and a light fluence rate of 96 mW/cm^2 at 5 cm distance.

2.1.2 Singlet oxygen release analysis

○ **TPCPD assay**

Singlet oxygen release by the compounds was assayed using the decolourisation of the marker 2,3,4,5-tetraphenylcyclopentadienone (TPCPD) in DMSO (Cincotta *et al.*, 1987). Initial stock concentrations of the candidate compounds and the marker (TPCPD) were prepared in DMSO (0.5 mg/ml). The candidate compounds were added, in a ratio of 1: 1, with the marker TPCPD and the absorbance, at a wavelength 506 nm, was monitored over time using a UV-Visible spectrophotometer (Shimadzu-UV-3600) in the presence or absence of blue light. The path length for best illumination was determined to be 5 cm from the blue light source and the standards used were aminoacridine, alloxazine, 10-phenylisoalloxazine, anthraquinone, anthrone and bianthrone. These standards were considered to be more likely to release singlet oxygen species due to their molecular structures typified by conjugated double bonds containing a

delocalised system of π-electrons (Wainwright *et al.*, 1997; Wu *et al.*, 2006). By assuming that the drop in TPCPD absorption at 506 nm is directly proportional to the reaction with singlet oxygen $^1O_2$, the decrease in absorption caused by tested derivatives compared to that of the corresponding standard when exposed to blue light under identical conditions thus gives a measure of its photosensitising effectiveness.

The Relative $^1O_2$ yield = Actual reduction of absorption (Standard) / Actual reduction of absorption (compounds).

2.1.3 Free radical release studies

o **DPPH assay**

2,2-Diphenyl-1-picrylhydrazyl (DPPH) assay was performed according to Brand-Williams *et al.*, (1995) with some modifications. The DPPH• is a stable radical in solution, absorbing at 515 nm in either DMSO or methanol. DPPH• accepts a hydrogen (H) atom and is reduced to DPPH, resulting in a colour change and a decrease in absorption at 515 nm (Brand-Williams *et al.*, 1995).

Initial stock concentrations of the test compounds 0.5mg/ml and equivalent concentration of DPPH were prepared in DMSO to give an OD of approximately 1.1 +/- 0.02 at 515 nm. The candidate compounds were added to DPPH solution at a ratio of 1:1 and the absorbance was monitored over time at 515 nm.

o **ABTS assay**

This assay depends on the reaction between 2,2′-Azino-bis(3-ethylbenzothiazoline-6-sulfonic acid) (ABTS) and potassium persulphate in order to generate ABTS•+ solution as described by (Re *et al.*, 1999). ABTS•+ solution, which has a maximum absorption at 734 nm, is reduced by antioxidants to ABTS. The extent of this decolourisation depends on the antioxidant activity and the amount of free radical species release. ABTS•+ was produced by reacting 7 mM ABTS, prepared in water, with 2.45 mM potassium persulphate (final concentration) and stored in the dark for 12-16 h.

The solution was then diluted with phosphate buffered saline (PBS) [0.8% NaCl, 0.02% KCl, 0.144% Na_2HPO_4, 0.024% KH_2PO_4] to give an absorbance of approximately 0.7 at 734 nm. The test compounds were added, and the

absorbance was monitored over time spectrophotometrically at 734 nm after exposing the candidate compound to blue light.

2.2   Microorganisms and growth media

Details of the yeast species and strains utilised are detailed in Table 2.1.

The fungal species utilised in the present study are *Saccharomyces cerevisiae (S. cerevisiae), Candida albicans (C. albicans)* and *Aspergillus fumigatus (A. fumigatus).*

These fungal species were maintained on agar plates, either yeast extract peptone dextrose (YPD) [2% dextrose, 1% peptone, 1% yeast extract] (*S. cerevisiae* and *C. albicans)* containing 2% agar or Sabouraud dextrose (SD) [4% dextrose, 1% peptone] (*A. fumigatus*), containing 1.5% agar. The bacterial species utilised were *Staphylococcus aureus (S. aureus)* and *Escherichia coli (E. coli),* which were maintained in Luria broth (LB) [1% tryptone, 0.5% yeast extract, 1% NaCl] containing 2% agar.

The fungal species, *S. cerevisiae* and *C. albicans,* were incubated in YPD at 30°C with shaking at 180 rpm. *A. fumigatus* (spore-forming mould) was grown on solid medium Sabouraud dextrose agar (SDA) at 35°C because it readily pellets in liquid. While the bacterial species, *S. aureus and E. coli*, were incubated in LB at 37°C with shaking at 180 rpm.

Microbial growth was measured via optical density (OD) using a spectrophotometer at either 595 nm, for fungi, or 600 nm, for bacteria.

Table 2.1 Microbial species and strains utilised in the present study. Strain information for fungal and bacterial species and strains used in the present study. (Δ) means deletion yeast species. NBRP: National BioResource Project (Japan).

Microbial species	Strain	Genotype	Reference
Saccharomyces cerevisiae wild type	BY4741a (derivative of S288C)	*MATa his3Δ1 leu2Δ0 met15Δ0 ura3Δ0*	(Brachmann *et al.*, 1998)
Candida albicans	SC5314	n/a	(Gillum *et al.*, 1984)
Aspergillus fumigatus	NCPF 2140	n/a	Public Health Culture Collection
Staphylcoccus aureus	NCTC 6571	n/a	Public Health Culture Collection (Heatley, 1944)
Escherichia coli	NCTC 12241	n/a	Public Health Culture Collection
*Saccharomyces cerevisiae hog*1Δ	BY23209	*MATαhog1::URA3 leu2 his3 trp1 ura3*	NBRP of the MEXT, Japan
Saccharomyces cerevisiae msn2/4Δ	BY23752	MTA *msn2::HIS3 msn4::URA3 ade2-1 his3-11,15 leu2-3,112 trp1-1 urα3-1 can1-100*	NBRP of the MEXT, Japan

2.3　Growth analysis

Growth curves were conducted on fungal and bacterial cells by pre-culturing cells overnight in the corresponding media at 30°C and 37°C, respectively, before diluting in new media to OD of approximately 0.1. Growth was monitored at hourly intervals via OD using a spectrophotometer at either 595 nm, for fungi, or 600 nm, for bacteria. Analysis of the data enabled the time to reach mid-exponential phase for each species to be determined.

To determine the relationship between optical density (OD) and cell number, viable cells were plated onto the corresponding plates at a variety of dilutions. The number of colonies were counted after 24 h incubation and related back to the starting OD. Density of 5×10^6 cells/ml for *S. cerevisiae* and 10×10^6 cells/ml for *C. albicans* were related to OD_{595} approximately 0.1 and density of 15×10^7 cells/ml for *S. aureus* and 45×10^7 cells/ml for *E. coli* were related to OD_{600} approximately 0.1. For *A. fumigatus*, conidia density of 2.5×10^5 cfu/ml was related to OD_{530} approximately 0.01.

2.4　Effect of blue light on microbial growth

The effect of visible light alone on fungal and bacteria cell growth was studied by determining the effect on cell growth with and without exposure.

3-(N-morpholino) propanesulfonic acid (MOPS) (Sigma-Aldrich) at a final concentration of 0.165 M pH 7 was the recommended buffer for preparation of RPMI 1640 Medium (HyClone, USA) [2.08% RPMI 1640, 6.906% MOPS, 3.6% glucose] was prepared by dissolving the components in distilled water and adjusting pH to 7 with 1 M sodium hydroxide [4% NaOH].

RPMI was then filter sterilised using a 0.22 μm pore size filter (Stericup Filter Unit) to reduce the media's insoluble particle content. Exponentially growing fungal cells were diluted and a final inoculum of 2.5×10^5 cfu/ml, prepared in sterilised distilled water, was added to each well. Conidia suspension 2.5×10^5 cfu/ml of *A. fumigatus* was prepared in sterilised distilled water and was shaken in a vortex mixer if clumps were detected. Cells were then exposed to blue light for either 0, 10, 20, 30 and 60 min before being incubated overnight at 30°C for *S. cerevisiae* and 35°C for *C. albicans* and *A. fumigatus*. Optical density readings at 530 nm

were taken to measure the growth of cells in the absence and presence of blue light for *S. cerevisiae* and *C. albicans.* For *A. fumigatus* the growth inhibition was determined by visual inspection. These experiments were done three times in triplicate, n=3.

The effect of visible light alone on bacterial cells was studied by measuring the optical density (OD_{600}) for *S. aureus* and *E. coli* in the absence and presence of blue light exposure. Similar volumes of 100 µl Mueller-Hinton [beef extract 0.2%, acid hydrolysate of casein 1.75%, starch 0.15%] and an inoculum of 1×10^6 cfu/ml bacterial cells (resulting in a final inoculum of 5×10^5) were dispensed in 96-well plates. Cells were then exposed to blue light for either 0, 10, 20, 30 and 60 min before being incubated overnight in a 35ºC static incubator. Optical density readings at 600 nm were taken to measure the growth of cells in the absence and presence of blue light for *S. aureus* and *E. coli*. The experiment was repeated three times in triplicate, n=3.

2.5   Photoantifungal susceptibility test

The EUCAST microbroth dilution method (EUCAST 7.3: Arendrup *et al*., 2015a) for yeast was used to evaluate the susceptibility of *S. cerevisiae* and *C. albicans* to the compounds. The susceptibility of *A. fumigatus* was measured using (EUCAST 9.3: Arendrup *et al*., 2015b) for moulds. For each compound, the minimum inhibitory concentration (MIC) in µg/ml was determined in the absence and presence of blue light.

Cultures of *S. cerevisiae* and *C. albicans* were grown in YPD broth at 30ºC with shaking at 180 rpm until they reached the mid-exponential phase. Varying concentrations (0-250 µg/ml) of the compounds were prepared in DMSO (≤ 5%) and RPMI 1640 culture medium and dispensed into 96-well plate before inoculation with the same volume of cells, 5×10^5 cfu/ml. The final drug concentration and inoculum density was half the starting amount i.e. final inoculum = 2.5×10^5 cfu/ml. Plates were illuminated for either 10 or 20 min using blue light (470 nm) giving a light irradiance of 96 mW/cm^2 and, as a control, in the absence of blue light.

The plates were incubated for 24 h at 30ºC for *S. cerevisiae* and 35ºC for *C. albicans*, before the optical density at a wavelength of 530nm for each well was

determined. The MIC values of the compounds were determined to be the well showing growth inhibition of ≥ 50% of that of the drug-free control. In contrastfor *A. fumigatus*, the culture was incubated for 48 h at 35 ⁰C and the MIC value considered as the concentration of compound providing no visible growth by eye. The standard antifungal drug fluconazole was used against *S. cerevisiae* and *C. albicans* and amphotericin B against *A. fumigatus*. Experiments were either performed twice, in duplicate (n=2), if no effect on growth was observed or three times, in duplicate (n=3), if an antimicrobial effect was observed. Where possible the resulting MIC values were analysed using two-way ANOVA with Tukey's post-hoc test to calculate significant difference, with results found to be significant when $p ≤ 0.05$.

To determine whether the compounds had a static or cidal effect, 100 μl of sample was removed from wells which showed complete inhibition of growth and sub-cultured into fresh YPD broth medium and incubated for 24 h at 30 ⁰C. The static or cidal effect was identified by investigating their growth visually and was repeated on three separate occasions.

2.6   Photoantibacterial susceptibility test

The EUCAST microbroth dilution method (EUCAST 5.1: EUCAST, 2003) for bacteria was used to evaluate the susceptibility of Gram-positive *S. aureus* and Gram-negative *E. coli* to the candidate compounds. For each compound, the minimum inhibitory concentration (MIC) was determined in the absence and presence of blue light.

Cultures of *S. aureus* and *E. coli* were grown in LB broth at 37⁰C with shaking at 180 rpm until they reached the mid-exponential phase. Varying concentrations (0-256 μg/ml) of the compounds were prepared in DMSO (≤ 5%), PBS and Mueller-Hinton culture medium and dispensed into 96-well plate before the inoculation with the same volume of 1 x 10^6 cfu/ml. The final drug concentration and inoculum density is half the starting amount i.e. final inoculum = 5 x 10^5 cfu/ml. Plates were illuminated for either 10 or 20 min using blue light (470 nm) giving a light irradiance of 96 mW/cm^2 and, as a control, in the absence of blue light.

The plates were incubated for 16-20 h at 35ºC for both bacteria, before the optical density at a wavelength of 600 nm for each well was determined. The MIC values of the compounds were determined to be the first well showing no visible growth. Experiments were either performed twice, in duplicate (n=2), if no effect on growth was observed or three times, in duplicate (n=3), if an antimicrobial effect was observed. Where possible the resulting MIC values were analysed using two-way ANOVA with Tukey's post-hoc test to calculate significant difference, with results found to be significant when $p \leq 0.05$.

To determine whether the compounds had a static or cidal effect, 100 µl of sample was removed from wells which showed complete inhibition of growth and sub-cultured into fresh LB broth media and incubated for 20 h at 35 ºC. The static or cidal effect was identified by investigating their growth visually and was repeated on three separate occasions.

2.7 Mechanism of action of photoactivated antimicrobial compounds

To investigate the mechanism of action of the five shortlisted compounds, which showed maximal growth inhibition following initial testing, they were tested against two mutant strains of *S. cerevisiae* deleted for either *HOG1* or *MSN2/4* genes involved in the stress response (Table 2.1). The MIC values of the compounds were determined using the EUCAST antifungal susceptibility testing method against both *hog1* and *msn2/4* genomic deletion strains of *S. cerevisiae* and compared the wildtype *S. cerevisiae.*

2.8 Development of resistance to photoactivated compounds

To investigate the development of resistance by fungal and bacterial species to the shortlisted candidate compounds, cells were repeatedly exposed to the compounds. Following initial screening by the EUCAST method, surviving cell suspensions were grown and screened again, using the same compound and 20-minute blue light illumination. The MIC was then determined before the assay was repeated again. This procedure was repeated until third exposures were reached. In each passage, three independent cultures were examined. The

resulting MIC values were analysed using two-way ANOVA with Tukey's post-hoc test to calculate significant difference, with results found to be significant when $p \leq 0.05$.

2.9 Effect of pH and EDTA on growth inhibition activity of photoactivated compounds

2.9.1 pH effect

The effect of pH on the growth inhibition activity of the shortlisted compounds against *S. cerevisiae* and *C. albicans* was tested.

Susceptibility testing was performed using a broth microdilution method, according to EUCAST guidelines utilising pH 7 (EUCAST 7.3: Arendrup *et al.*, 2015a). Compound concentrations tested were 0-250 µg/ml and fluconazole concentrations range was 0-64 µg/ml. 100 µl inoculum of 5×10^5 cfu/ml (resulting in final inoculum of 2.5×10^5 cfu/ml) was added to the same volume of compound solution in each well and illuminated for 20 min with blue light. The MIC was determined to be the lowest compound concentration giving growth inhibition of $\geq 50\%$ of that of the compound-free control. Antifungal susceptibility testing was carried out for *S. cerevisiae* and *C. albicans* by adjusting pH to 4, 5, 6 and 8 using 1 M sodium hydroxide [4% NaOH] or 1 M hydrogen chloride [96 ml of 32% HCl added to distilled water to make a total of 1 L], as required. These experiments were repeated in the presence and absence of MOPS, which is a buffer used to minimise pH changes and the MICs values were compared at different pH values 4, 5, 6, 7 and 8.

2.9.2 EDTA effect

The effect of Ethylenediaminetetraacetic acid (EDTA) on the growth inhibition activity of the shortlisted compounds against *S. cerevisiae* and *C. albicans* was tested.

Susceptibility testing was performed using a broth microdilution method, according to EUCAST guidelines (EUCAST 7.3: Arendrup *et al.*, 2015a). Compounds' concentrations (0-250 µg/ml) and fluconazole concentrations (0-64 µg/ml) were prepared with 1 mM EDTA (final concentration) at pH 7 with and without MOPS. 100 µl inoculum of 5×10^5 cfu/ml (a final inoculum of 2.5×10^5

cfu/ml) was added to the same volume of compound solution in each microdilution well and illuminated for 20 min with blue light. Antifungal susceptibility testing was carried out for *S. cerevisiae* and *C. albicans* in the absence and presence of EDTA and MIC was determined to be the lowest compound concentration giving growth inhibition of ≥ 50% of that of the compound-free control. MICs were compared and antifungal activity of EDTA was determined by analysing MICs results using two-way ANOVA with Tukey's post-hoc test to calculate significant difference, with results found to be significant when $p ≤ 0.05$.

2.10 *In Vitro* antifungal susceptibility testing Of *C. albicans* biofilms

The antifungal susceptibility test to determine MICs of planktonic cells was conducted using EUCAST broth microdilution (EUCAST 7.3: Arendrup *et al.*, 2015a). Testing was conducted in triplicate.

Biofilms cells were prepared following method described by (Ramage *et al.*, 2001), a fresh culture of *C. albicans* was grown in YPD at 30 ºC to ensure growing cells were in the budding yeast phase. Cells were harvested by centrifugation for 3 min at 1438 x g, washed twice in sterile PBS, and resuspended in RPMI 1640 with L-glutamine and 0.165 M MOPS. The optical density of the culture was adjusted to 0.1, which is equivalent to approximately 1 x 10^6 cfu/ml, by dilution with RPMI 1640. Biofilm cells were prepared by pipetting 100 µl of 1 x 10^6 cfu/ml suspension into a flat bottom 96-well microtiter plates before incubating for 48 h at 37 ºC. Photoantifungal tested compounds were prepared in RPMI 1640 and added to the biofilms at varying final concentrations (0-25 µg/ml). Samples were exposed to blue light for 20 min before being incubated for 24 h at 35ºC. MICs of compounds and fluconazole were determined using the XTT reduction assay to assess their effects on biofilm cells.

XTT [2,3-bis(2-methoxy-4-nitro-5-sulfophenyl)-2H-tetrazolium-5-carboxanilide] was prepared at 0.5 g/l in PBS and then filter sterilised using a stericup vacuum (0.22 µm pore size). Menadione (10 mM dissolved in acetone) was added to a final concentration of 1 µM and then 100 µl of the XTT-menadione mixture was added to biofilm cells and control wells. The 96-well plates were incubated in the

dark over a two-hour period at 37 ℃ and a colorimetric change was examined in a microtiter plate reader at 490 nm to compare the metabolic activity of the biofilm cells, as XTT is converted only in viable fungal cells into an orange-coloured formazan derivative by mitochondrial dehydrogenase activity (Meletiadis *et al.*, 2001).

2.11 Perseverance parameter measurement

Perseverance is defined by the ability of fungal cells to grow at drug concentrations above the MIC, and is measured as the degree of supra-MIC growth (SMG) in broth microdilution assays (Rosenberg *et al.*, 2018).

Supra-MIC growth (SMG) was quantified as the average growth per well obtained after 24h and 48h above the MIC_{50} at 24 h normalised to growth level in the drug-free control.

$$SMG = \frac{\text{average 48 h growth above MIC}_{50}}{\text{growth without compound}}$$

EUCAST broth microdilution assay was used to measure MIC value, the lowest drug concentration that inhibits 50% of growth, in *S. cereviseae* and *C. albicans* strains. The plates were incubated for 24 h at 30℃ and 35℃ for *C. albicans*, before the optical density at a wavelength of 530 nm for each well was determined. MICs values were determined to be the first well giving growth inhibition of ≥ 50% of that of drug-free control. MICs were determined after 24 h and 48 h. SMG and MICs values were compared at 24 h and 48 h and analysed using two-way ANOVA with Tukey's post-hoc test to calculate significant difference, with results found to be significant when $p ≤ 0.05$.

2.12 Mammalian screening

2.12.1 Cell maintenance

HeLa cells were maintained in Eagles Minimum Essential Medium (EMEM), supplemented with 10 % Fetal Bovine Serum (FBS), L-glutamine (2 mM), 1 % Non-Essential Amino Acids (NEAA) and sodium pyruvate (1 mM). The cell lines

were cultured in a 37 ºC humidified atmosphere containing 5% CO_2. When a maximum confluence of 80-90% was obtained in a T75 flask, cells were washed with phosphate buffered saline (PBS) solution, before being incubated with 3 ml of 1 X trypsin (0.25%) at 37ºC for 3 min. The trypsin was neutralised by the addition of EMEM before cells were centrifuged for 5 min at 169 x g. Cells were then resuspended in EMEM. Cells were passaged 1:5 into flasks to maintain the HeLa cell line or seeded into dishes for practical analysis.

2.12.2   Growth curves

To determine the growth rate of the HeLa cell line, growth curve analysis was performed over a period of four days. Cells were seeded in a 12-well plate at a density of 2,000 cells per well. After 24, 48, 72 and 96 h incubation, three wells on each day were trypsinised and viable cell number was determined by counting cells manually using a haemocytometer and trypan blue exclusion test of cell viability, as cells which had taken up trypan blue staining were considered non-viable and excluded from counting. This process was repeated three times.

2.12.3   PrestoBlue® viability assay

PrestoBlue® is a resazurin-based cell permeable viability indicator that is quickly reduced by metabolically active cells, changing in colour from blue to red and becoming highly fluorescent. PrestoBlue® assay was used to provide a quantitative measure of viability and cytotoxicity by changing fluorescence in the presence of compounds or blue light alone.

As the greatest variable in viability assays is cell number, linearity of fluorescence versus cell number was determined to find a suitable working range of cell density. Cells were seeded at 500, 1,000, 2,000, 2,500, 5,000 and 10,000 cells/well in EMEM in 96-well plates and incubated at 37ºC for 24, 48, and 72 h before adding PrestoBlue® (Invitrogen) at ratio 1:10 for one hour and measuring the fluorescence with excitation at 535 nm and emission at 610 nm by Tecan GENios PRO plate reader. This process was repeated three times in triplicate.

To characterise the effects of blue light alone on cell viability, HeLa cells were seeded at 2,000 cells per well and incubated for 24 h before 20-minute blue light treatment. The cell viability was then measured by taking fluorescence readings on three consecutive days following treatment. 10 µl was withdrawn from wells and 10 µl PrestoBlue® added and incubated at 37°C for 2 h. Fluorescence was measured with excitation at 535 nm and emission at 612 nm using a spectrophotometer.

To test the effect of the shortlisted antimicrobial compounds, HeLa cells were seeded at 2,000 cells per well, incubated for 24 h before treatment with the compounds alone and following exposure to blue light for 20 min. HeLa cells were treated with two different concentrations 25 and 32 µg/ml, which showed the highest MICs against fungal and bacterial species. The cell viability was measured using the PrestoBlue® assay by taking fluorescence readings throughout three consecutive days after compound treatment. The controls used in this experiment were HeLa cells treated with 0.625% DMSO (the highest DMSO concentration used in antimicrobial testing) and untreated HeLa cells. The experiment was conducted in triplicate, n=3.

2.13 Statistical analysis

All data are shown as means ±SEM of either two or three independent experiments. Comparison between tested groups was conducted by means of two-way ANOVA with Tukey's post-hoc test using GraphPad Prism software. Significant results were determined statistically as follows: *** $p \leq 0.001$,** $p \leq 0.01$, * $p \leq 0.05$.

3. Acridines

3.1 Introduction

Acridine-based compounds are important small nitrogen tricyclic heteroaromatic agents with anti-infective properties. Acridines in general possess a high degree of positive ionisation and sufficient planar surface space for DNA intercalation, which are considered necessary for antibacterial effectiveness (Albert, 1951).

Two aminoacridines, proflavine and acriflavine, were first developed and subjected to clinical uses during the First World War as antibacterials against sepsis in wounds and hospital infections. Another effective acridine antimicrobial drug, aminacrine, was used widely in dermatology, ear and eye surgery due to its safety in mammalian host cells. Acridines, such as mepacrine, were used as antimalarial drugs and, at higher doses, to treat immune system disorders such as lupus erythematosus (Albert, 1951). Additionally, the cytotoxic activities of several acridine derivatives have been intensively examined to test their ability as potential anticancer drugs (Lin *et al.*, 2017).

To improve their effectiveness as antimicrobial agents, Albert and his co-workers attempted to identify parameters necessary to optimise their activity, such as cationic ionisation. They focused on the mechanism of action of aminoacridines and showed that those with electronic conjugation between the ring nitrogen and the amino group were the most effective because of the high cationic ionisation of these compounds. This led Albert to find a correlation of antimicrobial efficacy via DNA intercalation with acridine planar area and cationic ionisation (Albert, 1951).

With respect to photosensitising activity, a variety of acridine derivatives such as proflavine, acridine orange, acriflavine and 9-aminoacridine have been demonstrated to be active photosensitisers by releasing reactive oxygen species (ROS) under irradiation with an ultraviolet (UV) lamp (Ito *et al.*, 1978). The production of these species may be due to the molecular structures of these compounds, typified by conjugated double bonds containing a delocalised system of π-electrons. Therefore, the acridines exposed to visible light are likely to be more effective in killing unwanted clinically important microbes, compared to acridines without light activation (Wainwright *et al.*, 1997).

Initial studies have found that photoactivated acridines have an antimicrobial effect across a number of microorganisms. Various acridine compounds such as acriflavine, proflavine and acridine orange are shown to have photodynamic biological activities in the haploid yeast, *Saccharomyces cerevisiae*. Following exposure to UV light (315-400 nm) for 30 min, these acridines inhibited the yeast cells viability more significantly significantly when compared to that of the dark control (Iwamoto *et al.,* 1987).

Photoactivated aminoacridines have shown a significant increase in antibacterial activity under illumination with white light (a mixture of wavelengths of the visible spectrum) against a range of pathogenic microorganisms including both Gram-positive (*Staphylococcus aureus*, *Enterococcus faecalis*, *Bacillus cereus*) and Gram-negative (*Escherichia coli*, *Pseudomonas aeruginosa*) bacteria (Wainwright *et al.*, 1997).

Based on the well-established *in vitro* photosensitising and photoantimicrobial activity (Iwamoto *et al.*, 1987; Wainwright *et al.*, 1997) and to optimise their potential antimicrobial activity, a library of novel aromatic substituted acridine compounds has been synthesised (Johns *et al.*, 2014). The substitution pattern at different positions on acridine was hoped to lead to some dyes with interesting photophysical, photochemical and biological properties. The wavelength of maximum absorbance λ_{max} of novel synthesised acridines ranged between 424-445 nm, which corresponds with blue light.

This study utilised these novel substituted acridines to determine their potential use in photodynamic therapy (PDT) for microbial infections following blue light illumination. To determine their antimicrobial activity, the European Committee for Antimicrobial Susceptibility Testing (EUCAST) microbroth dilution method was utilised. All compounds were screened against key microbial pathogens, including *Staphylococcus aureus and Escherichia coli* and the fungi *Candida albicans (C. albicans)* which has high mortality rate of 40% and *Aspergillus fumigatus (A. fumigatus),* which is complicated to treat and often fatal with a mortality rate of 50-90% (Liu *et al.*, 2013; Miceli *et al.*, 2011). In addition, the yeast model organism, *Saccharomyces cerevisiae* (*S. cerevisiae*), was also included within the study.

3.2   Results

Acridine moieties have been of interest to medicinal chemists for many years and they exhibit significant pharmaceutical importance due to their potential photodynamic biological activities (Wainwright, 2001). A series of novel acridine-based compounds was previously synthesised by Dr Rob Smith (Figure 3.1, Tables 3.1 and 3.2; Johns *et al.*, 2014).
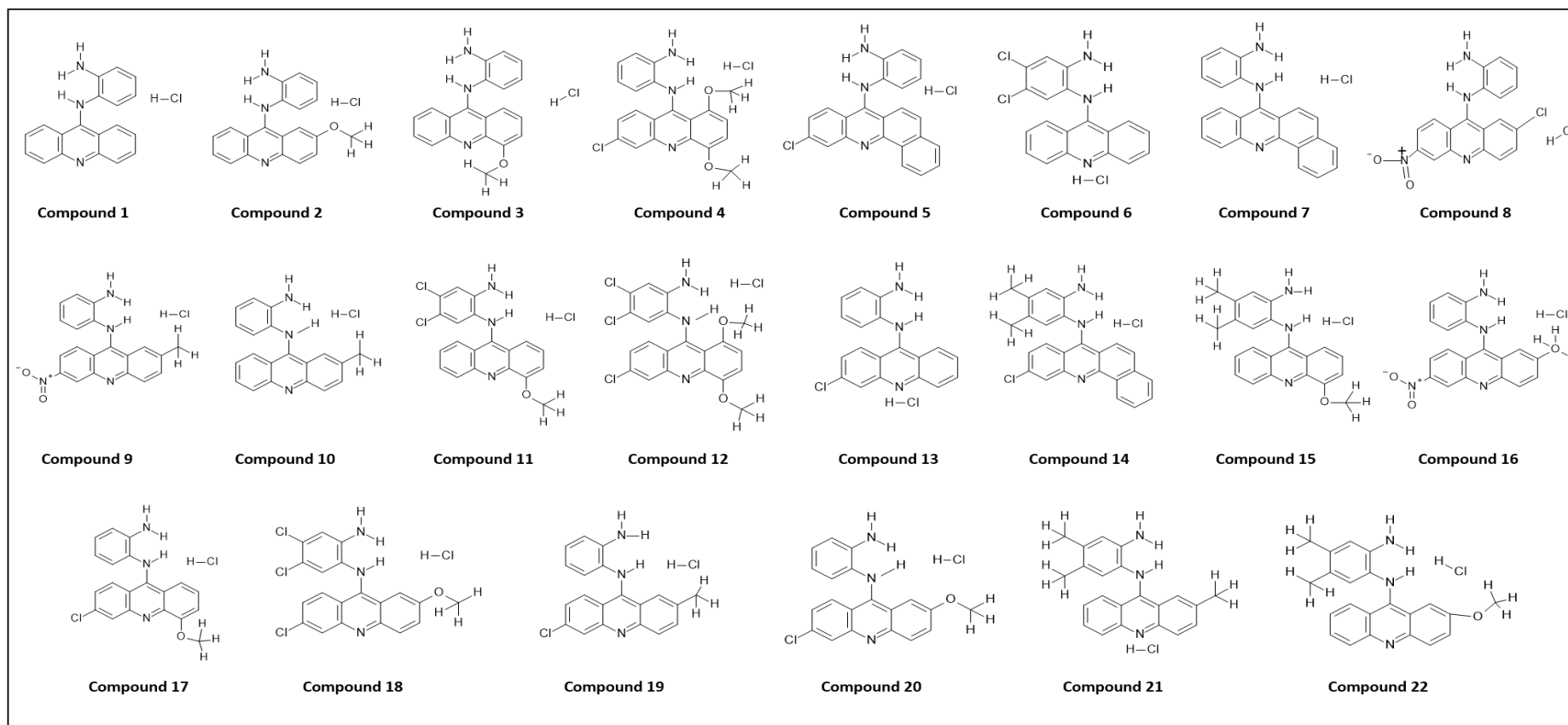
Figure 3.1 Chemical structures of novel acridine derivatives.

47

Table 3.1 Structures of substituted aminoacridine containing different R groups R$_1$, R$_2$, R$_3$, R$_4$, R$_5$ and R$_6$

Compound	R$_1$	R$_2$	R$_3$	R$_4$	R$_5$	R$_6$
1	H	H	H	H	H	H
2	H	H	OCH$_3$	H	H	H
3	H	H	H	OCH$_3$	H	H
4	Cl	OCH$_3$	H	OCH$_3$	H	H
6	H	H	H	H	Cl	Cl
8	NO$_2$	H	Cl	H	H	H
9	NO$_2$	H	CH$_3$	H	H	H
10	H	H	CH$_3$	H	H	H
11	H	H	H	OCH$_3$	Cl	Cl
12	Cl	OCH$_3$	H	OCH$_3$	Cl	Cl
13	Cl	H	H	H	H	H
15	H	H	H	OCH$_3$	CH$_3$	CH$_3$
16	NO$_2$	H	OCH$_3$	H	H	H
17	Cl	H	H	OCH$_3$	H	H
18	Cl	H	OCH$_3$	H	Cl	Cl
19	Cl	H	CH$_3$	H	H	H
20	Cl	H	OCH$_3$	H	H	H
21	H	H	OCH$_3$	H	CH$_3$	CH$_3$
22	H	H	CH$_3$	H	CH$_3$	CH$_3$

Table 3.2 Structures of substituted phenyl-aminoacridine containing different R groups R_1, R_2 and R_3
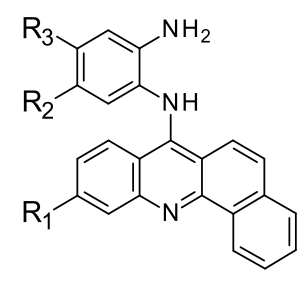
Compound			
	R_1	R_2	R_3
5	Cl	H	H
7	H	H	H
14	Cl	CH_3	CH_3

The structure shown in the table header features a phenyl ring with R_3, NH_2, R_2, and NH substituents connected to a benzo-fused acridine ring system bearing an R_1 substituent.

3.2.1 Photochemical characterisation of acridine compounds

3.2.1.1 Singlet oxygen ($^1O_2$) data

Firstly, the wavelength of maximum absorbance, λmax, was determined for each of the compounds in order to identify the corresponding visible light range for best excitation. As such, the absorption spectrum between the wavelengths 250-800 nm for each of the compounds was taken (Table 3.3). For all acridine compounds, the λmax of the compounds ranged between 424-445 nm, suggesting that all the novel acridine compounds were activated by blue light (400-495 nm).

The radical and $^1O_2$ species released from photosensitisers, under visible light illumination, can give a phototoxic response against microbial infections (Hamblin *et al.,* 2004; Jori *et al.,* 2006). Therefore, to measure singlet oxygen species produced following the exposure of candidate compounds to blue light, they were assayed using the decolourisation of the marker 2,3,4,5-tetraphenylcyclopentadienone (TPCPD) in DMSO. The absorbance of the marker alone and the active mixture, at a wavelength of 506 nm, was monitored over time using a UV-Visible spectrophotometer (Shimadzu-UV-3600) in the presence of blue light. It was assumed that the resultant drop in absorption of TPCPD in DMSO at 506 nm, due to decolourisation, is proportional to its reaction with singlet oxygen species. As such, the level of singlet oxygen release from each of

the compounds could be determined. An example set of data is shown in Figure 3.2, where the absorbance of TPCPD decreases over a period of 20 min following exposure of compound 5 to blue light. By determining the gradient of the linear portion of the graph, the half-life of the compound can be calculated. However, in 21 compounds the half-life was not reached, over the 20-minute monitoring period, instead the percentage reduction of absorption over 20 min was determined (Table 3.3).
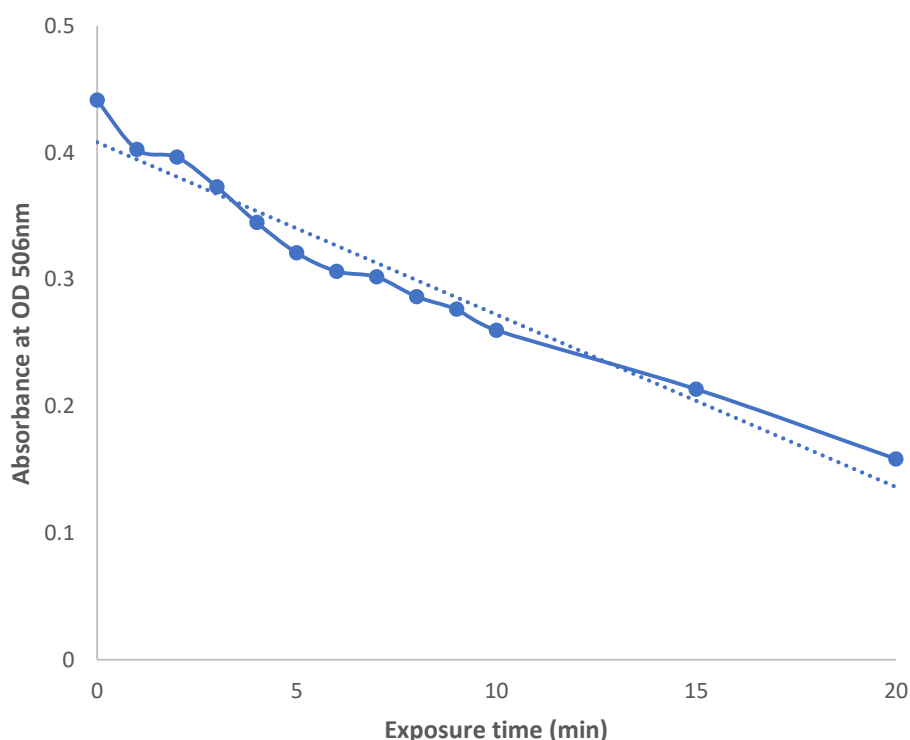
Figure 3.2 Absorbance degradation after blue light illumination. The singlet oxygen release of Compound 5 was monitored by absorbance reduction of TPCPD at 506 nm after excitation with blue light for 20 min. The half-life was reached after 15 min blue light exposure. Absorbance measurement was conducted three times, n=3.

The illuminated compounds were ranked according to the half-life or the percentage reduction in absorbance resultant from blue light illumination. It was assumed that the higher the actual reduction of absorption of TPCPD for the acridine compounds following blue light exposure, the greater their $^1O_2$ yield (Table 3.3). Twenty-one acridine compounds did not show a half-life except Compound 5, which has a half-life $t_{1/2}$ of 15 min. This data suggests that Compound 5 released the most singlet oxygen within the acridine compounds

tested. It was followed by Compounds 3 (43%), 17 (37%), 7 (24%) and 4 (27%), which showed a reduction in the percentage absorption (Table 3.3). Conversely, Compounds 19 and 20 did not show any measurable release of singlet oxygen following blue light illumination.

By measuring singlet oxygen release following excitation with blue light over a 60-minute period, it was noted that most singlet oxygen was released from candidate compounds after 20-minute blue light excitation.

Table 3.3 Compounds characterised according to the percentage reduction in absorbance or half-life obtained following 20 min blue light exposure. As the decrease of absorption of TPCPD at 506 nm is directly proportional to singlet oxygen release and the lower half-life the more singlet oxygen production. λmax is determined to be the wavelength at which absorbance is highest.

Compounds	λmax	Percentagereduction in absorbance in 20 min	Half-life (min)	Relative singlet oxygen
1	437	12%	83.33	1.00
2	440	11%	90.9	0.92
3	429	43%	23.25	3.58
4	442	16%	62.5	1.33
5	432	64%	15	5.33
6	426	13%	76.92	1.08
7	443	11%	90.9	0.92
8	444	26%	38.46	2.17
9	427	2%	500	0.17
10	431	8%	125	0.67
11	435	10%	100	0.83
12	441	6%	166.66	0.5
13	426	6%	166.66	0.5
14	424	6%	166.66	0.5
15	427	4%	250	0.33
16	433	9%	111.11	0.75
17	438	30%	33.33	2.5
18	445	10%	100	0.83
19	441	0%	No half-life	0
20	432	0%	No half-life	0
21	427	4%	250	0.33
22	426	7%	142.85	0.58

3.2.1.2 Radical species data

Due to the damaging effect of ROS released during PDT on microbes, radical species produced from the acridine compounds were then measured *in vitro.*

3.2.1.2.1 DPPH assay

The aim of this DPPH assay is to assess the antioxidant activity resultant from the candidate compounds during exposure to 60-minute blue light. DPPH· is reduced by free radical scavenger and the decrease in absorbance is monitored at 515 nm (Shimamura *et al.*, 2014).

The DPPH· 0.1 mM and 0.2 mM dissolved in DMSO was stable in the presence and absence of blue light as its absorbance was not degraded. However, its absorbance showed far greater degradation after the addition of acridine compounds in the presence and absence of blue light illumination.

After the compounds were added to DPPH·, they were exposed to blue light and then absorbance readings were taken. It has been demonstrated that the absorbance of the DPPH· was degraded directly after the addition of compounds. For example, the DPPH· absorbance was 1.6, which decreased dramatically to 0.045 when Compound 2 added at different points of concentration in the presence or absence of blue light. All the tested acridines caused dramatic degradation of the absorbance of DPPH· when added to it.

To investigate whether solvents can have effect on absorbance degradation of the marker DPPH when compound is mixed, different solvents were used to solubilise the compounds. The solvents tested were methanol, chloroform, acetone, isohexane and acetonitrile. In all cases, degradation of the maker was observed in the presence of the photosensitiser regardless of the availability of blue light.

3.2.1.2.2 ABTS assay

This method measures the antioxidant activity resultant from the candidate compounds during exposure to 60-minute blue light by determining the decolourisation of the ABTS· + through measuring the reduction of this radical cation as the percentage inhibition of absorbance at 734 nm (Miller *et al.*, 1997).

The ABTS assay was improved to prevent any possible effect on radical reduction. To achieve that, radical cation ABTS$^{\cdot+}$ was pre-generated before addition to the compounds, rather than the formation of the radical occurring continually in the presence of tested compounds (Re *et al.*, 1999).

Antioxidant activity was expressed using the total contribution to the antioxidant activity during 60-minute blue light exposure. The results in the presence of the compounds demonstrate that there was a drop in absorbance in the presence and absence of blue light, which means that the marker may be not stable when mixed with the acridines.

After the compounds were added to ABTS$^{\cdot+}$, they were exposed to blue light and then absorbance readings taken. It has been demonstrated that the absorbance of the ABTS$^{\cdot+}$ was degraded directly after the addition of acridines in the presence and absence of blue light. For example, the ABTS$^{\cdot+}$ absorbance was 1.3, which decreased markedly to 0.13 when the Compound 2 added at different points of concentration in the presence or absence of blue light.

3.2.2 Blue light alone has no effect on the growth of fungal and bacterial species

Based on previous data (Table 3.3), the λmax for all the acridine compounds was in the blue region between 426-445 nm. In order to determine the effect of the photoactivated compounds, exposure of fungal (*S. cerevisiae*, *C. albicans* and *A. fumigatus*) and bacterial cells (*S. aureus* and *E. coli)* to blue light alone was studied. The effect of blue light alone on growth was studied following exposure for 0, 10, 20, 30 and 60 min. As previously studied in photochemistry experiments (Section 3.2.1), the maximum level of singlet oxygen was released following 10 and 20-minute blue light exposure. Following 24 h incubation either the optical density was measured, or visual inspection of the plates was used to determine the level of microbial growth.

The experiment was conducted in triplicate, n=3, and the values expressed by the mean ±SEM. Two-way ANOVA analysis of results was used to test the degree to which untreated cells differ from cells treated with blue light.

ANOVA analysis of results, showed no significant effect of the *S. cerevisiae* and *C. albicans* cells treated with blue light in comparison with untreated cells after 24 h of treatment, as shown in Figures 3.3 and 3.4.

The percentage growth of blue light treated *A. fumigatus* did not change visually when compared to the untreated control (data not shown).
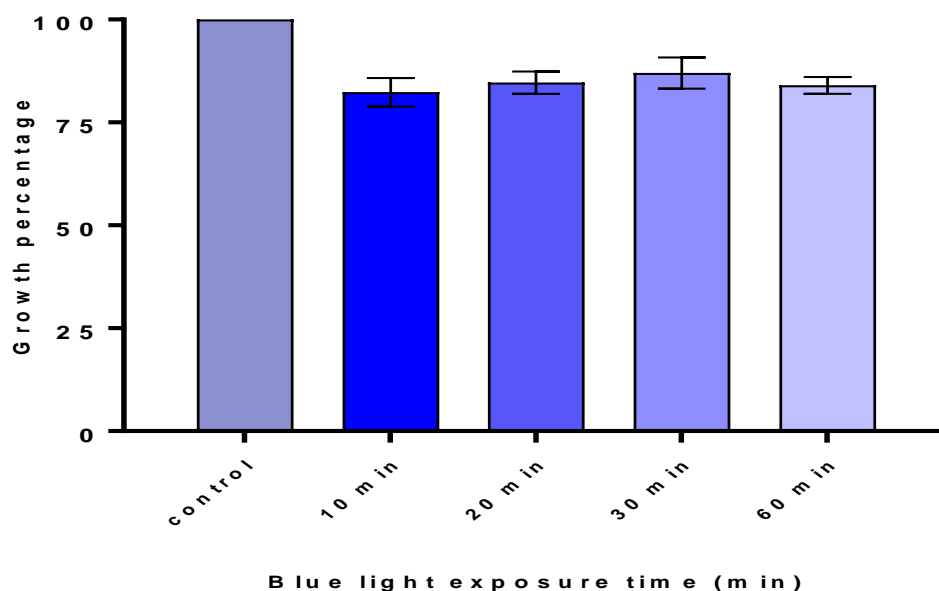
Figure 3.3 Blue light has no effect on the growth of *Saccharomyces cerevisiae*. 0.5-2.5 x 10^5 cells/ml (corresponding to approximately OD_{595} 0.002) of exponentially growing *S. cerevisiae* were inoculated in RPMI 1640 medium, exposed to blue light and incubated overnight at 30ºC without shaking. Optical density readings at the wavelength 530 nm were taken to measure the growth concentration of the growing cultures in 96-well plates in the absence and presence of blue light exposure over a period of 10, 20 and 60 min. *n*=3 (pooled from triplicate experiments). Values are the mean ±SEM. Data analysed by two-way ANOVA test.
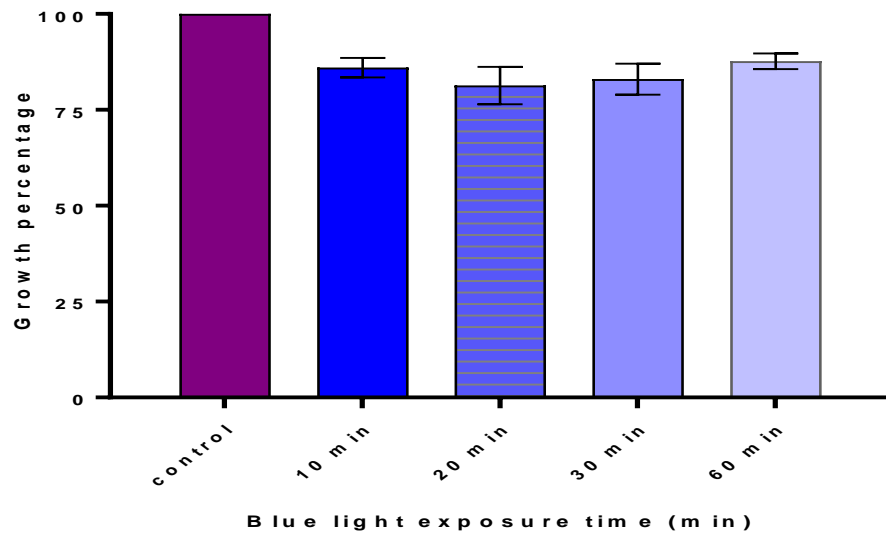
Figure 3.4 Blue light has no effect on the growth of _Candida albicans._ 0.5-2.5 x 10^5 cells/ml (corresponding to approximately OD_{595} 0.001) for _C. albicans_ were inoculated in RPMI 1640 medium, exposed to blue light and incubated overnight at 35ºC without shaking. Optical density readings at the wavelength 530 nm were taken to measure the growth concentration of the growing cultures in 96-well plates in the absence and presence of blue light exposure over a period of 10, 20, 30 and 60 min. _n_=3 (pooled from triplicate experiments). Values are the mean ±SEM. Data analysed by two-way ANOVA test.

ANOVA analysis of results, showed no significant effect of the bacterial cells treated with blue light in comparison with untreated cells after 24 h of treatment. As shown in Figures 3.5 and 3.6, the percentage growth of blue light treated _S. aureus_ and _E. coli_ strains did not change significantly when compared to the control (the standardised inoculum without blue light exposure).
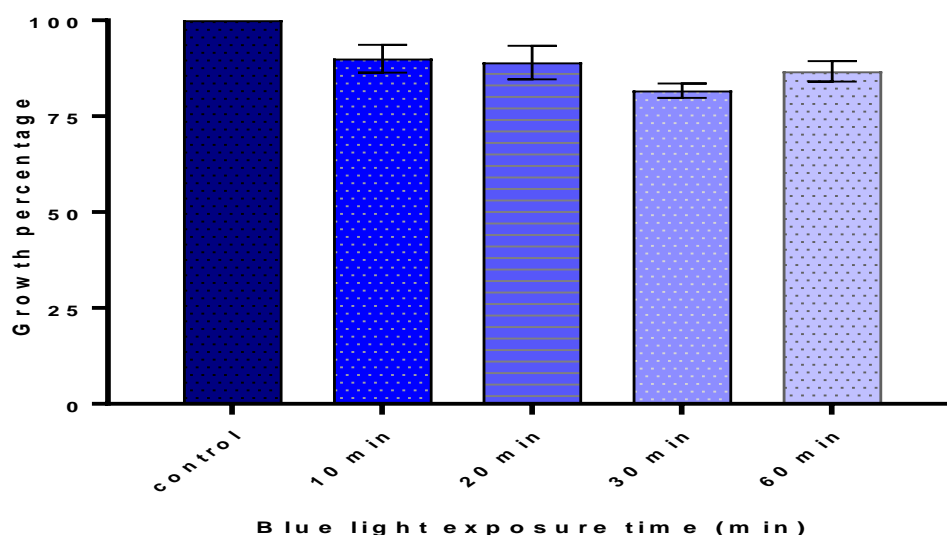
Figure 3.5 Blue light has no effect on the growth of *Staphylococcus aureus*. 5 x 10^5 cells/ml (corresponding to approximately OD_{600} 0.0003) for *S. aureus* were inoculated in Mueller-Hinton medium, exposed to blue light and incubated overnight at 35ºC without shaking. Optical density readings at the wavelength 600 nm were taken to measure the growth concentration of the growing cultures in 96-well plates in the absence and presence of blue light exposure over a period of 10, 20, 30 and 60 min. *n*=3 (pooled from triplicate experiments). Values are the mean ±SEM. Data analysed by two-way ANOVA test.
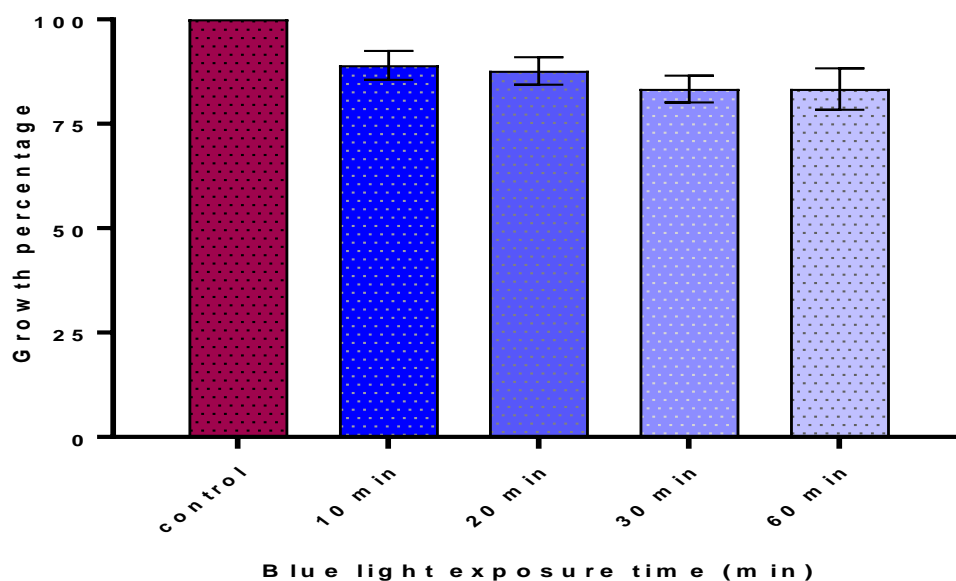
Figure 3.6 Blue light has no effect on the growth of *Escherichia coli*. 5 x 10^5 cells/ml (corresponding to approximately OD_{600} 0.0001) for *E. coli* were inoculated in Mueller-Hinton medium, exposed to blue light and incubated overnight at 35ºC without shaking. Optical density readings at the wavelength 600 nm were taken to measure the growth concentration of the growing cultures in 96-well plates in the absence and presence of blue light exposure over a period of 10, 20, 30 and 60 min. *n*=3 (pooled from triplicate experiments). Values are the mean ±SEM. Data analysed by two-way ANOVA test.

These results demonstrate that blue light did not inhibit the growth of the studied microbes significantly; therefore, the novel acridine compounds were then screened for photoantimicrobial activity.

3.2.3 Antifungal screening

Following photochemical characterisation of the compounds, they were then screened *in vitro* for their phototoxicity against a range of fungal species.

The 22 acridine compounds were screened using the EUCAST microbroth dilution method for antifungal activity against *S. cerevisiae, C. albicans* and *A. fumigatus* (EUCAST 7.3, 2015a; EUCAST 9.3, 2015b; Arendrup *et al.*, 2015). These species were exposed to a range of concentrations of the acridine compounds (0 to 250 µg/ml) in the presence and absence of blue light. Growth was determined by using OD at 530nm for *S. cerevisiae* and *C. albicans* and visually for *A. fumigatus.*

The heat maps shown in Figures 3.7 and 3.8 summarise the percentage growth determined from the OD_{530nm} readings for fungal growth for concentrations of fluconazole and compounds exposed to blue light for 20 min at 24 h incubation. The concentrations of fluconazole (control) used were 0 to 64 µg/ml, while concentrations of the compounds were 0 to 250 µg/ml. The colour in the heatmap indicates the percentage growth with black, indicating complete growth, and red, indicating no growth (100% inhibition). Yellow indicates 50% growth inhibition, which aligns with the minimal growth inhibition (MIC), as determined by the EUCAST method (EUCAST 7.3: Arendrup *et al.*, 2015a; Figures 3.7 and 3.8).
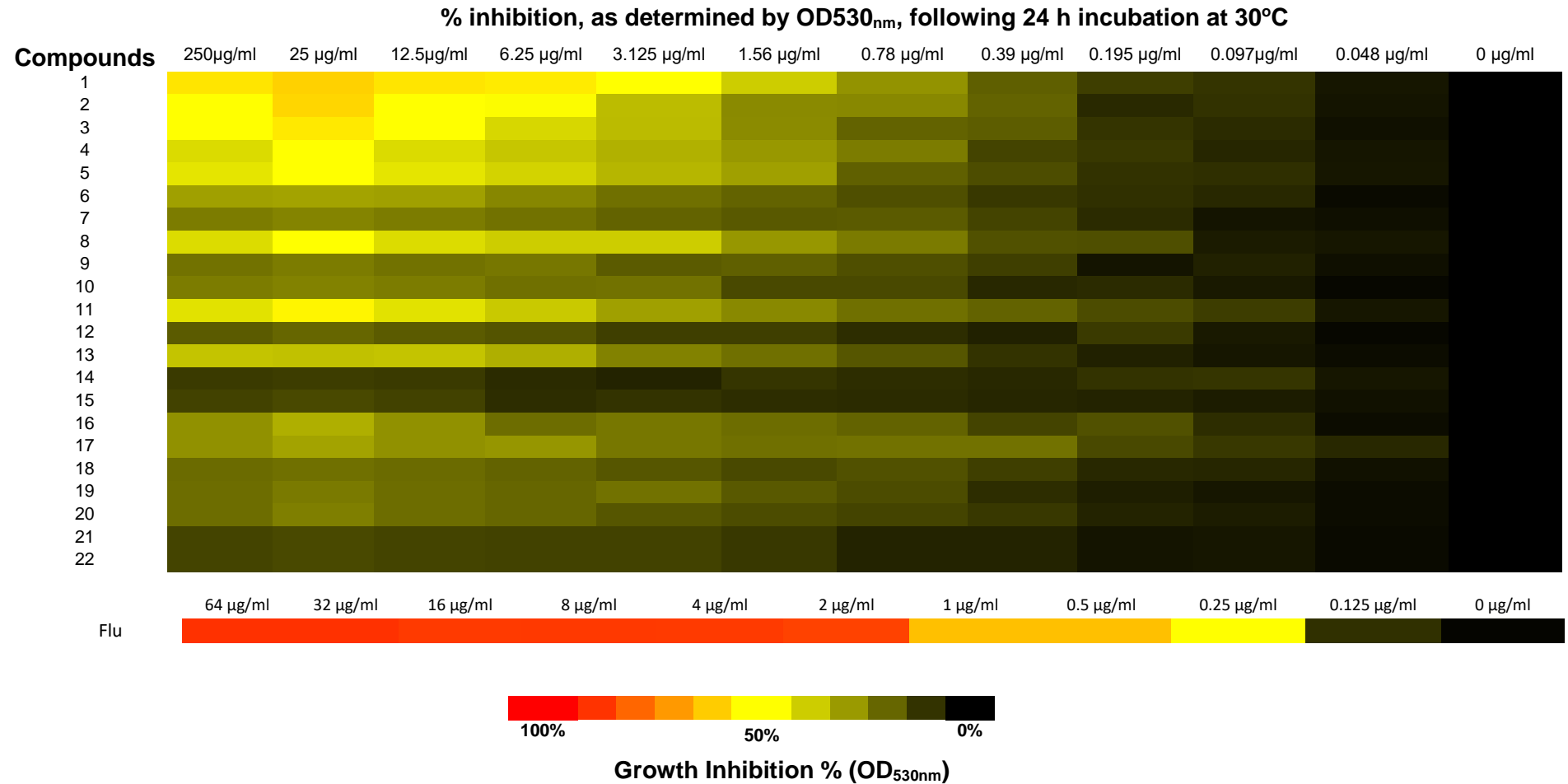
Figure 3.7 Heatmap illustrating OD$_{530nm}$ levels for varying concentrations of a list of 22 compounds (0 to 250 µg/ml) against *S. cerevisiae*. The yellow bar shows 50% growth inhibition while the red bar illustrates the maximum growth inhibition.
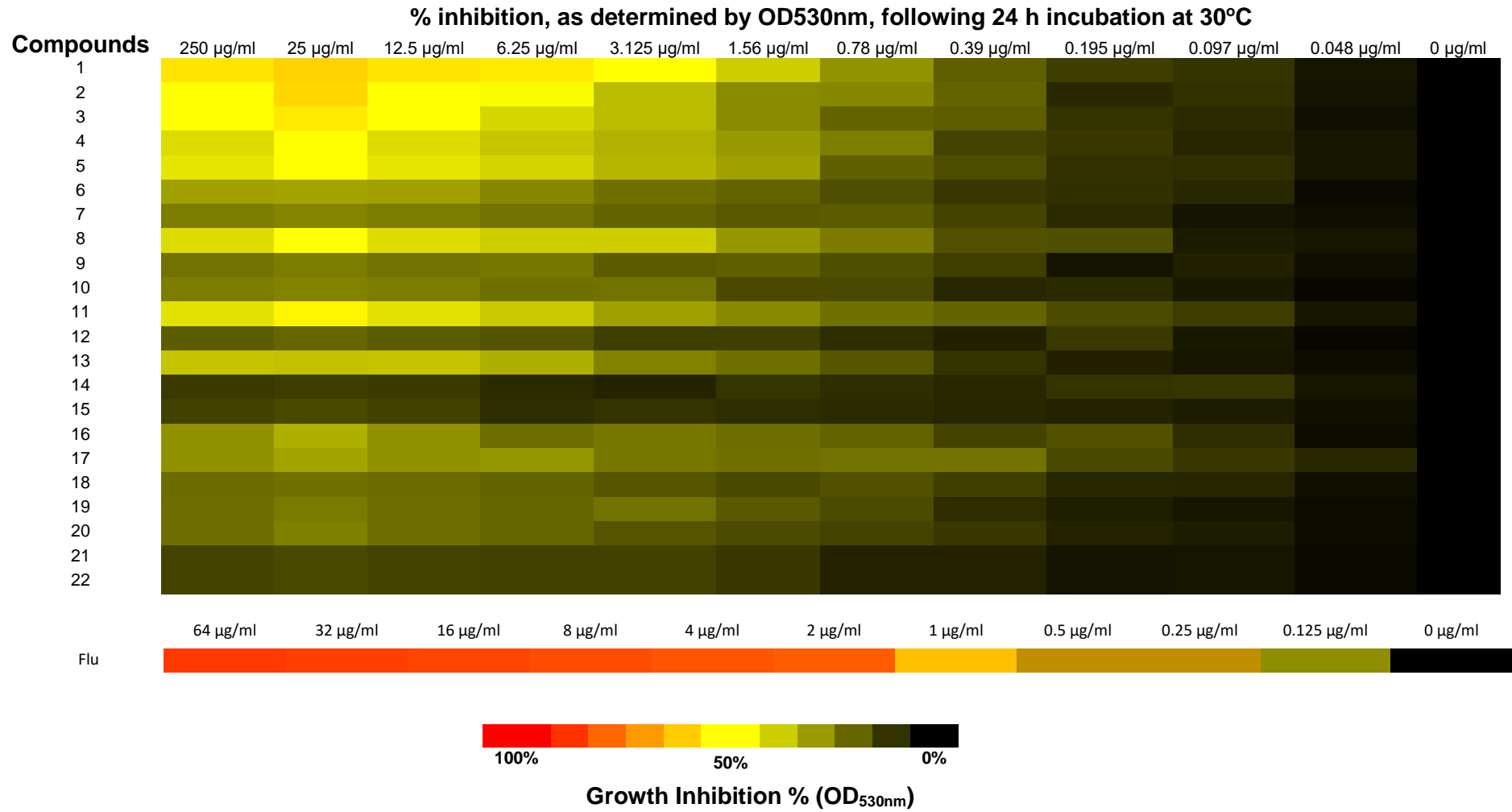
Figure 3.8 Heatmap illustrating OD$_{530nm}$ levels for varying concentrations of a list of 22 compounds (0 to250 µg/ml) against *C. albicans*. The yellow bar shows 50% growth inhibition while the red bar illustrates the maximum growth inhibition.

The EUCAST microdilution method was used to determine the susceptibility of studied fungi against a series of final concentrations of compounds of 0-250 µg/ml and fluconazole of 0.125-64 µg/ml and to identify the minimum inhibitory concentration MIC (50% growth inhibition compared to the control) of the tested compounds (EUCAST 7.3: Arendrup *et al.*, 2015a). To determine percentage growth inhibition, the optical density OD_{530nm} readings for *S. cerevisiae* and *C. albicans* growth were taken for each concentration of fluconazole and compounds exposed to blue light for 10 and 20 min at 24 h incubation.

The graphs show the mean ±SEM (standard error of the mean) of percent growth inhibition for the highest concentration of acridine compounds in the absence and presence of blue light, after 10 and 20-minute exposure and that for fluconazole at 64 (µg/ml) in *S. cerevisiae* and *C. albicans* (Figures 3.9 to 3.30). Table 3.4 shows the determined MIC (50% growth inhibition compared to the control) of each of the candidate compounds in *S. cerevisiae* and *C. albicans*. Fluconazole was utilised as a positive control in each of the studies. In all cases, growth inhibition of less than 17% was seen in the no blue light control. The experiments were repeated on two separate occasions in duplicate, except for the active compounds, which were repeated on three occasions in duplicate.
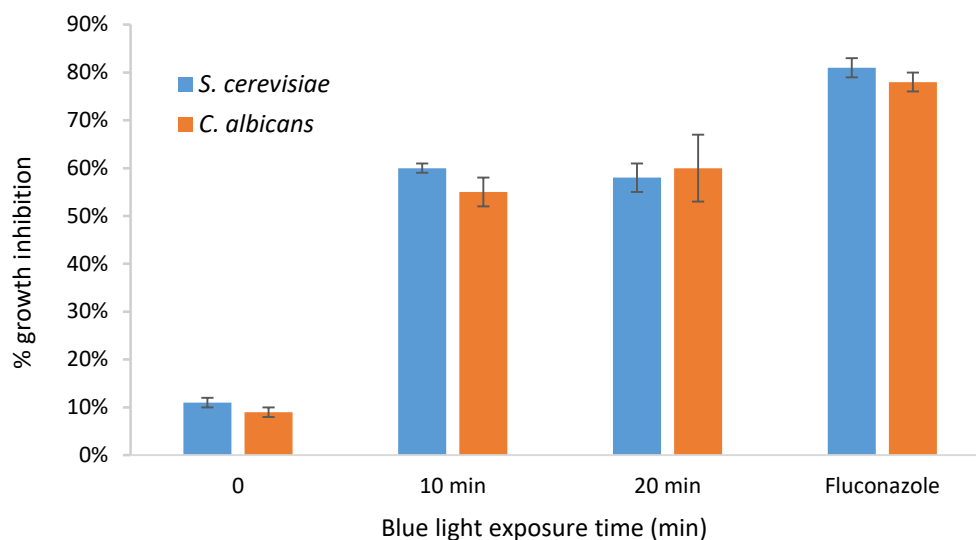
Figure 3.9 Percentage growth inhibition of *S. cerevisiae* and *C. albicans* with Compound 1 in absence and presence of blue light. Comparison of Compound 1 with fluconazole on both *S. cerevisiae* and *C. albicans* growth inhibition percentage obtained in the absence and presence of blue light. 0 means no blue light exposure. The experiment was conducted using EUCAST broth microdilution method and standardised inoculum of 0.5-2.5 x 10^5 cfu/ml. The experiment was conducted in duplicate, n=3. Values are the mean ±SEM.
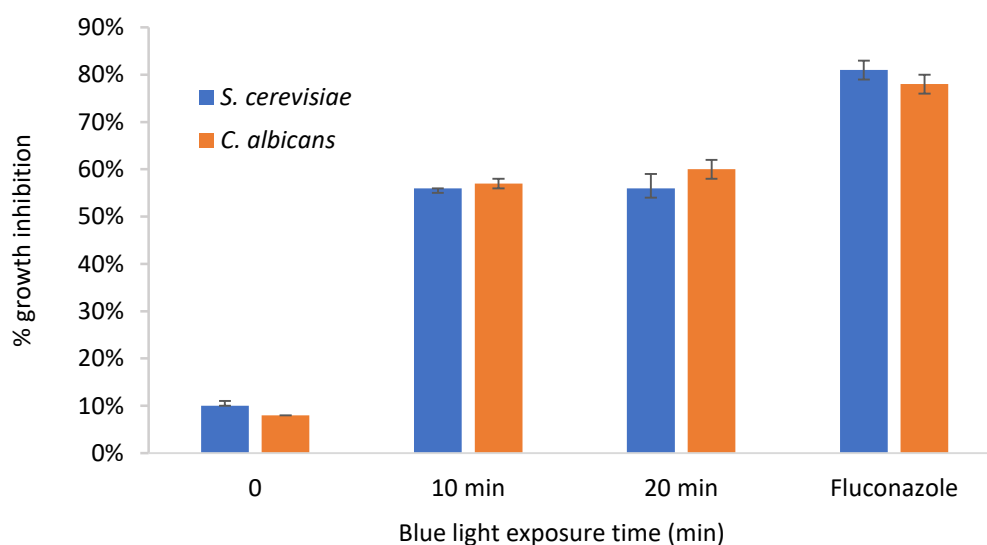
Figure 3.10 Percentage growth inhibition of *S. cerevisiae* and *C. albicans* with Compound 2 in absence and presence of blue light. Comparison of Compound 2 with fluconazole on both *S. cerevisiae* and *C. albicans* growth inhibition percentage obtained in the absence and presence of blue light. 0 means no blue light exposure. The experiment was conducted using EUCAST broth microdilution method and standardised inoculum of 0.5-2.5 x 10^5 cfu/ml. The experiment was conducted in duplicate, n=3. Values are the mean ±SEM.
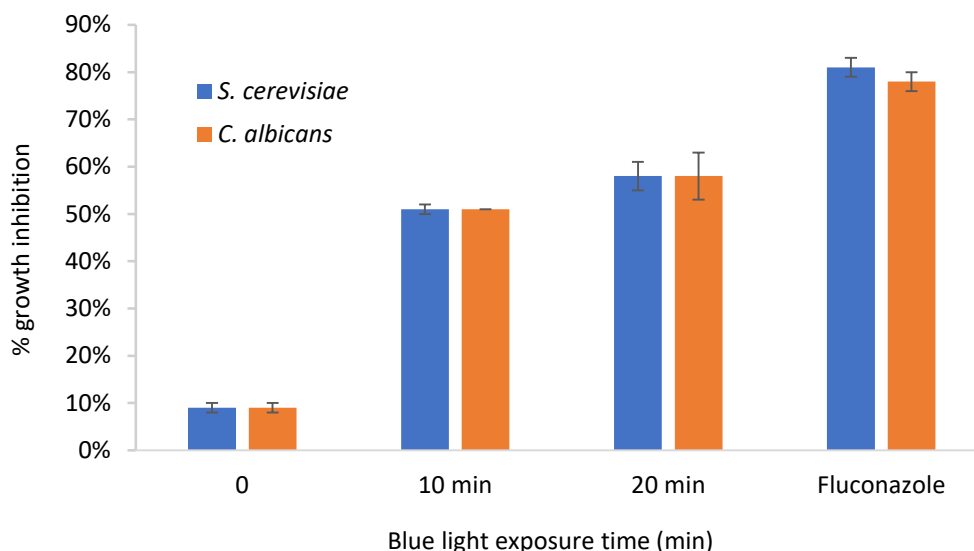
Figure 3.11 Percentage growth inhibition of *S. cerevisiae* and *C. albicans* with Compound 3 in absence and presence of blue light. Comparison of Compound 3 with fluconazole on both *S. cerevisiae* and *C. albicans* growth inhibition percentage obtained in the absence and presence of blue light. 0 means no blue light exposure. The experiment was conducted using EUCAST broth microdilution method and standardised inoculum of 0.5-2.5 x 10^5 cfu/ml. The experiment was conducted in duplicate, n=3. Values are the mean ±SEM.
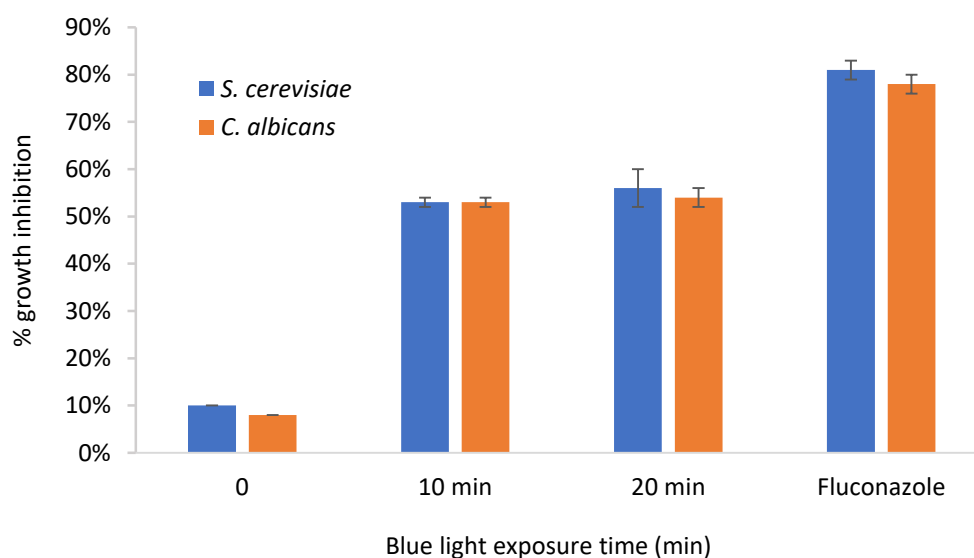
Figure 3.12 Percentage growth inhibition of *S. cerevisiae* and *C. albicans* with Compound 4 in absence and presence of blue light. Comparison of Compound 4 with fluconazole on both *S. cerevisiae* and *C. albicans* growth inhibition percentage obtained in the absence and presence of blue light. 0 means no blue light exposure. The experiment was conducted using EUCAST broth microdilution method and standardised inoculum of 0.5-2.5 x 10^5 cfu/ml. The experiment was conducted in duplicate, n=3. Values are the mean ±SEM.
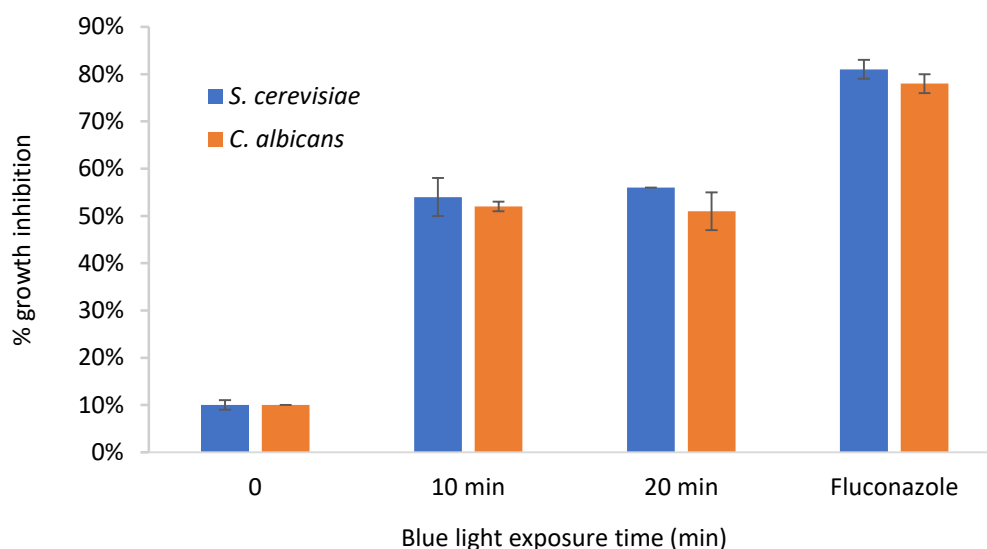
Figure 3.13 Percentage growth inhibition of *S. cerevisiae* and *C. albicans* with Compound 5 in absence and presence of blue light. Comparison of Compound 5 with fluconazole on both *S. cerevisiae* and *C. albicans* growth inhibition percentage obtained in the absence and presence of blue light. 0 means no blue light exposure. The experiment was conducted using EUCAST broth microdilution method and standardised inoculum of 0.5-2.5 x 10^5 cfu/ml. The experiment was conducted in duplicate, n=3. Values are the mean ±SEM.
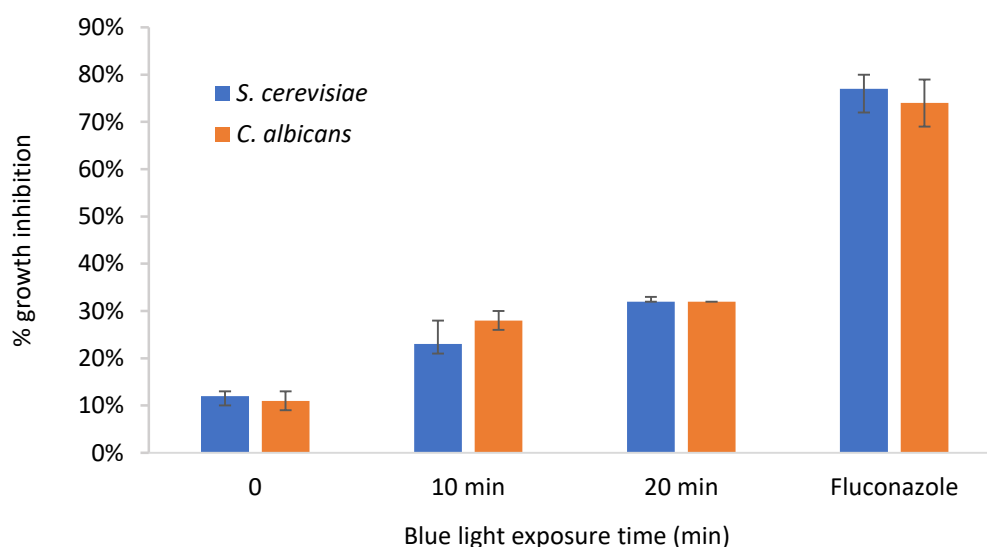
Figure 3.14 Percentage growth inhibition of *S. cerevisiae* and *C. albicans* with Compound 6 in absence and presence of blue light. Comparison of Compound 6 with fluconazole on both *S. cerevisiae* and *C. albicans* growth inhibition percentage obtained in the absence and presence of blue light. 0 means no blue light exposure. The experiment was conducted using EUCAST broth microdilution method and standardised inoculum of 0.5-2.5 x 10^5 cfu/ml. The experiment was conducted in duplicate, n=2. Values are the mean ±SEM.
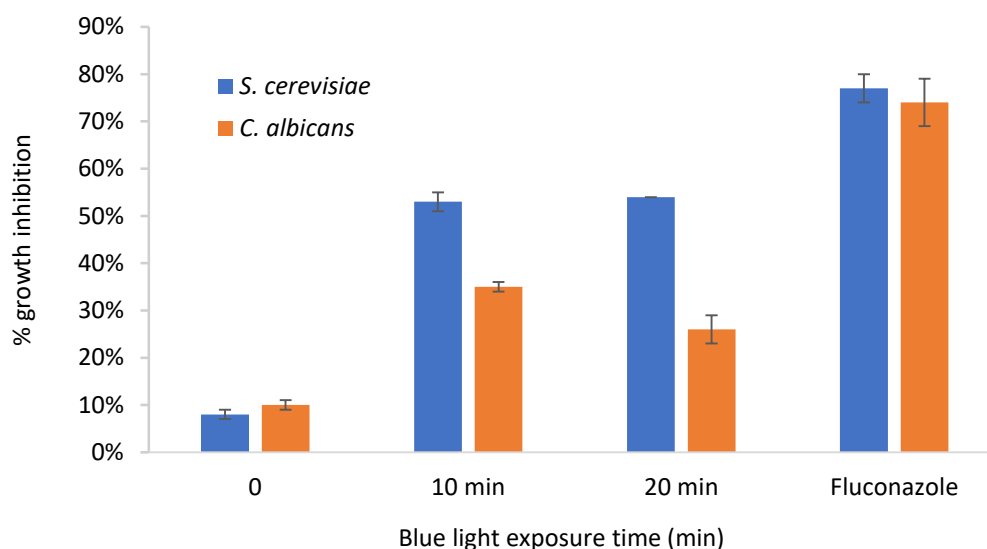
Figure 3.15 Percentage growth inhibition of *S. cerevisiae* and *C. albicans* with Compound 7 in absence and presence of blue light. Comparison of Compound 7 with fluconazole on both *S. cerevisiae* and *C. albicans* growth inhibition percentage obtained in the absence and presence of blue light. 0 means no blue light exposure. The experiment was conducted using EUCAST broth microdilution method and standardised inoculum of $0.5\text{-}2.5 \times 10^5$ cfu/ml. The experiment was conducted in duplicate, n=3. Values are the mean ±SEM.
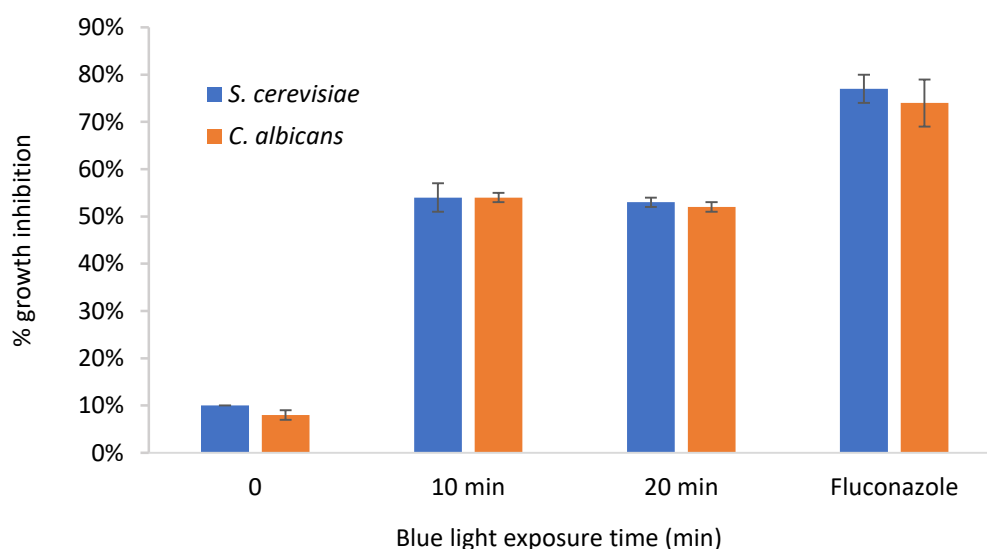
Figure 3.16 Percentage growth inhibition of *S. cerevisiae* and *C. albicans* with Compound 8 in absence and presence of blue light. Comparison of Compound 8 with fluconazole on both *S. cerevisiae* and *C. albicans* growth inhibition percentage obtained in the absence and presence of blue light. 0 means no blue light exposure. The experiment was conducted using EUCAST broth microdilution method and standardised inoculum of $0.5\text{-}2.5 \times 10^5$ cfu/ml. The experiment was conducted in duplicate, n=3. Values are the mean ±SEM.
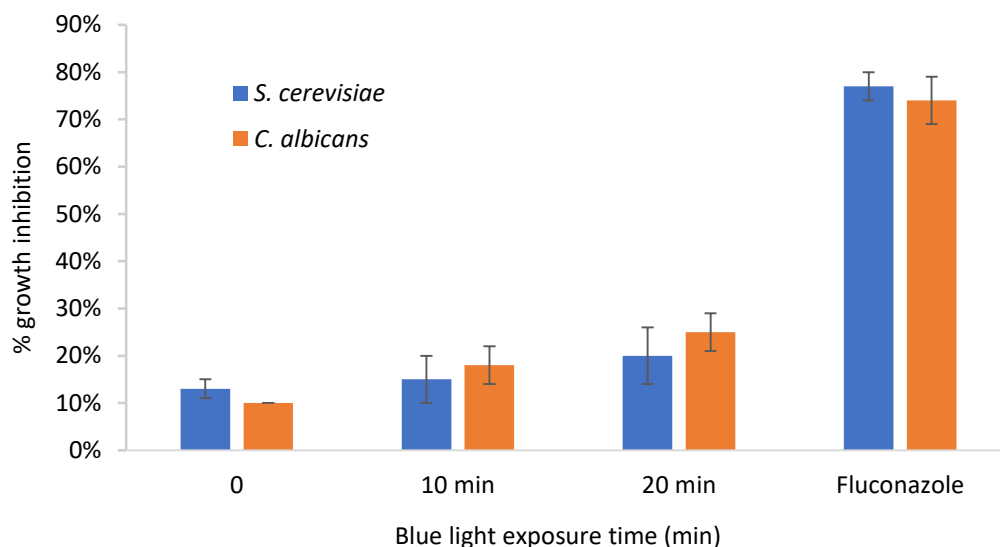
Figure 3.17 Percentage growth inhibition of *S. cerevisiae* and *C. albicans* with Compound 9 in absence and presence of blue light. Comparison of Compound 9 with fluconazole on both *S. cerevisiae* and *C. albicans* growth inhibition percentage obtained in the absence and presence of blue light. 0 means no blue light exposure. The experiment was conducted using EUCAST broth microdilution method and standardised inoculum of 0.5-2.5 x 10^5 cfu/ml. The experiment was conducted in duplicate, n=2. Values are the mean ±SEM.
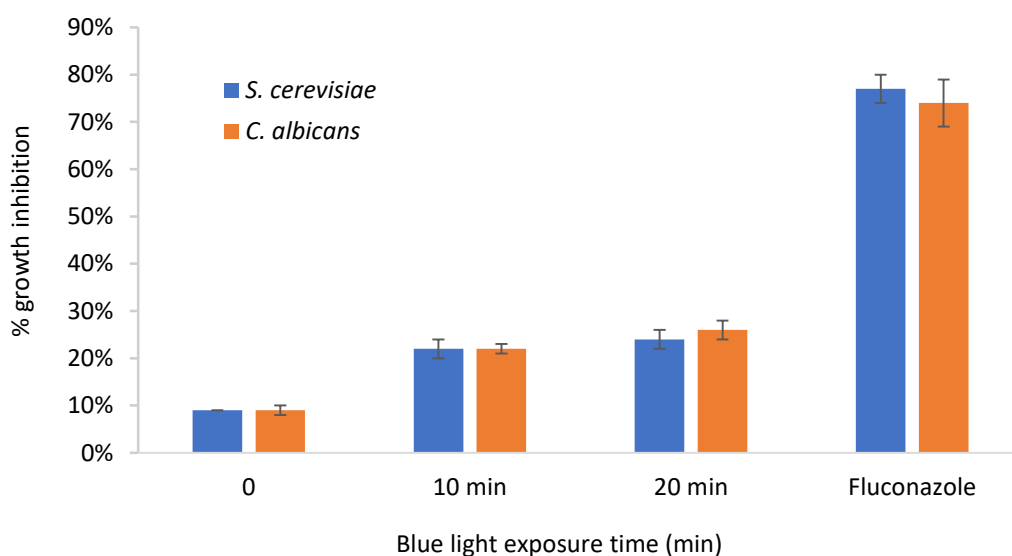
Figure 3.18 Percentage growth inhibition of *S. cerevisiae* and *C. albicans* with Compound 10 in absence and presence of blue light. Comparison of Compound 10 with fluconazole on both *S. cerevisiae* and *C. albicans* growth inhibition percentage obtained in the absence and presence of blue light. 0 means no blue light exposure. The experiment was conducted using EUCAST broth microdilution method and standardised inoculum of 0.5-2.5 x 10^5 cfu/ml. The experiment was conducted in duplicate, n=2. Values are the mean ±SEM.
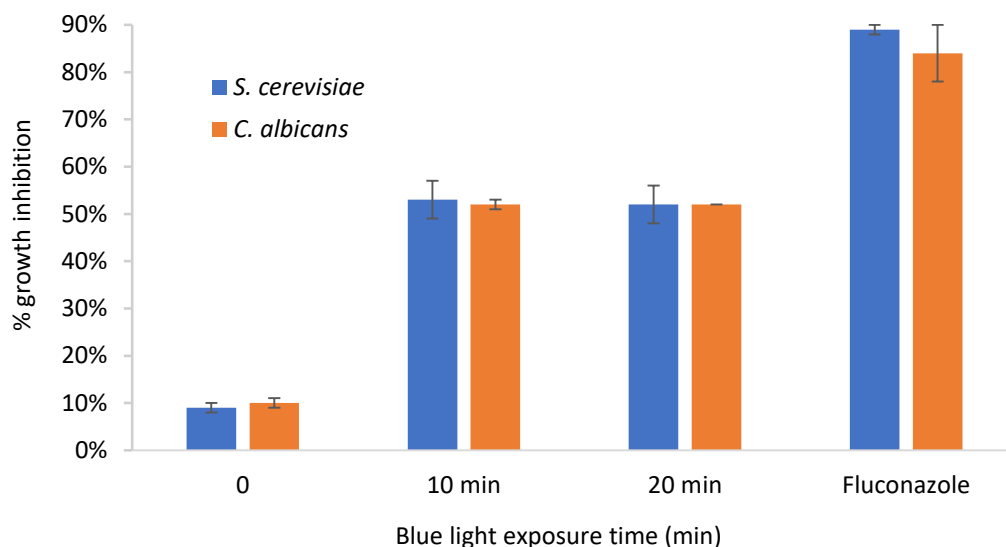
Figure 3.19 Percentage growth inhibition of *S. cerevisiae* and *C. albicans* with Compound 11 in absence and presence of blue light. Comparison of Compound 11 with fluconazole on both *S. cerevisiae* and *C. albicans* growth inhibition percentage obtained in the absence and presence of blue light. 0 means no blue light exposure. The experiment was conducted using EUCAST broth microdilution method and standardised inoculum of 0.5-2.5 x 10^5 cfu/ml. The experiment was conducted in duplicate, n=3. Values are the mean ±SEM.
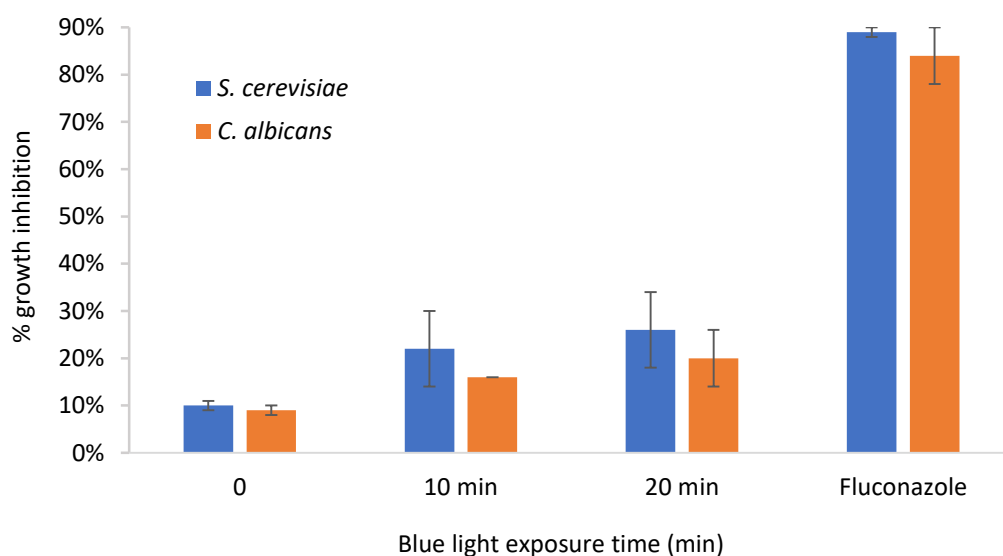
Figure 3.20 Percentage growth inhibition of *S. cerevisiae* and *C. albicans* with Compound 12 in absence and presence of blue light. Comparison of Compound 12 with fluconazole on both *S. cerevisiae* and *C. albicans* growth inhibition percentage obtained in the absence and presence of blue light. 0 means no blue light exposure. The experiment was conducted using EUCAST broth microdilution method and standardised inoculum of 0.5-2.5 x 10^5 cfu/ml. The experiment was conducted in duplicate, n=3. Values are the mean ±SEM.
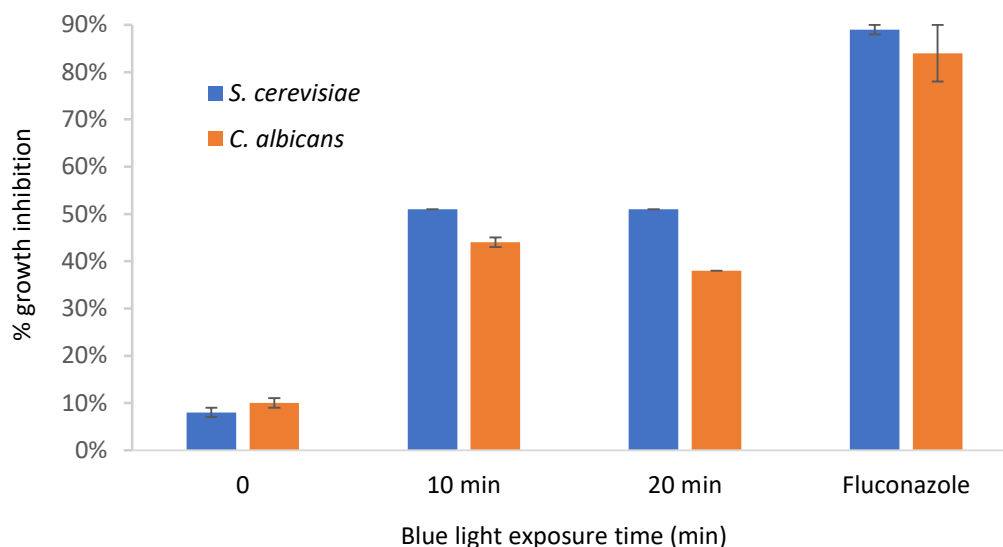
Figure 3.21 Percentage growth inhibition of *S. cerevisiae* and *C. albicans* with Compound 13 in absence and presence of blue light. Comparison of Compound 13 with fluconazole on both *S. cerevisiae* and *C. albicans* growth inhibition percentage obtained in the absence and presence of blue light. 0 means no blue light exposure. The experiment was conducted using EUCAST broth microdilution method and standardised inoculum of 0.5-2.5 x 10^5 cfu/ml. The experiment was conducted in duplicate, n=3. Values are the mean ±SEM.
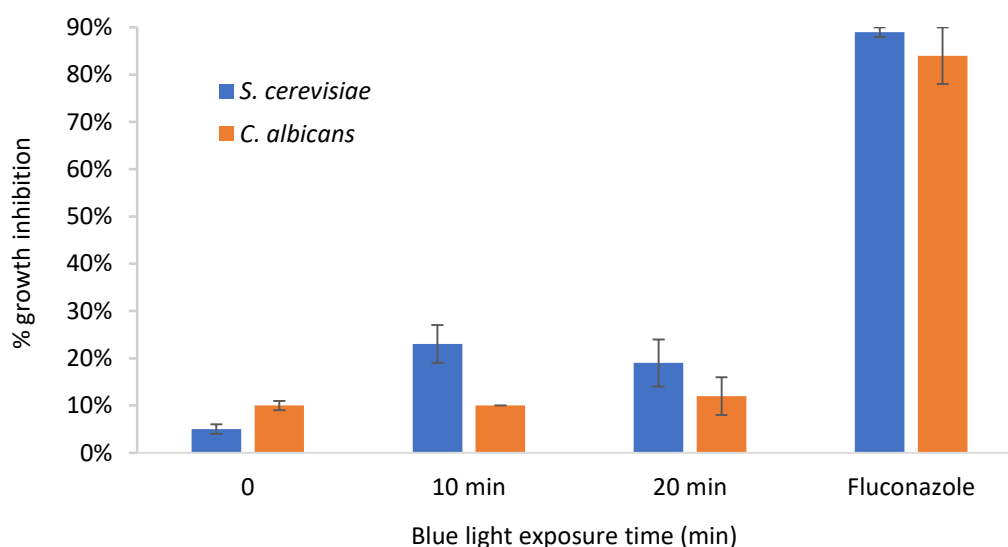
Figure 3.22 Percentage growth inhibition of *S. cerevisiae* and *C. albicans* with Compound 14 in absence and presence of blue light. Comparison of Compound 14 with fluconazole on both *S. cerevisiae* and *C. albicans* growth inhibition percentage obtained in the absence and presence of blue light. 0 means no blue light exposure. The experiment was conducted using EUCAST broth microdilution method and standardised inoculum of 0.5-2.5 x 10^5 cfu/ml. The experiment was conducted in duplicate, n=3. Values are the mean ±SEM.
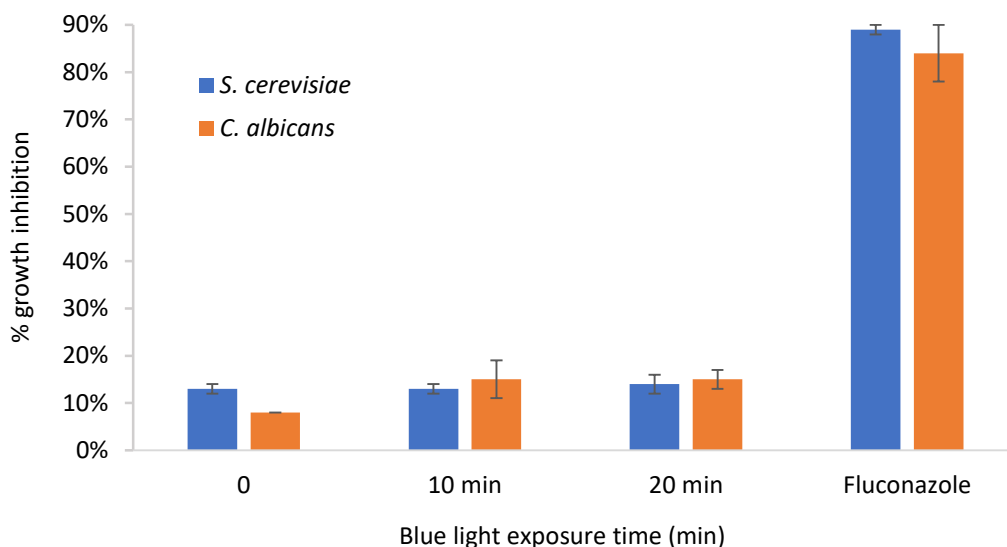
Figure 3.23 Percentage growth inhibition of *S. cerevisiae* and *C. albicans* with Compound 15 in absence and presence of blue light. Comparison of Compound 15 with fluconazole on both *S. cerevisiae* and *C. albicans* growth inhibition percentage obtained in the absence and presence of blue light. 0 means no blue light exposure. The experiment was conducted using EUCAST broth microdilution method and standardised inoculum of 0.5-2.5 x 10^5 cfu/ml. The experiment was conducted in duplicate, n=2. Values are the mean ±SEM.
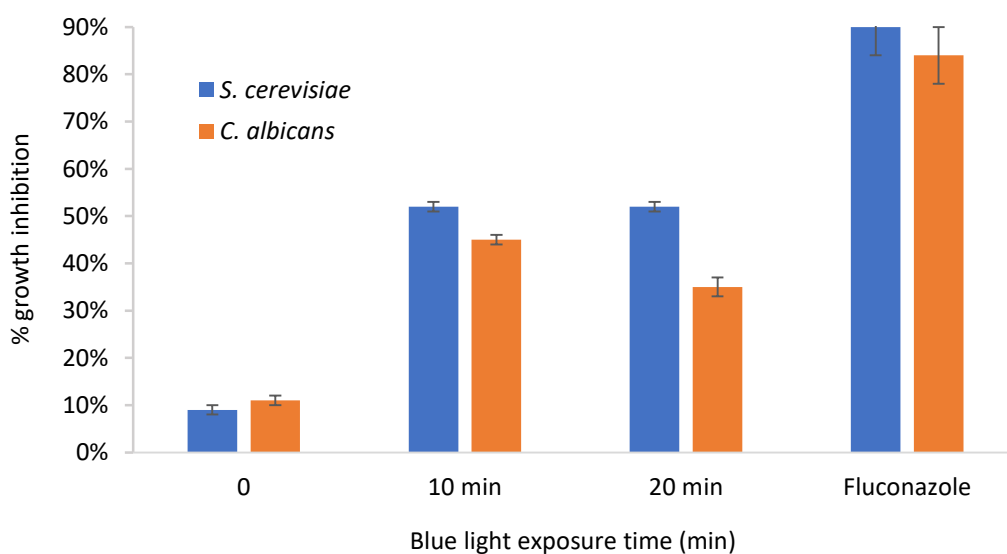
Figure 3.24 Percentage growth inhibition of *S. cerevisiae* and *C. albicans* with Compound 16 in absence and presence of blue light. Comparison of Compound 16 with fluconazole on both *S. cerevisiae* and *C. albicans* growth inhibition percentage obtained in the absence and presence of blue light. 0 means no blue light exposure. The experiment was conducted using EUCAST broth microdilution method and standardised inoculum of 0.5-2.5 x 10^5 cfu/ml. The experiment was conducted in duplicate, n=3. Values are the mean ±SEM.
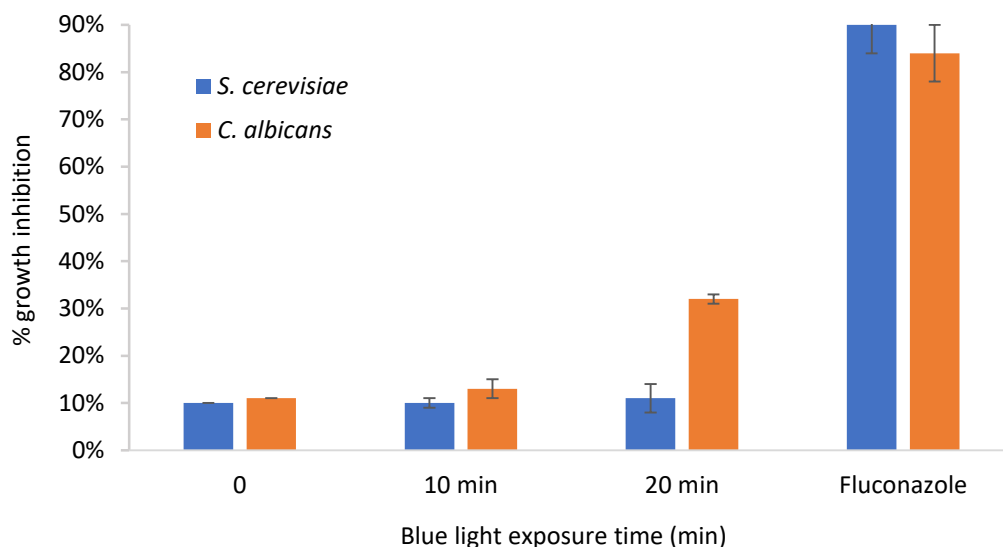
Figure 3.25 Percentage growth inhibition of *S. cerevisiae* and *C. albicans* with Compound 17 in absence and presence of blue light. Comparison of Compound 17 with fluconazole on both *S. cerevisiae* and *C. albicans* growth inhibition percentage obtained in the absence and presence of blue light. 0 means no blue light exposure. The experiment was conducted using EUCAST broth microdilution method and standardised inoculum of 0.5-2.5 x 10^5 cfu/ml. The experiment was conducted in duplicate, n=2. Values are the mean ±SEM.
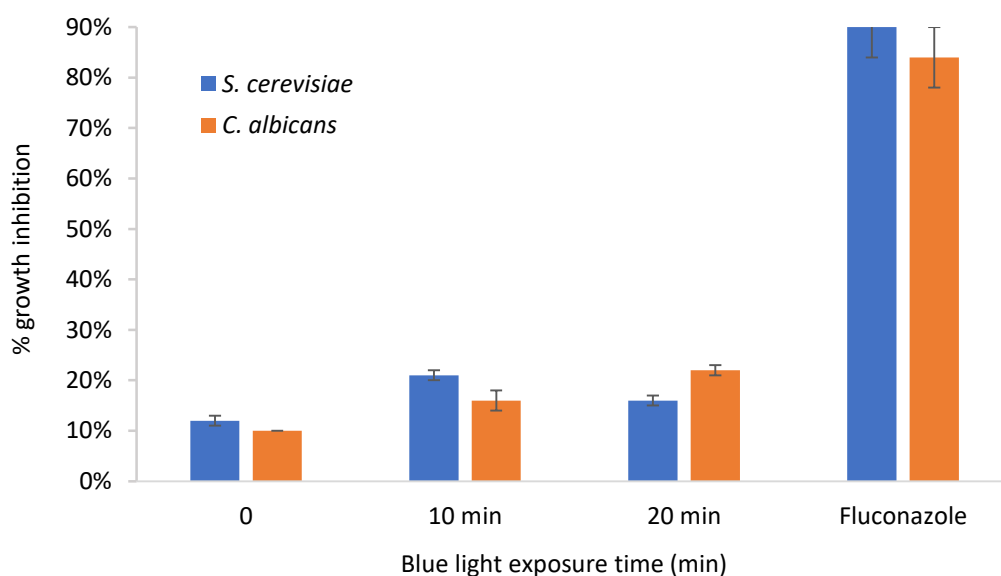
Figure 3.26 Percentage growth inhibition of *S. cerevisiae* and *C. albicans* with Compound 18 in absence and presence of blue light. Comparison of Compound 18 with fluconazole on both *S. cerevisiae* and *C. albicans* growth inhibition percentage obtained in the absence and presence of blue light. 0 means no blue light exposure. The experiment was conducted using EUCAST broth microdilution method and standardised inoculum of 0.5-2.5 x 10^5 cfu/ml. The experiment was conducted in duplicate, n=2. Values are the mean ±SEM.
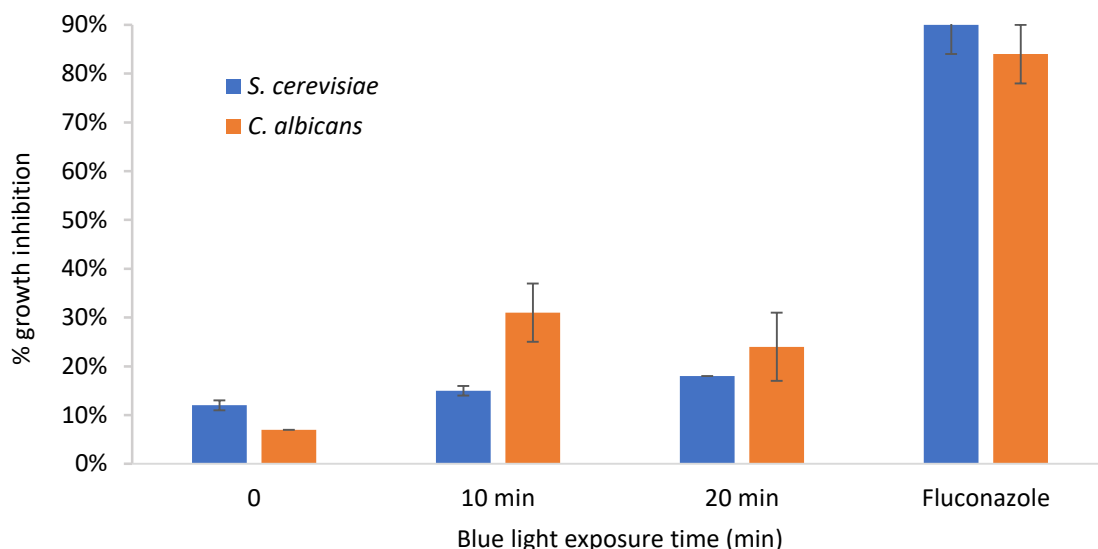
Figure 3.27 Percentage growth inhibition of *S. cerevisiae* and *C. albicans* with Compound 19 in absence and presence of blue light. Comparison of Compound 19 with fluconazole on both *S. cerevisiae* and *C. albicans* growth inhibition percentage obtained in the absence and presence of blue light. 0 means no blue light exposure. The experiment was conducted using EUCAST broth microdilution method and standardised inoculum of 0.5-2.5 x 10^5 cfu/ml. The experiment was conducted in duplicate, n=2. Values are the mean ±SEM.
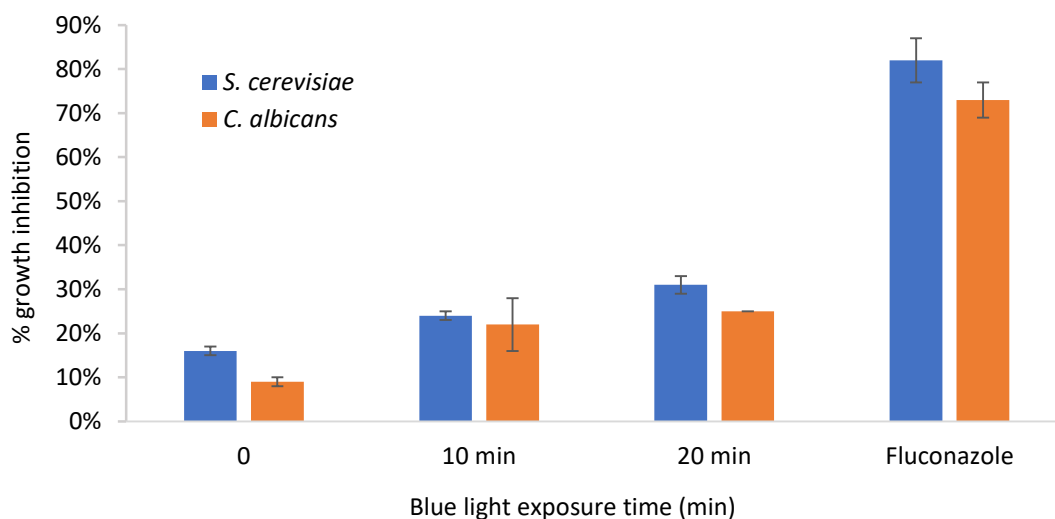
Figure 3.28 Percentage growth inhibition of *S. cerevisiae* and *C. albicans* with Compound 20 in absence and presence of blue light. Comparison of Compound 20 with fluconazole on both *S. cerevisiae* and *C. albicans* growth inhibition percentage obtained in the absence and presence of blue light. 0 means no blue light exposure. The experiment was conducted using EUCAST broth microdilution method and standardised inoculum of 0.5-2.5 x 10^5 cfu/ml. The experiment was conducted in duplicate, n=2. Values are the mean ±SEM.

71
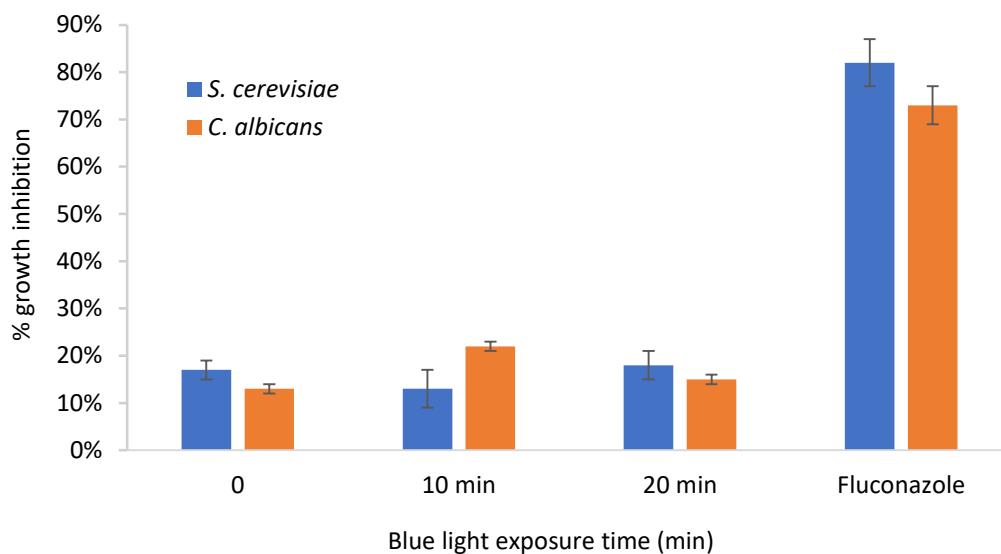
Figure 3.29 Percentage growth inhibition of *S. cerevisiae* and *C. albicans* with Compound 21 in absence and presence of blue light. Comparison of Compound 21 with fluconazole on both *S. cerevisiae* and *C. albicans* growth inhibition percentage obtained in the absence and presence of blue light. 0 means no blue light exposure. The experiment was conducted using EUCAST broth microdilution method and standardised inoculum of 0.5-2.5 x 10^5 cfu/ml. The experiment was conducted in duplicate, n=2. Values are the mean ±SEM.
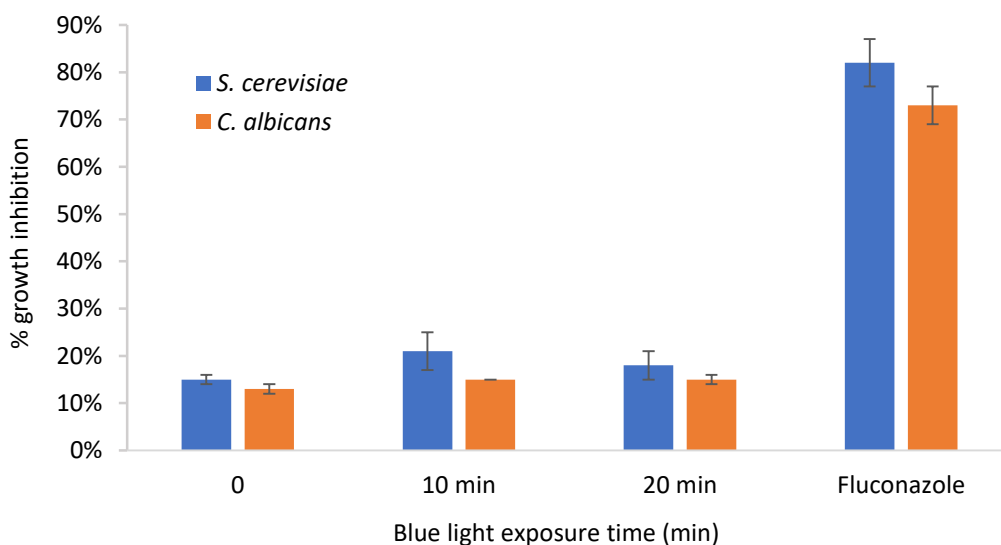
Figure 3.30 Percentage growth inhibition of *S. cerevisiae* and *C. albicans* with Compound 22 in absence and presence of blue light. Comparison of Compound 22 with fluconazole on both *S. cerevisiae* and *C. albicans* growth inhibition percentage obtained in the absence and presence of blue light. 0 means no blue light exposure. The experiment was conducted using EUCAST broth microdilution method and standardised inoculum of 0.5-2.5 x 10^5 cfu/ml. The experiment was conducted in duplicate, n=2. Values are the mean ±SEM.

Table 3.4 Summary of the minimum inhibitory concentrations (MICs) of the acridine compounds in *S. cerevisiae* and *C. albicans* using the EUCAST method after 10 and 20 min blue light exposure. MIC is the concentration at which 50% growth inhibition is seen. (-) means MIC value could not be determined at the maximum concentration tested (25 µg/ml). The rest of the candidate compounds did not show any minimum inhibitory concentrations against *S. cerevisiae* and *C. albicans* over both 10 and 20 min blue light exposure.

Studied compounds	Fungi			
	10 min blue light exposure		20 min blue light exposure	
	MIC (µg/ml) against *C. albicans*	MIC (µg/ml) against *S. cerevisiae*	MIC (µg/ml) against *C. albicans*	MIC (µg/ml) against *S. cerevisiae*
Fluconazole	1	0.25	1	0.25
Compound 1	4.2	4.2	4.2	4.2
Compound 2	8.3	5.2	8.3	5.2
Compound 3	21	21	25	12.5
Compound 4	25	25	25	25
Compound 5	21	21	21	21
Compound 6	-	-	-	-
Compound 7	-	25	-	12.5
Compound 8	25	25	25	25
Compound 9	-	-	-	-
Compound 10	-	-	-	-
Compound 11	25	25	25	12.5
Compound 12	-	-	-	-
Compound 13	-	25	-	25
Compound 14	-	-	-	-
Compound 15	-	-	-	-
Compound 16	-	25	-	25
Compound 17	-	-	-	-
Compound 18	-	-	-	-
Compound 19	-	-	-	-
Compound 20	-	-	-	-
Compound 21	-	-	-	-
Compound 22	-	-	-	-

To ensure consistency of the results, EUCAST antifungal susceptibility testing of *S. cerevisiae* and *C. albicans* to the control fluconazole was performed. The average MIC of fluconazole obtained was 0.25 µg/ml against *S. cerevisiae* and 1 µg/ml against *C. albicans*. Regarding *S. cerevisiae*, the obtained MIC of 0.25 µg/ml was in the region of published data (MIC and zone distributions and ECOFFs) (EUCAST 7.3: Arendrup *et al.*, 2015a). The resultant MIC of 1 µg/ml against *C. albicans* corresponded with the EUCAST Antifungal Clinical Breakpoints (EUCAST 7.3: Arendrup *et al.*, 2015a).

Furthermore, none of the compounds exhibited a significant antifungal effect in the absence of blue light against both strains. As the acridine compounds showed no significant effect on growth of cells in the absence of blue light, any antifungal activity will be attributed to blue light treated compounds.

A lower MIC value suggests that a lower concentration of drug is required for inhibiting growth of microbes, therefore the lower the MIC, the more effective the antimicrobial drug. By analysing the MIC results in Table 3.4, it can be noted that Compound 1 showed more effectiveness than other compounds with MICs of 4.2 µg/ml over 10 and 20 min against *C. albicans* and *S. cerevisiae*. It was followed by Compound 2, which showed MICs of 8.3 and 5.2 µg/ml over 10 and 20 min, respectively against *C. albicans* and *S. cerevisiae*. The data demonstrates that, amongst all the screened compounds, Compound 1 and Compound 2 showed the lowest MIC, and were determined to be the most potent. Furthermore, none of the drugs showed a lower MIC than that of fluconazole. The results of photoactivated acridines in the presence of blue light against *S. cerevisiae* and *C. albicans* were significantly different from those of non-light acridines.

Compounds 7, 13 and 16 exhibited antifungal activity against *S. cerevisiae* but demonstrated no effect on *C. albicans* at the maximum concentration tested. The remaining seven compounds showed a similar trend in activity against both species, except of *S. cerevisiae* being more susceptible to fluconazole, Compound 2, Compound 3 and Compound 11 compared *to C. albicans* (Table 3.4)*.*

A. fumigatus was also screened using EUCAST antifungal MIC microdilution method for moulds. Due to the growth of *A. fumigatus*, instead of measuring the

optical density to determine percentage growth inhibition, a visual inspection was undertaken (EUCAST 9.3: Arendrup *et al.*, 2015b). In this case, the MIC was determined to be the first well where the concentration of compound resulted in complete absence of growth. The concentration range tested for the control drug amphotericin B was 0-16 µg/ml. The control drug amphotericin B used in the EUCAST method was effective against *A. fumigatus* showing MIC of 0.125 µg/ml, which was matching the MIC EUCAST breakpoint in *A. fumigatus* (EUCAST 9.3: Arendrup *et al.*, 2015b) The antifungal screening demonstrated that acridines, following exposure to blue light, did not exhibit any efficacy against *A. fumigatus* at the concentrations tested (0 to 250 µg/ml) by checking the growth visually.

The first row of Figure 3.31 illustrates the complete growth inhibition of amphotericin B starting from well number 8 (0.125 µg/ml), while the rest of the rows illustrate the complete growth of *A. fumigatus* in the presence of Compounds 1 and 2 exposed to blue light.
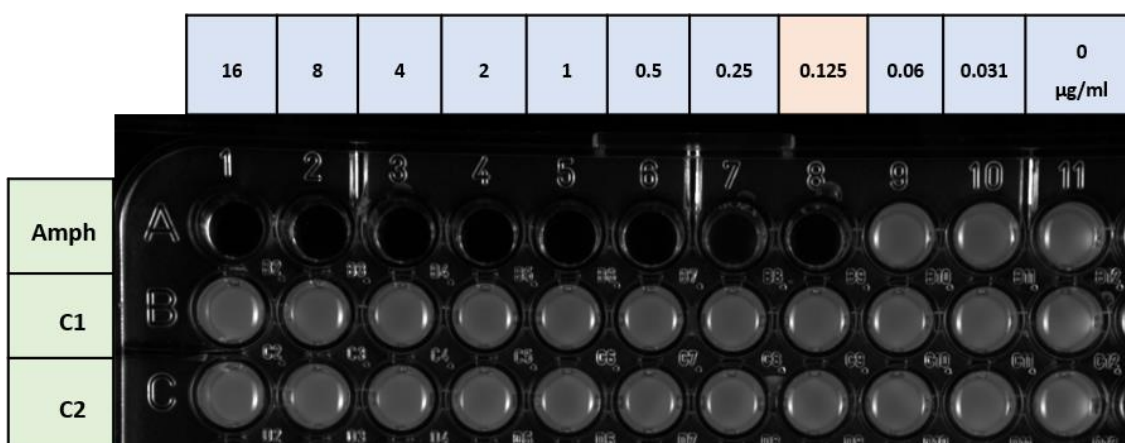
Figure 3.31 Comparing the effect of amphotericin B in the first row and photosensitisers in the next two rows against *A. fumigatus*. Amphotericin B showed MIC of 0.125 µg/ml while no acridine compound showed MIC against *A. fumigatus.* The experiment was conducted using EUCAST broth microdilution method and standardised inoculum of 0.5-2.5 x 10^5 cfu/ml. The MIC value considered as the concentration of compound providing no visible growth by eye.

3.2.4 Antibacterial screening

Following antifungal screening of the compounds, the compounds were then screened *in vitro* for their antibacterial effectiveness under blue light exposure against two clinically important bacteria, Gram-positive *S. aureus* and Gram-negative *E. coli*.

The acridine compounds were screened using the European Committee for Antimicrobial Susceptibility Testing (EUCAST) microbroth dilution method, for antibacterial activity (EUCAST 5.1; EUCAST, 2003). The antibacterial drug, gentamicin, was used as a control due to its broad antibacterial activity against both Gram-negative and Gram-positive bacteria. The bacterial species were exposed to a range of concentrations of the compounds (0 to 256 µg/ml) in the presence and absence of blue light. A 20-minute illumination period was used, due to the release of most singlet oxygen from the compounds. The MIC was determined, by visual inspection, to be the lowest concentration that completely inhibited growth. Data of MIC of compounds and fluconazole against *S. aureus* and *E. coli* are shown as means of two separate occasions in duplicate, except for the active compounds, which were repeated on three occasions in duplicate (Table 3.5).

Table 3.5 Summary of the minimum inhibitory concentrations (MICs) of the acridine compounds in *S. aureus* and *E. coli* using the EUCAST method after 10 and 20 min blue light exposure. (-) means MIC value could not be determined at the maximum concentration tested. The rest of the candidate compounds did not show any minimum inhibitory concentrations against *S. aureus* and *E. coli* over 10 and 20 min blue light exposure.

Studied compounds	Bacteria			
	10 min blue light exposure		20 min blue light exposure	
	MIC (µg/ml) against *S. aureus*	MIC (µg/ml) against *E. coli*	MIC (µg/ml) against *S. aureus*	MIC (µg/ml) against *E. coli*
Gentamicin	0.25	0.125	0.25	0.125
Compound 1	2	16	2	24
Compound 2	8	32	8	24
Compound 3	24	-	24	32
Compound 4	32	-	16	-
Compound 5	8	-	8	24
Compound 6	-	-	-	-
Compound 7	24	-	24	-
Compound 8	32	-	32	32
Compound 9	-	-	-	-
Compound 10	-	-	-	-
Compound 11	8	32	8	24
Compound 12	16	32	8	32
Compound 13	8	-	32	32
Compound 14	24	-	24	-
Compound 15	-	-	-	-
Compound 16	8	32	8	32
Compound 17	32	-	24	-
Compound 18	-	-	-	-
Compound 19	-	-	-	-
Compound 20	-	-	-	-
Compound 21	-	-	-	-
Compound 22	-	-	-	-

EUCAST antibacterial susceptibility testing of *S. aureus* and *E. coli* to the control gentamicin was performed and the resultant MICs of 0.25 and 0.125 µg/ml corresponded with EUCAST Antibacterial Clinical Breakpoints (EUCAST 5.1: EUCAST, 2003), which confirms the accuracy of the assay. Since the acridine compounds showed no remarkable visual effect on growth in the absence of blue light, any growth inhibition observed following the exposure to blue light is attributed to photoactivation of the compounds.

A lower MIC value is indicative that a lower concentration of drug is required for inhibiting growth of bacteria, therefore the lower MIC the more effective the antibacterial activity. By analysing the MIC results (Table 3.5) nine acridine compounds showed little effect on bacterial growth. Compound 1 and Compound 2 showed the lowest MICs of all the compounds tested with 2 and 8 µg/ml respectively, against *S. aureus* and the same MIC of 24 µg/ml against *E. coli*. Compounds 4, 7, 14 and 17 only exhibited an effect following 20-minute blue light exposure against *S. aureus* but not against *E. coli*. This suggests that the Gram-positive bacteria, *S. aureus*, is more sensitive to the activated compounds as compared to the Gram-negative bacteria, *E. coli* (Table 3.5).

By combining the MIC values of the acridine compounds against bacterial and fungal species following 20-minute blue light illumination in Table 3.6, it can be noted that there is a marked difference in the sensitivity of fungi and bacteria to the light activated acridine compounds. Compounds 12, 14 and 17, for instance, showed only antibacterial activity without any antifungal effect (Table 3.6).

Table 3.6 Summary of the minimum inhibitory concentrations (MICs) of the candidate compounds in *S. cerevisiae*, *C. albicans* and *S. aureus*, *E. coli* using the EUCAST method after 20 min blue light exposure. (-) means MIC value could not be determined at the maximum concentration tested.

Studied compounds	20 min blue light exposure		20 min blue light exposure	
	MIC (µg/ml) against *C. albicans*	MIC (µg/ml) against *S. cerevisiae*	MIC (µg/ml) against *S. aureus*	MIC (µg/ml) against *E. coli*
Fluconazole	1	0.25		
Gentamicin			0.25	0.125
Compound 1	4.2	4.2	2	24
Compound 2	8.3	5.2	8	24
Compound 3	25	12.5	24	32
Compound 4	25	25	16	-
Compound 5	21	21	8	24
Compound 6	-	-	-	-
Compound 7	-	12.5	24	-
Compound 8	25	25	32	32
Compound 9	-	-	-	-
Compound 10	-	-	-	-
Compound 11	25	12.5	8	24
Compound 12	-	-	8	32
Compound 13	-	25	32	32
Compound 14	-	-	24	-
Compound 15	-	-	-	-
Compound 16	-	25	8	32
Compound 17	-	-	24	-
Compound 18	-	-	-	-
Compound 19	-	-	-	-
Compound 20	-	-	-	-
Compound 21	-	-	-	-
Compound 22	-	-	-	-

3.3 Discussion

In this chapter, the aim was to investigate a series of novel synthesised acridine compounds for their possible use as antimicrobial photodynamic agents. Photochemical characterisation and antimicrobial investigations were carried out on these acridine compounds, in the absence and presence of blue light. Their antimicrobial activity was assessed against a range of clinically important fungi (*S. cerevisiae, C. albicans* and *A. fumigatus*) and bacteria (*S. aureus* and *E. coli*) using the European Committee for Antimicrobial Susceptibility Testing (EUCAST) method (EUCAST 5.1: EUCAST, 2003).

To identify the visible light source required to photoactivate the acridines, the absorption spectrum between the wavelengths 250-800 nm was taken. The wavelength of maximum absorbance, λmax, was then determined for each of the compounds tested to choose the corresponding visible region. It has been demonstrated that λmax of the acridine compounds ranges between 424-445 nm, which corresponds with the blue light region (400-500 nm) (Table 3.3). The obtained values are consistent with other published acridines, which generally show their λmax in the range between 400-500 nm (Albert, 1951).

The absorption of acridine-based compounds may be extended into the red or near infrared regions by utilising the acidic carbon functionality of 9-methyl quaternary acridines to produce styryl derivatives (Wainwright, 2015). It has been demonstrated that the selection of red wavelength in antimicrobial photodynamic therapy leads to significant reduction in adverse effects when compared to UV and blue light, which can lead to DNA cleavage and thus cause greater toxicity to mammalian cells (Bumah *et al.*, 2017). Additionally, longer wavelength such as red and infrared have the ability to penetrate more deeply in tissues than UV and blue light, which allows their use in surgery and dentistry applications (Jin *et al.*, 2010; Hill *et al.*, 2014). However, limited work has been published on the photosensitising and photoantimicrobial activity of those acridine compounds absorbing in red or infrared light. In this study all the tested compounds absorb strongly in the blue light region. This method has not been done with any of the compounds used in this study, which absorbed strongly in the blue light region.

3.3.1 Acridines are photosensitised following exposure to blue light and release singlet oxygen

Due to the well-characterised photosensitising activity of a variety of acridine compounds such as euflavine, proflavine and acridine orange (Iwamoto *et al.*, 1993; Iwamoto *et al.*, 1987), set of novel synthesised acridines has been characterised photochemically in the present study.

The photochemical reactions of the triplet state of photosensitisers such as acridines following blue light exposure can be divided into two different pathways, either the Type 1 mechanism involving electron transfer reaction from the PS to O_2 and results in $O_2^{\cdot-}$, H_2O_2 and $\cdot OH$, or the Type 2 mechanism involving energy transfer to O_2 and form $^1O_2$. It has been demonstrated that the most prevalent damaging ROS are $\cdot OH$ and $^1O_2$, which have the ability to react with many molecules in microbial cells (Vatansever *et al.*, 2013). Therefore, this present study has studied both $\cdot OH$ and $^1O_2$ species and attempted to quantify them following activation by blue light over a 60-minute period. Within this study, a radical scavenging assay using DPPH, a stabilised radical, was used to assess the amount of radical species produced from blue light treated acridines by monitoring the absorbance at 517 nm (Brand-Williams *et al.*, 1995). Although DPPH$\cdot$ showed stability in the solvent used, DMSO, it demonstrated instability following the addition of acridine compounds in the presence and absence of blue light. This is indicative of degradation of DPPH$\cdot$ when mixing with acridines. Following failure to measure the radical using DPPH$\cdot$, another popular radical scavenging assay was conducted using the ABTS radical. This ABTS method has extra flexibility, as it can be used at different pH levels (unlike DPPH, which is sensitive to acidic pH). Furthermore, ABTS$^{\cdot+}$ is pre-generated directly in a stable form prior to the addition of acridines, while DPPH$\cdot$ is ready to use free radical. Following generation of ABTS$^{\cdot+}$, it is recommended to store it in the dark for 12 h for completion of the radical formation reaction. Subsequently, the resultant decolourisation was monitored by spectrophotometer at wavelength 724 nm. Radical cation ABTS$^{\cdot+}$ was pre-formed in order to achieve a more stable synthetic coloured radical. However, ABTS$^{\cdot+}$ was degraded following the addition of acridines and radical release data was not obtained due to its instability in the presence and absence of blue light. The two assays were chosen because the λ_{max} of DPPH$\cdot$ and ABTS$^{\cdot+}$at 517 and 734 nm did not overlap with the λ_{max} of

acridines (426-446 nm). The experiments in this study were conducted without the addition of acridines and revealed that synthetic radicals dissolved in DMSO were stable in the presence and absence of blue light (Floegel *et al.*, 2011; Thaipong *et al.*, 2006).

With respect to the measurement of radical species release, the amount of radical released from 20-minute blue light treated acridines is not known. It may be possible that the radical markers used in these antiradical activity assays are unstable in solution with acridines, which makes radical release investigation challenging. Furthermore, highly reactive radical species such as hydroxyl radical ·OH may be quite difficult to detect, due to their extremely short lifetimes. There are alternative methods to measure radical species such as using fluorescent probes such as HPF for the specific detection of hydroxyl radical with insensitivity to $^1O_2$ (Price *et al.*, 2010). Additionally, EPR spectroscopy performed by EPR spin-trapping is considered the method of choice to detect and identify free radicals in biological systems (Hawkins, 2004). This highly sensitive method depends on the reaction between radicals with a diamagnetic probe containing a nitrone function, the spin trap, to produce a stable radical adduct (a nitroxide derivative) that can be detected by EPR (Augusto *et al.*, 2007). Also, the EPR method has the ability to identify and quantify distinct radical species such as $O_2^{\cdot-}$ and ·OH, which could otherwise not be detected by other assays (Mitchell *et al.*, 2013). However, the requirements of high cost, knowledge of operation and upkeep of this large complicated piece of equipment are drawbacks of this type of investigation (Davies, 2016).

In the screening of the second most damaging ROS ($^1O_2$) for 60 min, it appeared that most singlet oxygen was released from acridine compounds after 20 min using the TPCPD assay. It was established in this study that 20 acridine compounds produced singlet oxygen upon exposure to blue light for 20 min when compared with the standard's yield in the *in vitro* photochemical test (Table 3.3). The *in vitro* photosensitising activity of acridines and their abilities to release singlet oxygen upon exposure to blue light support findings by (Iwamoto *et al.*, 1987), who found that several acridines such as acriflavine (AF), proflavine (PF), acridine orange (AO) and 9-aminoacridine (AA) showed singlet oxygen activity, upon irradiation with an ultraviolet (UV) lamp for 30 min, which is unsurprising given the spectral proximity of UV and blue light. The singlet oxygen production

in the aforementioned study was detected and quantified by measuring the signal intensity of TEMPO detected by (ESR) spectrometry inside the cell, which is considered less sensitive than the method used in the present study (TPCPD) and may show misleading increase of singlet oxygen production due to the possibility of electron transfer interference by the excited photosensitiser as well as the spin trap TEMPO is considered very sensitive to pH and its penetration into tissue is limited (Koh *et al.*, 2016).

Conversely, a group of acridine compounds such as ethacidine, aminacrine, salacrine, acridine orange and proflavine was screened for $^1O_2$ using *in vitro* spectrophotometric testing. None of the compounds yielded any measurable amount of $^1O_2$ after one hour's illumination by white light of 1.7 mW/cm^2 (Wainwright *et al.*, 1997). The reason for the absence of $^1O_2$ release in that study is potentially due to the insufficient irradiance dose to photoactivate the compounds, while the irradiance rate used in this present study was far higher at 96 mW/cm^2 for 20 min, which was sufficient to release $^1O_2$.

The photochemical data presented in this study demonstrated that six acridine compounds, 3, 4, 5, 6, 8 and 17, out of 22 compounds were more efficient singlet oxygen producers than the standard, aminoacridine (Compound 1). Aminoacridine is an unsubstituted photosensitiser, which demonstrates that substitutions made by adding the groups Cl, NO_2, CH_3 and OCH_3 at C1, C2, C3, C4, C5 and C6 of the aminoacridine led to enhanced singlet oxygen release (Table 3.6). Similarly, substitutions made on toluidine blue (standard lead photosensitiser for the phenothiazinium group) produced analogues releasing more $^1O_2$ than that of standard with relative values ranging between 1.24 and 1.87, by replacing methyl group at C2 in toluidine blue with the groups ethyl, propyl, butyl and phenyl (Wainwright *et al.*, 2016). The relative $^1O_2$ measurements in this study cannot be directly compared with relative $^1O_2$ released from the phenothiazinium group, which used a different standard as lead compound due to their missing data of half-life.

It has been demonstrated that acridine orange possesses photosensitising activity and can release both singlet oxygen and hydroxyl radicals. Investigations of $^1O_2$ and radicals were conducted by using acridine orange with L-histidine hydrochloride monohydrate, a scavenger of $^1O_2$, and D-mannitol, a scavenger of

hydroxyl radicals. The survival rate of tumour cells under ultrasonic irradiation at 2 W/cm^2 was significantly higher in the presence of two scavengers than that in the presence of acridine orange alone, which reveals the killing effect of both $^1O_2$ and hydroxyl radicals. In the previous study, L-histidine and D-mannitol both suppressed the antitumour effect when combined with acridine orange. Therefore, both singlet oxygen and hydroxyl radicals may play a role in ultrasonic cell damage in the presence of acridine orange, however no quantitative results were obtained. No published data measured radicals released from acridines.

3.3.2 Acridines have no significant effect on microbial growth in the absence of blue light

Acridines such as acridine orange are cell-permanent compounds that can diffuse into the cytoplasm of living cells to accumulate in lysosomes, mitochondria or to bind to the DNA and RNA (Iwamoto *et al.*, 1987; Lin *et al.*, 2017). The accumulation of AO may give us an indication of how the tested compounds in this study may behave. Acridines have been shown to enter the fungal and bacterial cell as this localisation of acridines has been facilitated by cationic ionisation and sufficient molecular planarity. The high cationic ionisation of acridines results from electronic conjugation between the ring nitrogen and the amino group (Albert, 1951). It has been demonstrated that all acridine compounds screened in this study showed limited activity in the absence of blue light illumination, a growth inhibition of less than 15% in the no blue light control against *S. cerevisiae* and *C. albicans*, measuring growth by the optical density method. Because there is no effect of acridines on microbial growth in the absence of light, this suggests they are either unable to enter the cell or the cellular effect is limited. For example, intracellularly they may bind to mitochondria or lysosomes only or they enter the nucleus without DNA intercalation and then release ROS under illumination, which destroys DNA. Furthermore, the assessment of microbial growth inhibition using the optical density method in this study does not reflect accurately the viable cells count and thus the effect of acridines alone on microbial growth may be present.

3.3.3 Blue light (470 nm with irradiance rate of 11 5 J/cm^2) has no significant effect on microbial growth

The novel acridine compounds in this study are activated in response to blue light (Table 3.3). Before biological testing of these compounds was undertaken, the effect of the activating light source alone on cell growth was determined. The data within this chapter demonstrates that 470 nm blue light alone (20 min, 115 J/cm^2) cannot be utilised as an effective antimicrobial therapy against *S. cerevisiae*, *C. albicans, A, fumigatus, S. aureus* and *E. coli*, as no significant effect on growth was obtained as measured by optical density or checking visual growth (Figures 3.3 to 3.6). The insignificant antimicrobial effect observed in this study can be attributed to the weak activation of endogenous photosensitisers chromophores such as coproporphyrin, which were not completely activated. This in turn leads to the release of low amounts of cytotoxic oxidative agents ROS, causing lack of significant growth inhibition. This result is in contrast to other studies where blue light alone, particularly in the wavelength range of 405-470 nm, has shown potential antimicrobial effects (Gwynne *et al.*, 2018).

Exposure of *S. aureus, E. coli* and *C. albicans* to blue light has been shown to have an antimicrobial effect (Halstead *et al.*, 2016; Zhang *et al.*, 2016; Maclean *et al.*, 2009). However, although many of these studies use a similar blue light dose (115 J/cm^2 versus 108 J/cm^2), the wavelength of blue light is much shorter (400 – 415nm). A study by (Murdoch *et al.*, 2013) required short wavelength and much higher levels of irradiance dose to achieve significant CFU inactivation in fungal suspensions of *S. cerevisiae*, *C. albicans* and *A. niger.* The previous results may suggest why this current study did not demonstrate a significant growth inhibition. These results suggest that the shorter the wavelength of blue light, the more effect it has on the growth of microbial cells. This suggests the availability of endogenous photosensitisers inside microbial cells, which can be photoactivated only by shorter wavelength, then produce ROS and kill the cell. Most of the studies undertaken on the effect of blue light on microorganisms concentrate on the blue/ultra violet range - 405 nm. This is a significantly shorter wavelength than was used in this study (470 nm). Comparison of same energy doses but varying wavelengths indicates that a shorter wavelength is more effective in inactivating microbes (405 nm vs 470 nm) (Roh *et al.*, 2016). Due to the use of longer wavelength of blue light (470 nm) in this study, no effect seen

can be interpreted. The antimicrobial blue light effect obtained by other studies was mainly attributed to the presence of endogenous photosensitisers chromophores such as coproporphyrin, which were activated and led to the release of cytotoxic oxidative agents ROS and thus inactivated microbial cells (Zhang *et al.*, 2016). In this study the activity of 470 nm blue light was not sufficient to activate endogenous porphyrins, which are well known for their importance as if their synthesis pathway is knocked out, the susceptibility of microbial cells to blue light decreases significantly (Galbis-Martínez *et al.*, 2012; Grinholc *et al.*, 2015). The amount of endogenous coproporphyrin was shown to be different between Gram-positive and negative bacteria (Nitzan *et al.*, 2004; Kumar *et al.*, 2015). There is evidence that Gram-positive bacteria are generally more susceptible to blue light than Gram-negative bacteria when using a shorter wavelength at 405 nm (Gupta *et al.*, 2015). This difference in susceptibility is due to the difference in concentration of flavins, endogenous photosensitisers present inside the cell, which can vary between bacterial species (Kumar *et al.*, 2015). However, within this study no significant effect of blue light was observed in all tested microorganisms.

There is also evidence that a higher dose of blue light can have an antimicrobial effect with a 60-minute blue light illumination, producing a total higher dose of 216 J/ cm^2, which inhibited growth for *C. albicans (*Trzaska *et al.,* 2017*).* This is consistent with Roh *et al.*, 2016, who utilised a similar wavelength and method for determining an antimicrobial effect to show that bacterial cells were significantly inactivated after 24 h blue light irradiation at a dose of 1,150 J/cm^2. This suggested that the absence of effect in this study was obtained due to using a much lower irradiance dose when compared to the aforementioned studies. Furthermore, exposure time can have impact on the level of porphyrins as adjusting low irradiance with longer exposure exhibited a greater effect of antimicrobial inactivation than high irradiance with short exposure (Murdoch *et al.*, 2012). It has been demonstrated that *A. fumigatus* spores were significantly inactivated by using a much longer illumination period with low irradiance Fuller *et al.*, (2013). In contrast, this study used high irradiance with short exposure time, which may affect the result obtained. It was also reported that the endogenous porphyrin patterns *in vitro* such as porphyrin quantity and porphyrin species are highly affected by the whole culturing conditions such as time of

culturing, passaging and nature of culture media. Since porphyrin levels and antimicrobial activity can be affected by various factors, there is a need to find an antimicrobial blue light standardised method to achieve a significant effect on microbial cells.

Furthermore, differences in blue light effect might have also resulted from a number of other factors including size of the inoculum, the endogenous levels of porphyrins, the method used to measure antimicrobial effectiveness and how cells were exposed to blue light treatment. Regarding inoculum cells, studies have shown that a higher concentration of cells reduces antimicrobial activity. In this study the cell concentration was 2×10^5 cells/ml. This is significantly less than that used in the study of Bumah *et al.,* 2015 at (3×10^6 cells/ml), which would suggest that this would not influence the effects of blue light alone. In contrast to other studies, this study did not show an effect. It seems the effect seen with blue light exposure is due to endogenous porphyrins and the reason for not seeing the effect in this study could be that bacterial strains have different levels of porphyrins. As it has been shown that strains of *P. aeruginosa* Gram-negative bacteria showed significant difference in inactivation using the same conditions, possibly due to the lack of sufficient amount of flavins in the bacterial strain used(Abana *et al.*, 2017). Also, the effectiveness of inactivation in log phase which was used in this study was less than lag phase due to the presence of more porphyrin inside cells in lag phase that acted as endogenous photosensitisers (Keshishyan *et al.*, 2015). The previous studies conducted used a different method to determine antimicrobial activity by utilising the viable count method (colony forming unit - CFU), while the present work used optical density measurements or visual inspection to determine growth inhibition obtained. The use of CFU, where actually a significant inactivation was seen, is more accurate due to the measurement of viable cells. While this work determined growth inhibition by taking ODs or visually without measuring how many viable cells were there. In addition, the cells were removed from the treated samples and plated on agar, then incubated for 24 h before counting. In this study the cells were left in the treated media which have antioxidant properties. The effect of blue light with approximately the same wavelength and irradiance dose to this present study was shown to significantly reduce number of CFU of the same *E. coli* strain DH5α as used in this study (Abana *et al.*, 2017). This dissimilarity between their

results and the present study is probably due to using agar plate method (Abana *et al.*, 2017) while this work utilised the suspension method. It has been demonstrated that *in vitro* studies performed using the in suspension method require a higher irradiance dose to achieve microbial inactivation than studies performed on agar plates (Murdoch *et al.*, 2012). The bacterial cells exposed to blue light in buffer suspensions and on agar plates were compared. It has been found that using suspensions required significantly more energy doses to obtain similar effect to that on agar, which ensures more exposure to blue light and direct effect on cells (Murdoch *et al.*, 2012). Various studies have been conducted with using cell suspension, as this study, but to improve the antimicrobial efficacy, blue light should be exposed to microbial cells on agar plates (Murdoch *et al.*, 2012). Therefore, there is no need for blue light to penetrate the solution. This suggests that using the suspension method in this study may have affected the results obtained in this work.

In this study, no antimicrobial effect of blue light was seen against the spores of *A. fumigatus*. This supports the findings of Moorhead *et al.* (2016), who found previously *Aspergillus* species resistant at an energy dose of 504 J/cm^2, which is higher than the dose used in this study. An increased resistance to blue light is also seen in bacterial endospores, which have similar hardy properties to the spore-forming *A. fumigatus* used in this study (Maclean *et al.*, 2013). The high resistance of *Aspergillus* species is most probably due to the multilayered pigmented spore coat containing aspergillin (Ray *et al.*, 1975).

3.3.4 Blue light activation of acridines has an effect on microbial growth

Based on blue light results and the absence of significant effect of acridines alone on microbial growth, any growth inhibition observed following illumination of the novel acridine compounds would be attributed to photoactivation of these compounds. Following photochemical screening of the 22 acridine compounds, the photoantifungal activity of these compounds under blue light illumination was measured against a range of fungi: *S. cerevisiae, C. albicans* and *A. fumigatus.*

The synthesised compounds were tested *in vitro* to determine growth inhibitory activity in the absence and presence of blue light. Minimum inhibitory concentration (MIC) values were measured using the EUCAST broth microdilution method (EUCAST 7.3: Arendrup *et al.*, 2015a).Two different types of antimicrobial susceptibility test available are the solid media-based disk diffusion method and the liquid media-based microbroth dilution method. The disk diffusion method offers the ability to detect subpopulations of resistant bacteria that would be visualised as inner colonies in the zone of inhibition, view growth on the plate rather than in a well and set up easily. However, the disk diffusion method must be visually read and does not provide quantitative MIC values for the comparison of *in vitro* efficacy of different agents (Balouiri *et al.*, 2016). Additionally, not all fastidious bacteria can be tested accurately by using the disk diffusion method, such as *Helicobacter pylori* and *Brucella spp*, which require particular cultural conditions to grow. On the other hand, the broth microdilution method has become a more widely referenced method for antimicrobial susceptibility testing. Using this method secures quantitative measurement of minimum inhibitory concentration (MICs) of antimicrobial drugs, reproducibility and result accuracy (Kahlmeter *et al.*, 2006; Mayrhofer *et al.*, 2008). However, broth microdilution as a method has its associated disadvantages as being relatively difficult to setup and more expensive (Reller *et al.*, 2009).

The most popular standardising breakpoint guidelines of broth microdilution method used in antimicrobial susceptibility testing worldwide are the Clinical Laboratory Standards Institute (CLSI) and the European Committee on Antimicrobial testing (EUCAST). Both the CLSI and EUCAST methods establish MIC breakpoints, which can identify whether the microorganism is sensitive or resistant to a given antimicrobial agent (Pfaller *et al.*, 2011) . Due to the free availability and standardisation property of EUCAST guidelines, they were chosen in the present study.

Two control bioassays with fluconazole against *S. cerevisiae* and *C. albicans* and amphotericin B against *A. fumigatus* were conducted. Fluconazole inhibits cell membrane formation by inhibition of a key enzyme, lanosterol 14-alpha demethylase, with decreasing effect against *A. fumigatus* due to the emergence of resistance (Carrillo-Munoz *et al.*, 2006). Amphotericin B targets ergosterol, the essential component of fungal cell membrane, leading to cell death (Vandeputte

et al., 2012). No effect on the activity of fluconazole and amphotericin B was seen in the presence of blue light. This has not been previously investigated, consequently there is no literature to support this observation.

To ensure consistency of the antifungal susceptibility testing and allow the obtained data to be compared across experiments, two control bioassays with fluconazole against *S. cerevisiae* and *C. albicans* and amphotericin B against *A. fumigatus* were carried out. The obtained MIC of 0.25 µg/ml against *S. cerevisiae* was located in the fluconazole wildtype distributions of *S. cerevisiae* that include data collected from multiple sources, geographical areas and time periods (MIC distributions-ECOFFs). In addition, the resultant MIC of 1 µg/ml against *C. albicans* corresponded with the EUCAST Antifungal Clinical Breakpoints (EUCAST 7.3: Arendrup *et al.*, 2015a). Finally, the MIC of amphotericin B against *A. fumigatus* of 0.125 µg/ml matched the previous published MIC EUCAST breakpoint.

The photoantimicrobial activity of acridine compounds was studied using the EUCAST broth microdilution method following 20-minute blue light (470 nm). The microbiological screening used in this study identified seven compounds with photoantifungal activity as these compounds reached MIC values against both *S. cerevisiae* and *C. albicans* with limited growth inhibition in the absence of blue light (Table 3.4). The MIC of acridines was determined using the same method as the reference drug fluconazole, to be the lowest concentration giving inhibition of growth of ≥ 50 % of that of compound-free control (EUCAST 7.3: Arendrup *et al.*, 2015a).

The spectrophotometric assay determined that five acridine compounds, 3, 4, 5, 8, 17 were more efficient singlet oxygen producers than the standard with relative $^1O_2$ of 3.58, 1.33, 5.33, 2.17, and 2.5, respectively (Table 3.3). Compounds 3 and 5 that released the highest levels of *in vitro* singlet oxygen compared to Compound 1 (Table 3.3); however, their high levels of singlet oxygen following blue light activation were not proportional to their respective photoantimicrobial effectiveness. For example, Compound 1 showed an MIC of 2 µg/ml against *S. aureus*, while the MIC of Compounds 3 and 5 was 24 and 8 µg/ml, respectively (Table 3.6). Indeed, Compound 17 produced a high level of singlet oxygen, with a half-life of 33 min, but had limited effect on the growth of bacteria and fungi following blue light illumination. Additionally, although Compounds 2 and 11

released less $^1O_2$ than Compound 5 in the spectrophotometric assay, they showed similar photoantibacterial activity (Table 3.3 and 3.5). This means that the increased *in vitro* photoantibacterial efficacy for Compounds 2 and 11 was not reflected in their respective singlet oxygen production (Table 3.3 and 3.5). This means that the *in vitro* photoantimicrobial efficacy for acridine compounds was not reflected in their respective singlet oxygen production.

The photoantifungal data demonstrated that acridines 7, 13 and 16 showed antifungal activity against *S. cerevisiae* with no effect on *C. albicans*, while acridines 2, 3 and 11 exhibited antifungal activity against *C. albicans* but less than against *S. cerevisiae*. As *C. albicans* is a diploid microorganism, it contains two copies of its entire genome including genes responsible for resistance such as *CDR1, CDR2, MDR1,* which act by an efflux pumps mechanism (White *et al.*, 2002; Franz *et al.*, 1998). Therefore, this genomic property may make *C. albicans* more resistant to antimicrobial acridine compounds than *S. cerevisiae* (Cowen *et al.*, 2002). This is the same trend as with other antifungal agents, as the incidence of fluconazole resistance in *C. albicans* is higher than in *S. cerevisiae* (Anderson *et al.*, 2004).

No effect of acridines following blue light illumination was observed against *A. fumigatus*. *A. fumigatus,* in general, is more resistant than bacteria and other fungi. This can be attributed to the fact that *A. fumigatus* conidia accumulate trehalose and mannitol which play a protective role by scavenging reactive oxygen species (ROS) and preventing the aggregation of proteins (Ruijter *et al.*, 2003). Conversely, PDT has been shown to be effective against the conidial form of *A. fumigatus* but at a longer exposure time and higher wavelength than used in the study (Friedberg *et al.*, 2001).

In order to improve the efficacy of these compounds against microbes, the chemical structures should be reviewed to increase the production of singlet oxygen, which is considered to play the major role in microbial inactivation (Castano *et al.*, 2004). The higher the singlet oxygen release the longer triplet excited state lifetime of a photosensitiser, which can be obtained by increasing intersystem crossing (ISC) efficiency. One way to increase ISC is by incorporating heavy atoms such as Br and I into the structure of the sensitiser. None of the current structures incorporate with those heavy atoms. Additionally, the cationic charge of molecules can make them more effective photosensitisers against

Gram-negative bacteria and Gram-positive bacteria as the positive charge on the PS molecule promotes a tight electrostatic interaction with negatively charged sites at the outer surface of the bacterial cells, increasing the efficiency of the photoinactivation process (Alves *et al.*, 2009; Minnock *et al.*, 1996).

An additional way to enhance the efficacy of acridine compounds could be by synergism of acridines with other antimicrobial agents such as fluconazole, as this combination leads to a stronger effect than that of acridine alone in the equivalent dose (Lu *et al.*, 2017; Cokol *et al.*, 2011).

The photoactivation of the 22 acridine compounds was examined against Gram-positive bacteria (*S. aureus*) and Gram-negative bacteria (*E. coli*) using blue light. The obtained data showed nine acridine compounds with photoantibacterial efficacy against both bacterial species (Table 3.5).

Despite singlet oxygen release being detected from the novel compounds in this study, this did not reflect their effectiveness against bacterial and fungal target cells. In photoantimicrobial therapy, the two most damaging ROS are $\cdot OH$ and $^1O_2$, which are able to react with many biomolecules in microbial cells (Vatansever *et al.*, 2013). Since data in this study shows there is no correlation between photochemical results of singlet oxygen (Type 2) and biological results, this can explain that acridine compounds also tend to produce free radicals via Type 1 photochemistry; however, the amount of radicals could not be measured in this study. Consistent with the previous suggestion are the findings of a study by (Vatansever *et al.*, 2013) in which non-tetrapyrrole based compounds (which match acridines) are more likely to undergo both Type 1 and Type 2 photochemistry. Examples of these PS include phenothiazinium salts, such as toluidine blue O (TBO) (Martin *et al.*, 1987) and methylene blue (MB) (Sabbahi *et al.*, 2008). While it is thought that photosensitisers with different molecular frameworks (tetrapyrrole-based compounds) such as porphyrins and chlorins tend to undergo mainly Type 2 photochemical mechanisms ($^1O_2$ generation) (Maisch, 2007). This means that acridines tested in this study probably tend to undergo Type 1 and Type 2 reactions and thus produce radicals and singlet oxygen, respectively. Therefore, the absence of correlation between singlet oxygen release and photoantimicrobial effect in this present study could mean other factors, such as radical hydroxyl $\cdot OH$, could be responsible.

Additionally, photosensitisers in free solution may behave differently in the clinical environment. The composition of synthetic culture media is important for the behaviour of cultured cells *in vitro* and may affect the results of the photoantimicrobial experiments. The total antioxidant capacity of RPMI 1640 medium used in photoantimicrobial screening has been estimated using the ABTS decolourisation assay and the ferric ion reducing antioxidant power assay and it has been shown that this culture medium has antioxidant properties using both assays (Lewinska *et al.*, 2007). It has been found that components of the RPMI 1640 medium such as phenol red, cysteine, tyrosine and tryptophan are important contributors to the total antioxidant capacity of cell culture media (Van Overveld *et al.*, 2000; Watanabe *et al.*, 2002). Therefore, the use of RPMI 1640 as a medium in photoantimicrobial screening within this study can weaken the killing effect of radicals released from acridines under irradiation. In this study it has been found that photoantimicrobial activity did not correlate with the amount of $^1O_2$ released, which has previously been shown by Iwamoto *et al.*, who measured singlet oxygen release and found that acridine and quinacrine produced a large amount of $^1O_2$ but had less inactivation effect on viable *S. cerevisiae* cells than acridine yellow which produced the same amount of $^1O_2$ (Iwamoto *et al.*, 1987). This supports the findings in this present study, which demonstrated that the resultant phototoxicity effects did not have a clear correlation with the related $^1O_2$ efficiencies.

The generation of $^1O_2$ is very sensitive to oxygen concentration, which may play a role in photodynamic inactivation (Maisch, 2007). Because $^1O_2$ originates from energy transfer from the excited photosensitiser to ground state oxygen, consuming oxygen, photoinactivation critically depends on oxygen levels (Kwiatkowski *et al.*, 2018; Juzeniene *et al.*, 2007). The measured oxygen levels at the site of singlet oxygen generation inside the microbial cells decreased as a result of normal oxygen consumption thus with decreasing oxygen concentration, the quantum yield of singlet oxygen released following exposure of acridines to blue light also decreases (Maisch, 2007). This means that the amount of singlet oxygen produced from acridines in microbiological screening may be less than that released under blue light illumination within the photochemical experiments of this study.

To carry out PDT effectively in microbial cells, it is necessary to ensure sufficient light delivery to the cells with the least proportion of scatter and absorption scattering and absorbing (Castano *et al.*, 2004; Castano *et al.,* 2014). Additionally, the areas of photosensitiser localisation can directly affect the outcome of PDT in microbial cells because of the high reactivity and short life of both $^1O_2$ and ·OH (Moan *et al.*, 1991).

The discrepancies in the growth inhibition effect among the studied fungi (Table 3.4) may be due to the fact that *A. fumigatus* is a spore-forming mould and its susceptibility testing was performed using a fungal conidial suspension. Compared to unicellular fungi such as *S. cerevisiae* and *C. albicans*, *A. fumigatus* fungi have supplementary mechanisms to handle ROS. For example, such mechanisms include a larger number of antioxidant enzymes such as the catalases *CATA*, *CAT1*, *CAT2* and superoxide dismutases (SODs), which play important roles in the resistance of *A. fumigatus* to oxidative stress (Paris *et al.*, 2003; Jukic *et al.*, 2017). Furthermore, the role of AtfA and the HOG MAPK pathway in stress tolerance in conidia of *A. fumigatus* has been reported, particularly AtfA, which can regulate several stress protection-related genes such as *catT, dprA, scf1* and *conJ* at the conidiation stage (Paris *et al.*, 2003; Hoi *et al.*, 2011). Therefore, due to the availability of two ROS-detoxifying systems, catalases (CATs) and superoxide dismutases (SODs), *A. fumigatus* resists the ROS released following the exposure of acridines to blue light (Jukic *et al.*, 2017; Emri *et al.*, 2015).

It is apparent in this study that the Gram-positive bacterium *S. aureus* was more sensitive to acridine compounds illuminated by blue light than Gram-negative bacterium *E. coli* (Table 3.5). Various studies have also reported fundamental difference in susceptibility to PDT between Gram-positive and negative bacteria (Nitzan *et al.*, 2004; Maclean *et al.*, 2009). Data within this chapter shows Gram-positive bacteria are more susceptible to acridines than Gram-negative bacteria. This may be related to their morphology and physiology properties, as their cytoplasmic membrane is surrounded by a relatively porous layer of peptidoglycan and lipoteichoic acid that allows acridine and ROS to cross. Gram-negative *E. coli* were more resistant to blue light treated acridines, which may be due to the existence of lipopolysaccharides (LPSs) in the extra outer membrane which forms a physical and functional barrier between the cell and its

surroundings, which may prevent penetration of acridines and ROS into the cells (Vatansever *et al.*, 2013; Hamblin *et al.,* 2004). Therefore, the different susceptibilities between Gram-positive and Gram-negative bacteria in this study can be explained by the difference in their cell wall structures.

The data in this study demonstrated that Gram-positive bacteria are more sensitive to PDT than Gram-negative bacteria and this has been shown in other studies (Jori *et al.*, 2006; Costa *et al.*, 2012). In contrast, another study has previously shown no difference in susceptibility between Gram-positive and Gram-negative bacteria (Wainwright *et al.*, 2016). The existence of more strongly cationic charges on molecules will increase the spectrum antimicrobial efficacy against Gram-negative bacteria (Vatansever *et al.*, 2013).

It is clear that there is a marked difference in the sensitivity of fungi and bacteria against our compounds. Compounds 12, 14 and 17, for instance, showed only antibacterial activity without any antifungal effect (Table 3.7). The higher resistance of fungi *S. cerevisiae* and *C. albicans* to photodynamic inactivation (PDI) in this study is probably due to the great difference in size and surface area between the bacterial and fungal cells. Because bacterial cells are significantly smaller than fungal cells that means fewer oxygen radicals less $^1O_2$ are needed to kill them (Demidova *et al.*, 2004).

In conclusion, the data reported here will be important in designing experiments concerning antimicrobial PDT for infections. The photoantimicrobial activity of some compounds and the low no-light toxicity prompt future research to study their chemical structures and improve their effectiveness.

4. Flavins

4.1 Introduction

Flavins are compounds with the basic structure of tricyclic isoalloxazine (Figure 4.1; Knappe, 1977). They have been of interest to scientific research over the past decades, due to the discovery of many flavin-containing enzymes, which have a pivotal role in several important biological reactions. Flavin derivatives can absorb in the visible light range of spectrum because of the conjugation of the isoalloxazine ring. This absorption property allows flavins to be activated by UV-blue light.
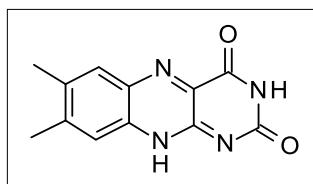
Figure 4.1 7,8-Dimethylisoalloxazine structure (Knappe, 1977).

 Flavin molecules act as important cofactors, which have the ability to take part in either one or two electron transfer reactions (Heelis, 1982).

Flavin dependent enzymes perform a wide variety of functions in the absence or presence of light. For example, flavoprotein dehydrogenases and reductases transfer electrons between substrates in non-light conditions (Edwards, 2006). Another group of flavins containing enzymes such as DNA photolyase can obtain their catalytic functions following light exposure. This enzyme can be photoactivated by blue or near UV light of 360-500 nm and use its energy for the DNA repair function (Losi, 2007)

Flavins such as riboflavin (RF), lumiflavin, flavin adenine dinucleotide (FAD), flavin mononucleotide (FMN), β-nicotinamide adenine dinucleotide (NAD) and β-nicotinamide adenine dinucleotide phosphate (NADPH) showed to have a photosensitising activity when excited in the ultraviolet-blue (UV-blue) spectral band due to the production of either hydrogen peroxide and other radical species via electron transfer (Type 1) or singlet oxygen $^1O_2$ via energy transfer to oxygen (Type 2). The release of singlet oxygen and radical species is attributed to the

highly delocalised π-orbitals capable of transferring electrons or energy to molecular oxygen (Heelis, 1982).

It has been further identified, in a study by (Ruane *et al.*, 2004), that two selected bacterial pathogens *Staphylococcus epidermidis* and *Escherichia coli* can be inactivated by exposing riboflavin to 10 min UV light (Ruane *et al.*, 2004) . Additionally, the antibacterial activity of photosensitising riboflavin using UV irradiation against *Staphylococcus aureus*, *Staphylococcus epidermidis* and *Pseudomonas aeruginosa* was evaluated by using a combination of 60 min UV light and riboflavin, which decreased the viable bacterial count (CFU), by an average of 95% in all bacteria tested (Makdoumi *et al.*, 2010). A device known as Mirasol Technology was developed for the reduction of microbes by using UV light (280-360 nm) and riboflavin (vitamin B2) as photosensitiser to inactivate *E. coli* cells' viability (Kumar *et al.*, 2004). However, the negative effect of UVA ionisation on the biological tissues and its mutagenesis mechanism can cause additive effects (Ahgilan *et al.*, 2016).

It has been shown that riboflavin and two novel derivatives, FLASH-01a and FLASH-07a, can produce singlet oxygen and radicals following UV-blue light illumination, which means they are involved in two pathways, Type 1 and Type 2 reactions under visible light illumination (380-600 nm) (Wainwright, 2009). These new flavin photosensitisers exhibited a phototoxicity effect upon light exposure duration between 10 and 180 s against multidrug resistant bacteria such as MRSA (methicillin-resistant *Staphylococcus aureus*) and EHEC (enterohemorrhagic *Escherichia coli*) (Maisch*,* 2007). Another study by Maisch, proved the photodynamic effect of these two novel riboflavin derivatives against *Bacillus atrophaeus.* Their results showed that the combination of the photosensitisers with blue light for 10 s effectively inactivated the Bacillus spores (Maisch*,* 2007).

Due to the photosensitisation effect and phototoxicity properties of flavins under UV-blue light irradiation, a set of new flavin derivatives was produced to evaluate the antibacterial efficacy of theses photoactivated derivatives using blue light on clinically important microorganisms (Heelis, 2018).

The work presented in this chapter describes the possible photochemical inactivation of selected microbes using the novel flavin derivatives and blue light irradiation. The singlet oxygen ($^1O_2$) released from these flavin compounds was measured previously and these compounds were then tested to determine their photoantimicrobial activities. To determine their antimicrobial efficacy, the European Committee for Antimicrobial Susceptibility Testing (EUCAST) microbroth dilution method was utilised (EUCAST 7.3: Arendrup *et al.*, 2015a). All flavin compounds were screened against key microbial pathogens, including *Staphylococcus aureus (S. aureus) and Escherichia coli (E. coli)* and the fungi *Candida albicans (C. albicans)*, which has high mortality rate of 40%, and *Aspergillus fumigatus (A. fumigatus),* which is complicated to treat and often fatal with a mortality rate 50-90%. In addition, the yeast model organism, *Saccharomyces cerevisiae* (*S. cerevisiae*), was also included in this study.

4.2   Results

Riboflavine (Vitamin B2) is a natural photosensitiser and well known to undergo Type 1 and 2 photosensitisation under illumination with blue light (λ = 475nm) (Wainwright, 2009). The reported photoantimicrobial activity of riboflavin demonstrates activity across a broad spectrum of Gram-positive and Gram-negative bacteria (Kumar *et al.*, 2004; Makdoumi *et al.*, 2010). Inspired by this, a series of novel flavin compounds, based on the core alloxazine structure as shown in Table 4.1, was synthesised by Dr Rob Smith, UCLan (Figure 4.1). (Table 4.1; Johns *et al.,* 2014). The aim was to investigate how singlet oxygen production and the subsequent antimicrobial effects of these compounds would change, if the ribose sugar unit was replaced with a p-substituted phenyl derivative. This is because the removal of the sugar unit could change the ability of the microbe to take up the flavin compounds. Indeed, it was hypothesised that when the substituted atom was a Cl, Br or I, the singlet oxygen yield would increase due to the heavy atom effect. This in turn should increase photoantimicrobial activity due to the higher rate of singlet oxygen production, which can enable more targets to be attacked within the microbial cell.
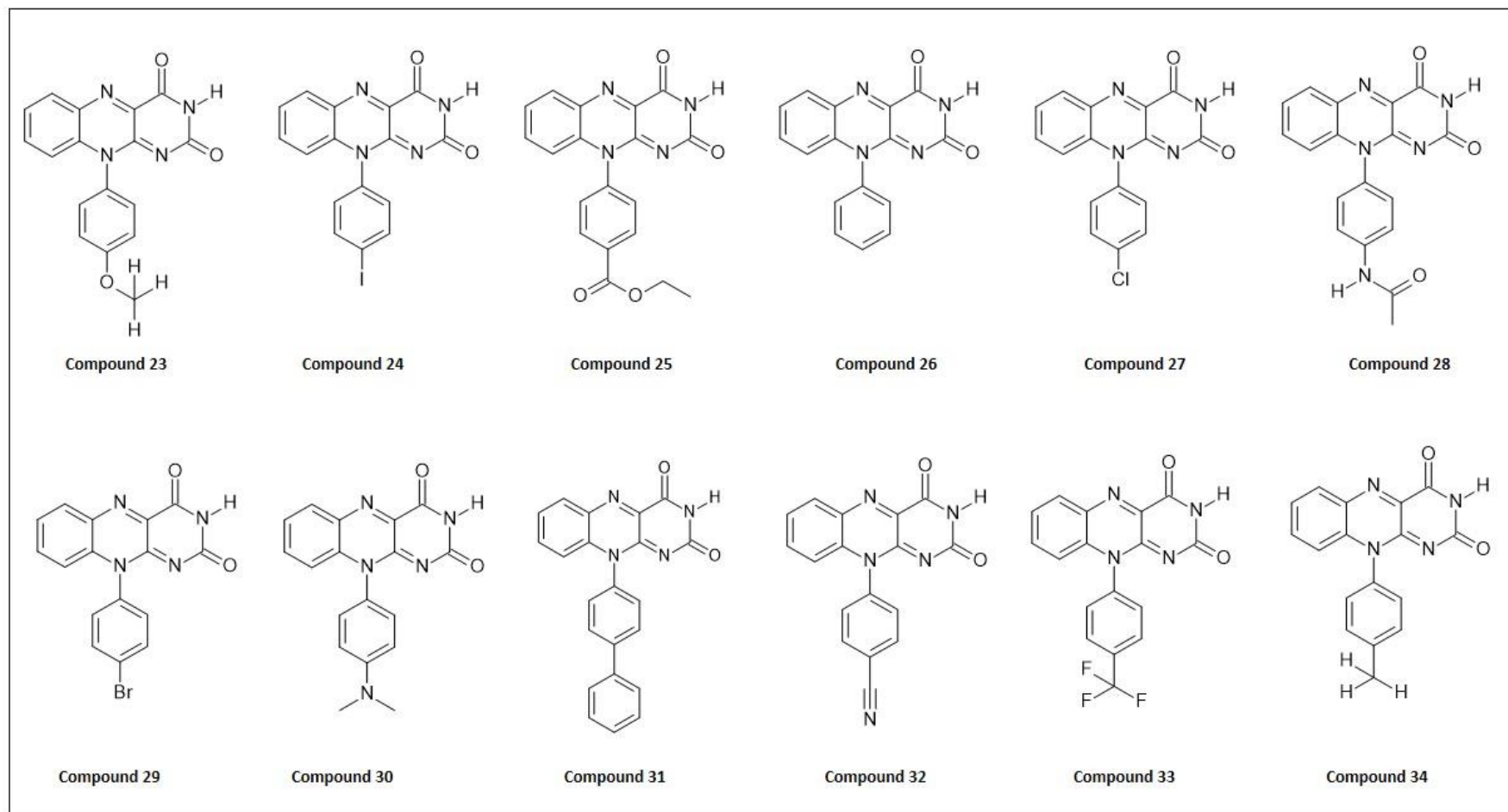
Figure 4.2 Chemical structures of novel flavin derivatives.

Table 4.1 Structures of substituted flavins containing different R groups.
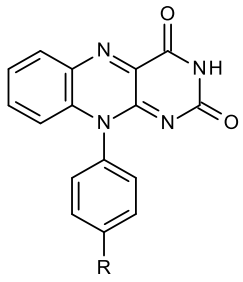
Compounds	R
23	OCH_3
24	I
25	$CO_2(CH_3)_2$
26	H
27	Cl
28	$NHCOCH_3$
29	Br
30	$N(CH_3)_2$
31	C_6H_5
32	CN
33	CF_3
34	CH_3

4.2.1 Photochemical characterisation of flavin compounds

4.2.1.1 Singlet oxygen ($^1O_2$) data

The absorption spectrum for all flavins was taken to identify the matching wavelength of visible light for best activation. For all flavin compounds, the λmax (which shows the wavelength at the highest energy peak) ranged between 260-269 nm (Table 4.2). Two other low energy peaks were located in the blue light region between 425-435 nm, which can activate flavins. Following absorption of visible light of a specific wavelength, free radicals and singlet oxygen species are produced, which then cause cellular damage. The singlet oxygen produced following blue light exposure was measured using TPCPD assay by determining the half-life of these compounds.

The half-life and singlet oxygen levels of flavins were measured following the exposure to blue light. All the flavins demonstrated a half-life. The data in this study finds that Compound 29 produced the most amount of singlet oxygen by showing the lowest half-life at 6 min among all flavin derivatives. It was followed by Compounds 24, 27 and 33 with half-life values of 6, 8 and 9 min, which showed decreasing values of relative singlet oxygen (Table 4.2). It was seen that the amount of singlet oxygen peaked after 20-minute blue light illumination.

Table 4.2 Compounds characterised according to the half-life obtained following 60 min blue light exposure. The lower the half-life the more singlet oxygen production. λmax is determined to be the wavelength at which absorbance is highest.

Compounds	λmax nm	Half-life min	Relative singlet oxygen
Alloxazine	260	100	1
23	266	25	7
24	267	6	27.5
25	268	20	8.7
26	268	13	14
27	269	8	21.7
28	269	60	3
29	268	6	29
30	266	23	8
31	269	11	15.7
32	263	53	3.3
33	253	9	20.4
34	267	12	14.4

4.2.1.2 Radical species data

The measurement of radicals released from flavins during PDT on microbes was not measured in this study. It may possible that the radical markers used in this assay were inactivated by flavins, which makes radical release investigation difficult.

4.2.2 Antifungal screening

The 12 candidate compounds based on flavins were screened using the EUCAST microbroth dilution method for antifungal activity against *S. cerevisiae, C. albicans* and *A. fumigatus*. These species were exposed to a range of concentrations of the flavin compounds (0 to 250 µg/ml) in the presence and absence of blue light. The concentration range of 0 to 250 µg/ml was consistently chosen as higher concentrations often showed limited solubility. Growth was determined by measuring OD at 530 nm for *S. cerevisiae* and *C. albicans* and visually for *A. fumigatus*.

The growth inhibition percentage for each concentration of compound, in the presence and absence of blue light, was calculated against the OD$_{530nm}$ of the drug-free control (100%). The well-characterised antifungal agents, fluconazole and amphotericin B, were used as the controls. The experiments were repeated on two separate occasions in duplicate.

The heat maps shown in Figures 4.3 and 4.4 illustrate the percentage growth inhibition determined from the OD$_{530nm}$ readings for fungal growth for concentrations of fluconazole and compounds exposed to blue light for 20 min at 24 h incubation. The concentrations of fluconazole (control) used were 0 to 64 µg/ml due to the expected MIC range of fluconazole according to the EUCAST method, while concentrations of the compounds were 0 to 250 µg/ml. The colour of the table cells indicates the percentage growth, with black indicating complete growth (0% inhibition), and red indicating no growth (100% inhibition). Yellow indicates 50% growth inhibition, which aligns with the minimal growth inhibition (MIC), as determined by the EUCAST method. In Chapter 3 it has been demonstrated that there is no effect of blue light alone on the growth of fungal and bacterial species (Figure 3.3 to 3.6). Therefore, any antimicrobial activity will be due to the tested photoactivated compounds.

% inhibition, as determined by OD$_{530nm}$, following 24 h incubation at 30˚C

Figure 4.3 Heatmap illustrating OD$_{530nm}$ levels for varying concentrations of a list of 12 compounds (0 to 250 µg/ml) against *S. cerevisiae*. The yellow bar shows 50% growth inhibition while the red bar illustrates the maximum growth inhibition.
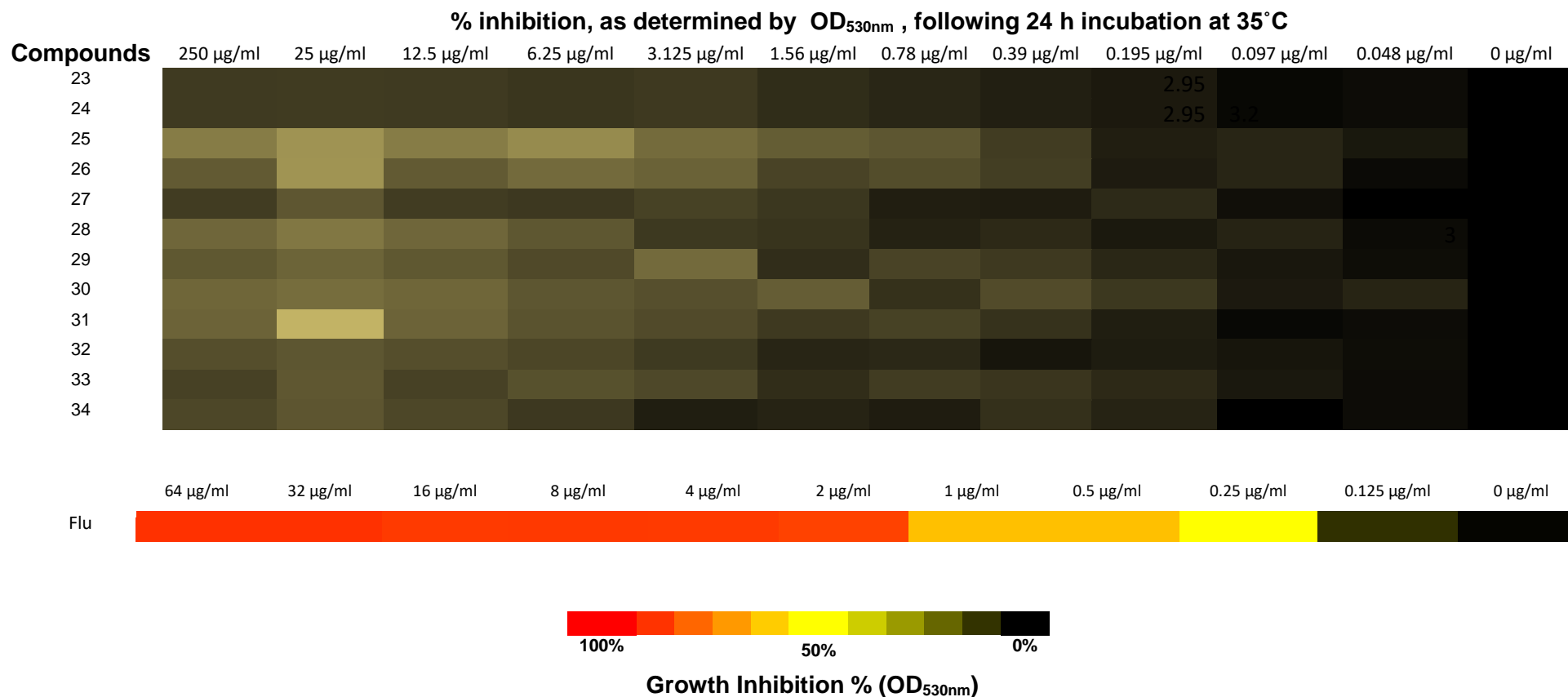
Figure 4.4 Heatmap illustrating OD$_{530nm}$ levels for varying concentrations of a list of 12 compounds (0 to 250 µg/ml) against *C. albicans*. The yellow bar shows 50% growth inhibition while the red bar illustrates the maximum growth inhibition.

The EUCAST microdilution method was used to determine the susceptibility of the studied fungi against a series of concentrations to identify the minimum inhibitory concentration MIC (50% growth inhibition compared to the control) of the tested compounds. To determine percentage growth inhibition, the optical density OD_{530nm} readings for fungal growth were taken for each concentration of compounds exposed to blue light for 20 min at 24 h incubation and compared with that of the compound-free control.

The graphs (Figures 4.5 to 4.16) show the mean ±SEM (standard error of the mean) of the highest percentage growth inhibition which has been recorded for all flavin compounds at 25 µg/ml in the absence and presence of blue light and for fluconazole at 64 µg/ml in *S. cerevisiae* and *C. albicans*.
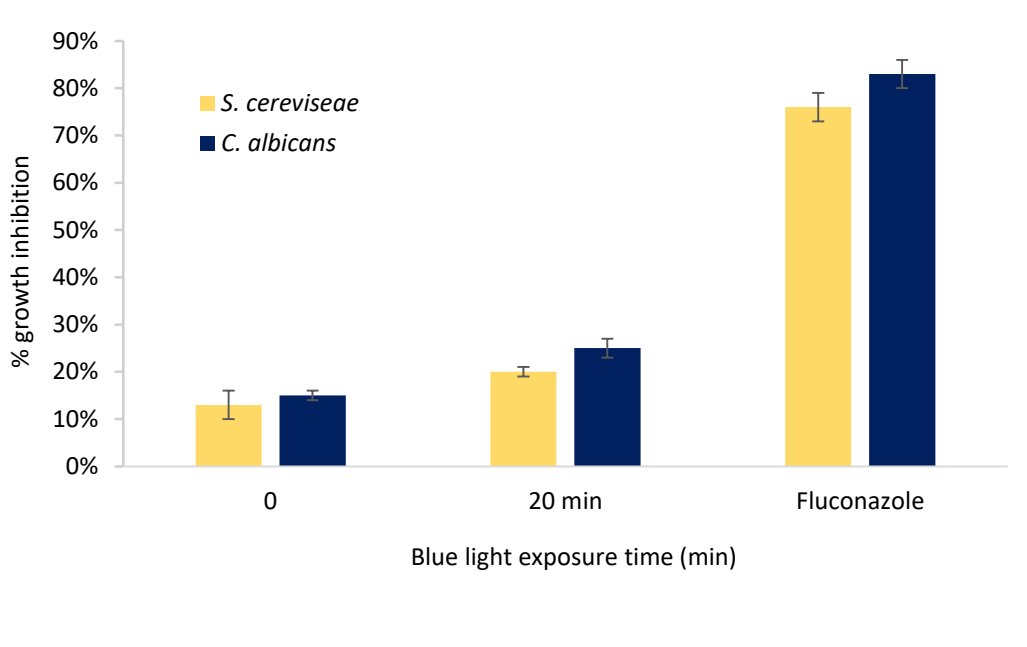
Figure 4.5 Percentage growth inhibition of *S. cerevisiae* and *C. albicans* with Compound 23 in absence and presence of blue light. Comparison of Compound 23 with fluconazole on both *S. cerevisiae* and *C. albicans* growth inhibition percentage obtained in the absence and presence of blue light. 0 means no blue light exposure. The experiment was conducted using EUCAST broth microdilution method and standardised inoculum of 0.5-2.5 x 10^5 cfu/ml. The experiment was conducted in duplicate, n=2. Values are the mean ±SEM.
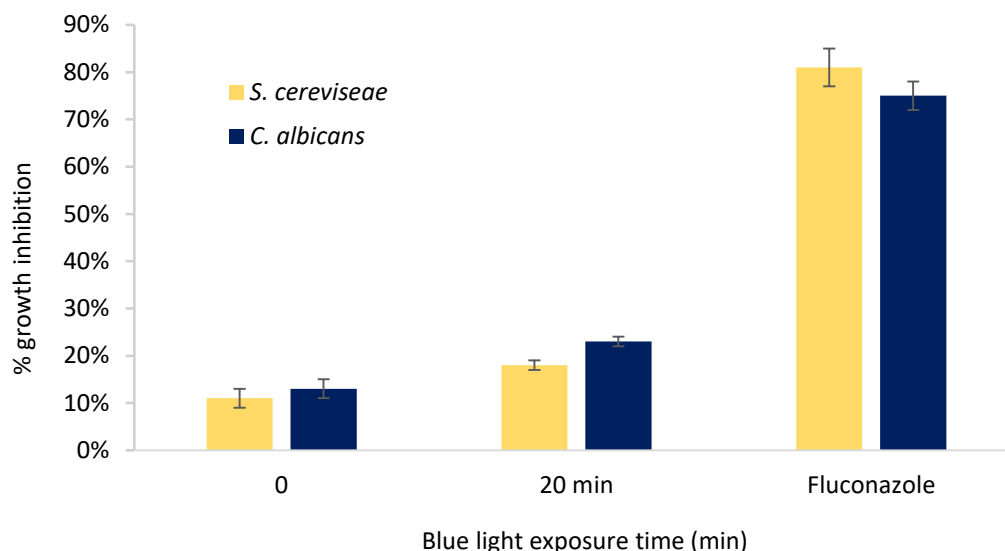
Figure 4.6 Percentage growth inhibition of *S. cerevisiae* and *C. albicans* with Compound 24 in absence and presence of blue light. Comparison of Compound 24 with fluconazole on both *S. cerevisiae* and *C. albicans* growth inhibition percentage obtained in the absence and presence of blue light. 0 means no blue light exposure. The experiment was conducted using EUCAST broth microdilution method and standardised inoculum of 0.5-2.5 x 10^5 cfu/ml. The experiment was conducted in duplicate, n=2. Values are the mean ±SEM.
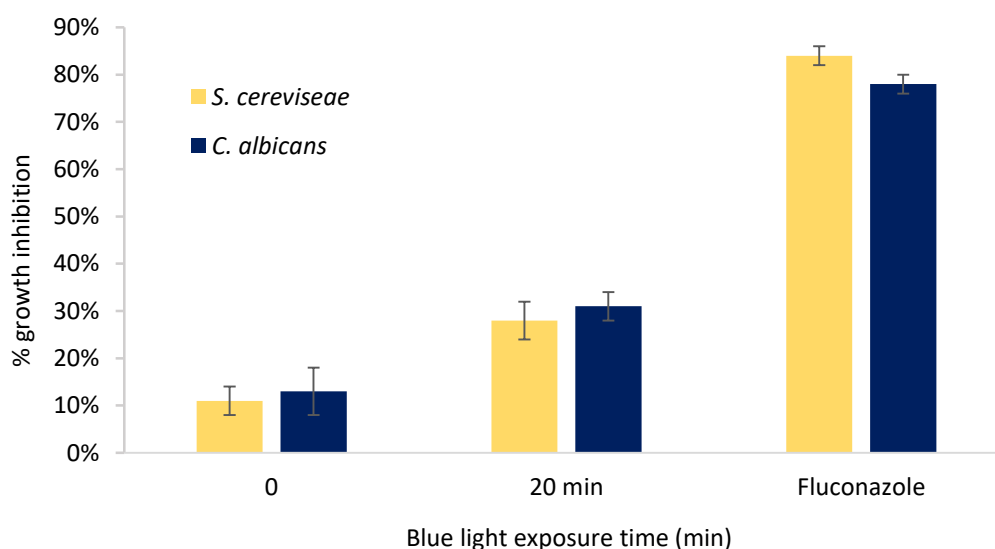
Figure 4.7 Percentage growth inhibition of *S. cerevisiae* and *C. albicans* with Compound 25 in absence and presence of blue light. Comparison of Compound 25 with fluconazole on both *S. cerevisiae* and *C. albicans* growth inhibition percentage obtained in the absence and presence of blue light. 0 means no blue light exposure. The experiment was conducted using EUCAST broth microdilution method and standardised inoculum of 0.5-2.5 x 10^5 cfu/ml. The experiment was conducted in duplicate, n=2. Values are the mean ±SEM.
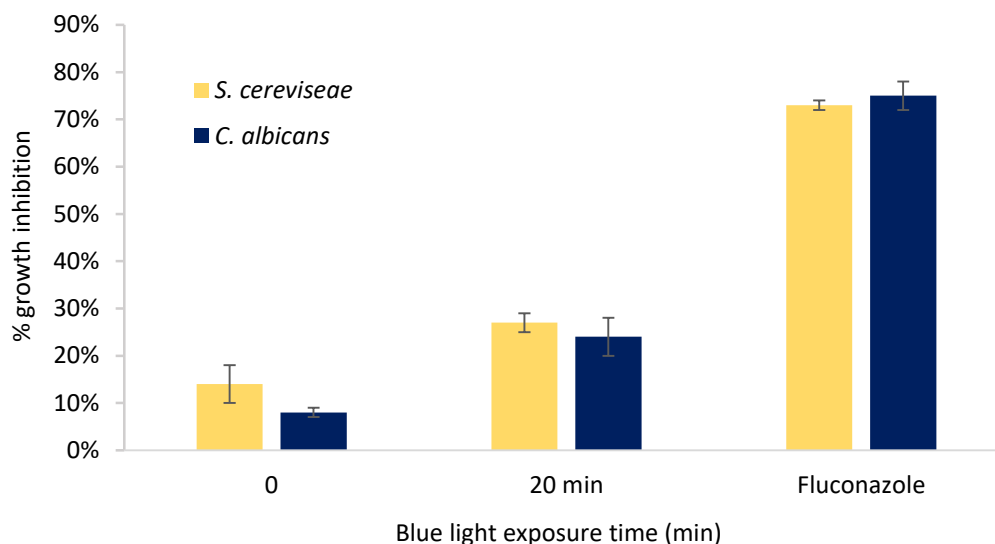
Figure 4.8 Percentage growth inhibition of *S. cerevisiae* and *C. albicans* with Compound 26 in absence and presence of blue light. Comparison of Compound 26 with fluconazole on both *S. cerevisiae* and *C. albicans* growth inhibition percentage obtained in the absence and presence of blue light. 0 means no blue light exposure. The experiment was conducted using EUCAST broth microdilution method and standardised inoculum of 0.5-2.5 x 10^5 cfu/ml. The experiment was conducted in duplicate, n=2. Values are the mean ±SEM.
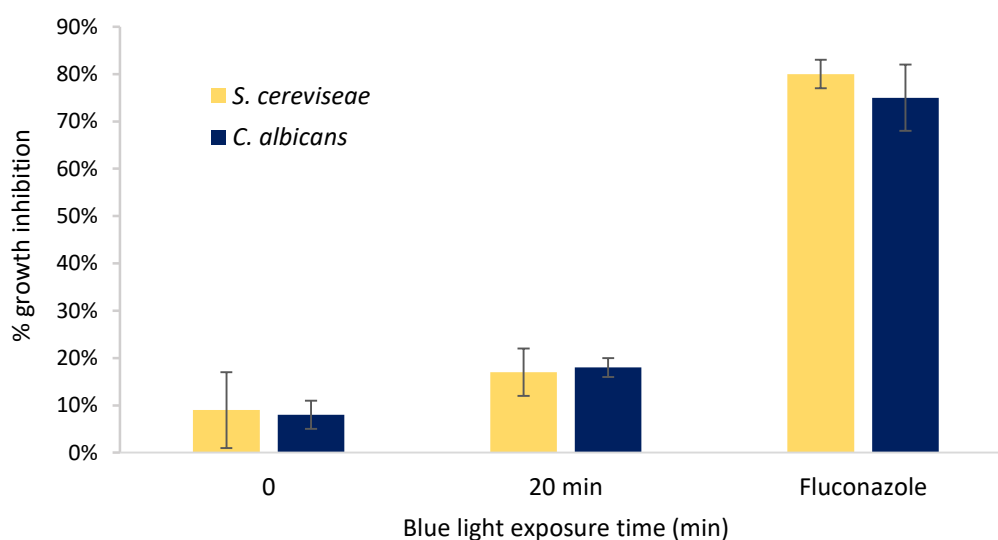
Figure 4.9 Percentage growth inhibition of *S. cerevisiae* and *C. albicans* with Compound 27 in absence and presence of blue light. Comparison of Compound 27 with fluconazole on both *S. cerevisiae* and *C. albicans* growth inhibition percentage obtained in the absence and presence of blue light. 0 means no blue light exposure. The experiment was conducted using EUCAST broth microdilution method and standardised inoculum of 0.5-2.5 x 10^5 cfu/ml. The experiment was conducted in duplicate, n=2. Values are the mean ±SEM.
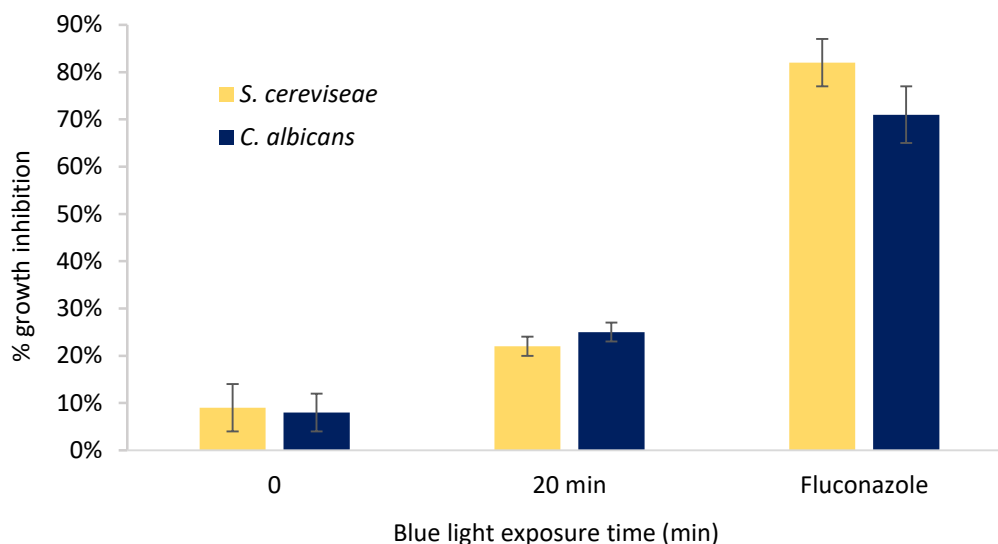
Figure 4.10 Percentage growth inhibition of *S. cerevisiae* and *C. albicans* with Compound 28 in absence and presence of blue light. Comparison of Compound 28 with fluconazole on both *S. cerevisiae* and *C. albicans* growth inhibition percentage obtained in the absence and presence of blue light. 0 means no blue light exposure. The experiment was conducted using EUCAST broth microdilution method and standardised inoculum of 0.5-2.5 x 10^5 cfu/ml. The experiment was conducted in duplicate, n=2. Values are the mean ±SEM.
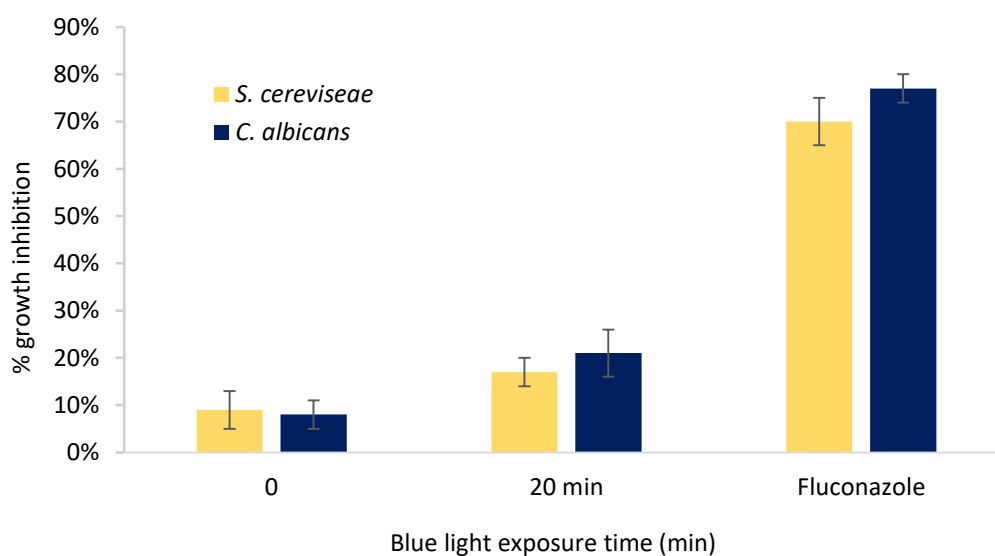
Figure 4.11 Percentage growth inhibition of *S. cerevisiae* and *C. albicans* with Compound 29 in absence and presence of blue light. Comparison of Compound 29 with fluconazole on both *S. cerevisiae* and *C. albicans* growth inhibition percentage obtained in the absence and presence of blue light. 0 means no blue light exposure. The experiment was conducted using EUCAST broth microdilution method and standardised inoculum of 0.5-2.5 x 10^5 cfu/ml. The experiment was conducted in duplicate, n=2. Values are the mean ±SEM.
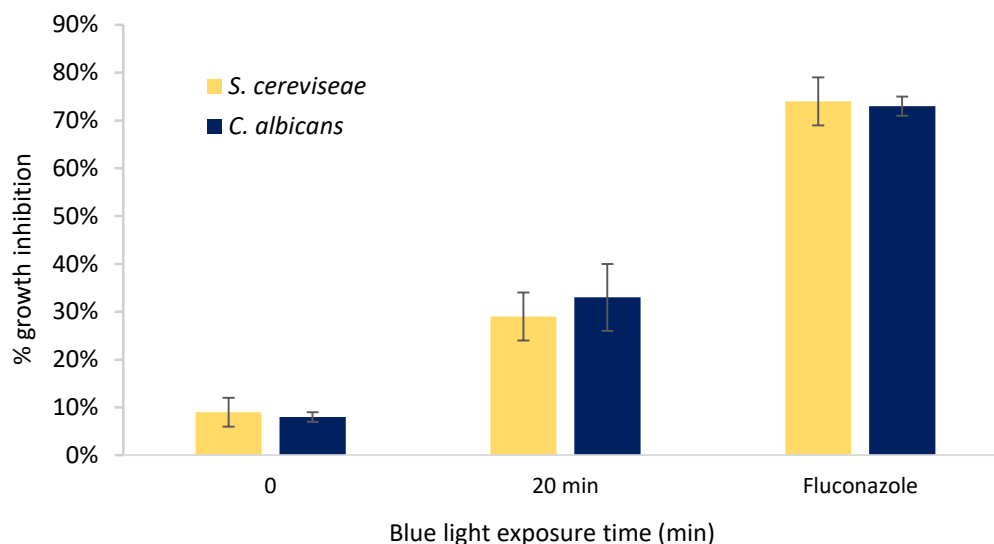
Figure 4.12 Percentage growth inhibition of *S. cerevisiae* and *C. albicans* with Compound 30 in absence and presence of blue light. Comparison of Compound 30 with fluconazole on both *S. cerevisiae* and *C. albicans* growth inhibition percentage obtained in the absence and presence of blue light. 0 means no blue light exposure. The experiment was conducted using EUCAST broth microdilution method and standardised inoculum of 0.5-2.5 x 10^5 cfu/ml. The experiment was conducted in duplicate, n=2. Values are the mean ±SEM.
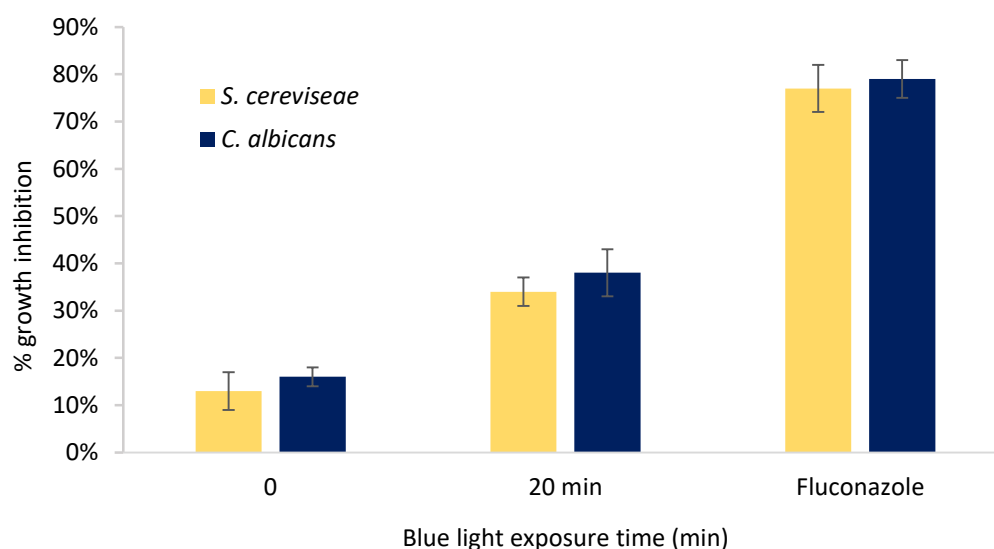
Figure 4.13 Percentage growth inhibition of *S. cerevisiae* and *C. albicans* with Compound 31 in absence and presence of blue light. Comparison of Compound 31 with fluconazole on both *S. cerevisiae* and *C. albicans* growth inhibition percentage obtained in the absence and presence of blue light. 0 means no blue light exposure. The experiment was conducted using EUCAST broth microdilution method and standardised inoculum of 0.5-2.5 x 10^5 cfu/ml. The experiment was conducted in duplicate, n=2. Values are the mean ±SEM.
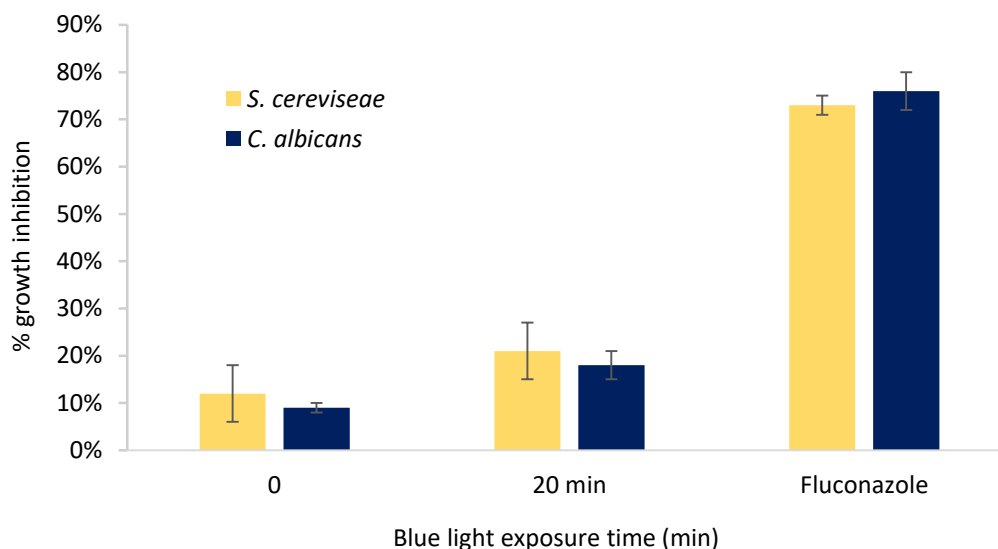
Figure 4.14 Percentage growth inhibition of *S. cerevisiae* and *C. albicans* with Compound 32 in absence and presence of blue light. Comparison of Compound 32 with fluconazole on both *S. cerevisiae* and *C. albicans* growth inhibition percentage obtained in the absence and presence of blue light. 0 means no blue light exposure. The experiment was conducted using EUCAST broth microdilution method and standardised inoculum of 0.5-2.5 x 10^5 cfu/ml. The experiment was conducted in duplicate, n=2. Values are the mean ±SEM.
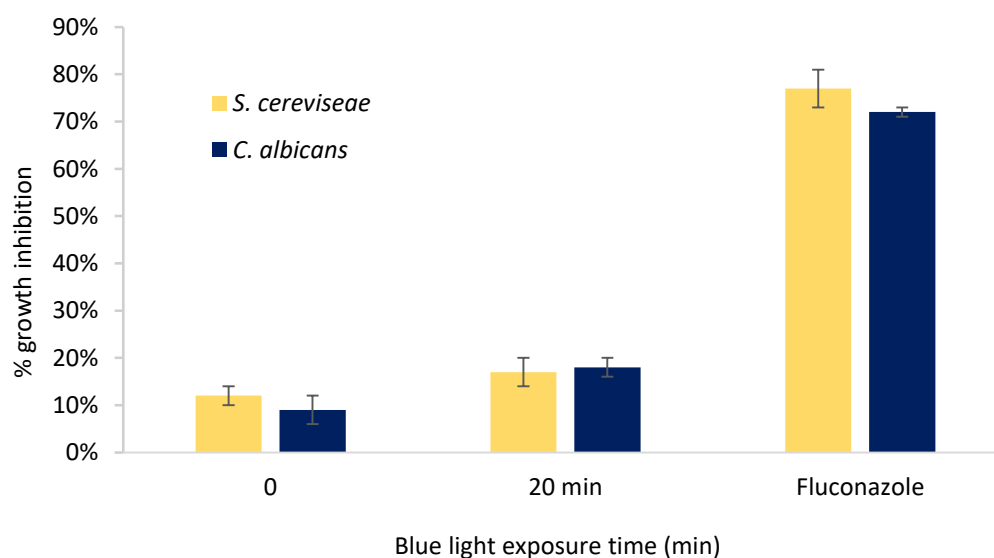
Figure 4.15 Percentage growth inhibition of *S. cerevisiae* and *C. albicans* with Compound 33 in absence and presence of blue light. Comparison of Compound 33 with fluconazole on both *S. cerevisiae* and *C. albicans* growth inhibition percentage obtained in the absence and presence of blue light. 0 means no blue light exposure. The experiment was conducted using EUCAST broth microdilution method and standardised inoculum of 0.5-2.5 x 10^5 cfu/ml. The experiment was conducted in duplicate, n=2. Values are the mean ±SEM.
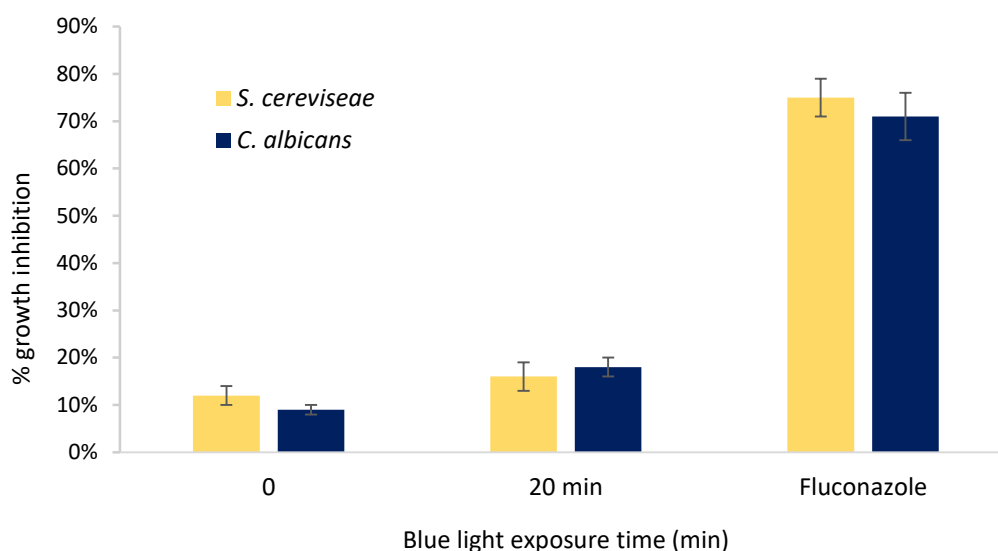
Figure 4.16 Percentage growth inhibition of *S. cerevisiae* and *C. albicans* with Compound 34 in absence and presence of blue light. Comparison of Compound 34 with fluconazole on both *S. cerevisiae* and *C. albicans* growth inhibition percentage obtained in the absence and presence of blue light. 0 means no blue light exposure. The experiment was conducted using EUCAST broth microdilution method and standardised inoculum of 0.5-2.5 x 10^5 cfu/ml. The experiment was conducted in duplicate, n=2. Values are the mean ±SEM.

To ensure consistency of the results, EUCAST antifungal susceptibility testing of *S. cerevisiae* and *C. albicans* was performed using fluconazole as the control. Regarding *S. cerevisiae*, the resultant MIC of 0.25 µg/ml was identified to be within the published range (MIC and zone distributions and ECOFFs). The resultant MIC of 1 µg/ml against *C. albicans* corresponded with the EUCAST Antifungal Clinical Breakpoints (EUCAST 7.3: Arendrup *et al*., 2015a).

None of the compounds have significant antifungal activity in the absence of blue light against both species. Since the tested compounds showed no measurable effect on the growth of cells in the absence of blue light, any possible antifungal efficacy will be due to blue light treated flavins.

The data shows that the blue light treated flavins had limited effect on the growth of *S. cerevisiae* or *C. albicans*, with growth inhibition determined to be ≤ 50% compared to the compound-free control. As such, the MIC could not be determined for these compounds.

Although the MIC value was not reached, the flavin Compounds 25, 30 and 31 showed the highest growth inhibition among all the 12 compounds after 20-minute blue light illumination (Figures 4.7, 4.12 and 4.13). The highest percentage growth inhibition was obtained at a concentration of 25 µg/ml with maximum growth inhibition levels of between 30-40% in *S. cerevisiae* and *C. albicans*. There was no significant difference in the susceptibility of *S. cerevisiae* and *C. albicans* to the activated flavins. The nine remaining flavins demonstrated slightly more growth inhibition when excited by 20-minute blue light when compared to the unactivated compounds against the both species (Figures 4.5, 4.6, 4.8, 4.9, 4.10, 4.11, 4.14, 4.15 and 4.16). Compounds 23 and 24, for example, showed growth inhibition of 15%, and 13% against *C. albicans* in the absence of blue light which increased to 25% and 23% respectively when exposed to 20-minute blue light (Figures 4.5 and 4.6). In all cases, growth inhibition of less than 12% was seen in the no blue light control.

A. fumigatus was also screened using the EUCAST antifungal MIC microdilution method for moulds (EUCAST 9.3: Arendrup *et al.*, 2015a). Due to the growth of *A. fumigatus*, instead of using the optical density to determine percentage growth inhibition, a visual inspection was undertaken. In this case the MIC was determined to be the first well where the concentration of compound resulted in complete absence of growth. It has been demonstrated that amphotericin B is effective against *A. fumigatus* showing MIC of 0.125 µg/ml, which matched the MIC EUCAST breakpoint in *A. fumigatus.* The antifungal screening demonstrated that flavins, following exposure to blue light, did not exhibit any efficacy against *A. fumigatus* at the concentrations tested (0 to 250 µg/ml) by checking the growth visually (data not shown).

4.2.3 Antibacterial screening

The flavin compounds were then screened using the European Committee for Antimicrobial Susceptibility Testing (EUCAST) microbroth dilution method, for antibacterial activity following blue light illumination for 20 min against two clinically important bacterial species, *S. aureus* and *E. coli.*

The antibacterial drug gentamicin was used as a control due to its broad antibacterial activity against both Gram-negative and Gram-positive bacteria (Jao *et al.*, 1964). The bacterial species were exposed to a range of concentrations of the flavin compounds (0 to 256 µg/ml) in the presence and absence of blue light. A 20-minute illumination period was used due to the release of most singlet oxygen from the compounds during that time. The MIC was determined, by visual inspection, to be the lowest concentration that completely inhibits growth. The experiments were repeated two times in duplicate.

EUCAST antibacterial susceptibility testing of *S. aureus* and *E. coli* to the control gentamicin was performed and the resultant MICs of 0.25 and 0.125 µg/ml corresponded with EUCAST Antibacterial Clinical Breakpoints which confirms the accuracy of the assay.

All the compounds showed little effect on bacterial growth after blue light exposure and no MIC was reached at the maximum concentration tested of 256 µg/ml (data not shown).

4.3   Discussion

In this study, the aim was to evaluate the antimicrobial activity of a set of novel photoactivated flavins using blue light irradiation. Flavin compounds, previously characterised photochemically, were tested in the absence and presence of blue light against a range of clinically important fungi including *S. cerevisiae, C. albicans* and *A. fumigatus*, and the bacteria *S. aureus* and *E. coli,* using the European Committee for Antimicrobial Susceptibility Testing (EUCAST) method (EUCAST 7.3: Arendrup *et al.*, 2015a).

4.3.1 Flavins are photosensitised following exposure to blue light and release singlet oxygen

Due to the reported photosensitising activity of flavins, such as riboflavin (Khaydukov *et al.*, 2016; Ha *et al.*, 2009; Huang *et al.*, 2006), a set of novel synthesised flavins has been characterised photochemically.

The absorption spectrum between the wavelengths 250-800 nm was taken for each flavin compound to determine the wavelength of maximum absorbance, λmax, which identified the visible light source required to photoactivate the flavins. Although flavins absorbed maximally in the UV light region, as λmax ranges between 260-269 nm (Table 4.2), the absorption spectrum consists of two additional peaks centred in the blue light region at around 415 and 435nm, which can activate flavins. This finding supports the results of Heelis *et al.,* (1982), who found that riboflavin was absorbed in the UV-blue light region as four maximum peaks centred at 446, 375, 265 and 220nm. This is also consistent with other published data conducted on flavins, flavin adenine dinucleotide (FAD) and flavin mononucleotide (FMN), which show their longest absorption wavelengths in the range between 400-500 nm at the λmax of 450 and 446 nm, respectively. Absorption peaks of a compound can be obtained by electron jump from π-bonding orbitals to π-anti-bonding orbitals, non-bonding orbitals to π-anti-bonding orbitals and non-bonding orbitals to sigma anti-bonding orbitals. This means that in order to absorb light in the region from 200- 800 nm, the molecule must contain at least one π bond or atom with a non-bonding orbital (Huang *et al.*, 2006). The carbon-oxygen double bond in flavins obviously has π electrons as part of the double bond, and also has a non-bonding orbital. The non-bonding orbital has higher energy than a π-bonding orbital which means that flavins can

absorb light of different wavelengths. The structures of flavins tested within this study have two carbon-oxygen double bonds, producing additional absorption peaks. The substitutions added to the basic flavin structure did not affect the λmax.

Flavins are suggested to be involved in two photochemical reactions, Type 1 and Type 2, producing free radicals and singlet oxygen, respectively. These released species are highly reactive and thus can cause cellular damage (Martins *et al.*, 2008; Sauer *et al.*, 2010). Therefore, singlet oxygen release following activation by blue light over a 60-minute period was quantified using the TPCPD assay, which demonstrated that most singlet oxygen species were produced from flavins following 20 min of blue light illumination (Table 4.2).

The 12 flavin derivatives, following 20 min of blue light illumination, all released more singlet oxygen than the standard, alloxazine. The relative singlet oxygen values for the novel flavins ranged between 3 and 29 (Table 4.2). This finding was in agreement with a study by Sikorska *et al.*, 1998, who found that derivatives of alloxazine also showed higher levels of singlet oxygen production, when compared to alloxazine alone. However, the $^1O_2$ measurements between the studies are difficult to compare, owing to the use of two different measurement methods of $^1O_2$ as well the use of UV light instead of blue light.

These results indicate that the flavins tested in this study can act as effective singlet oxygen producers. The most important method of generating $^1O_2$ is via the photosensitising process, which is triggered by the absorption of photons by the photosensitiser (PS). The resultant singlet excited state can decay via intersystem crossing (ISC) to generate the excited triplet state (T_1). Subsequently, the energy of the excited triplet state of PS is transferred directly to molecular oxygen, resulting in the generation of $^1O_2$. Consequently, the quantum yield of $^1O_2$ strongly depends on the efficiency of ISC and the triplet excited state T_1 (Jeong *et al.*, 2016). Therefore, enhancing the ISC process is considered a fundamental approach for producing a high T_1 population of PS and thus more $^1O_2$. This can be achieved by incorporation of heavy atoms (such as halogens) onto the photosensitiser, which can be explained using the principles of spin-orbit coupling, which leads to a bathochromic shift in absorption maxima, the first important step in the photosensitising process (Abrahamse *et al.*, 2016). This method supports the observations obtained in this study, which

demonstrated that flavin structures which have halogen atoms, such as iodine, bromine and chlorine, incorporated into the alloxazine moiety increased the singlet oxygen yield at least threefold when compared to compounds without halogens. It has been demonstrated that Compounds 29 and 24 which contain the halogens iodine and bromine released the most relative $^1O_2$ at values 29 and 27.5, respectively. It was followed by compounds incorporating the halogens chlorine and fluorine, which produced relative $^1O_2$ at 21.7 and 20.4, respectively (Table 4.2). The effect seen with halogenated substituents is consistent with several studies which demonstrated the same relationship between induction of halogens and amount of singlet oxygen release following the order $F < Cl < Br < I$ (Mehraban *et al.*, 2015; Pereira *et al.*, 2010; Azenha *et al.*, 2002). This suggests that halogens with a higher atomic mass induce a significant enhancement of the ISC, the excited triplet yield, and the quantum yield of $^1O_2$ generation (Jeong *et al.*, 2016).

Following the UV or blue light illumination, flavins such as riboflavin are converted into triplet excited state riboflavin. Radical $O_2{}^{\bullet-}$ (a precursor of H2O2 and hydroxyl radical $\cdot OH$) and $^1O_2$ are then produced through the reaction of the triplet excited state riboflavin (Liang *et al.*, 2017; Nielsen *et al.*, 2015). Various studies have investigated irradiation of riboflavin with blue light and determined the generation of radical species ($O_2{}^{\bullet-}$) by measuring the reduction of nitro blue tetrazolium (NBT). This release can be detected at 560 nm as the absorbance of NBT reduction increases with the generation of ($O_2{}^{\bullet-}$) (Yang *et al.*, 2018; Choi *et al.*, 2002; Apak *et al.*, 2007). This NBT method points to the significant generation of radicals when compared to the no-light control.

4.3.2 Flavins have no significant effect on microbial growth in the absence of blue light

All flavin compounds screened in this study demonstrated insignificant growth inhibition activity in the absence of blue light. At the highest concentrations tested (250 μg/ml), growth inhibition of less than 12% in *S. cerevisiae* and *C. albicans* was observed in the no blue light control. Additionally, no visual growth effect was observed against the fungus *A. fumigatus* and the bacteria *S. aureus* and *E. coli*.

The finding in this study was in agreement with a number of other studies that have found that riboflavin had no effect on cell viability in the absence of light. This includes both fungi (*C. albicans, Fusarium sp* and *Aspergillus fumigatus*) and bacteria (*E. coli*, *S. aureus* and *P. aeruginosa)* (Makdoumi *et al.*, 2010; Martins *et al.*, 2008; Nielsen *et al.*, 2015). In all cases, the concentration of riboflavin was significantly lower than that used in this study, ranging from 1 μg/ml to 150 μg/ml.

When flavins are taken up into the cell by flavin importers, the FMN and FAD enzymes inside the microbial cell, which have a relatively broad substrate specificity, will accept a variety of flavin analogues as substrates; among them are riboflavin (RF) and roseoflavin (RoF). The imported flavin analogues are phosphorylated and adenylated and consequently flavin-FMN and flavin-FAD rather than flavins will be the toxic compounds in the cytoplasm of target cells due to significantly altered redox potential (Biscaro Pedrolli *et al.*, 2013). However, some flavoenzymes may still be active after accepting flavin analogues without a decrease in activity. In bacteria, the flavin transporters, YpaA, RibZ, RibM and RibF, can uptake these flavin analogues, where they are phosphorylated and adenylated within the cytoplasm (Vogl *et al.*, 2007, Hemberger *et al.*, 2011; Gutiérrez-Preciado *et al.*, 2015). For fungi, transporters Mch5p, RibZ and RibE catalyse the uptake of riboflavin (Vogl *et al.*, 2007).

The impact of the absence of tested flavins in this study against fungal and bacterial cells is suggestive that these microorganisms did not recognise the tested flavins and thus no enzymatic conversion occurred. Furthermore, upon addition of the flavin compounds to the media, they could be taken up into the

cells and converted into flavin-FAD and flavin-FMN, which are potentially still active or marginally affected. To provide more antimicrobial activity to the flavins it has been suggested to make them more hydrophobic (through a methylation process), such as roseoflavin, which facilitates their binding to the target enzymes and fully inactivates flavoenzymes (Biscaro Pedrolli *et al.*, 2013; Kasai *et al.*, 1979). Since flavins tested in the present study lack methylation (making them less hydrophobic), this may give indication why no effect was observed against fungal and bacterial cells.

4.3.3 Three blue light activated flavins have a significant effect on microbial growth when compared to that of untreated flavins

To confirm that any effect on microbial cell growth is the result of blue light/compound combination rather than exposure to the activating light source, the effect of blue light alone (470 nm) on growth of fungal and bacterial cells, over 20-minute period of irradiation at 96 mW/cm^2, was investigated. The data presented in Chapter 3 demonstrated that 60-minute blue light illumination did not have a significant effect on the the growth of *S. cerevisiae*, *C. albicans, A, fumigatus, S. aureus* and *E. coli* when compared to that of untreated microbial cells (Figures 3.3-3.6).

Based on the blue light results, any growth inhibition observed following illumination of the novel flavin compounds, would be attributed to photoactivation of these compounds. Following photochemical screening of the 12 flavin compounds, the photoantimicrobial activity of these compounds was assessed against a range of fungi and bacteria and the minimum inhibitory concentration (MIC) values were measured using the EUCAST method (EUCAST 7.3: Arendrup *et al.*, 2015a).

Each of the controls in each individual species tested, fell within the published range, indicating that the assay was consistent.

Following microbiological screening, nine of the twelve flavin-based compounds showed no effect on growth in either *S. cerevisiae* or *C. albicans* (Figures 4.5 to

4.16). Only three of the light activated flavin compounds, 25, 30 and 31, showed significant growth inhibition in *S. cerevisiae* and *C. albicans* when compared with no blue light control (Figures 4.7, 4.12 and 4.13). However, no MIC could be determined as, at the highest concentration tested (250 µg/ml), total growth inhibition was less than 50%. In contrast, no growth inhibition was observed in either *A. fumigatus* or the bacterial species, *E. coli* and *S. aureus*, following exposure to the 12 flavin compounds.

Photoactivated riboflavin, by UV and visible light, has been extensively studied as an antimicrobial agent in a range of different microorganisms. Cellular damage occurs via ROS, which causes non-specific oxidative stress, and via intercalation of the molecule into the nucleic acids of the cell. In this study, nine of the light activated compounds showed no antimicrobial activity against fungi or bacteria.

This is supported by previous studies where various concentrations of photoactivated riboflavin exhibited no effect on growth in *C. albicans*, *A. fumigatus*, *S. aureus* or *E. coli* (Martins *et al.*, 2008; Nielsen *et al.*, 2015; Sauer *et al.*, 2010). However, it should be noted that the concentrations used were lower than this study (i.e. below 100 µg/ml versus 250 µg/ml) and the wavelengths of the activating light sources varied. There is no published data on the effect of activated flavin molecules on *S. cerevisiae*, thus this result could not be confirmed.

This effect was observed only in *S. cerevisiae* and *C. albicans* and not in bacteria within this study, suggesting that flavins did not experience metabolism (enzymatic conversion) inside fungi and thus they are activated by blue light and release ROS, which significantly impact growth. Whereas in bacteria, it is possible that the substituted flavins are converted so there are no molecules available to be photoactivated. Also, the weak effect of blue light treated flavins on bacteria may be explained also by the uncharged state of flavins, which may reduce the interaction with bacterial cell membrane (Maisch, 2007). Regarding *A. fumigatus,* it is generally accepted to be more resistant than bacteria and other fungi to compound penetration and ROS effect due to the presence of trehalose and mannitol in the spores which play a protective role by scavenging reactive oxygen species (ROS) and preventing the aggregation of proteins (Ruijter *et al.*, 2003).

Compounds 25, 30 and 31 had the lowest release of singlet oxygen release of the 12 flavins compounds tested, but caused the greatest level of fungal growth inhibition (Table 4.2; Figures 4.7, 4.12 and 4.13). As such, the levels of singlet oxygen production were not proportional to their respective photoantimicrobial activity. Indeed, Compounds 28 and 32 produced the highest level of singlet oxygen but had no effect on growth following blue light illumination (Figures 4.9 and 9.13). This means that the increased *in vitro* singlet oxygen release for Compounds 46 and 50 was not reflected in their respective photoantimicrobial activity.

The low half-life of flavins obtained in *in vitro* photochemical studies indicated that singlet oxygen release from flavins is high (Table 4.2), as the lower the half-life value, the greater the singlet oxygen production. Although flavins released more singlet oxygen photochemically, no MIC was observed at the maximum concentration following blue light activation. This is may be due to the lack of singlet oxygen release inside the microbial cell, which may be attributed to the rapid transportation of flavins into the cells, which employ them directly as enzyme cofactors. The absence of effective photoantimicrobial properties may be explained by the concept that *in vitro* photochemical investigation, which measures relative singlet oxygen released from flavins, may not reflect exact behaviour in the real microbiological systems. Since the production of singlet oxygen depends on the molecular environment of the photosensitiser, investigations in solution may not reflect exact behaviour in the microbiological situation. Both singlet oxygen and radical species can result in damaging effects on microbial cells, suggesting that photoantimicrobial effects may be influenced mainly by electron transfer/redox mechanism of action (Type 1 photosensitisation) represented by radicals such as ·OH, which could not be measured, as previously mentioned in this study. Significant NBT reduction by flavin in the presence of light can confirm photosensitivity of the compound whereas an increased dichlorofluoroscein (DCF) level in the microbial cells treated with photoactivated flavin shows significant intracellular ROS generation (Khan *et al.*, 2019). Furthermore, addition of radical scavenger to microbial solution will lead to hindrance in terms microbial inactivation, thus providing a clear evidence that the antimicrobial effect is mediated by radicals.

The present study shows that the flavins tested are not suitable as photoactivated compounds in photoantimicrobial therapy. This was because no antimicrobial efficacy was observed by using the combination of flavins and blue light against all the investigated species.

5. Acridine-isoalloxazine

5.1 Introduction

Acridine-isoalloxazine based compounds are composed of a combination of two moieties, acridine and isoalloxazine. As previously described in Chapter 3, acridine compounds are one of many groups of photosensitisers that are intensively studied in antimicrobial photodynamic therapy due to their ability to generate reactive oxygen species (ROS) and inactivate microbial cells under blue light illumination.

The most significant isoalloxazine derivatives are called flavins, (7,8-dimethyl substituted isoalloxazines), they are considered an important group of compounds in regard to their biological functions, photosensitisation activity and nutritional role. They can be seen in most cell types, mainly as riboflavin (vitamin B2) and two electron carriers, flavin mononucleotide (FMN) and flavin adenine dinucleotide (FAD). The wavelengths of maximum absorbance of isoalloxazine derivatives range between 326 and 460 nm, which match the UV and blue light regions (Sikorska *et al.*, 1998)

Isoalloxazine derivatives' photochemical and photophysical properties have been studied intensively over the past forty years (Penzer *et al.*, 1967). Isoalloxazine derivatives, including lumiflavin, riboflavin, flavin mononucleotide (FMN) and flavin adenine dinucleotide (FAD), demonstrated photosensitising activities *in vitro* by reacting with a number of substrates under illumination with a tungsten halogen lamp of 420-480 nm for 30 min. The production of singlet oxygen and radical species is due to the highly delocalised π-orbitals capable of transferring electrons or energy to molecular oxygen (Heelis, 1982).

Initial tests have found that photoactivated isoalloxazines have antimicrobial efficacy against several microorganisms. Riboflavin (RB) has been revealed to have a sensitising effect on DNA in *E. coli* when activated with UV light as this effect was observed by showing increased genomic DNA degradation (Kumar *et al.*, 2004).

Additionally, photoactivated riboflavin demonstrated *in vitro* antimicrobial activity by inhibiting growth of a range of pathogenic microorganisms including both

Gram-positive (*Staphylococcus aureus*, *Staphylococcus epidermidis*) and Gram-negative (*Pseudomonas aeruginosa*) bacteria under one hour-UV illumination (365 nm) and using a disk diffusion susceptibility test (Martins *et al.*, 2008).

Due to the well-established photosensitising and antimicrobial activities of both acridine and isoalloxazine, a range of novel acridine-isoalloxazine conjugates was synthesised by a chromatography-free route to determine their applicability for photodynamic antimicrobial treatment (Johns *et al.*, 2014).

This study will utilise these novel substituted acridine-isoalloxazine compounds, which have previously been characterised photochemically, to determine their potential use as effective PDT agents for microbial infections following blue light illumination. The European Committee for Antimicrobial Susceptibility Testing (EUCAST) microbroth dilution method was utilised to evaluate the antimicrobial activity against bacteria, including *S. aureus* and *E. coli* and the fungi *S. cerevisiae*, *C. albicans* and *A. fumigatus.*

5.2   Results

Acridine moieties have been of interest to medicinal chemists for many years and they exhibit significant pharmaceutical importance due to their potential photodynamic biological activities (Wainwright, 2001). Isoalloxazine derivatives absorb in the visible region and show photoantimicrobial activity through Type 1 and Type 2 photosensitisation (Ruane *et al.,* 2004). Inspired by the biological activity of both, a series of novel acridine-isoalloxazine conjugates was previously synthesised by Dr Rob Smith, UCLan (Figure 5.1, Table 5.1; Johns *et al.*, 2014).
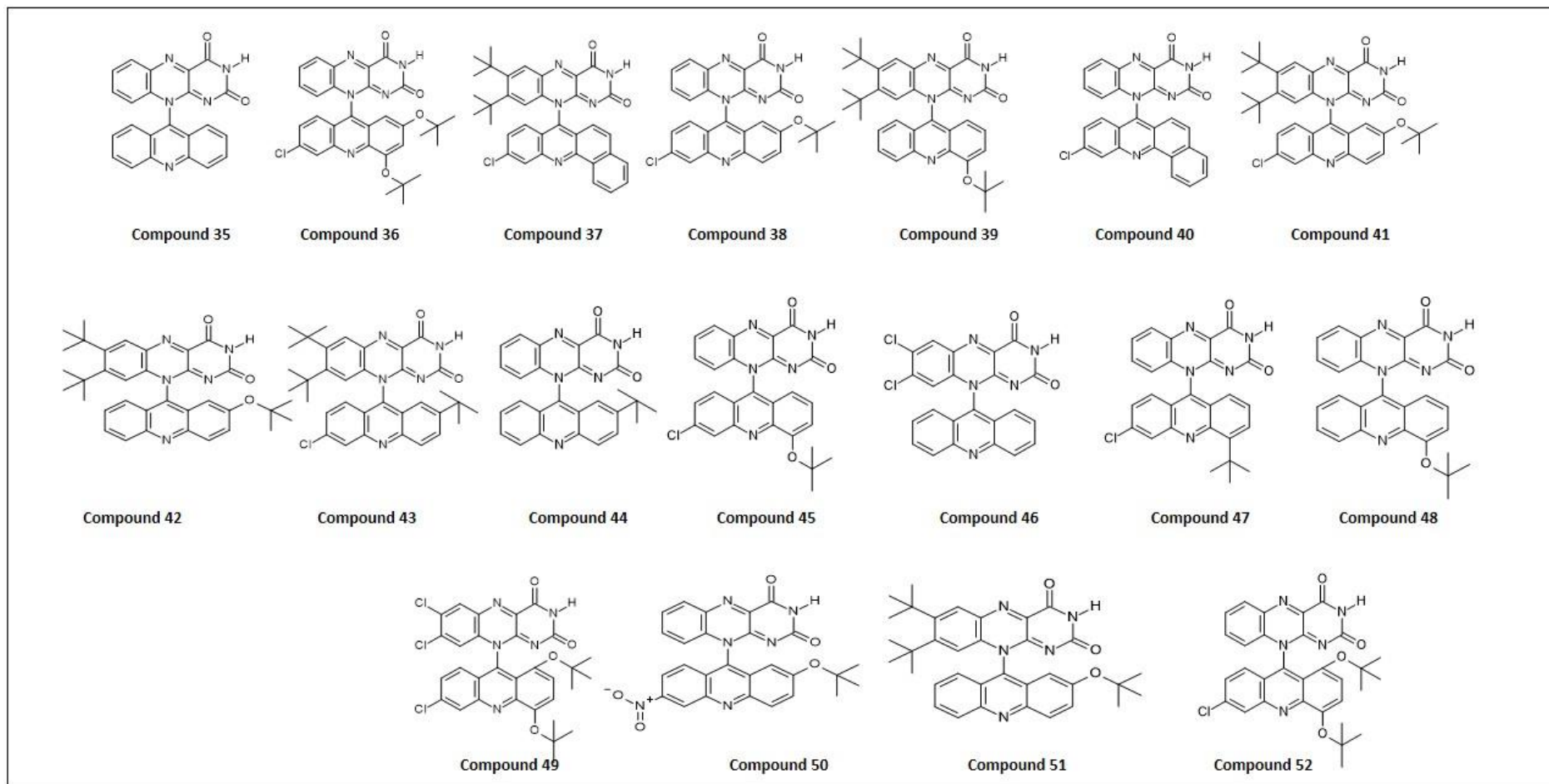
Figure 5.1 Chemical structures of novel acridine-isoalloxazine derivatives.

Table 5.1 Structures of substituted acridine-isoalloxazine containing different R groups.
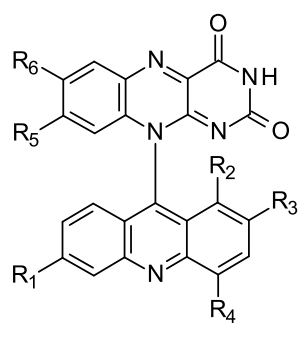
Compound	R_1	R_2	R_3	R_4	R_5	R_6
35	H	H	H	H	H	H
36	Cl	H	OCH_3	OCH_3	H	H
37	Cl	H	H	Fused Phenyl	CH_3	CH_3
38	Cl	H	OCH_3	H	H	H
39	H	H	H	OCH_3	CH_3	CH_3
40	Cl	H	H	Fused Phenyl	H	H
41	Cl	H	OCH_3	H	CH_3	CH_3
42	H	H	OCH_3	H	CH_3	CH_3
43	Cl	H	CH_3	H	CH_3	CH_3
44	H	H	CH_3	H	H	H
45	Cl	H	H	OCH_3	H	H
46	H	H	H	H	Cl	Cl
47	Cl	H	H	CH_3	H	H
48	H	H	H	OCH_3	H	H
49	Cl	OCH_3	H	H	Cl	Cl
50	NO_2	H	OCH_3	H	H	H
51	H	H	OCH_3	H	CH_3	CH_3
52	Cl	OCH_3	H	OCH_3	H	H

5.2.1 Photochemical characterisation of acridine-isoalloxazine compounds

5.2.1.1 Singlet oxygen ($^1O_2$) data

The acridine-isoalloxazine compounds were previously characterised by Dr Rob Smith's group at UCLan using the 2,3,4,5-tetraphenylcyclopentadienone (TPCPD) assay to measure the relative singlet oxygen of the compounds against alloxazine as a standard.

Firstly, the wavelength of maximum absorbance, λmax, was determined for each of the compounds in order to identify the corresponding visible light range for best excitation. As such, the absorption spectrum between the wavelengths 250-800 nm was taken for each of the compounds (Table 5.2). For all the novel acridine-isoalloxazine compounds, the λmax of the compounds ranged between 300-443 nm, which means they absorb in the UV-blue light region and thus are activated by blue light.

The radical and $^1O_2$ species released from photosensitisers, under visible light illumination, can inactivate microbial infections (Hamblin *et al.,* 2004; Jori *et al.,* 2006). Therefore, to measure singlet oxygen species released following the exposure of acridine-isoalloxazine compounds to blue light, they were assayed using the decolourisation of 2,3,4,5-tetraphenylcyclopentadienone (TPCPD) in DMSO. The absorbance of TPCPD alone and the active mixture, at a wavelength of 506 nm, was monitored over time using a UV-Visible spectrophotometer (Shimadzu-UV-3600) in the presence of blue light. It was assumed that the resultant drop in absorption of TPCPD in DMSO at 506 nm, due to decolourisation, is proportional to its reaction with singlet oxygen species. As such, the level of singlet oxygen release from each of the compounds could be determined. An example set of data is shown in Table 5.2, where the absorbance of TPCPD decreases over a period of 5 min following exposure of Compound 45 to blue light. By determining the gradient of the linear portion of the graph, the half-life of the compound can be calculated.

The illuminated compounds were ranked according to the half-life resultant from blue light illumination. It was assumed that the lower the half-life of TPCPD following exposure to acridine-isoalloxazine compounds and blue light, the greater its $^1O_2$ yield. Fourteen acridine-isoalloxazine compounds did not show a half-life over 20-minute illumination except Compounds 37, 45, 47 and 49. This data suggests that Compound 45 released the most singlet oxygen within the acridine-isoalloxazine compounds tested. It was followed by Compounds 47 ($t_{1/2}$ = 6.5 min), 49 ($t_{1/2}$ = 8 min) and 37 ($t_{1/2}$ = 12 min), which showed lower half-life (Table 5.2). Following excitation with blue light over a 60-minute period, it was noted that most singlet oxygen was released from the tested compounds after 20-minute blue light excitation.

Table 5.2 Acridine-isoalloxazine compounds characterised according to the half-life obtained following 20 min blue light exposure. As the decrease of absorption of TPCPD at 506 nm is directly proportional to singlet oxygen release and the lower the half-life the more singlet oxygen production. λmax is determined to be the wavelength at which absorbance is highest.

Compounds	λmax (nm)	Half-life min	Relative singlet oxygen
Alloxazine	391	145	1
35	343	137	1.23
36	421	45	3.78
37	401	12	14.430
38	380	52.5	3.298
39	345	76.06	2.28
40	401	45	3.78
41	348	27.5	6.297
42	353	210	0.85
43	443	39	4.2
44	365	245	0.73
45	350	5	34.633
46	348	47	3.4
47	360	6.5	26.64
48	343	105.87	1.636
49	367	8	21.645
50	388	218	0.81
51	300	166	0.92
52	353	110	1.71

5.2.1.2   Radical species data

Data on radical species, another damaging factor released within PDT, could not be measured *in vitro* using both assays DPPH and ABTS for the same reasons mentioned in Chapter 3.

5.2.1.2.1   DPPH assay

The absorbance of DPPH· has been degraded directly following the addition of compounds dissolved in DMSO. For instance, the DPPH· absorbance was 1.45, which decreased dramatically to 0.1 when adding Compound 36 in the presence or absence of blue light. The problem is that all tested acridine-isoalloxazines caused dramatic degradation of the absorbance of DPPH· when added to it in the absence and presence of blue light.

5.2.1.2.2   ABTS assay

After the compounds were added to ABTS·+, they were exposed to blue light and then absorbance readings taken. It has been shown that the absorbance of the ABTS·+ was degraded directly after the addition of acridine-isoalloxazines in the presence and absence of blue light. For instance, the ABTS·+ absorbance was 1.52, which decreased markedly to 0.89 when Compound 40 was added in the presence or absence of blue light.

5.2.2 Antifungal screening

The 18 candidate compounds, based on acridine-isoalloxazine, were screened using the EUCAST microbroth dilution method for antifungal activity against *S. cerevisiae, C. albicans* and *A. fumigatus*. These species were exposed to a range of concentrations of the candidate compounds (0 to 250 µg/ml) in the presence and absence of blue light. This range of concentrations of acridine-isoalloxazine compounds was chosen because higher concentrations of compounds showed limited solubility. Growth was determined by measuring the OD at 530 nm for *S. cerevisiae* and *C. albicans* and visually for *A. fumigatus*.

Growth inhibition percentage for each concentration of compound, in the presence and absence of blue light, was calculated against the OD_{530nm} of the drug-free control (100%). The well-characterised antifungal agents, fluconazole and amphotericin B, were used as positive controls. All compounds were tested on two separate occasions in duplicate. However, if a compound was identified as having antimicrobial activity based on these two assays, it was tested for a third time.

The heat maps shown in Figures 5.2 and 5.3 summarise the percentage growth inhibition determined from the OD_{530nm} readings for fungal growth for concentrations of fluconazole and compounds exposed to blue light for 20 min at 24 h incubation. The concentrations of fluconazole (control) used were 0 to 64 µg/ml, while concentrations of the compounds were 0 to 250 µg/ml. The colour in the heatmap indicates the percentage growth, with black indicating complete growth (0% inhibition), and red indicating no growth (100% inhibition). Yellow indicates 50% growth inhibition, which aligns with the minimal growth inhibition (MIC), as determined by the EUCAST method (EUCAST 7.3: Arendrup *et al*., 2015a)(Figures 5.2 and 5.3).

Previous data in Chapter 3 demonstrated that blue light alone has no significant effect on the growth of fungal and bacterial species (Figures 3.3 to 3.6). Therefore, any antimicrobial efficacy will be due to the tested photoactivated compounds.
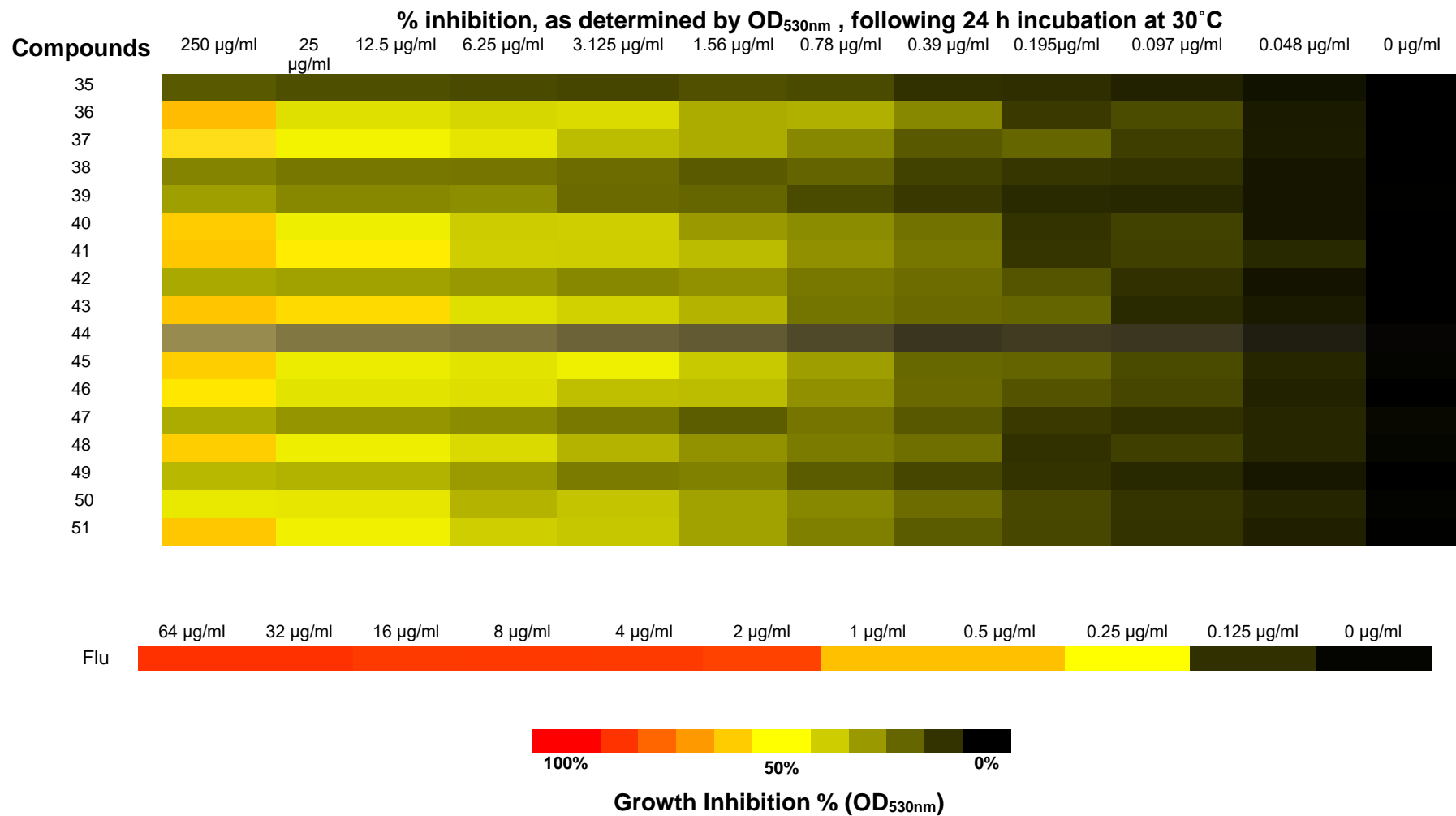
Figure 5.2 Heatmap illustrating OD$_{530nm}$ levels for varying concentrations of a list of 18 acridine-isoalloxazine compounds (0 to 250 µg/ml) against *S. cerevisiae*. The yellow bar shows 50% growth inhibition while the red bar illustrates the maximum growth inhibition
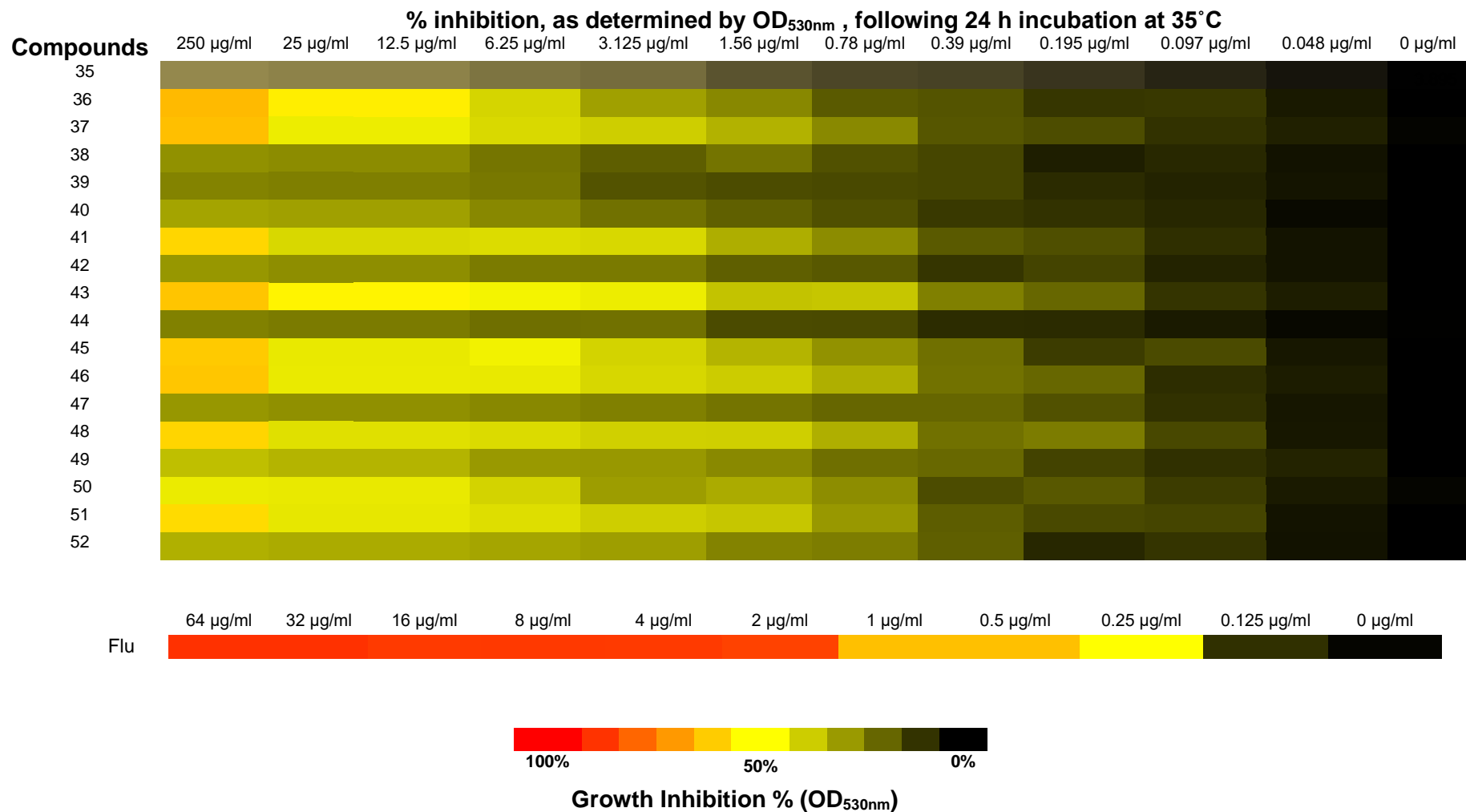
Figure 5.3 Heatmap illustrating OD$_{530nm}$ levels for varying concentrations of a list of 18 acridine-isoalloxazine compounds (0 to 250 μg/ml) against *C. albicans*. The yellow bar shows 50% growth inhibition while the red bar illustrates the maximum growth inhibition.

The minimum inhibitory concentration MIC of the tested compounds was identified to be the first concentration showing 50% growth inhibition compared to the drug-free control (EUCAST 7.3: Arendrup *et al.*, 2015a). To determine percentage growth inhibition, the optical density OD_{530nm} readings for fungal growth were taken for each concentration of fluconazole and compounds exposed to blue light for 10 and 20 min at 24 h incubation.

Following the EUCAST microdilution method, for each of the compounds the maximum growth inhibition was seen at 25 µg/ml in the presence of blue light, after 10 and 20-minute exposure. Regarding fluconazole, the maximum growth inhibition seen was at the concentration of 64 µg/ml. All graphs show the mean ±SEM (standard error of the mean) of the antifungal screening experiments in the presence and absence of blue light (Figures 5.4 to 5.21) and Table 5.3 shows the determined MIC (50% growth inhibition compared to the control) of each of the tested compounds in *S. cerevisiae* and *C. albicans*. In all cases, growth inhibition of less than 14% was seen in the no blue light control.
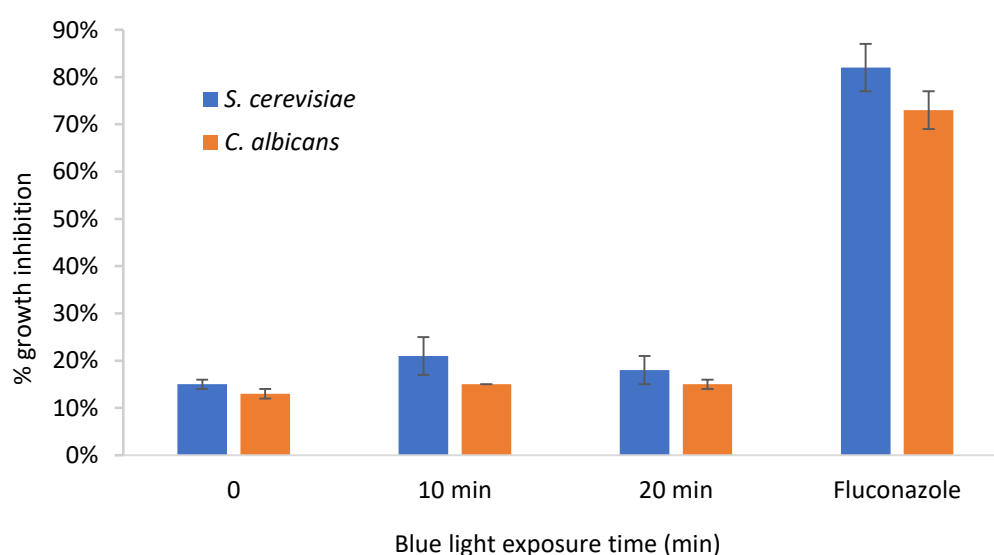
Figure 5.4 Percentage growth inhibition of *S. cerevisiae* and *C. albicans* with Compound 35 in absence and presence of blue light. Comparison of Compound 35 with fluconazole on both *S. cerevisiae* and *C. albicans* growth inhibition percentage obtained in the absence and presence of blue light. The experiment was conducted using EUCAST broth microdilution method and standardised inoculum of 0.5-2.5 x 10^5 cfu/ml. The experiment was conducted in duplicate, n=2. Values are the mean ±SEM.
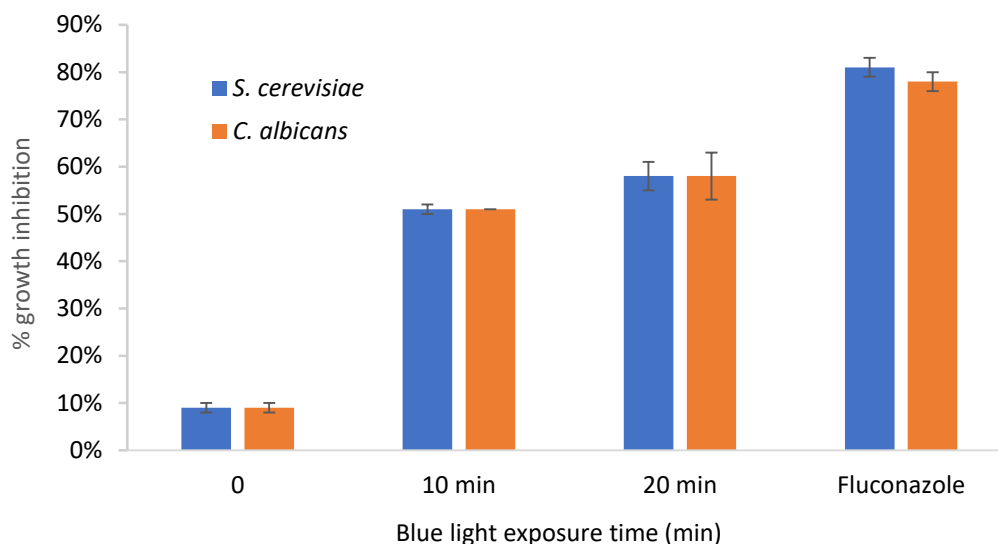
Figure 5.5 Percentage growth inhibition of *S. cerevisiae* and *C. albicans* with Compound 36 in absence and presence of blue light. Comparison of Compound 36 with fluconazole on both *S. cerevisiae* and *C. albicans* growth inhibition percentage obtained in the absence and presence of blue light. The experiment was conducted using EUCAST broth microdilution method and standardised inoculum of 0.5-2.5 x 10^5 cfu/ml. The experiment was conducted in duplicate, n=3. Values are the mean ±SEM.
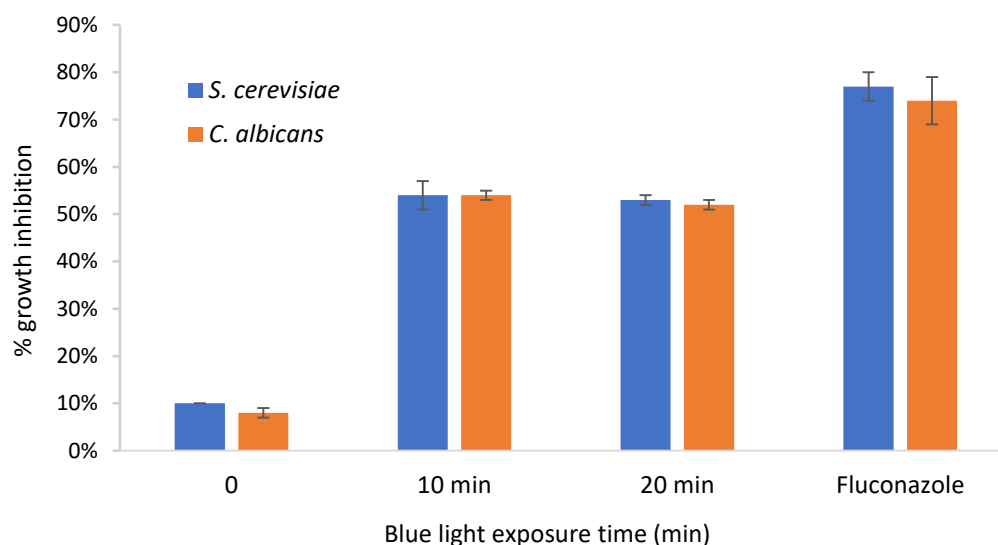
Figure 5.6 Percentage growth inhibition of *S. cerevisiae* and *C. albicans* with Compound 37 in absence and presence of blue light. Comparison of Compound 37 with fluconazole on both *S. cerevisiae* and *C. albicans* growth inhibition percentage obtained in the absence and presence of blue light. The experiment was conducted using EUCAST broth microdilution method and standardised inoculum of 0.5-2.5 x 10^5 cfu/ml. The experiment was conducted in duplicate, n=3. Values are the mean ±SEM.
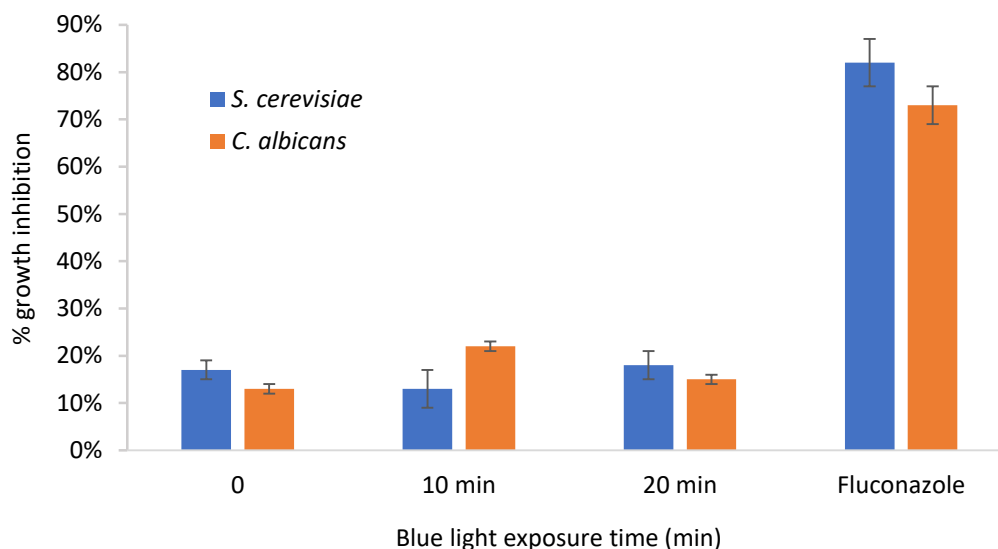
Figure 5.7 Percentage growth inhibition of *S. cerevisiae* and *C. albicans* with Compound 38 in absence and presence of blue light. Comparison of Compound 38 with fluconazole on both *S. cerevisiae* and *C. albicans* growth inhibition percentage obtained in the absence and presence of blue light. The experiment was conducted using EUCAST broth microdilution method and standardised inoculum of 0.5-2.5 x 10^5 cfu/ml. The experiment was conducted in duplicate, n=2. Values are the mean ±SEM.
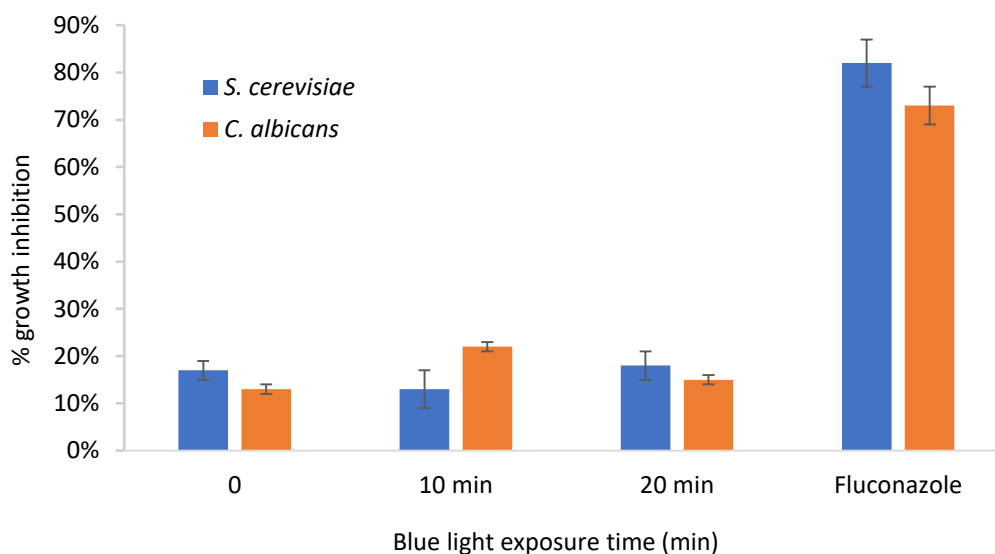
Figure 5.8 Percentage growth inhibition of *S. cerevisiae* and *C. albicans* with Compound 39 in absence and presence of blue light. Comparison of Compound 39 with fluconazole on both *S. cerevisiae* and *C. albicans* growth inhibition percentage obtained in the absence and presence of blue light. The experiment was conducted using EUCAST broth microdilution method and standardised inoculum of 0.5-2.5 x 10^5 cfu/ml. The experiment was conducted in duplicate, n=2. Values are the mean ±SEM.
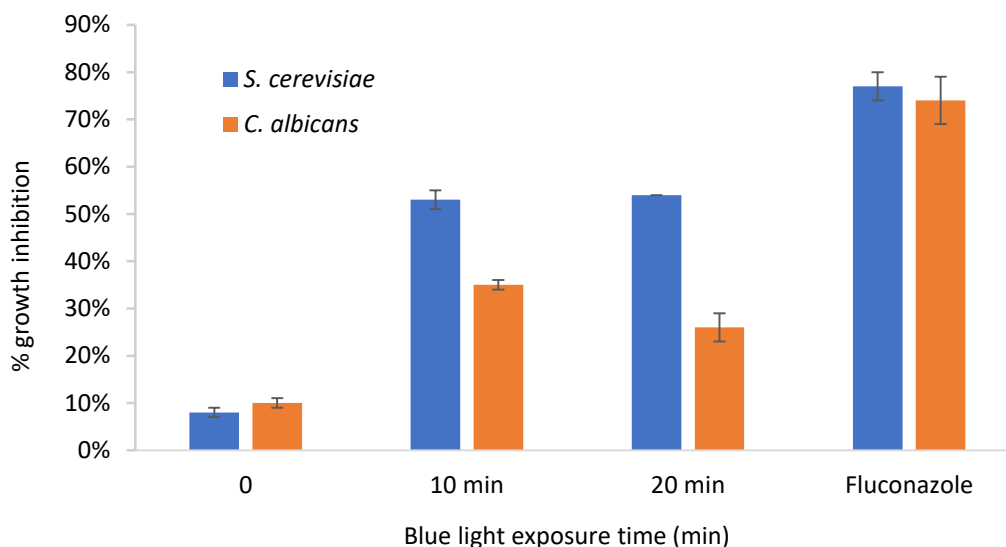
Figure 5.9 Percentage growth inhibition of *S. cerevisiae* and *C. albicans* with Compound 40 in absence and presence of blue light. Comparison of Compound 40 with fluconazole on both *S. cerevisiae* and *C. albicans* growth inhibition percentage obtained in the absence and presence of blue light. The experiment was conducted using EUCAST broth microdilution method and standardised inoculum of 0.5-2.5 x 10^5 cfu/ml. The experiment was conducted in duplicate, n=3. Values are the mean ±SEM.
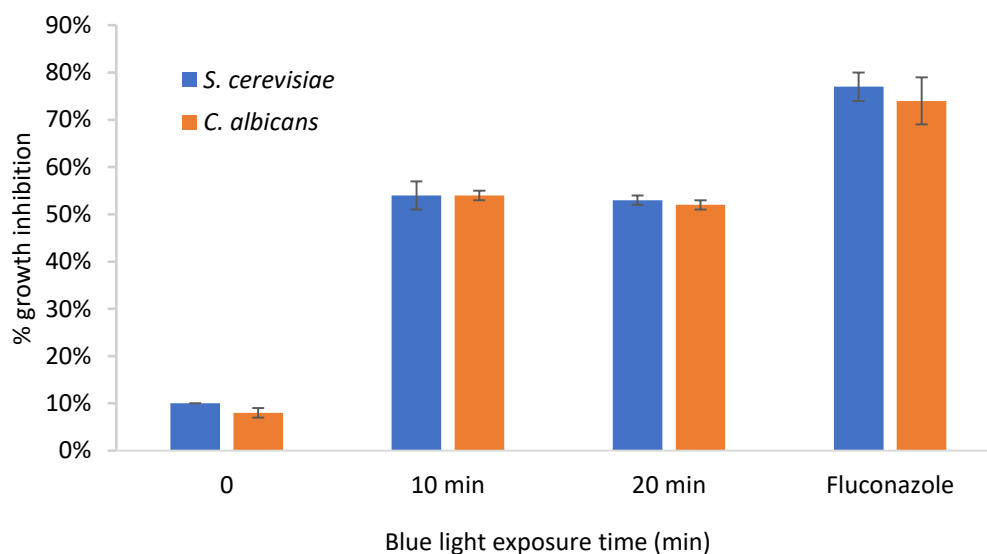
Figure 5.10 Percentage growth inhibition of *S. cerevisiae* and *C. albicans* with Compound 41 in absence and presence of blue light. Comparison of Compound 41 with fluconazole on both *S. cerevisiae* and *C. albicans* growth inhibition percentage obtained in the absence and presence of blue light. The experiment was conducted using EUCAST broth microdilution method and standardised inoculum of 0.5-2.5 x 10^5 cfu/ml. The experiment was conducted in duplicate, n=3. Values are the mean ±SEM.
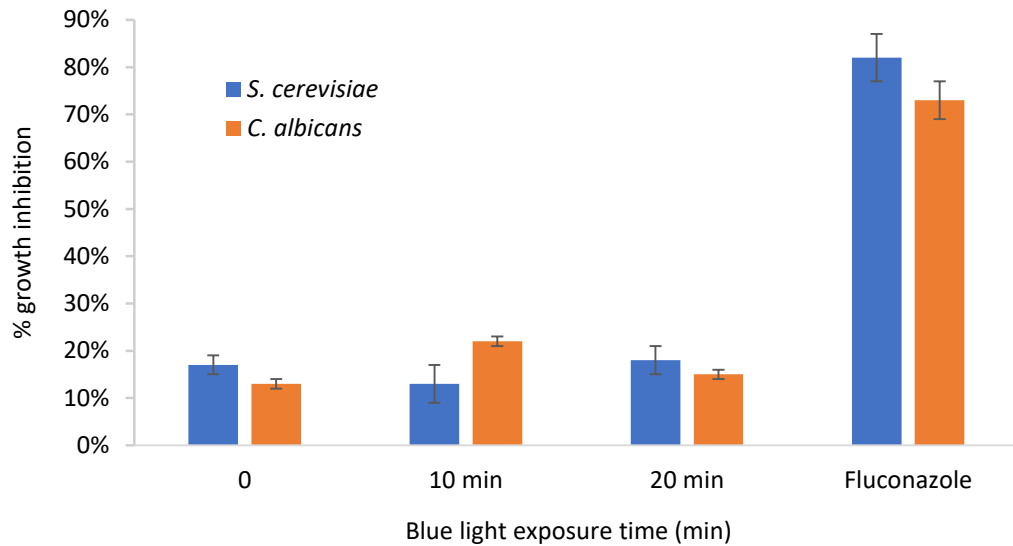
Figure 5.11 Percentage growth inhibition of *S. cerevisiae* and *C. albicans* with Compound 42 in absence and presence of blue light. Comparison of Compound 42 with fluconazole on both *S. cerevisiae* and *C. albicans* growth inhibition percentage obtained in the absence and presence of blue light. The experiment was conducted using EUCAST broth microdilution method and standardised inoculum of 0.5-2.5 x 10^5 cfu/ml. The experiment was conducted in duplicate, n=2. Values are the mean ±SEM.
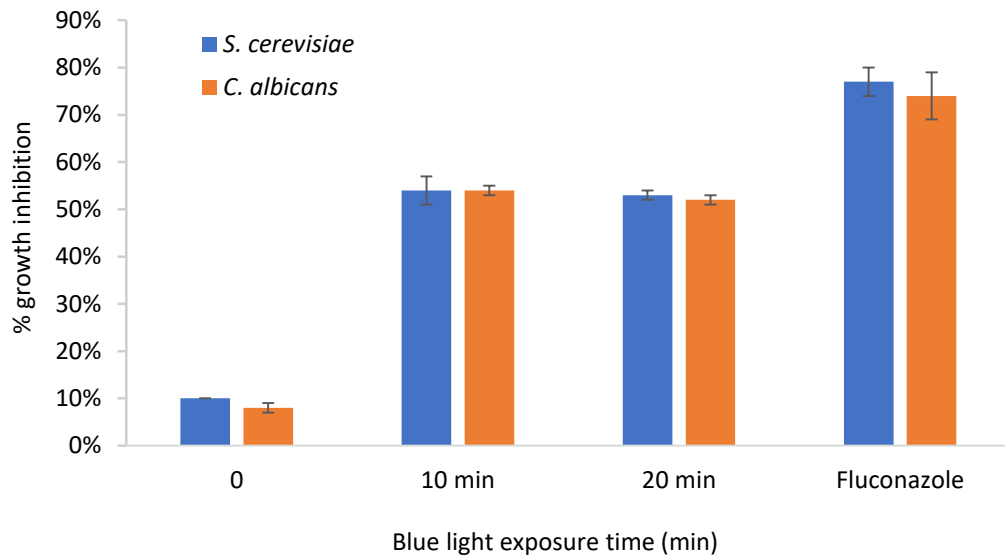
Figure 5.12 Percentage growth inhibition of *S. cerevisiae* and *C. albicans* with Compound 43 in absence and presence of blue light. Comparison of Compound 43 with fluconazole on both *S. cerevisiae* and *C. albicans* growth inhibition percentage obtained in the absence and presence of blue light. The experiment was conducted using EUCAST broth microdilution method and standardised inoculum of 0.5-2.5 x 10^5 cfu/ml. The experiment was conducted in duplicate, n=3. Values are the mean ±SEM.
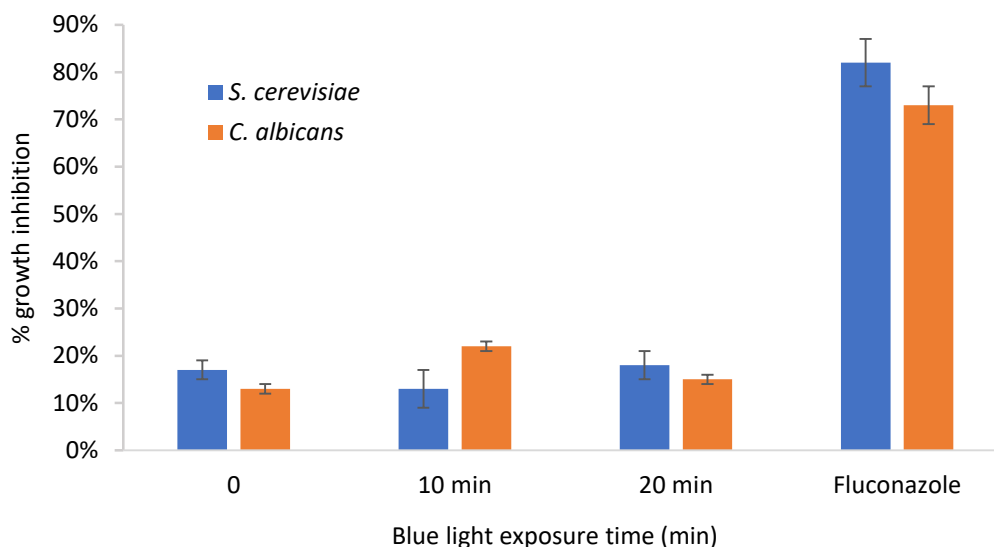
Figure 5.13 Percentage growth inhibition of *S. cerevisiae* and *C. albicans* with Compound 44 in absence and presence of blue light. Comparison of Compound 44 with fluconazole on both *S. cerevisiae* and *C. albicans* growth inhibition percentage obtained in the absence and presence of blue light. The experiment was conducted using EUCAST broth microdilution method and standardised inoculum of 0.5-2.5 x 10^5 cfu/ml. The experiment was conducted in duplicate, n=2. Values are the mean ±SEM.
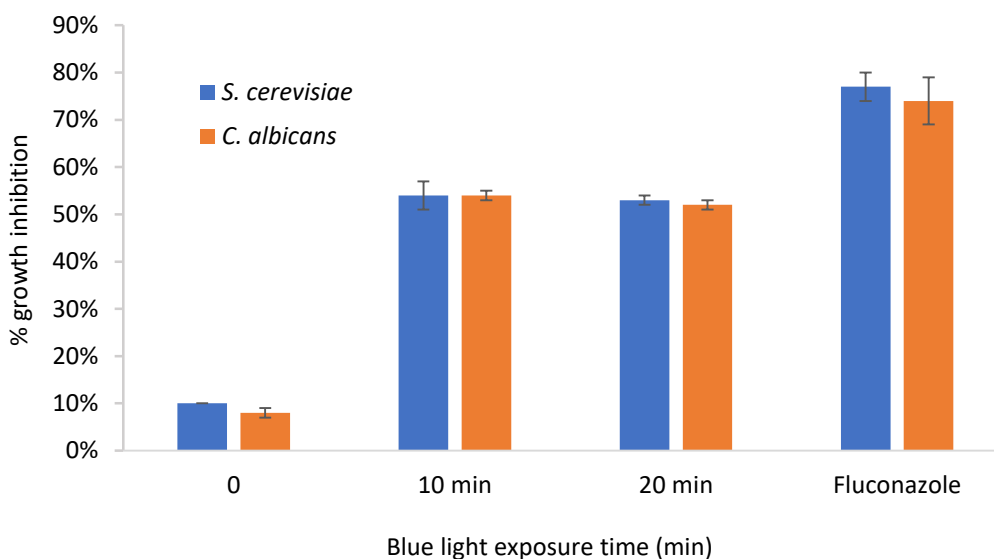
Figure 5.14 Percentage growth inhibition of *S. cerevisiae* and *C. albicans* with Compound 45 in absence and presence of blue light. Comparison of Compound 45 with fluconazole on both *S. cerevisiae* and *C. albicans* growth inhibition percentage obtained in the absence and presence of blue light. The experiment was conducted using EUCAST broth microdilution method and standardised inoculum of 0.5-2.5 x 10^5 cfu/ml. The experiment was conducted in duplicate, n=3. Values are the mean ±SEM.
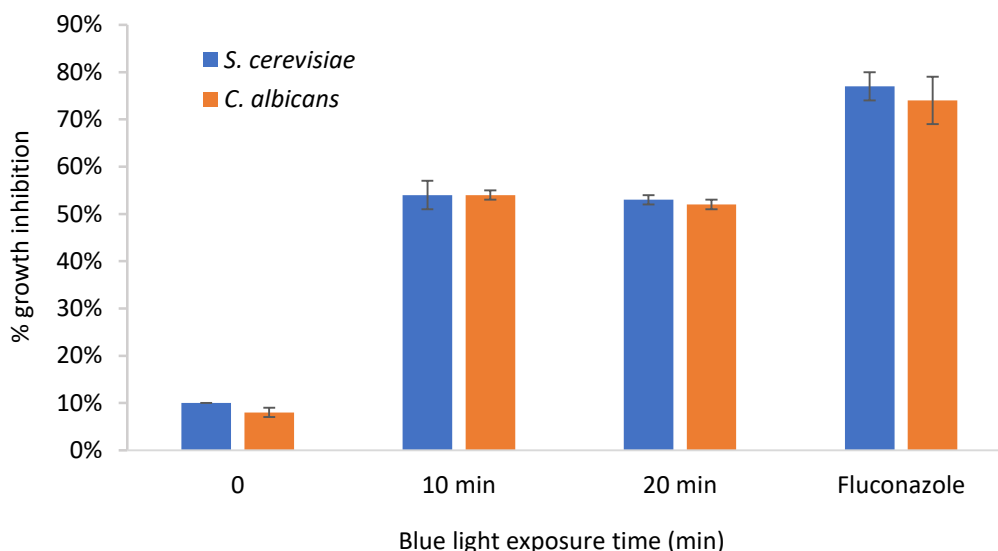
Figure 5.15 Percentage growth inhibition of *S. cerevisiae* and *C. albicans* with Compound 46 in absence and presence of blue light. Comparison of Compound 46 with fluconazole on both *S. cerevisiae* and *C. albicans* growth inhibition percentage obtained in the absence and presence of blue light. The experiment was conducted using EUCAST broth microdilution method and standardised inoculum of 0.5-2.5 x 10^5 cfu/ml. The experiment was conducted in duplicate, n=3. Values are the mean ±SEM.
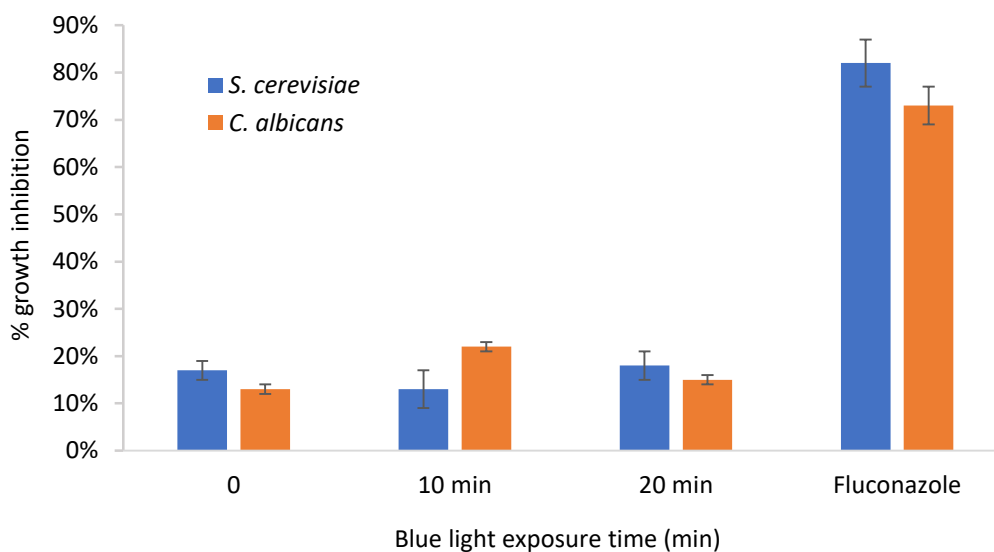
Figure 5.16 Percentage growth inhibition of *S. cerevisiae* and *C. albicans* with Compound 47 in absence and presence of blue light. Comparison of Compound 47 with fluconazole on both *S. cerevisiae* and *C. albicans* growth inhibition percentage obtained in the absence and presence of blue light. The experiment was conducted using EUCAST broth microdilution method and standardised inoculum of 0.5-2.5 x 10^5 cfu/ml. The experiment was conducted in duplicate, n=2. Values are the mean ±SEM.
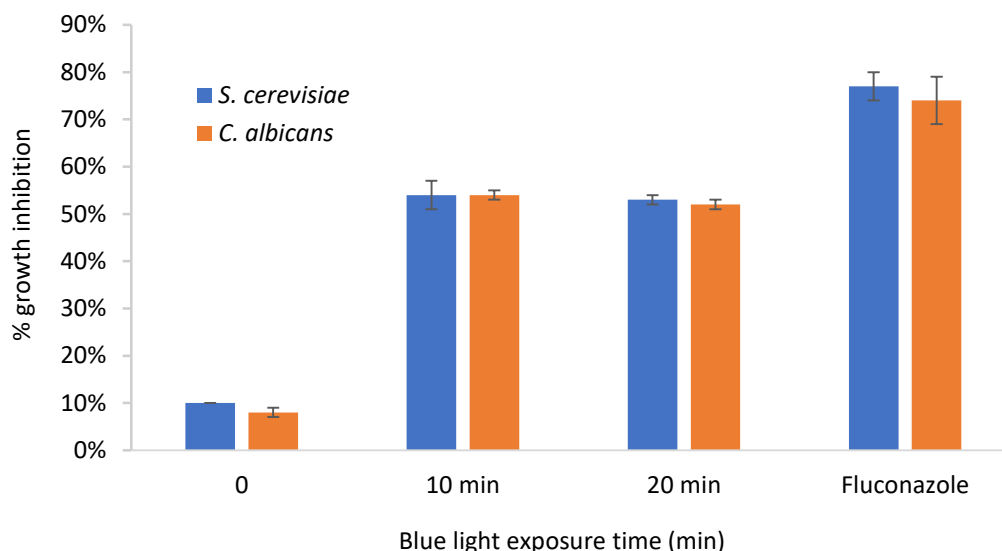
Figure 5.17 Percentage growth inhibition of *S. cerevisiae* and *C. albicans* with Compound 48 in absence and presence of blue light. Comparison of Compound 48 with fluconazole on both *S. cerevisiae* and *C. albicans* growth inhibition percentage obtained in the absence and presence of blue light. The experiment was conducted using EUCAST broth microdilution method and standardised inoculum of 0.5-2.5 x 10^5 cfu/ml. The experiment was conducted in duplicate, n=3. Values are the mean ±SEM.
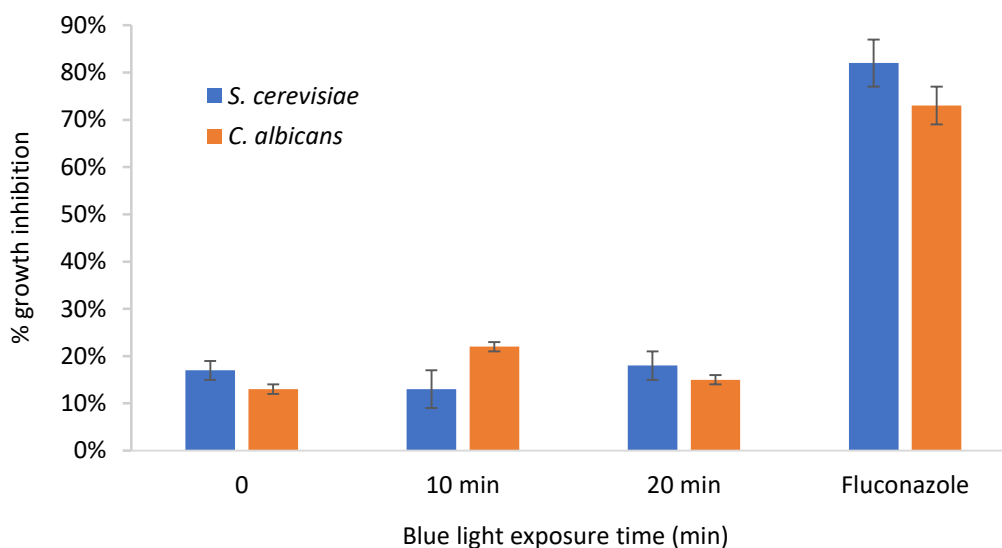
Figure 5.18 Percentage growth inhibition of *S. cerevisiae* and *C. albicans* with Compound 49 in absence and presence of blue light. Comparison of Compound 49 with fluconazole on both *S. cerevisiae* and *C. albicans* growth inhibition percentage obtained in the absence and presence of blue light. The experiment was conducted using EUCAST broth microdilution method and standardised inoculum of 0.5-2.5 x 10^5 cfu/ml. The experiment was conducted in duplicate, n=2. Values are the mean ±SEM.
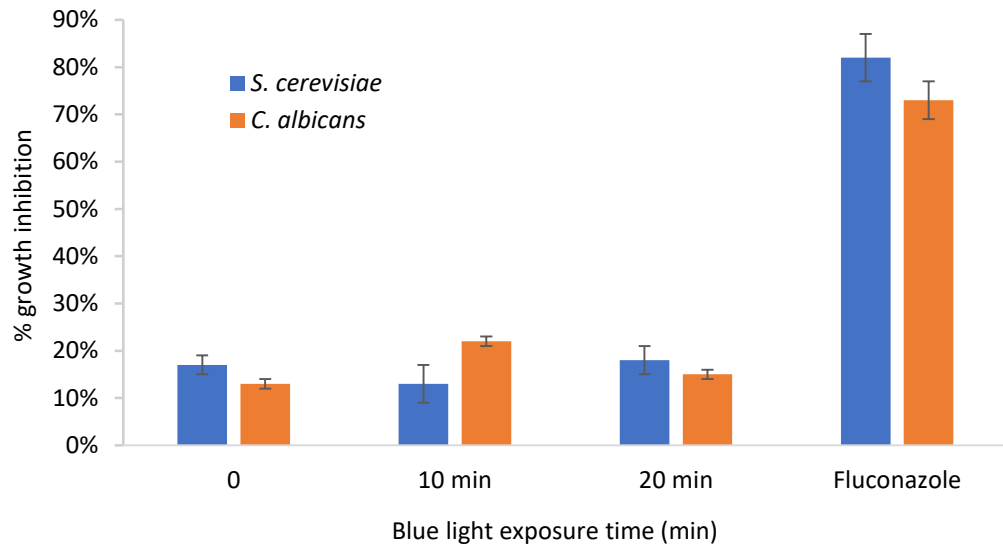
Figure 5.19 Percentage growth inhibition of *S. cerevisiae* and *C. albicans* with Compound 50 in absence and presence of blue light. Comparison of Compound 50 with fluconazole on both *S. cerevisiae* and *C. albicans* growth inhibition percentage obtained in the absence and presence of blue light. The experiment was conducted using EUCAST broth microdilution method and standardised inoculum of 0.5-2.5 x 10^5 cfu/ml. The experiment was conducted in duplicate, n=2. Values are the mean ±SEM.
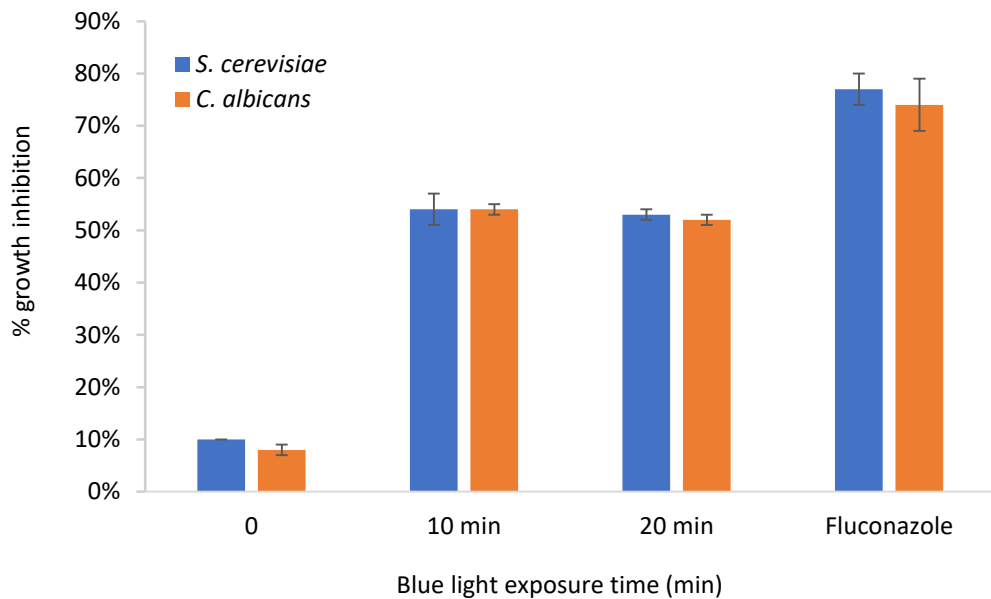
Figure 5.20 Percentage growth inhibition of *S. cerevisiae* and *C. albicans* with Compound 51 in absence and presence of blue light. Comparison of Compound 51 with fluconazole on both *S. cerevisiae* and *C. albicans* growth inhibition percentage obtained in the absence and presence of blue light. The experiment was conducted using EUCAST broth microdilution method and standardised inoculum of 0.5-2.5 x 10^5 cfu/ml. The experiment was conducted in duplicate, n=3. Values are the mean ±SEM.

Table 5.3 Summary of the minimum inhibitory concentrations (MICs) of the 18 acridine-isoalloxazine compounds in *S. cerevisiae* and *C. albicans* using the EUCAST method after 10 and 20 min blue light exposure. MIC is the concentration at which 50% growth inhibition is seen. (-) means MIC value could not be determined at the maximum concentration tested (250 µg/ml).

Studied compounds	Fungi			
	10 min blue light exposure		20 min blue light exposure	
	MIC (µg/ml) against *S. cerevisiae*	MIC (µg/ml) against *C. albicans*	MIC (µg/ml) against *S. cerevisiae*	MIC (µg/ml) against *C. albicans*
Fluconazole	0.25	1	0.25	1
Compound 35	-	-	-	-
Compound 36	16.5	25	12.5	25
Compound 37	25	25	16.5	25
Compound 38	-	-	-	-
Compound 39	-	-	-	-
Compound 40	25	-	25	-
Compound 41	12.5	12.5	12.5	12.5
Compound 42	-	-	-	-
Compound 43	12.5	16.5	12.5	12.5
Compound 44	-	-	-	-
Compound 45	-	-	-	-
Compound 46	21	21	21	21
Compound 47	-	-	-	-
Compound 48	25	25	16.5	25
Compound 49	-	-	-	-
Compound 50	-	-	-	-
Compound 51	21	21	21	21

To ensure consistency of the results, EUCAST antifungal susceptibility testing of *S. cerevisiae* and *C. albicans* to the control fluconazole was performed. The average MIC of fluconazole obtained was 0.25 µg/ml against *S. cerevisiae* and 1 µg/ml against *C. albicans*. In regard to *S. cerevisiae*, the resultant MIC of 0.25 µg/ml (Table 5.3) was located in the region of published data (MIC and zone distributions and ECOFFs; EUCAST 7.3: Arendrup *et al.*, 2015a). The resultant MIC of 1 µg/ml against *C. albicans* corresponded with the EUCAST Antifungal Clinical Breakpoints (EUCAST 7.3: Arendrup *et al.*, 2015a).

None of the compounds have a significant antifungal activity in the absence of blue light against both species. Since the tested compounds showed no significant effect on growth of cells in the absence of blue light, any possible antifungal efficacy will be due to blue light treated compounds.

A lower MIC value means that less amount of drug is required for inhibiting growth of microbes, therefore the lower the MIC, the more effective antimicrobial drugs. By analysing the MIC results in Table 5.3, it can be noted that among all the eight studied compounds, Compounds 36 (12.5, 25 µg/ml), 37 (16.5, 25 µg/ml), 40 (12.5, 12.5 µg/ml), 41 (12.5, 12.5 µg/ml), 43 (21, 21 µg/ml), 46 (21, 21 µg/ml), 48 (16.5, 25 µg/ml) and 51 (21, 21 µg/ml), showed antifungal efficacy following 20-minute blue light exposure against *S. cerevisiae* and *C. albicans*, respectively. The data shows that Compound 40 showed antifungal activity against *S. cerevisiae* with MIC of 25 µg/ml but showed no effect on *C. albicans* at the maximum concentration tested. Compounds 41, 46 and 51 showed a similar susceptibility against both species over 10 and 20-minute blue light exposure (Table 5.3)*. S. cerevisiae* showed more susceptibility to Compounds 36, 37 and 48 than *C. albicans* following 20-minute blue light illumination. While under 10-minute blue light exposure, the susceptibility of *S. cerevisiae to* Compounds 36 and 43 was more than *C. albicans,* showing MIC of 16.5, 12.5 µg/ml for Compound 36 and 12.5, 16.5 µg/ml for Compound 43, respectively (Table 5.3).

A. fumigatus was also screened using the EUCAST antifungal MIC microdilution method for moulds (EUCAST 9.3: Arendrup *et al.*, 2015b). Due to the growth of *A. fumigatus*, instead of measuring the optical density to determine percentage growth inhibition, a visual inspection was undertaken. In this case the MIC was determined to be the first well where the concentration of compound resulted in complete absence of growth. The concentrations range tested for the control drug

amphotericin B was 0-16 μg/ml. The control drug amphotericin B was effective against *A. fumigatus* showing MIC of 0.125 μg/ml, which matched the MIC EUCAST breakpoint in *A. fumigatus.* The antifungal screening demonstrated that acridine-isoalloxazine compounds, following exposure to blue light, did not exhibit any efficacy against *A. fumigatus* at the concentrations tested (0 to 250 μg/ml) by visual determination of growth (data not shown).

5.2.3 Antibacterial screening

Following antifungal screening of the acridine-isoalloxazine compounds, these compounds were then screened *in vitro* for their antibacterial efficacy under blue light exposure against two clinically important bacteria Gram-positive *S. aureus* and Gram-negative *E. coli*.

The acridine-isoalloxazine compounds were screened, using the European Committee for Antimicrobial Susceptibility Testing (EUCAST) microbroth dilution method, for antibacterial activity (EUCAST 5.1: EUCAST, 2003).

 The antibacterial drug gentamicin, was used as a control due to its broad antibacterial activity against both Gram-negative and Gram-positive bacteria (Jao *et al.*, 1964).The bacterial species were exposed to a range of concentrations of the compounds (0 to 256 μg/ml) in the presence and absence of blue light. A 20-minute illumination period was used due to the release of most singlet oxygen from the compounds. The MIC was determined, by visual inspection, to be the lowest concentration that completely inhibited growth. The experiments were repeated two times in duplicate, except for the active compounds (36, 37, 40, 41, 43, 45, 46, 48, 49, and 51), which were repeated on three occasions in duplicate.

Table 5.4 Summary of the minimum inhibitory concentrations (MICs) of the acridine-isoalloxazine compounds in _S. aureus_ and _E. coli_ using the EUCAST method after 10 and 20 min blue light exposure. (-) means MIC value could not be determined at the maximum concentration tested.

Studied compounds	Bacteria			
	10 min blue light exposure		20 min blue light exposure	
	MIC (µg/ml) against _S. aureus_	MIC (µg/ml) against _E. coli_	MIC (µg/ml) against _S. aureus_	MIC (µg/ml) against _E. coli_
Gentamicin	0.5	0.25	0.5	0.25
Compound 35	-	-	-	-
Compound 36	8	16	8	16
Compound 37	24	32	8	64
Compound 38	-	-	-	-
Compound 39	-	-	-	-
Compound 40	32	-	24	64
Compound 41	8	64	32	64
Compound 42	-	-	-	-
Compound 43	8	8	24	32
Compound 44	-	-	-	-
Compound 45	24	24	24	24
Compound 46	32	128	32	128
Compound 47	-	-	-	-
Compound 48	24	128	24	128
Compound 49	128	-	24	-
Compound 50	-	-	-	-
Compound 51	24	64	24	64

EUCAST antibacterial susceptibility testing of *S. aureus* and *E. coli* to the control gentamicin was performed and the resultant MICs of 0.5 and 0.25 µg/ml corresponded with EUCAST Antibacterial Clinical Breakpoints (EUCAST 9.3: Arendrup *et al*., 2015b), which confirms the accuracy of the assay (Table 5.4). Since the acridine-isoalloxazine compounds did not exhibit a significant antibacterial efficacy in the absence of blue light, any bacterial inactivation observed following blue light illumination must be due to photosensitisation of the compounds.

By analysing the MIC results (Table 5.4) ten acridine-isoalloxazine compounds showed little effect on bacterial growth after 20-minute blue light irradiation. Compound 36 showed the lowest MICs of all the compounds tested against *S. aureus* and *E. coli* with 8 and 16 µg/ml, respectively. Following 20-minute blue light exposure, only Compound 49 exhibited an antibacterial activity against *S. aureus* at 24 µg/ml without activity against *E. coli*.

S. aureus was more susceptible than *E. coli* against Compound 36 at 8, 16 µg/ml, Compound 37 at 8, 64 µg/ml, Compound 40 at 24, 64 µg/ml, Compound 41 at 32, 64 µg/ml, Compound 43 at 24, 32 µg/ml, Compound 46 at 32, 128µg/ml, Compound 48 at 24, 128 µg/ml and Compound 51 at 24, 64 µg/ml after 20-minute blue light exposure. Based on the data in Table 5.4, it is apparent that the Gram-positive bacterium, *S. aureus,* is more sensitive to the compounds, following exposure to blue light, than the Gram-negative bacterium, *E. coli*.

By combining the MIC values of the acridine-isoalloxazine compounds against bacterial and fungal species in Table 5.5, it can be noted that there is a difference in the sensitivity of fungi and bacteria to the tested compounds. Compound 45, for instance, showed only antibacterial activity at MIC 24 µg/ml without any antifungal effect while Compound 49 exhibited only antibacterial activity against *S. aureus* at MIC 24 µg/ml after 20-minute blue light exposure without any effect against *E. coli*, *S. cerevisiae* and *C. albicans* (Table 5.5).

Table 5.5 Summary of the minimum inhibitory concentrations (MICs) of the active acridine-isoalloxazine compounds in *S. cerevisiae*, *C. albicans* and *S. aureus*, *E. coli* using the EUCAST method after 20 min blue light exposure. (-) means MIC value could not be determined at the maximum concentration tested.

Studied compounds	Fungi		Bacteria	
	20 min blue light exposure		20 min blue light exposure	
	MIC (µg/ml) against *S. cerevisiae*	MIC (µg/ml) against *C. albicans*	MIC (µg/ml) against *S. aureus*	MIC (µg/ml) against *E. coli*
Fluconazole	0.25	1		
Gentamicin			0.5	0.25
Compound 36	12.5	25	8	16
Compound 37	16.5	25	8	64
Compound 40	25	-	24	64
Compound 41	12.5	12.5	32	64
Compound 43	12.5	12.5	24	32
Compound 45	-	-	24	24
Compound 46	21	21	32	128
Compound 48	16.5	25	24	128
Compound 49	-	-	24	-
Compound 51	21	21	24	64

5.3 Discussion

In this chapter, the aim was to screen a series of novel synthesised acridine-isoalloxazine compounds for their possible antimicrobial activity in the presence of blue light.

These compounds had previously undergone photochemical characterisation. This included identifying the relevant activating light source by examining the absorption spectrum of each compound between the wavelengths 250-800 nm. The wavelength of maximum absorbance, λmax, was then determined for each of the compounds tested to choose the light that can photosensitise them. It has been shown that λmax of the acridine compounds ranges between 300-443 nm, which corresponds with the blue light region (400-500 nm) (Table 5.2). The obtained values of acridine-isoalloxazine conjugates are consistent with other published acridines, which generally show their longest absorption wavelengths in the range between 400-500 nm (Albert, 1951) and isoalloxazines (flavins) which absorb also in the UV-blue light range (Baier *et al.*, 2006). The method of conjugating two photoactivated compounds in this study has not been previously investigated, so there is no literature to support this observation.

5.3.1 Acridine-isoalloxazines are photosensitised following exposure to blue light and release singlet oxygen

Due to the well-established photosensitising activity of various acridine compounds, such as acridine orange (Iwamoto *et al.*, 1987; Iwamoto *et al.*, 1993), and isoalloxazine derivatives, such as riboflavin (Heelis *et al.* 1982), a set of novel synthesised acridine-isoalloxazine derivatives has been synthesised and characterised photochemically to quantify singlet oxygen release following activation by blue light over a 60-minute period.

The photochemical reactions of the triplet state of photosensitiser such as acridine-isoalloxazines following blue light exposure can be divided into two different pathways, either the Type 1 mechanism that leads to the production of radical species or the Type 2 mechanism that results in $^1O_2$ release. Both these species, radicals and $^1O_2$, can inactivate microbial cells (Castano *et al.*, 2004). Therefore, this current work has tried to measure these species under 60-minute

blue light irradiation. Within this work, two radical scavenging assays, DPPH and ABTS, were chosen as described previously in Chapter 3 in order to measure the amount of radicals released following blue light illumination. As with previous data, neither of these two assays was able to measure radicals' production from these compounds, as explained in Chapter 3. Solvent type could have a potential impact on radical production, however, both reagents exhibited stability when dissolved in DMSO in the presence and absence of blue light, yet were degraded following the addition of acridine-isoalloxazines. Alternative methods have been used as radical screening assays for other acridines and isoallxazines, including: D-mannitol, a scavenger of hydroxyl radicals or electron paramagnetic resonance (EPR) spectroscopy combined with spin trap probes (Spin-trapping) (Augusto *et al.*, 2007).

By measuring $^1O_2$ under blue light excitation for 60 min it was shown that most singlet oxygen was released from acridine-isoalloxazine compounds after 20-minute blue light excitation. It was established by using TPCPD assay, that 18 acridine-isoalloxazine compounds released singlet oxygen upon exposure to blue light for 20 min when compared with the standard's yield (alloxazine) in the *in vitro* photochemical test (Table 5.2). This finding is consistent with a study of Iwamoto *et al.,* (1987), who found that several acridines such as acriflavine (AF), proflavine (PF), acridine orange (AO) and 9-aminoacridine (AA) showed singlet oxygen activity upon irradiation with an ultraviolet (UV) lamp for 30 min by measuring the signal intensity of TEMPO detected by (ESR) spectrometry (Iwamoto *et al.,* 1987). This finding also supports findings by Baier *et al.,* (2006), who proved that UVA light (320-400) nm has been shown to generate singlet oxygen by irradiating isoalloxazine derivatives such as flavin mononucleotide (FMN) and flavin dinucleotide (FAD).

In this study, 14 acridine-isoalloxazine compounds (35, 36, 37, 38, 39, 40, 41, 43, 45, 46, 47, 48, 49 and 52) were more efficient singlet oxygen producers than the standard alloxazine, which released $^1O_2$ of value 1. The relative $^1O_2$ values of the previous 15 acridine-isoalloxazine compounds ranged between 1.23 and 34.633 (Table 5.2). However due to the structural differences between the standard compounds, comparison between the singlet oxygen production can only be done based on the $^1O_2$ yield. Although there can be a direct comparison between compound half-lives, many papers do not include this information, instead only

presenting the $^1O_2$ yield. The only conjugation which occurred was between photoactivated compounds in nanoparticles, which does not affect ROS release, but increases selectivity.

Both the isoalloxazines and acridine orange have demonstrated their ability to produce both $^1O_2$ and radicals (Iwamoto *et al.*, 1987; Losi, 2007). Based on this evidence, it is expected that compounds tested in this study work via both mechanisms, Type 1 and 2, and thus release $^1O_2$ and radicals under blue light exposure. Even though radicals could not be measured, it is assumed that they are being released in our study. The incorporation of halogens onto the acridine-isoalloxazine structure was shown to exhibit significant increase in the singlet oxygen yield (a minimum twofold increase) when compared to non-halogenated compounds. Compounds 45 ($t_{1/2} = 5$ min), 47 ($t_{1/2} = 6.5$ min) and 49 ($t_{1/2} = 8$ min), all contain a chlorine, and show the highest release of of singlet oxygen (Table 5.2). This result indicates that the heavy atom effect increases the possibility of the transition into the excited triplet state, causing an increase in the amount of singlet oxygen produced (Mehraban *et al.*, 2015). Non-halogenated Compound 44 ($t_{1/2} = 245$ min), 50 ($t_{1/2} = 218$ min), 51 ($t_{1/2} = 166$ min), produced the lowest amount of relative singlet oxygen among all the compounds tested (Table 5.2).

5.3.2 Acridine-isoalloxazines have no significant effect on microbial growth in the absence of blue light

Both acridines and isoalloxazines can penetrate bacterial and fungal cells as described previously in Chapters 3 and 4. The penetration of both moieties into the microbial cell may indicate how the acridine-isoalloxazine compounds tested in this work may behave. All compounds tested in this study demonstrated limited activity in the absence of blue light irradiation, with limited growth inhibition observed in the fungal and bacterial cells tested. A key requirement for potential photoantimicrobial compounds is to have a small molecular weight with cationic charge (Wainwright, 2015). Therefore, it can be assumed that although these compounds have cationic charge, their large molecular weight may prevent them from penetrating into the cell and thus a limited effect of these compounds was

observed on microbial growth in the absence of blue light. These compounds have not been previously investigated, consequently there is no literature to support these observations.

5.3.3 Blue light activation of acridine-isoalloxazines has an effect on microbial growth

Based on the blue light results and the absence of significant effect of acridine-isoalloxazines alone on microbial growth, any growth inhibition observed following illumination with blue light would be attributed to photoactivation. Following photochemical characterisation of the 18 compounds, their photoantimicrobial activity under blue light illumination was measured against both fungi and bacteria.

The growth inhibitory activity of tested compounds was determined by measuring minimum inhibitory concentration (MIC) values using the EUCAST broth microdilution method. To ensure consistency of the antimicrobial susceptibility testing and compare the obtained results across experiments, three control bioassays with fluconazole against *S. cerevisiae* and *C. albicans* and amphotericin B against *A. fumigatus* as well as gentamicin against *S. aureus* and *E. coli* were conducted. The obtained MIC of 0.25 µg/ml against *S. cerevisiae* was in the fluconazole wildtype distributions determined by the EUCAST broth microdilution method. Additionally, the resultant MIC of 1 µg/ml against *C. albicans* corresponded with the EUCAST Antifungal Clinical Breakpoints (EUCAST 7.3: Arendrup *et al.*, 2015a). Finally, the MIC of amphotericin B against of 0.125 µg/ml matched the MIC EUCAST breakpoint in *A. fumigatus*. With respect to bacteria, the obtained MICs of 0.25 and 0.125 µg/ml against *S. aureus* and *E. coli* corresponded with EUCAST Antibacterial Clinical Breakpoints. All control assays were conducted on each run and all the results obtained were within the expected range.

Based on photochemical data, the compounds were investigated for antimicrobial activity following 20 min of blue light illumination (470 nm, 115 J/cm^2), using the EUCAST brothmicrodilution method. The microbiological screening used in this

work identified eight compounds with photoantifungal activity (Table 5.3) and ten compounds with photoantibacterial activity (Table 5.4).

A review of the antimicrobial results compared to the photochemical data indicated that there was no relationship between singlet oxygen release and MIC. For example, Compound 45, which released the highest amount of singlet oxygen with a half-life of 5 min, showed an MIC of 24 µg/ml against both *S. aureus* and *E. coli* but elicited no activity against fungi. However, Compound 37 released significantly lower $^1O_2$ than Compound 45, in the spectrophotometric assay, yet showed antimicrobial activity in both bacteria and fungi (Tables 5.2 and 5.3). Interestingly, Compound 47 which produced the second highest amount of $^1O_2$, showed no effect on bacterial and fungal growth following blue light illumination (Table 5.5). This suggests that measurement of singlet oxygen release is not an accurate reflection of antimicrobial activity of a compound. This is a theme that has been previously identified and can be attributed to the same reasons explained in detail within Chapter 3. These reasons include the possibility that Type 1 (radicals) has more antimicrobial impact than Type 2 ($^1O_2$) in this situation and the antioxidant capacity of RPMI 1640 and Mueller-Hinton media used in the photoantimicrobial screening assays (Lewinska *et al.*, 2007).

The photoantifungal results showed that *C. albicans* overall is more resistant than *S. cerevisiae* to the compounds tested (Table 5.3). This data is consistent with the data obtained for fluconazole, which is used as a control in this study, and other azole based antifungal agents (Anderson *et al.,* 2014). Compared with *S. cerevisiae*, which often shows great sensitivity to hydrogen peroxide (Lewinska *et al.*, 2007; Pedreño *et al.*, 2002), *C. albicans* has a high natural resistance to oxidative agents. *C. albicans* has the ability to induce specific genes encoding antioxidant enzymes including superoxide dismutase (SOD) and glutathione reductase (GR), which is considered important factor in the resistance of *C. albicans* to oxidative stress (Hwang *et al.*, 2002; Pedreño *et al.*, 2002). In addition, *C. albicans* is a diploid microorganism, and contains two copies of the efflux pump genes *CDR1, CDR2* and *MDR1,* which encode proteins responsible for resistance to accumulation of compounds inside the cells. This supports the higher resistance of *C. albicans* to photoactivated compounds observed in this study when compared to *S. cerevisiae*.

In the present study, no effect of acridine-isoalloxazines was seen against *A. fumigatus* under blue light illumination. *A. fumigatus* in general is more resistant than other fungi to antifungal drugs and ROS. This could be due to synthesis of high amounts of trehalose and mannitol intracellularly in conidia, these compounds work as antioxidant by quenching ROS (Ruijter *et al.*, 2003). This can explain why *A. fumigatus* was resistant to the ROS produced following the exposure of acridine-isoalloxazine to blue light. In this study both flavins and acridines moieties that form acridine-isoalloxazines, did not show antifungal activity against *A. fumigatus* when exposed to blue light. There are reports of PDT being effective against conidial forms of *A. fumigatus* but at longer exposure time and higher wavelength than used in the study (Friedberg *et al.*, 2001).

It has been demonstrated that the tested acridine-isoalloxazine compounds demonstrated better photoantimicrobial activity when compared to flavins (isoalloxazines) separately, however this was not significantly different to that of the tested acridines.

It has been shown in this study that the Gram-positive bacterium *S. aureus* was more sensitive to acridine-isoalloxazine compounds illuminated by blue light than the Gram-negative bacterium *E. coli* (Table 5.4). This finding was consistent with data obtained from several studies, which showed Gram-positive bacteria had increased susceptibility to PDT compared to Gram-negative bacteria (Nitzan *et al.*, 2004; Maclean *et al.*, 2009). The difference in susceptibility is due to the existence of lipopolysaccharides (LPSs) in the extra outer membrane of Gram-negative bacteria, which may prevent the penetration of compounds and ROS into the cells (Hamblin *et al.*, 2004). This finding is also consistent with other studies conducted with different PDT agents (Jori *et al.*, 2006). Conversely, a study by Wainwright *et al.,* 2015 showed no difference in susceptibility to PDT between Gram-positive and negative bacteria. This is suggested to be as a result of existence of more strongly constitutive cationic charges than that of our compounds which may increase the antibacterial activity against Gram-negative bacteria (Costa *et al.*, 2012; Vatansever *et al.*, 2013). This is because the use of cationic molecules would increase the susceptibility of Gram-negative bacteria due to their highly negatively charged surface.

In the case of Gram-negative bacteria, photoinactivation does not occur with ease as they are relatively impermeable to neutral or anionic compounds due to their

highly negatively charged surface. This offers a beneficial property of broad-spectrum activity as neutral and ionic compounds taken up by all classes of microbial cells; this can faciltate overcoming the hindrance of Gram-negative to the penetration process.

It was apparent that there was a remarkable difference in the susceptibility of fungi and bacteria against our tested compounds. The compounds that showed antifungal activity also demonstrated antibacterial activity, with the exception of Compounds 45 and 49, which only demonstrated antibacterial activity. The higher resistance of fungi *S. cerevisiae* and *C. albicans* to photodynamic inactivation (PDI) in this present study may be attributed to the great difference in size and surface area between bacterial and fungal cells. As bacterial cells are significantly smaller than fungal cells, lower ROS are needed to kill them (Jori *et al.*, 2006; Demidova *et al.*, 2004). This suggests that the amount of ROS released by photoactivated Compounds 45 and 49 was sufficient only to inactivate the tested bacteria. Additionally, as described previously in this chapter, fungi generally have the ability to survive oxidative stress due to the presence of genes encoding antioxidant enzymes.

In conclusion, the data reported here have shown the photosensitising activity and photoantimicrobial efficacy of some novel acridine-isoalloxazine compounds synthesised by combination of acridine and isoalloxazine moieties. The low toxicity of these compounds and their photoantimicrobial activity prompt further study intotheir chemical structures and improve their effectiveness.

6. Anthraquinone

6.1 Introduction

Anthraquinone derivatives are a group of quinone-containing compounds based on a rigid, planar three-ring aromatic system ,9,10-dioxoanthracene, and have the appearance of a yellow or light grey solid crystalline powder (Dave *et al.*, 2012) . They are considered one of the largest groups of natural pigments found in fungi and plants (Chien *et al.*, 2015, Gessler *et al.*, 2013). An important feature of anthraquinones is their absorption spectrum. They have small absorption peaks at 405 nm and stronger absorption peaks in the ultra violet region due to the system of conjugated double bonds (Gessler *et al.*, 2013, Uchimiya *et al.*, 2009). This property allows anthraquinones to be photosensitised under both UV and visible light region.

Naturally occurring quinone compounds such as anthraquinones have been used widely in the textile industry as dyes for fibres and in microelectronics as semiconductors. Furthermore, several anthraquinones have a broad spectrum of bioactivities, for example laxative, diuretic and anticancer activities (Dave *et al.*, 2012; Gholivand *et al.*, 2011; Uchimiya *et al.*, 2009). They can be used also as catalysts in a wide variety of chemical and biogeochemical reactions, such as reductive degradation of contaminants, due to their redox activity (Malik *et al.*, 2016). Due to the wide range of applications, there is interest in and efforts to develop novel anthraquinone compounds with important biological properties (Malik *et al.*, 2016).

Anthraquinones have been demonstrated to possess antimicrobial activities against a range of common pathogens. It has been shown that two anthraquinones, aloe-emodin and chrysophanol (Figure 6.1) have antifungal activity against *C. albicans* and *A. fumigatus* in the absence of light activation (Agarwal *et al.*, 2000).
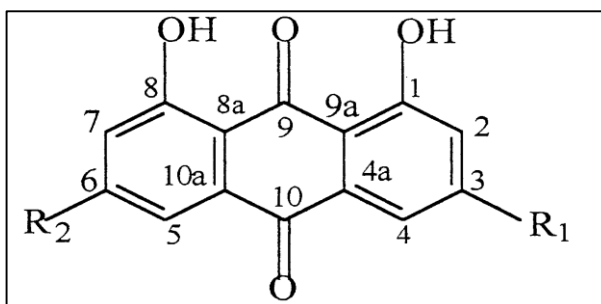
Figure 6.1 Aloe-emodin R_1 = COOH R_2 = H, Chrysophanol R_1 = CH$_3$ R_2= H (Agarwal *et al.,* 2000).

A new anthraquinone compound, 1-methyl-2-(3-methyl-but-2-enyloxy)-anthraquinone, isolated from the seeds of *Aegle marmelos* Correa showed significant antifungal activity against *Aspergillus fumigatus* and *Candida albicans* (Figure 6.2; Mishra, 2010).
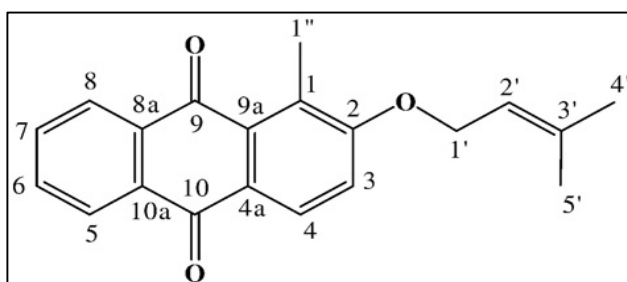
Figure 6.2 Structure of 1-methyl-2-(3-methyl-but-2-enyloxy)-anthraquinone (Mishra, 2010).

Anthraquinone derivatives have also been shown to have antibacterial activity against both Gram-positive and negative bacteria in the absence of light (Wu *et al.*, 2006; Mohanlall *et al.*, 2013). Two anthraquinones, soranjidiol and rubiadin were shown to have antibacterial activity on *S. aureus* with MICs of 32-64 µg/ml (Comini *et al.*, 2011). The mechanism of action of these compounds was suggested to be directly linked to the increase of $O2^{\cdot-}$ and/or $^1O_2$ levels resulting from the interaction between anthraquinones and bacteria without a photosensitising process (Comini *et al.,* 2011). Several mechanisms of actions of anthraquinones in microbes were reported in the absence of light including the inhibition of cell wall synthesis and membrane function by reducing membrane fluidity and integrity (Lu *et al.*, 2011) .Additionally, anthraquinones can inhibit

nucleic acid synthesis by binding with phosphate groups of DNA and affecting replication and transcription. Finally, production of singlet oxygen and radicals can occur in the presence and absence of light (Lu *et al.*, 2011).

It has been established that anthraquinones can have photosensitising activities and mediate one electron transfer to the oxygen molecule to produce the superoxide anion radical and form reactive oxygen species under visible light illumination (Comini *et al.*, 2011).

Two anthraquinones, barleriaquinone-I (BQ-I) and barleriaquinone-II (BQ-II), have been demonstrated to have photosensitising activity by releasing $O_2^{\cdot-}$ and $^1O_2$ on visible illumination via Type 1 and 2 reactions (Figure 6.3; Inbaraj *et al.*, 1999) .
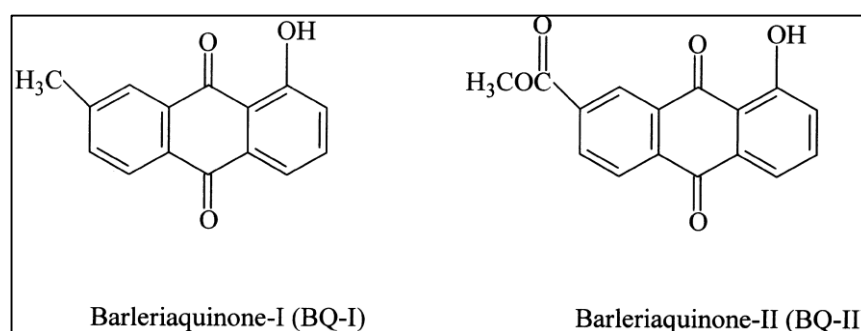
Figure 6.3 Chemical structures of BQ-I and BQ-II (Inbaraj *et al.,* 1999).

Naturally occurring anthraquinone hypericin was reported to have photoantibacterial activity when illuminated by 593 nm. Hypericin-mediated phototoxicity was found to be active against methicillin-susceptible *S. aureus* (MSSA), methicillin-resistant *S. aureus* (MRSA) and *E. coli* through photodynamic therapy (Liu *et al.*, 2015).

Additionally, the *in vitro* photodynamic production of superoxide radicals by quinone-containing compounds, such as doxorubicin, has been demonstrated by Comini *et al.,* (2011) upon visible light (300-600 nm) exposure.

Photoantibacterial efficacy of three anthraquinone compounds, rubiadin, soranjidiol and 5,5´-bisoranjidiol, have been shown on Gram-positive bacterium *S. aureus* under visible light illumination (410 nm, 0.65 mW/cm^2) for 20 min due

to the detected increase in the levels of singlet oxygen and superoxide anion (Comini *et al.*, 2011).

A combination of two anthraquinones, rubiadin and rubiadin-1-methyl ether, with blue light (420 nm, 0.65 mW/cm^2) was shown to produce superoxide radical anion O2$^{.-}$ and singlet oxygen and ^{1}O$_2$ (Figure 6.4). The photosensitisation of 15 µg/ml for each anthraquinone was capable of inactivating *C. tropicalis* biofilms (Marioni *et al.*, 2017).
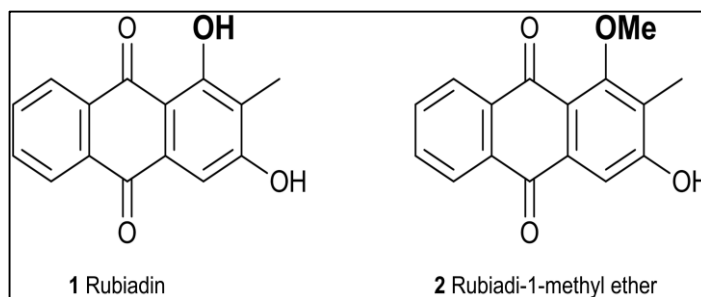
Figure 6.4 Chemical structures of rubiadin and rubiadin-1-methyl ether (Marioni *et al.,* 2017).

Based on the reported *in vitro* photosensitising and phototoxicity effect of anthraquinones (Gessler *et al.*, 2013) and to search for potential compounds for photodynamic antimicrobial treatment, a set of structures of novel anthaquinones was synthesised.

The work shown in this chapter illustrates the possible photochemical inactivation of selected microbes using the novel anthraquinone derivatives and blue light illumination. The singlet oxygen (^{1}O$_2$) released from these anthraquinone compounds was measured previously and these compounds were then tested to determine their photoantimicrobial activities.

In this present work, the susceptibility of fungi *S. cerevisiae*, *C. albicans* and *A. fumigatus* and bacteria including *S. aureus* and *E. coli* to these new anthraquinones was tested following blue light irradiation. The European Committee for Antimicrobial Susceptibility Testing (EUCAST) microbroth dilution method was utilised to test the antimicrobial activity of these blue light treated and untreated anthraquinones and their potential use in photodynamic therapy (PDT) for microbial infections.

6.2   Results

A series of quinone-based compounds, including anthraquinone (Table 6.1), anthrone (Table 6.2) and bianthrone (Table 6.3) was previously synthesised by Dr Rob Smith, UCLan. These compounds absorbe in the UV range and have chemical structures shown in (Figure 6.5). Due to the anthraquinones having three different structures, the singlet oxygen levels will be discussed separately. These compounds were screened for singlet oxygen production when compared to their standards and then screened for antimicrobial activities in the presence and absence of blue light.

Compound 57   Compound 58   Compound 59   Compound 60

Compound 61   Compound 62   Compound 63
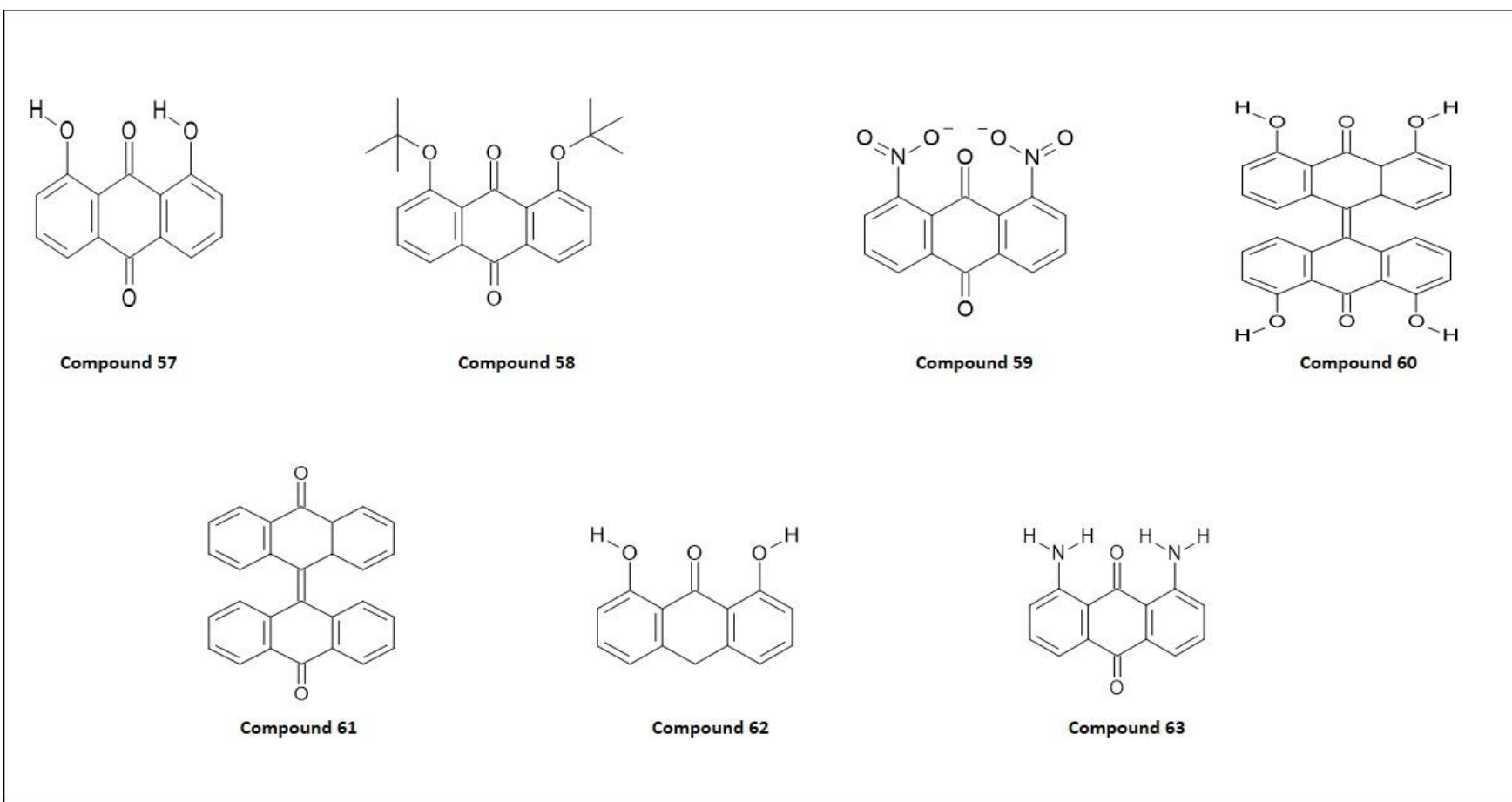
Figure 6.5 Chemical structures of anthraquinone derivatives.

Table 6.1 Structures of substituted anthraquinone containing different R groups R_1, R_2, R_3, R_4, R_5, R_6, R_7 and R_8.

Compound	R_1	R_2	R_3	R_4	R_5	R_6	R_7	R_8
57	OH	H	H	H	H	H	H	OH
58	OCH_3	H	H	H	H	H	H	OCH_3
59	NO_2	H	H	H	H	H	H	NO_2
63	NH_2	H	H	H	H	H	H	NH_2

Table 6.2 Structures of substituted bianthrone containing different R groups R_1, R_2, R_3, R_4, R_5, R_6, R_7 and R_8.

Compound	R_1	R_2	R_3	R_4	R_5	R_6	R_7	R_8
61	H	H	H	H	H	H	H	H
60	OH	H	H	H	H	H	H	OH

Table 6.3 Structures of substituted anthrone containing different R groups R_1, R_2, R_3, R_4, R_5, R_6, R_7 and R_8.

Compound	R_1	R_2	R_3	R_4	R_5	R_6	R_7	R_8
62	OH	H	H	H	H	H	H	OH

6.2.1 Photochemical characterisation of anthraquinone compounds

6.2.1.1   Singlet oxygen ($^1O_2$) data

The photochemical data was collected and analysed by Dr Rob Smith's group, UCLan, and then characterised biologically in this study. For all anthraquinone compounds, two λmax were identified, the first in the UVC region between 223-265 nm and the second in the blue light visible region between 400-450 nm. This information confirms that all anthraquinones can be activated in the blue light range (400-495 nm) (Tables. 6.1 to 6.3).

The $^1O_2$ release for the prepared anthraquinones was assayed using the decolourisation 2,3,4,5-tetraphenylcyclopentadienone (TPCPD assay) in DMSO under visible light illumination. The illuminated compounds were ranked according to the half-life.

The half-life and singlet oxygen of anthraquinones were measured after blue light exposure. All anthraquinone compounds demonstrated a half-life, with a shorter half-life indicating increased singlet oxygen release. The data suggests that both Compounds 57 and 60 produced the most singlet oxygen within the compounds tested due to showing the lowest half-life of 2 min (Table 6.5). Compound 63 showed the longest half-life, which means it released the least amount of singlet oxygen among all compounds tested (Table 6.4).

By measuring singlet oxygen release following excitation with blue light over a 60-minute period, it was noted that no further increase in singlet oxygen release was observed after 20-minute blue light excitation.

Table 6.4 Anthraquinone compounds characterised according to the half-life obtained following 20 min blue light exposure. As the decrease of absorption of TPCPD at 506 nm is directly proportional to singlet oxygen release and the lower half-life the more singlet oxygen production. λmax is determined to be the wavelength at which absorbance is highest.

Compounds	λmax nm	Half-life min	Relative singlet oxygen
57	253	2	52.94
58	254	4	26.5
59	247	7	16
63	251	16	6.625

Table 6.5 Bianthrone compounds characterised according to the half-life obtained following 20 min blue light exposure. As the decrease of absorption of TPCPD at 506 nm is directly proportional to singlet oxygen release and the lower half-life the more singlet oxygen production. λmax is determined to be the wavelength at which absorbance is highest.

Compounds	λmax nm	Half-life min	Relative singlet oxygen
61	228	7	1
60	223	2	3.5

Table 6.6 Anthrone compound characterised according to the half-life obtained following 20 min blue light exposure. As the decrease of absorption of TPCPD at 506 nm is directly proportional to singlet oxygen release and the lower half-life the more singlet oxygen production. λmax is determined to be the wavelength at which absorbance is highest.

Compounds	λmax nm	Half-life min	Relative singlet oxygen
62	265	7	1

6.2.1.2   Radical species data

The measurement of radicals released from anthraquinones following blue light exposure was not performed within this study as explained in Chapter 3.

6.2.2 Antifungal screening

The anthraquinone compounds, which have previously been characterised photochemically, were then screened *in vitro* to determine their photoantifungal activity against a range of fungal species.

The seven anthraquinone compounds were screened using the EUCAST microbroth dilution method for antifungal activity against*, S. cerevisiae, C. albicans* and *A. fumigatus.*These species were exposed to a range of concentrations of the anthraquinone compounds (0 to 500 µg/ml) in the presence and absence of blue light. This range of concentrations is different to the previously studied groups because this group showed higher solubility. Growth was determined by using OD at 530nm for *S. cerevisiae* and *C. albicans* and visually for *A. fumigatus.*

The percentage growth inhibition for each concentration of the anthraquinones, in the presence and absence of blue light, was calculated against the OD_{530nm} of the drug-free control (100%). The well-characterised antifungal agents, fluconazole and amphotericin B, were used as the controls. Data on percentage growth inhibition of *S. cerevisiae* and *C. albicans* with the highest concentration used of fluconazole and anthraquinone compounds in presence and absence of blue light are shown as means ±SEM (Figures 6.8 to 6.14). Experiments were repeated on two separate occasions (n=2) in duplicate.

The heat maps shown in Figures 6.6 and 6.7 show the percentage growth determined from the OD_{530nm} readings for fungal growth after 24 h incubation for concentrations of fluconazole and the compounds following exposure to blue light for 20 min. The concentrations of fluconazole (control) used were 0-64 µg/ml, while concentrations of the compounds were 0-500 µg/ml. The colour in the heat map indicates the percentage growth, with black indicating complete growth (0% inhibition), and red indicating no growth (100% inhibition). Yellow indicates 50% growth inhibition, which aligns with the minimal growth inhibition (MIC), as determined by the EUCAST method (Figures 6.6 and 6.7).
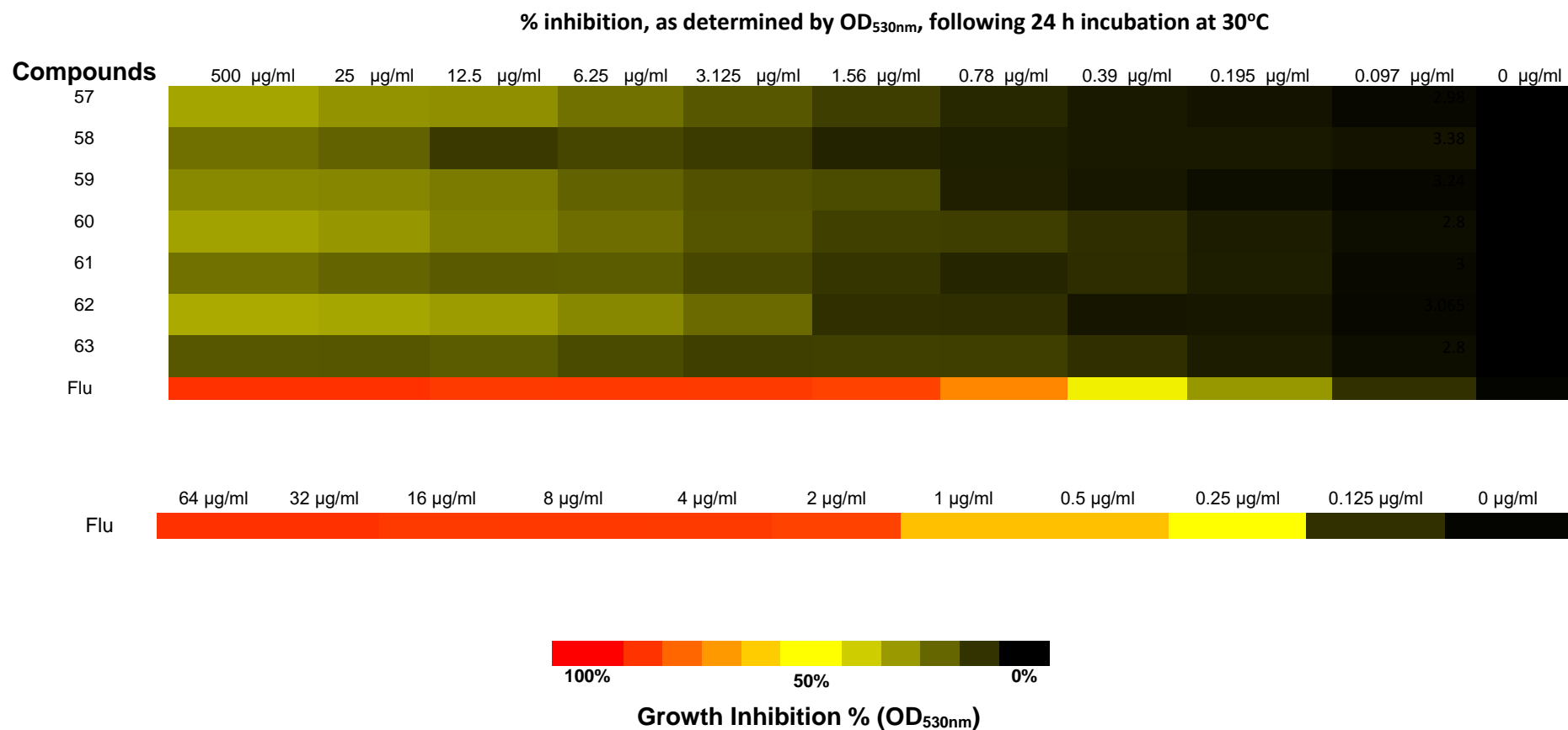
Figure. 6.6 Heatmap illustrating OD$_{530nm}$ levels for varying concentrations of a list of seven anthraquinone compounds (0 to 500 µg/ml) against *S. cerevisiae*. The yellow bar shows 50% growth inhibition while the red bar illustrates the maximum growth inhibition.
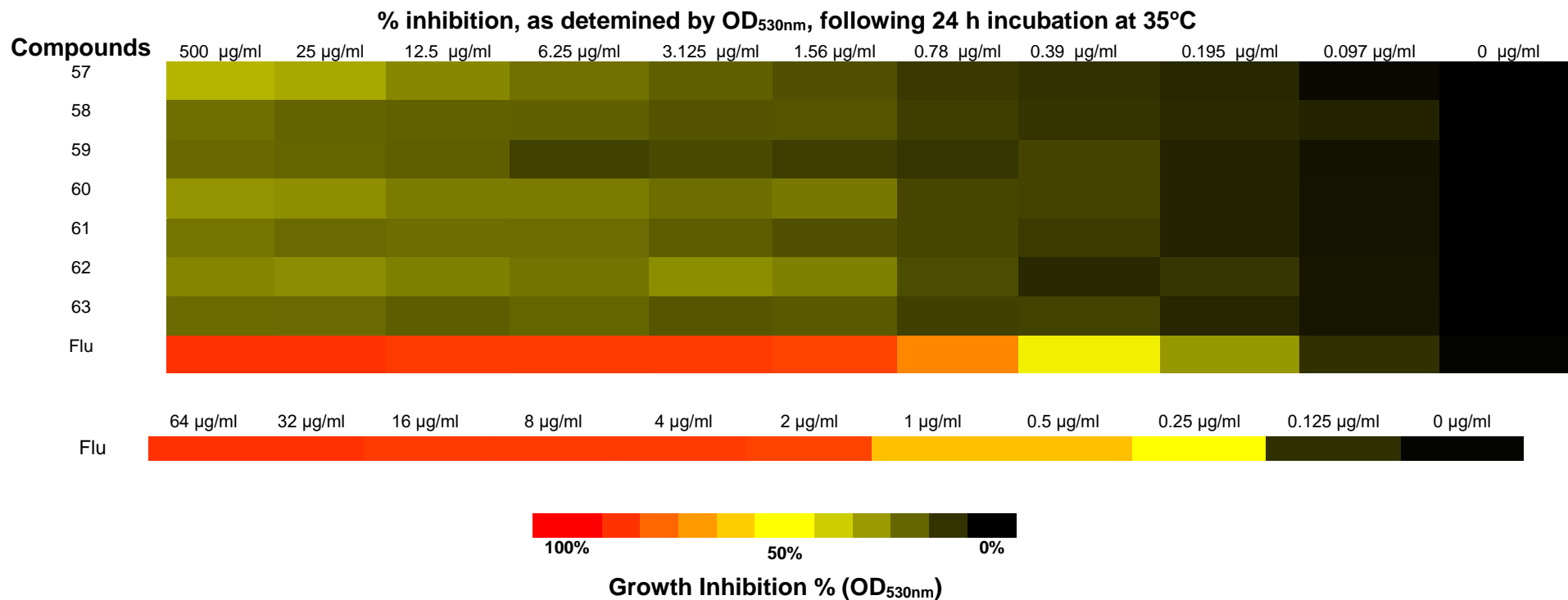
Figure. 6.7 Heatmap illustrating OD$_{530nm}$ levels for varying concentrations of a list of 7 anthraquinone compounds (0 to 500 µg/ml) against *C. albicans*. The yellow bar shows 50% growth inhibition while the red bar illustrates the maximum growth inhibition.

The graphs (Figures 6.8 to 6.14) show the mean ±SEM (standard error of the mean) of highest percentage growth inhibition that has been recorded at concentration 64 (μg/ml) fluconazole and 50 (μg/ml) anthraquinones in the absence and presence of blue light, after 20-minute exposure in *S. cerevisiae* and *C. albicans* (Figures 6.9 to 6.15). In all cases, growth inhibition of less than 23% was seen in the no blue light control.
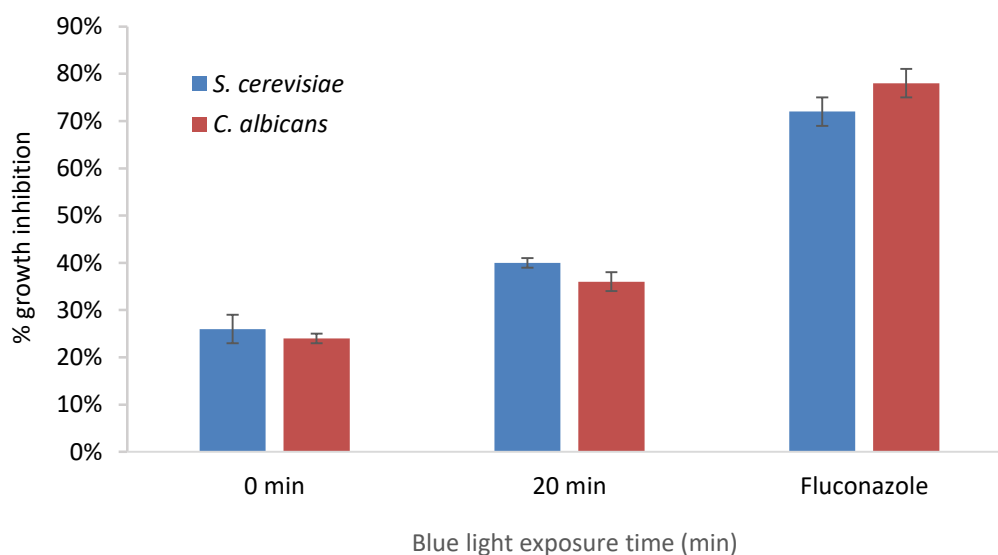
Figure 6.8 Percentage growth inhibition of *S. cerevisiae* and *C. albicans* with Compound 57 in absence and presence of blue light. Comparison of Compound 57 with fluconazole on both *S. cerevisiae* and *C. albicans* growth inhibition percentage obtained in the absence and presence of blue light. 0 min means no blue light exposure. The experiment was conducted using EUCAST broth microdilution method and standardised inoculum of 0.5-2.5 x 10^5 cfu/ml. The experiment was conducted in duplicate, n=2. Values are the mean ±SEM.
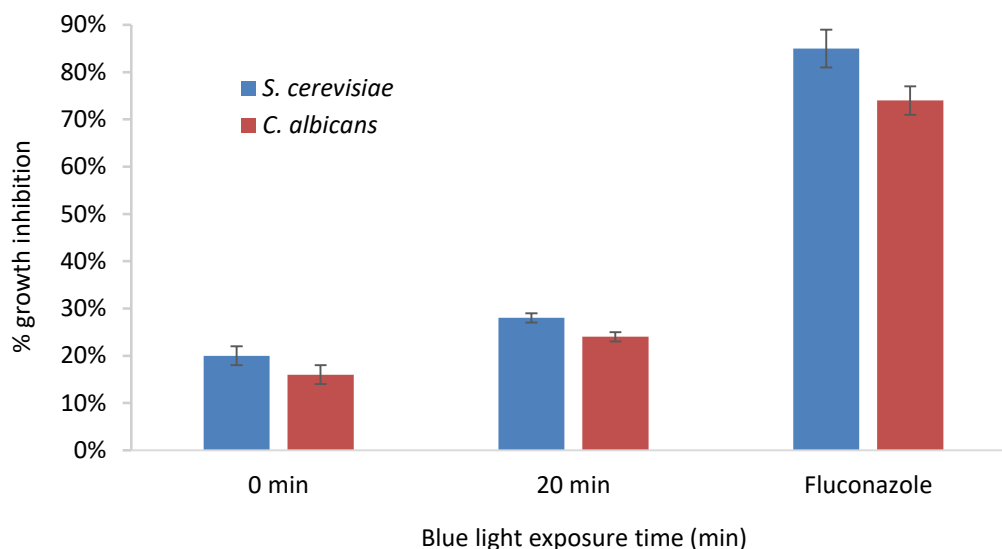
Figure 6.9 Percentage growth inhibition of *S. cerevisiae* and *C. albicans* with Compound 58 in absence and presence of blue light. Comparison of Compound 58 with fluconazole on both *S. cerevisiae* and *C. albicans* growth inhibition percentage obtained in the absence and presence of blue light. 0 min means no blue light exposure. The experiment was conducted using EUCAST broth microdilution method and standardised inoculum of 0.5-2.5 x 10^5 cfu/ml. The experiment was conducted in duplicate, n=2. Values are the mean ±SEM.
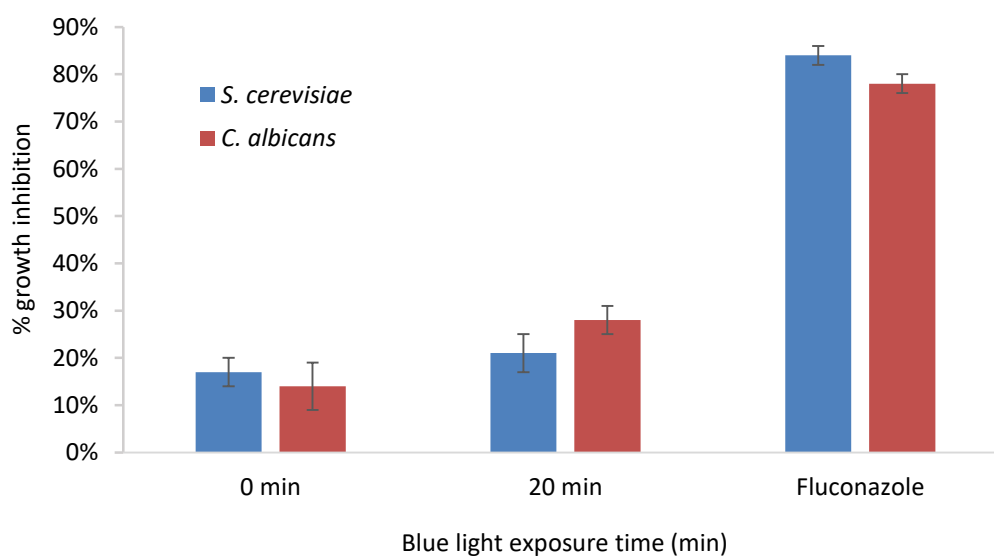
Figure 6.10 Percentage growth inhibition of *S. cerevisiae* and *C. albicans* with Compound 59 in absence and presence of blue light. Comparison of Compound 59 with fluconazole on both *S. cerevisiae* and *C. albicans* growth inhibition percentage obtained in the absence and presence of blue light. 0 min means no blue light exposure. The experiment was conducted using EUCAST broth microdilution method and standardised inoculum of 0.5-2.5 x 10^5 cfu/ml. The experiment was conducted in duplicate, n=2. Values are the mean ±SEM.

170
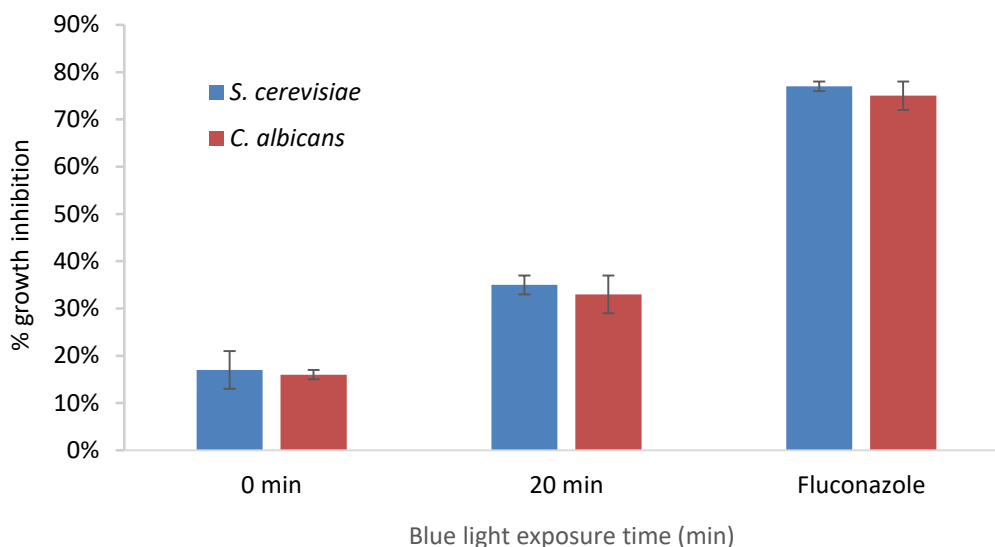
Figure 6.11 Percentage growth inhibition of *S. cerevisiae* and *C. albicans* with Compound 60 in absence and presence of blue light. Comparison of Compound 60 with fluconazole on both *S. cerevisiae* and *C. albicans* growth inhibition percentage obtained in the absence and presence of blue light. 0 min means no blue light exposure. The experiment was conducted using EUCAST broth microdilution method and standardised inoculum of 0.5-2.5 x 10^5 cfu/ml. The experiment was conducted in duplicate, n=2. Values are the mean ±SEM.
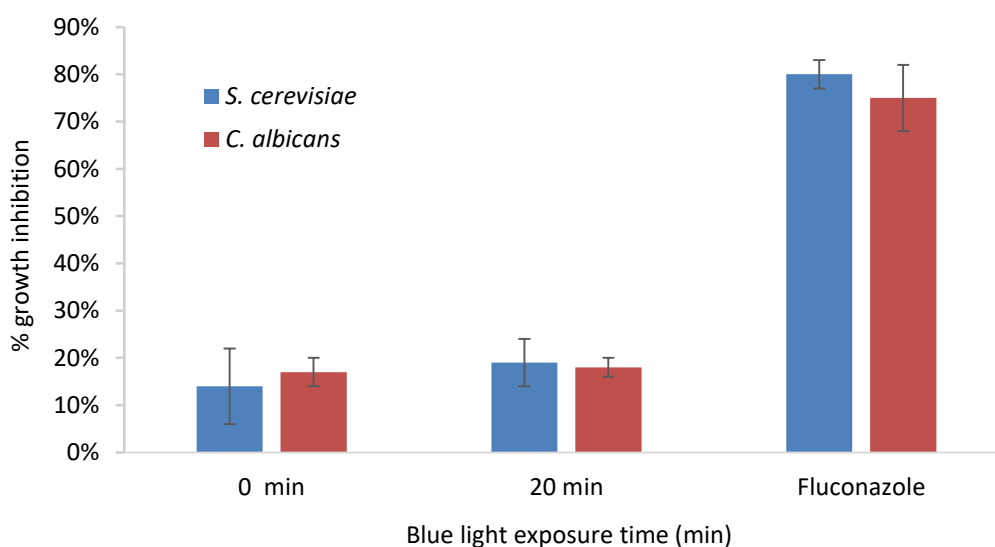
Figure 6.12 Percentage growth inhibition of *S. cerevisiae* and *C. albicans* with Compound 61 in absence and presence of blue light. Comparison of Compound 61 with fluconazole on both *S. cerevisiae* and *C. albicans* growth inhibition percentage obtained in the absence and presence of blue light. 0 min means no blue light exposure. The experiment was conducted using EUCAST broth microdilution method and standardised inoculum of 0.5-2.5 x 10^5 cfu/ml. The experiment was conducted in duplicate, n=2. Values are the mean ±SEM.
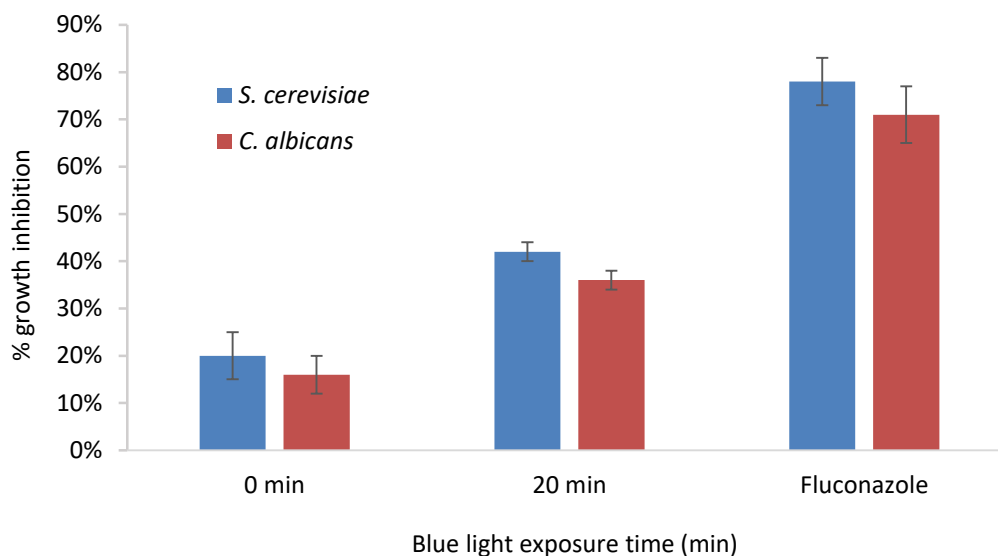
Figure 6.13 Percentage growth inhibition of *S. cerevisiae* and *C. albicans* with Compound 62 in absence and presence of blue light. Comparison of Compound 62 with fluconazole on both *S. cerevisiae* and *C. albicans* growth inhibition percentage obtained in the absence and presence of blue light. 0 min means no blue light exposure. The experiment was conducted using EUCAST broth microdilution method and standardised inoculum of 0.5-2.5 x 10^5 cfu/ml. The experiment was conducted in duplicate, n=2. Values are the mean ±SEM.
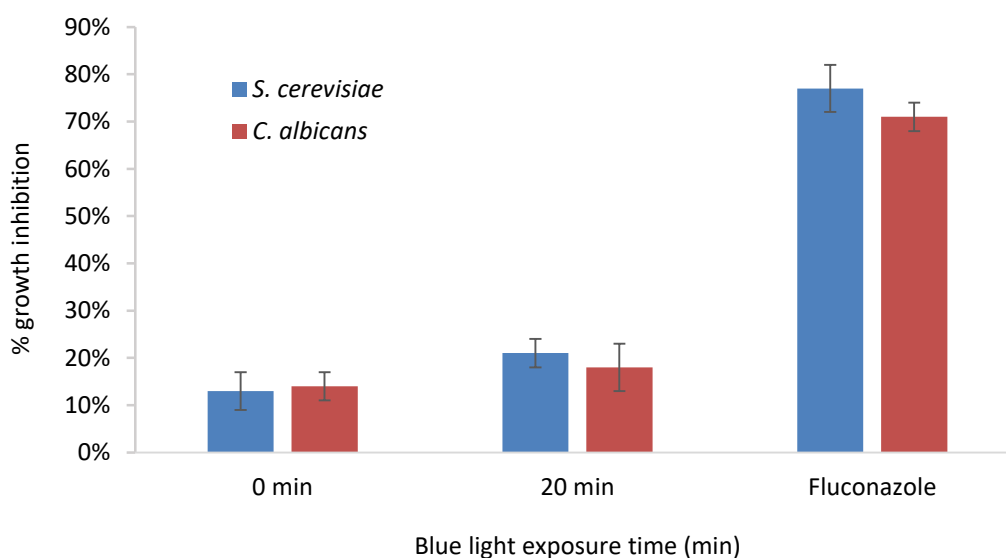
Figure 6.14 Percentage growth inhibition of *S. cerevisiae* and *C. albicans* with Compound 63 in absence and presence of blue light. Comparison of Compound 63 with fluconazole on both *S. cerevisiae* and *C. albicans* growth inhibition percentage obtained in the absence and presence of red light. 0 min means no blue light exposure. The experiment was conducted using EUCAST broth microdilution method and standardised inoculum of 0.5-2.5 x 10^5 cfu/ml. The experiment was conducted in duplicate, n=2. Values are the mean ±SEM.

To ensure consistency of the results, EUCAST antifungal susceptibility testing of *S. cerevisiae* and *C. albicans* to the control antifungal agent, fluconazole, was performed. The resultant MIC of 1 µg/ml against *C. albicans* corresponded with the EUCAST Antifungal Clinical Breakpoints (EUCAST 7.3: Arendrup *et al.*, 2015a). Regarding *S. cerevisiae* the resultant MIC of 1 µg/ml was identified to be within the published MIC range (MIC and zone distributions and ECOFFs; EUCAST 7.3: Arendrup *et al.*, 2015a).

Only Compound 57 had a significant effect in the absence of blue light against both species (Figure 6.8). None of the six remaining compounds (58, 59, 60, 61, 62 and 63) showed significant antifungal activity in the absence of blue light. As such, for these compounds, any antifungal efficacy will be due to blue light treated anthraquinones.

The data shows that none of the blue light treated anthraquinones showed growth inhibition of ≥50% compared to that of the compound-free control, which means that no MIC could be determined against both *S. cerevisiae* and *C. albicans.*

Although the MIC value was not reached, the anthraquinone Compounds 57, 58 and 60 showed the highest growth inhibition among all the seven compounds after 20-minute blue light exposure. The highest percentage growth inhibition of Compounds 57, 58 and 60 was recorded at a concentration of 50 µg/ml, with maximum growth inhibition levels of 40%, 41% and 42% against *S. cerevisiae* and 36%, 33% and 36% against *C. albicans*, respectively. In general, the sensitivity of *S. cerevisiae* was more than that of *C. albicans* (Figures 6.8, 6.11 and 6.13).

All the four remaining anthraquinones exposed to 20-minute blue light exhibited slightly more growth inhibition than the no-light control against both species. For example, Compound 59 inhibited growth of *S. cerevisiae* and *C. albicans* at 20% and 16%, in the absence of blue light that increased to 28% and 24%, respectively, when light activated (Figures 6.9).

A. fumigatus was also screened using the EUCAST antifungal MIC microdilution method for moulds. Due to the growth of *A. fumigatus*, instead of measuring the optical density to determine percentage growth inhibition, a visual inspection was

undertaken. In this case the MIC was determined to be the first well where the concentration of compound resulted in complete absence of growth. The concentrations range tested for the control drug amphotericin B was 0-16 (μg/ml). It has been demonstrated that amphotericin B was effective against *A. fumigatus* showing MIC of 0.125 μg/ml, which matched the MIC EUCAST breakpoint in *A. fumigatus*. The antifungal screening demonstrated that anthraquinones, following exposure to blue light, did not exhibit any efficacy against *A. fumigatus* at the concentrations tested (0 to 500 μg/ml) by checking the growth visually (data not shown).

6.2.3 Antibacterial screening

The anthraquinone compounds were then screened, using the European Committee for Antimicrobial Susceptibility Testing (EUCAST) microbroth dilution method, for antibacterial activity following 20-minute blue light exposure against two clinically important bacterial species *S. aureus* and *E. coli* (EUCAST 7.3: Arendrup *et al.*, 2015a).

 The antibacterial drug gentamicin, was used as a control due to its broad antibacterial activity against both Gram-negative and Gram-positive bacteria (Jao *et al.*, 1964). The bacterial species were exposed to a range of concentrations of the anthraquinone compounds (0-500 μg/ml) in the presence and absence of blue light. The MIC was determined, by visual inspection, to be the lowest concentration that completely inhibits growth. The experiments were repeated twice in duplicate.

EUCAST antibacterial susceptibility testing of *S. aureus* and *E. coli* to the control gentamicin was performed and the resultant MICs of 0.25 and 0.125 (μg/ml) corresponded with EUCAST Antibacterial Clinical Breakpoints, which confirms the accuracy of the assay.

Compounds 57, 58 and 60 showed effect on visible growth against *S. aureus* and *E. coli* following 20-minute blue light exposure. The remaining compounds did not show an effect on bacteria when exposed to blue light (data not shown).

6.3 Discussion

In this study, the aim was to evaluate the antimicrobial effectiveness of a set of novel photoactivated anthraquinones using blue light illumination. The anthraquinone compounds had previously been characterised photochemically and, in this study, they were investigated biologically against a range of clinically important microorganisms.

6.3.1 Anthraquinones are photosensitised following exposure to blue light and release singlet oxygen

Due to the studied photosensitising activity of anthraquinones and their ability to release free radicals and singlet oxygen within Type 1 and Type 2 reactions, a set of novel synthesised anthraquinones was characterised photochemically (Comini *et al.*, 2011).

To identify the required light source to photoactivate anthraquinones, the wavelength of maximum absorbance, λmax, was determined by taking the absorbance spectrum between the wavelengths 250-800 nm. The tested anthraquinones absorbed maximally in the UV light region, with the λmax located between 223 to 265 nm. The photophysical properties of the anthraquinone compounds can be seen in Table 6.4. The reduction of one of the carbonyl groups causes an increase in the absorption spectra. In the case of Compound 62, when compared to Compound 57 there is an increase of 12 nm and this could be a result of the reduction in the polarity of the molecule, which affects the interaction with the microbial cell membrane. This result is supported by another study which found that anthraquinones, such as rubiadin and rubiadin-1-methyl ether, absorbed in UV and blue light regions of the spectrum, showing maximum absorbance at 360 nm and 411 nm, respectively. This is also consistent with various published studies conducted on bis(4-oxybenzoic acid)-1,8-anthraquinone and bis(3-oxybenzoic acid)-1,8-anthraquinone, sornjidiol and damnacanthal, which demonstrate their maximum absorption in the range between 316-349 nm (Babanzadeh *et al.*, 2018; Comini *et al.,* 2017).

The studied anthraquinones have been demonstrated to absorb mainly in the UV light region between 220-300 nm (Tables 6.1, 6.2 and 6.3). Due to the UV-based mutagenesis effect, blue light can potentially be a safer activating light source. However, blue light has the associated disadvantages of potentially not activating the anthraquinone tested compounds.

Following anthraquinones exposure to 20-minute blue light in the present study, singlet oxygen species were produced and relative $^1O_2$ calculated when compared to their unsubstituted standards. The data suggests that most singlet oxygen species were released from the anthraquinones following 20-minute blue light exposure. All anthraquinone derivatives produced higher singlet oxygen than their relevant standards, anthraquinone and bianthrone. The relative singlet oxygen values for these derivatives ranged between 3.5 and 53 (Table 6.4 and 6.5), with the singlet oxygen yield of Compound 57 showing the highest increase at 53-fold. Similarly, the singlet oxygen of Compound 60 also showed an increase when compared to the standard bianthone, at a 3.5-fold increase.

Compounds which produced high levels of singlet oxygen were hydroxyl and methoxyl derivatives (Compounds 57, 58 and 60; Tables 6.4 and 6.5). The TPCPD assay for singlet oxygen measurement showed that light activation of Compounds 57 and 60 resulted in a half-life of 2 min, when compared with standards anthraquinone and bianthrone, respectively (Tables 6.1 and 6.2). These observations indicate that the addition of hydroxyl groups to the parental compound increases singlet oxygen production (Tables 6.4 and 6.5). This data is supported by data from four anthraquinones, erythroglaucin (ERG), teloschistin (TEL), 1-hydroxy-2-methylanthraquinone (HYQ) and 1-methoxy-2-hydroxyanthraquinone (MEQ), which contain both hydroxyl and methoxyl substitute groups and have exhibited effective photosensitising activity (Rajendran *et al.*, 2004). These results cannot be compared with the data shown in this study because of the different reference standards and also due to the data only being stated as $^1O_2$ yield.

6.3.2 The majority of anthraquinones have no significant effect on microbial growth in the absence of blue light

Anthraquinones have been shown to possess antimicrobial activity against a range of common pathogens in the absence of activating light (Wu *et al.*, 2006, Mohanlall *et al.*, 2013, Rhea *et al.*, 2012). In this study, the anthraquinones alone were tested against the fungi and bacteria. Only Compound 57 showed a significant growth inhibition activity against *S. cerevisiae* and *C. albicans* when compared to the untreated control, however the MIC was not reached. The remaining compounds showed some growth inhibition in fungi, but it was less than 23% at the highest concentrations tested (500 μg/ml). No visual growth effect was observed against the fungus *A. fumigatus* and the bacteria *S. aureus* and *E. coli* in the absence of blue light.

Both anthraquinones, rhein and emodin, were shown to be inactive against *E. coli* and *C. albicans* at the highest concentration tested (500 μg/ml) (Chukwujekwu *et al.*, 2006, Malmir *et al.,* Ayo *et al.*, 2007). Additionally, the antimicrobial activity of a popular anthraquinone, emodin, was studied and the MIC was found to be 2,000 μg/ml against *S. aureus,* 3,000 μg/ml against *E. coli* and 4,000 μg/ml against *C. albicans* using the disk diffusion method (Ayo *et al.*, 2007) . These findings support the observations made in this study that the MIC was higher than the maximum concentration tested at 500 μg/ml.

Comparison of the activities of the anthraquinones revealed that the effects of emodin, rhein and physcion against all microbial species were significant while our compounds showed no antimicrobial activity. It is suggested that antibacterial activity of the anthraquinone derivatives may be related to the type of substituent groups on the molecular structure. All of the anthraquinones tested in this study and the various reported studies have the same hydroxyanthraquinone nucleus composed of two ketone groups at C9 and C10, while different groups are substituted at C1, C3, C6 and C8 of the phenyl ring. The active anthraquinones, including rehin and emodin, have polar substituent carboxyl, hydroxyl, and hydroxymethyl groups at these positions. This is because these polar functional

groups can increase antibacterial activity due to the ability of these groups to bind strongly to the polar phospholipids region in the microbial membrane (Echeverría *et al.*, 2017; Lu *et al.*, 2011). This is consistent with the results for Compound 57 within this study, which contains two hydroxyl groups. In comparison with the other anthraquinone compounds tested, this seems to increase the growth inhibition effect.

This means Compound 57 could enter the cell and, as described for other anthraquinones, bind and insert into the cell membrane, leading to loss of cytoplasmic membrane integrity. Additionally, these compounds may also bind with the phosphate group of DNA and intercalate into the base pairs of the DNA helix, which may affect replication and transcription, repress expression and even lead to cell death. Other mode of actions might be involved in the observed antimicrobial activity of anthraquinones including the inhibition of activity of nicotinamide adenine dinucleotide (NADH) oxidase and succinate oxidase of mitochondria and thus this could lead to uncoupling of oxidative phosphorylation, restraining of active transport, and loss of pool metabolites (Lu *et al.*, 2011). The six remaining tested anthraquinones lack these polar groups, which may limit their ability to enter the cell and, therefore, explain why they have no antimicrobial effect in the absence of light.

The activity of anthraquinones in the absence of activating light may be improved by having a long unsaturated aliphatic chain methoxy group substituted in position C2 of the basic anthraquinone structure to facilitate interaction and disruption of cell walls (Sikkema *et al.*, 1995; Kemegne *et al.*, 2017). This is the case of 1-methyl-2-(3′-methyl-but-2′-enyloxy)-anthraquinonem, which showed significant efficacy against both *C. albicans* and *A. fumigatus* at MIC of 31.25 µg/ml (Mishra *et al.*, 2010), while our compounds tested in this study do not possess such a long unsaturated chain.

6.3.3 Blue light activation of three tested anthraquinones showed a significant effect on microbial growth when compared to that of untreated-anthraquinones

It has been demonstrated in Chapter 3 that 60-minute blue light illumination did not have a significant effect on the the growth of any of the test microorganisms when compared to that of untreated microbial cells, due to the wavelength and irradiance dose (Figures 3.3-3.6). Based on the blue light results and the observations of no-light effect, any growth inhibition observed following illumination of the novel anthraquinones other than Compound 57, would be attributed to the of photoactivation of the compounds.

The results for all the control bioassays undertaken within this study against each of the species tested were within the published ranges, which ensured the accuracy and consistency of the antimicrobial susceptibility testing (EUCAST 7.3: Arendrup *et al.*, 2015a).

The phototoxicity effect of these anthraquinones using blue light irradiation was investigated against a range of clinically important microorganisms. The minimum inhibitory concentration (MIC) were determined for each compound using the EUCAST method (EUCAST 7.3: Arendrup *et al.*, 2015a).

Following microbiological screening of seven quinone-based compounds, four compounds demonstrated no significant effect on growth in either *S. cerevisiae* and *C. albicans* (Figures 6.10, 6.12, 6.13 and 6.14). Only Compounds 57, 58 and 60 of the light activated compounds exhibited significant growth inhibition in *S. cerevisiae* and *C. albicans* when compared with no-light compounds (Figures 6.8, 6.9 and 6.11). However, no MIC could be determined as, at the highest concentration tested (500 µg/ml), total growth inhibition was less than 50%. No growth inhibition was observed in either *A. fumigatus* or the bacterial species, *E. coli* and *S. aureus*, following exposure to the seven anthraquinone compounds. It has been demonstrated that two anthraquinones, rubiadin and rubiadin-1-methyl ether, showed significant antifungal activity against *Candida* species when exposed to blue light (Marioni *et al.*, 2017). However, the previous study used a shorter wavelength than that used in this

research (420 nm versus 470nm), which may have had a cumulative effect on *Candida*. The two tested anthraquinones have been substituted with methoxyl and methyl groups as well as two hydroxyl groups, which may increase the polarity, facilitating penetration into the microbial cells. The test compounds are less polar, possibly reducing their ability to enter the cell. Although not measured in this study, a number of other anthraquinone-related compounds, such as rubiadin and rubiadin-1-methyl ether, have also been shown to release both radical and $^1O_2$ species following light activation. As such, we can predict that lack of penetration into the cell of the test compounds is reducing their ability to affect the microbial cells and reduce their growth (Marioni *et al.*, 2017).

Three blue light activated anthraquinones, Compounds 57, 58 and 60, have significantly greater photoantimicrobial activity against *S. aureus* and *E. coli* compared to the controls. However, although they were tested up to 500 µg/ml, the MIC was not reached. In comparison, the blue light activation of anthraquinones soranjidiol and rubiadin showed *in vitro* bactericidal effect against *S. aureus* using a different method, the agar diffusion method, with a minimum reduction of 10^3 cfu/ml (3.0 log_{10}). The higher antibacterial activity of soranjidiol and rubiadin in comparison to the compounds tested in this research is suggested to be related to hydroxyl and methyl groups substituted at C2, C3 and C4 of the basic phenyl ring, which increase the penetration into the cells.

The aforementioned anthraquinones are different to our compounds in respect to position of hydroxyl groups and including a substituent methyl group, which are suggested to have influence on activity due to additional polarity obtained (Wang *et al.*, 2010).

One of the limitations regarding using anthraquinones as drugs is the possible toxicity associated with quinone-containing derivatives that could lead to mammalian cell damage (Malik *et al.*, 2016). Anthraquinones are widely used as laxatives, however several side effects, such as; electrolyte imbalance, metabolic alkalosis, hypotension and dehydration are generally associated with their use (Malik *et al.*, 2016) . The toxicity associated with quinones is caused by their ability to interact with essential nucleophiles inside the cell as well as the result

of taking part in redox reactions, which produce damaging reactive oxygen species (ROS) mainly $^1O_2$ as well as radicals, however radicals were not measured in this present study (Malik *et al.,* 2016). Therefore, the limited photoantimicrobial activity and potential toxicity of the novel anthraquinones tested within this study may be a limiting factor in their use within photodynamic therapy.

7. Characterisation of candidate compounds

7.1 Introduction

The treatment of infectious diseases is one of the most challenging problems in medicine due to the increased resistance of microbes to current antimicrobial drugs, their side effects and their spectrum of activity (Liang *et al.*, 2016; Cieplik *et al.*, 2018). Therefore, there is a requirement to develop new therapeutic strategies which target unique characteristics of bacterial and fungal cells, without affecting the patient. Photodynamic therapy is a potential alternative therapy that can be utilised to treat microbial infections.

There are certain characteristics required of an ideal PDT antimicrobial agent:

1. Broad spectrum of antimicrobial activity at a low MIC, which indicates that less of the drug is required to inhibit growth of the microbe.
2. They cannot easily induce the development of microbial resistance. Many current antimicrobial therapies target a limited number of sites within the microbial cell, which increases the chances that resistance may develop. Multiple targets will increase efficacy of the PDT agent and limit the development of resistance against the compound.
3. Effective antimicrobial activity against biofilms that often have reduced susceptibility towards conventional antimicrobial treatments and are linked to various human diseases.
4. Selective toxicity so that the compound is lethal to microorganisms without causing significant damage to the mammalian host cells. This will help reduce side effects within the patient.

Following biological screening of all acridine, flavine, acridine-isoalloxazine and anthraquinone compounds (Chapters 3, 4, 5 and 6), a shortlist of five compounds showing the lowest MICs values against fungi and bacteria was chosen. The shortlisted compounds were acridine (Compounds 1, 2 and 11) and acridine-isoalloxazine (Compounds 36 and 43), which have the lowest MICs of all the compounds tested for both antifungal and antibacterial activity following photoactivation (Table 7.1). In order to determine their clinical potential, the shortlisted compounds need to be further characterised to determine whether

they meet the characteristics required for an effective antimicrobial agent in a clinical setting.

A common dogma in the medical field is that cidal drugs are more efficient than static agents, because they eliminate bacteria rather than limiting their growth. Knowing the mechanism of action of any novel antimicrobial is important to determine its clinical use. The majority of PDT agents show cidal effects on microbial cells by releasing ROS, which disrupts multiple cellular targets. Therefore, the shortlisted compounds will be reviewed for cidial or static effects following treatment of microbial cells.

Photosensitisers work via the release of ROS ($\cdot$OH and H_2O_2) via Type 1 or/and ($^1O_2$) via Type 2 reactions, which is able to kills cells as a result of oxidative stress (Baltazar *et al.*, 2015). The initial chemical characterisation of these compounds within this study demonstrates no biological relevance to their antimicrobial activity. Therefore, an alternative method is required to determine their biological effect. A large number of stresses are signalled through the high osmolarity glycerol (HOG*)* pathway, including the general stress response. One of the targets of this pathway are a key set of transcription factors, Msn2/4p, which are activated in response to oxidative stress. Deletion of the *MSN2/4* genes encoding these proteins results in sensitivity of cells to oxidative stress (Pascual-Ahuir *et al.*, 2007; Martinez Pastor *et al.*, 1996). Therefore, the MIC of the candidate compounds within these mutant strains can help inform the mechanism of action of these compounds.

The mechanism of action of these compounds is important as this may impact on the development of resistance within treated microbial cells. There is an increasing resistance to traditional antimicrobial treatments, which has resulted in the persistence of a number of infections (Alanis, 2005, Hawkey, 2008). Therefore, an important effort is being made to find alternative antimicrobial therapies, where development of resistance is limited. Various studies have shown that no development of resistance is observed in fungal and bacterial cells in response to PDT due to the absence of a specific target (Jori *et al.*, 2006; Vandeputte *et al.*, 2012; Vatansever *et al.*, 2013). Therefore, any new PDT agents

will need to be reviewed to determine the possibility of resistance developing in the treated microorganisms.

Microorganisms can cause persistent infections in clinical situations despite showing susceptibilities to antimicrobial treatment when testing *in vitro*. It has been suggested a parameter termed perseverance correlates with the clinical responses and is defined by the ability of fungal cells to grow at drug concentration above the MIC (Rosenberg *et al.,* 2018). This parameter is measured as the degree of supra-MIC growth (SMG) in broth microdilution assays. The SMG and MIC of the examined compounds were studied to check the proportion of cells that form colonies at SMG concentration and compared with the MIC, which is often not sufficient to explain clinical outcomes.

The clinical effectiveness of a potential antimicrobial compound is influenced by the external environment (Şen *et al.*, 1997; Sherrington *et al.*, 2017). This includes availability of metal ions and changes in pH, which can occur at the treatment site or intracellularly (Mayer *et al.*, 2013; Weckwerth *et al.*, 2012). For example, to treat microbes found in the vagina (pH 4-4.5), the compound must retain activity within acidic conditions (George *et al.*, 2009). Further, medium pH and EDTA have been shown to have an effect within *in vitro* susceptibility testing against microbial species (Marr *et al.*, 1999). These aspects can be assessed by testing the novel antimicrobial compounds in combination with EDTA, a magnesium and calcium metal chelator, and at varying pHs to determine their effectiveness.

To investigate if the different medium conditions could have effects during PDT (Carvalho *et al.*, 2009), the antimicrobial susceptibility testing of the PDT shortlisted compounds was investigated in buffered and unbuffered medium using MOPS as a buffer.

Many PDT agents have been shown to have an effect on fungal and bacterial sessile cells of biofilms, which are often resistant to conventional antimicrobial therapies and host immune defences (Pereira *et al.*, 2010). Therefore, in this chapter the photoantifungal activity of the shortlisted compounds against *C.*

albicans biofilms following exposure to 20-minute blue light was evaluated by conducting a colorimetric method using XTT reduction assay.

As any new antimicrobial reagent would be required to have minimal effect in host cells, the shortlisted compounds were tested to determine their toxicity in mammalian cells. The assays were performed using HeLa cells, an immobilised human cell line derived from cervical cancer cells, which have been used widely in toxicity testing due to their ability to thrive indefinitely and easily in biomedical research and their susceptibility to infections (Limban *et al.*, 2008; Franchini *et al.*, 2009; Wasson *et al.*, 2012). The toxicity in mammalian cells has been evaluated by investigating cell viability in the presence of the photosensitisers.

This chapter will present data from a range of experiments utilised to assess whether the shortlisted compounds have the characteristics required to enable them to move forward as potential antimicrobial compounds for clinical use.

7.2   Results

Following photoantimicrobial screening of all tested compounds under 20-minute blue light illumination, a shortlist of compounds with the lowest MIC against the fungi *S. cerevisiae* and *C. albicans* and bacteria *S. aureus* and *E. coli* was chosen and moved through into further characterisation (Figure 7.1, Table 7.1). The five shortlisted compounds were three acridine-based compounds (1, 2 and 11) as well as two acridine-isoalloxazine based compounds, 36 and 43 (Figure 7.1). The MICs of *S. aureus* were lower than those of *E. coli* bacteria while *C. albicans* showed more resistance than *S. cerevisiae* by showing higher MIC values in general.

Table 7.1 Summary of the minimum inhibitory concentrations (MICs) of shortlisted compounds, which have been chosen according to the compounds showing the lowest MICs values against bacteria and fungi.

Studied compounds	Fungi		Bacteria	
	20 min blue light exposure		20 min blue light exposure	
	MIC (µg/ml) against *S. cerevisiae*	MIC (µg/ml) against *C. albicans*	MIC (µg/ml) against *S. aureus*	MIC (µg/ml) against *E. coli*
Fluconazole	0.25	1		
Gentamicin			0.25	0.125
Compound 1	4.2	4.2	2	24
Compound 2	5.2	8.3	8	24
Compound 11	12.5	25	8	24
Compound 36	12.5	25	8	16
Compound 43	12.5	12.5	24	32
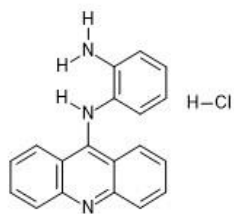
Compound 1
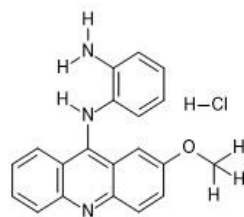
Compound 2
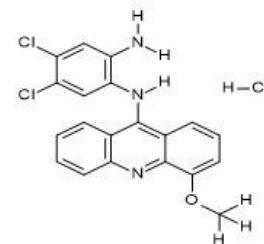
Compound 11
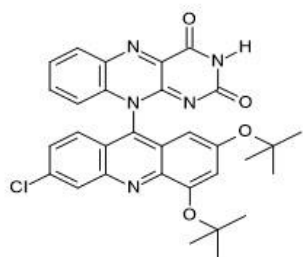
Compound 36
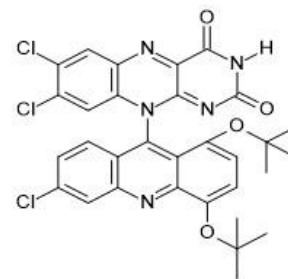
Compound 43

Figure 7.1 Chemical structures of novel shortlisted acridine and acridine-isoalloxazine derivatives.

7.2.1 All shortlisted compounds are static against the tested fungi, *S. cerevisiae* and *C. albicans*, and bacteria, *S. aureus* and *E. coli.*

Based on the phototoxicity of the shortlisted compounds against fungal species *S. cerevisiae* and *C. albicans* and bacterial species *S. aureus* and *E. coli* (Table 7.2), it was investigated whether this effect was static or cidal.

Following treatment with the shortlisted compound and a 24 h incubation, samples were taken from the first well where no visible growth could be observed. These samples were diluted into the corresponding fresh broth media and incubated for 24 h. The regrowth was determined by observing turbidity visually, with samples treated with compound where growth was seen classified as static and those with no further growth determined to be cidal.

The experiment was conducted on the shortlisted compounds, fluconazole and gentamicin three times in duplicate, n=3.

Table 7.2 Determination if the compounds and control drugs are cidal or static to microbial cells. It has been determined by investigating their growth visually after 20 min blue light exposure.

Compounds	Fungi		Bacteria	
	S. cerevisiae	*C. albicans*	*S. aureus*	*E. coli*
Compound 1	Static	Static	Static	Static
Compound 2	Static	Static	Static	Static
Compound 11	Static	Static	Static	Static
Compound 36	Static	Static	Static	Static
Compound 43	Static	Static	Static	Static
Fluconazole	Static	Static		
Gentamicin			Cidal	Cidal

As expected, fluconazole showed a static effect against all fungal cells, with gentamicin showing a cidal effect against all bacterial cells (Lewis *et al.*, 1998; Natarajan *et al.*, 1998).

The data suggests that compounds treated with blue light were static to bacterial and fungal cells due to the regrowth of cells observed.

7.2.2 Development of resistance of PDT

The emergence and spread of resistance to antimicrobial drugs is becoming an increasingly serious threat to global public health (Vandeputte *et al.*, 2012; Hawkey, 2008). As a result, traditional and standard treatments become ineffective, and microbial infections persist and may spread to others, which lead to prolonged illness and death (Cosgrove *et al.*, 2003; Hurley, 2005). Therefore, there is always a demand for new antimicrobial approaches where cells have a limited ability to develop resistance.

In this study the development of microbial resistance following repeated exposure to the blue light activated compounds was investigated. The well before that showing MIC was chosen to move into the next round, and over three rounds of repeated exposure, the MICs of the cells to each shortlisted compound were determined. This is consistent with a study by Rosenberg who measured the MIC change throughout three successive exposures (Rosenberg *et al.,* 2018).

The determined minimum inhibitory concentrations of blue light treated compounds are shown as means ±SEM (Figures 7.2 to 7.5). The experiments were repeated on three separate occasions, n=3. Two-way ANOVA analysis was performed, and a significant result was determined to have a *p* value of < 0.05.

7.2.2.1 No development of fungal resistance to the candidate compounds

Two fungal species, *S. cerevisiae* and *C. albicans,* were repeatedly treated with five blue light activated compounds to evaluate the probability of resistance developing to the tested compounds. EUCAST antifungal susceptibility testing was performed and the MICs determined after repeated exposure to Compounds 1, 2, 11, 36 and 43 in the presence of blue light for three successive exposure cycles.
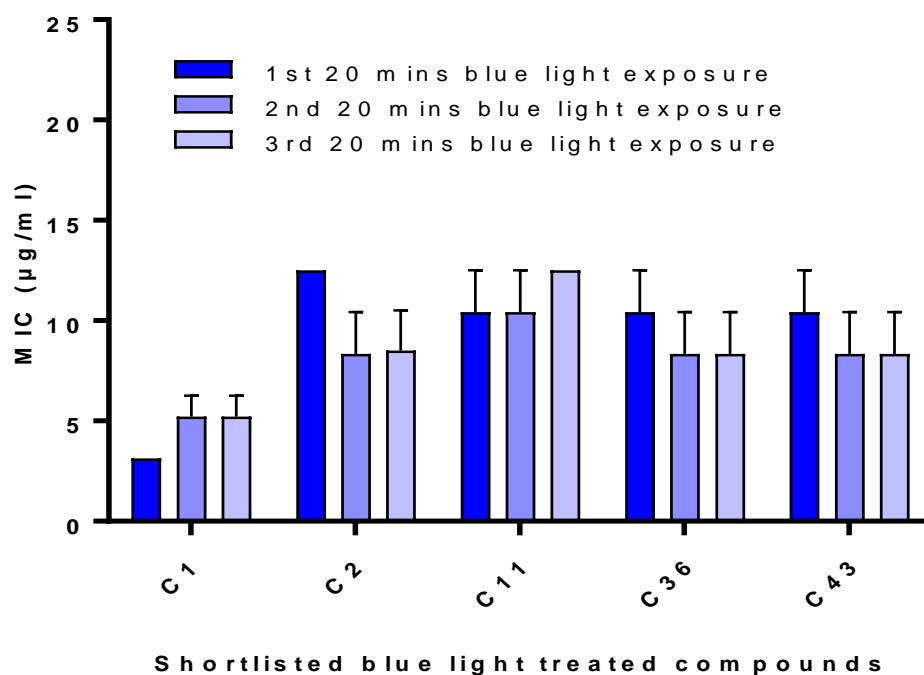
Figure 7.2 Development of resistance to Compound 1, 2, 11, 36 and 43 in *S. cerevisiae*. Comparison of the MICs of five shortlisted compounds against *S. cerevisiae* following three exposures with excitation with blue light for 20 min. The MIC was defined by broth dilution (EUCAST method) as the lowest concentration, recorded in µg/ml, of a compound that gives inhibition of growth of ≥50% of that of the drug-free control. *n*=3 (pooled from duplicate experiments). Values are the means ±SEM. ANOVA analysis of results shows no significant effect of repeated blue light exposure on the development of resistance to these shortlisted compounds in *S. cerevisiae.*
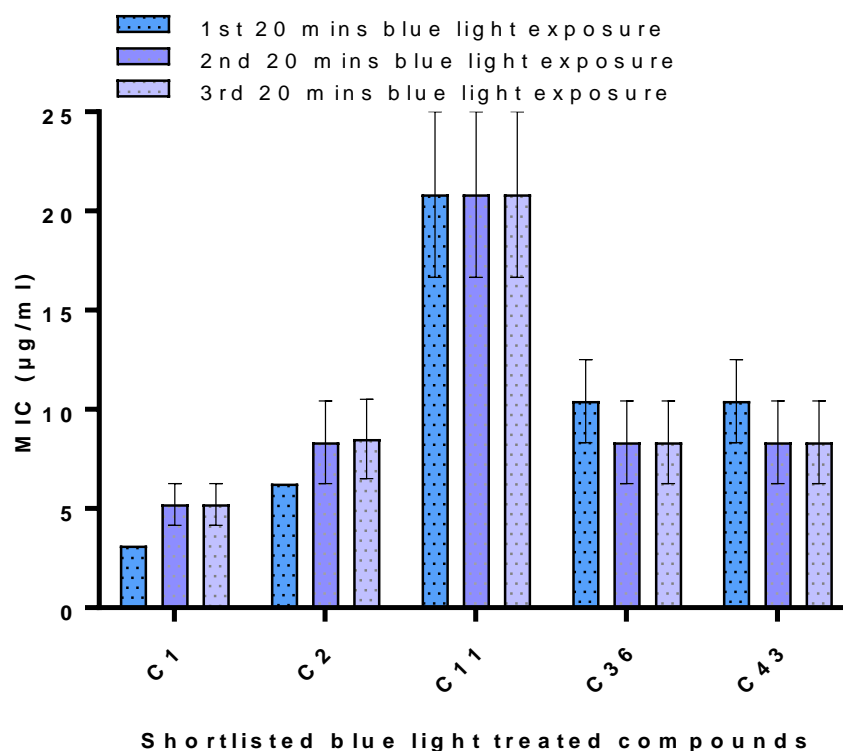
Figure 7.3 Development of resistance to Compounds 1, 2, 11, 36 and 43 in *C. albicans*. Comparison of the MICs of five shortlisted compounds against *C. albicans* following three exposures with excitation with blue light for 20 min. The MIC was defined by broth dilution (EUCAST method) as the lowest concentration, recorded in µg/ml, of a compound that gives inhibition of growth of ≥50% of that of the drug-free control. *n*=3 (pooled from duplicate experiments). Values are the means ±SEM. ANOVA analysis of results shows no significant effect of repeated blue light exposure on the development of resistance to these shortlisted compounds in *C. albicans.*

S. cerevisiae and *C. albicans* suspensions were serially passaged three times on 20-minute blue light illumination and Figures 7.2 and 7.3 demonstrate the changes in MIC obtained with increasing numbers of passages. Two-way ANOVA analysis exhibited no significant difference in the photoantifungal activity between 1st and 3rd passage.

Overall, both fungal species showed no change in susceptibility to the compounds.

7.2.2.2 No development of bacterial resistance to the candidate compounds

Two bacterial species, *S. aureus* and *E. coli,* were repeatedly treated with five blue light activated compounds to evaluate the probability resistance developing to the examined compounds. EUCAST antibacterial susceptibility testing of *S. aureus* and *E. coli* was performed and the MICs determined after repeated exposures to Compounds 1, 2, 11, 36 and 43 in the presence of blue light for three successive exposure cycles.
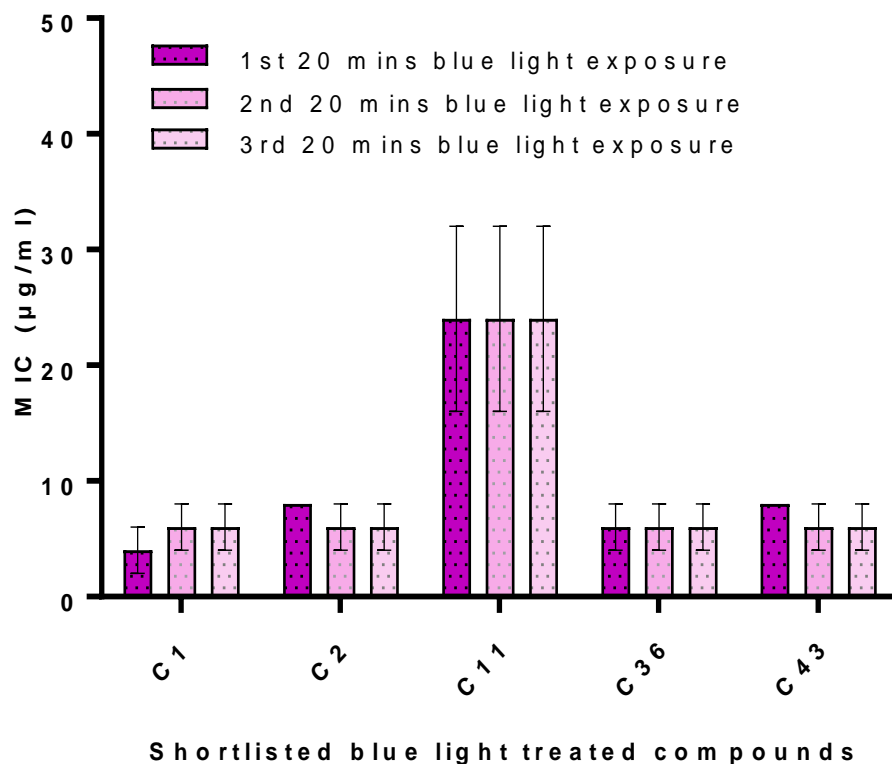
Figure 7.4 Development of resistance to Compounds 1, 2, 11, 36 and 43 in *S. aureus*. Comparison of the MICs of five shortlisted compounds against *S. aureus* following three exposures with excitation with blue light for 20 min. The MIC was defined by broth dilution (EUCAST method) as the lowest concentration, recorded in μg/ml, of a compound that completely inhibits the growth of *S. aureus. n*=3 (pooled from duplicate experiments). Values are the means ±SEM. ANOVA analysis of results shows no significant effect of repeated blue light exposure on the development of resistance to these shortlisted compounds in *S. aureus.*
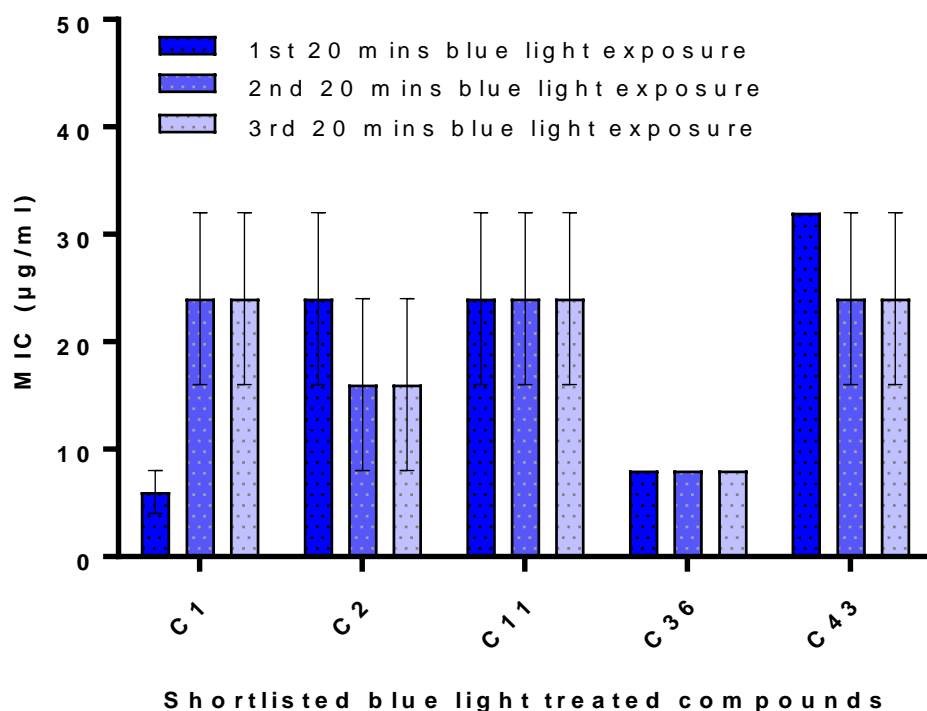
Figure 7.5 Development of resistance to Compounds 1, 2, 11, 36 and 43 in *E. coli*.
Comparison of the MICs of five shortlisted compounds against *E. coli* following three
exposures with excitation with blue light for 20 min. The MIC was defined by broth dilution
(EUCAST method) as the lowest concentration, recorded in µg/ml, of a compound that
completely inhibits the growth of *E. coli*. *n*=3 (pooled from duplicate experiments). Values
are the means ±SEM. ANOVA analysis of results shows no significant effect of repeated
blue light exposure on the development of resistance to these shortlisted compounds in
E. coli.

S. aureus and *E. coli* suspensions were serially passaged three times on 20-
minute blue light illumination and Figures 7.4 and 7.5 demonstrate the changes
in MIC obtained with increasing numbers of passages. However, two-way
ANOVA analysis exhibited no significant difference in the photoantibacterial
activity between 1st and 3rd passage.

Overall, both bacterial species showed no change in susceptibility to the
compounds.

7.2.3 Effect of pH and EDTA on in vitro susceptibility to photoactivated compounds

7.2.3.1 *S. cerevisiae* and *C. albicans* susceptibility decreases when pH reduces

The treatment of vulvovaginal candidiasis (VVC) due to *Candida* species is challenging, with limited therapeutic options. Various studies have found a frequent *in vivo* failure of antifungal drugs in women with vaginitis caused by *Candida* species, which is possibly due to the decrease in susceptibility of *Candida* species to antifungals with more acidic vaginal pH (4 to 4.5) (Marr *et al.*, 1999; Danby *et al.*, 2012). The exact mechanism of pH-induced reduced susceptibility has not been established yet and could be attributed to the pH impact on chemical structure of antifungal drug or on microbial cell. This study evaluated whether a change in media pH had an effect on *in vitro* susceptibility of *S. cerevisiae* and *C. albicans* to fluconazole and blue light treated shortlisted compounds, in order to explain the effectiveness of the compounds under conditions of reduced pH.

The antifungal susceptibility testing was conducted using the broth microdilution EUCAST method and the concentrations tested were 0-64 µg/ml for fluconazole and 0-25 µg/ml for shortlisted compounds, as the MICs obtained for these compounds were within these concentration ranges as shown in Chapters 3 and 4. The MICs were determined as the lowest concentration giving inhibition of growth of ≥50% compared to growth in compound-free growth wells for all tested compounds.

Antifungal susceptibility testing was conducted for *S. cerevisiae* and *C. albicans* by adjusting the pH to 4, 5, 6 and 8, using either 1M hydrochloric acid or sodium hydroxide. The resultant antifungal activities were then compared with the pH of initial experiments that identified the shortlisted compounds (pH=7). This experiment was conducted in the presence and absence of MOPS buffer solution to identify the relationship between the photoantifungal results and the ability of the medium to permit changes in the pH values. The experiments were conducted three times, n=3, in duplicate. Two-way ANOVA analysis was carried out and a significant result was determined to have a *p* value of < 0.05.

Regarding fluconazole, it has been demonstrated that *S. cerevisiae* and *C. albicans* species showed MICs located in the published region, which means that no change in susceptibility was determined. However, as the pH decreased an obvious increase in MIC was noted. For example, in the presence of MOPS, the MIC of fluconazole against *S. cerevisiae* was 0.33 µg/ml at both pH 7 and 8, before increasing approximately threefold, to 0.83 µg/ml at pH 4 (Figure 7.6). While against *C. albicans*, the MIC of fluconazole in the presence of MOPS was 0.21 µg/ml at pH 7 and 8, which increased twofold at pH 4 to 0.42 µg/ml (Figure 7.8).

The results of testing compounds in *S. cerevisiae* and *C. albicans* in *in vitro* exhibited that blue light treated compounds behaved similarly with a drop in pH and showed an increase in MIC, particularly at pH 4. This was a trend noted for all five of the shortlisted compounds, with MIC increasing with a decrease in pH.

With a decrease in pH from 8 to 4 it was seen a 3-fold rise in MIC of Compound 2 in the presence of MOPS from 5.21 to 16.67 µg/ml against *S. cerevisiae* and twofold rise in MIC of Compound 2 from 5.21 to 10.42 µg/ml against *C. albicans.*

In general, for both fluconazole and the shortlisted compounds, the MICs in the absence of MOPS were not significantly different from those in the presence of MOPS (Figures 7.7 and 7.9).
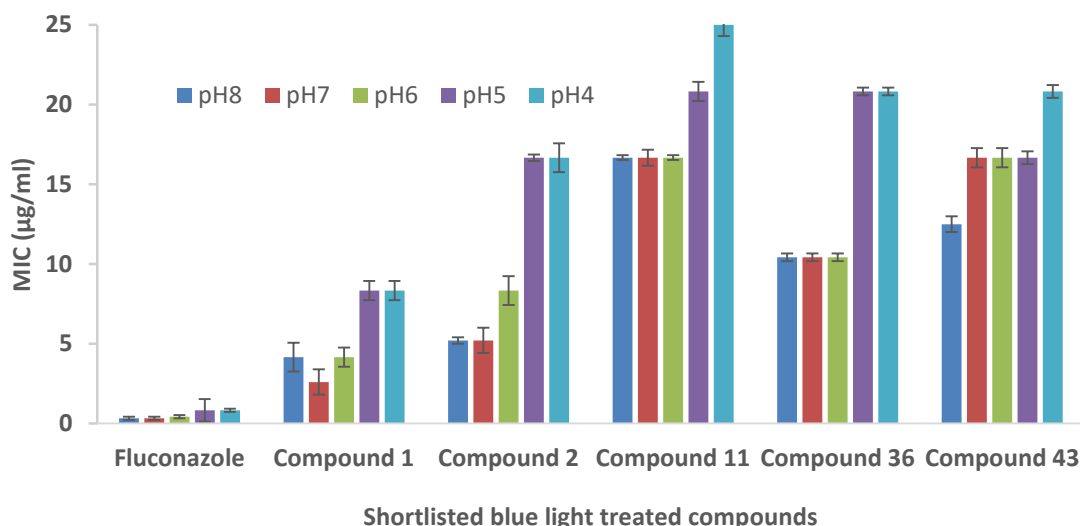
Figure 7.6 Minimum inhibitory concentrations MICs$_{50}$ susceptibility results for *S. cerevisiae* at pH 8, 7, 6, 5 and 4 in the presence of MOPS buffer solution. The experiment was conducted in duplicate, n=3. Values are the means ±SEM. Data analysed by two-way ANOVA analysis and significance indicated between susceptibility in pH 4 and pH 7 *p <0.01.
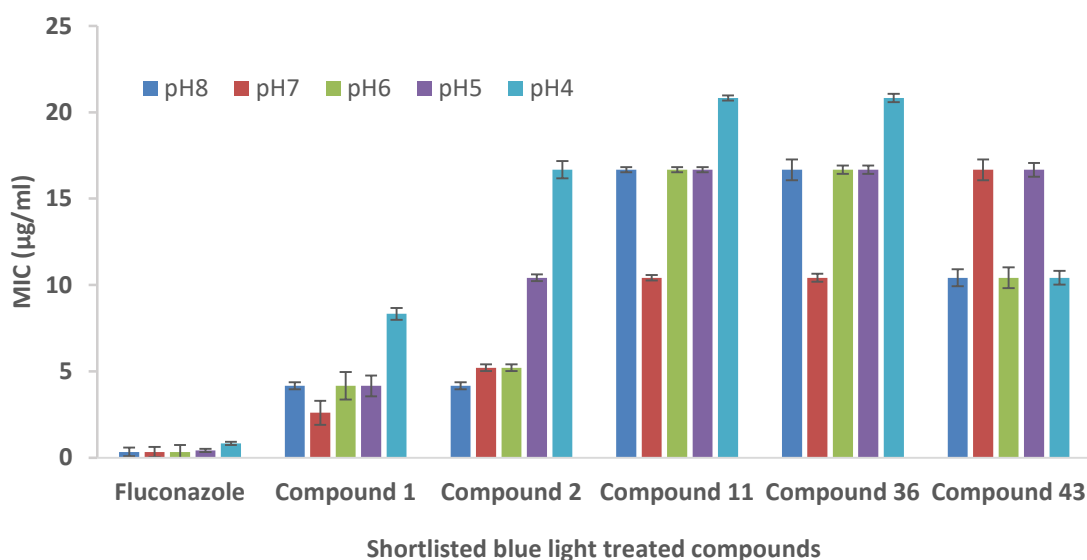
Figure 7.7 Minimum inhibitory concentrations MICs$_{50}$ susceptibility results for *S. cerevisiae* at pH 8, 7, 6, 5 and 4 in the absence of MOPS buffer solution. The experiment was conducted in duplicate, n=3. Values are the means ±SEM. Data analysed by two-way ANOVA analysis and significance indicated between susceptibility in pH 4 and pH 7 *p <0.01.
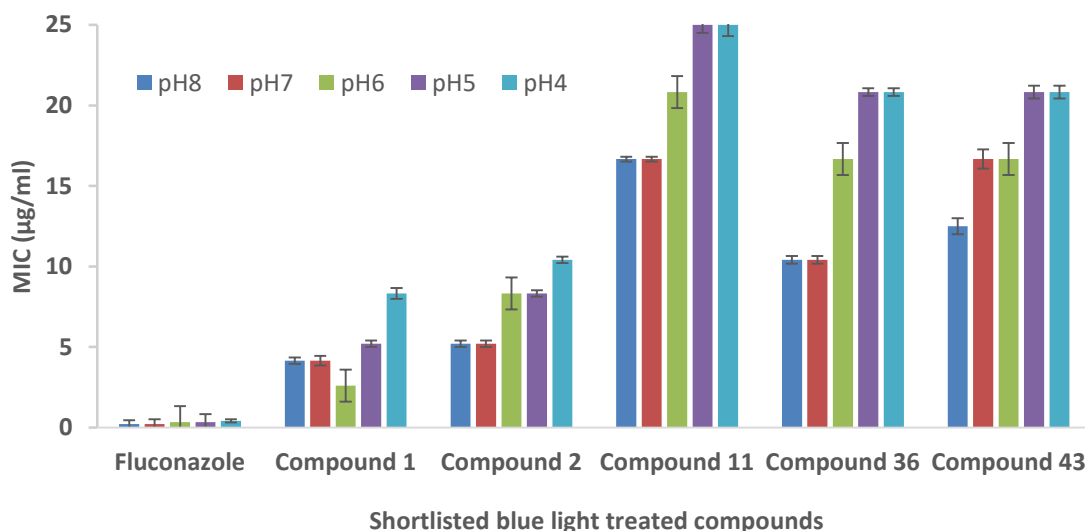
Figure 7.8 Minimum inhibitory concentrations MICs$_{50}$ susceptibility results for *C. albicans* at pH 8, 7, 6, 5 and 4 in the presence of MOPS buffer solution. The experiment was conducted in duplicate, n=3. Values are the means ±SEM. Data analysed by two-way ANOVA analysis and significance indicated between susceptibility in pH 4 and pH 7 *p <0.01.
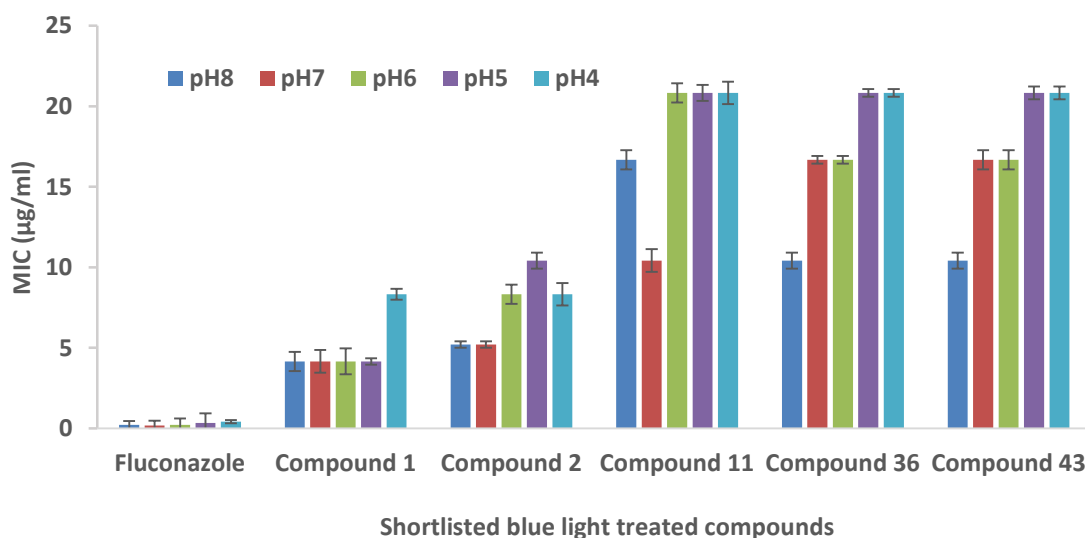
Figure 7.9 Minimum inhibitory concentrations MICs$_{50}$ susceptibility results for *C. albicans* at pH 8, 7, 6, 5 and 4 in the absence of MOPS buffer solution. The experiment was conducted in duplicate, n=3. Values are the means ±SEM. Data analysed by two-way ANOVA analysis and significance indicated between susceptibility in pH 4 and pH 7 *p< 0.01.

7.2.3.2 EDTA addition increases the susceptibility of *S. cerevisiae* and *C. albicans* to the shortlisted compounds

The antibacterial effects of EDTA have been investigated widely and proved to be limited (Orstavik *et al.*, 1990; Heling *et al.*, 1998). However, EDTA may have antifungal potential with its chelating property because calcium ions have a critical role in morphogenesis and pathogenesis of *C. albicans*. Additionally, EDTA can reduce the fungal growth by removing calcium from the cell wall and causing collapse in the cell wall, and by inhibiting enzyme reactions (Holmes *et al.*, 1991).

Therefore, the aim of this study was to determine the susceptibility of *S. cerevisiae* and *C. albicans* to the combination of photoactivated compounds and fluconazole with and without 10 mM EDTA. The MOPS buffer solution effect was studied to investigate the influence of pH change on the photoantifungal results. The susceptibility testing using the broth microdilution method was performed according to EUCAST guidelines. The concentrations tested were 0-64 µg/ml for fluconazole and 0-25 µg/ml for shortlisted compounds, as the MICs obtained for these compounds were within these concentration ranges as shown in Chapters 3 and 4. The MICs were determined as the lowest concentration giving inhibition of growth of ≥ 50% compared to growth in compound-free growth wells for all tested compounds. The experiments were conducted on three different occasions, n=3. ANOVA analysis was conducted to determine the significant results.

The *S. cerevisiae* and *C. albicans* cells were exposed to 10 mM EDTA alone at pH 7 in the absence of the compounds. No significant impact on growth was observed.

Fluconazole showed MICs located in the region of published results against *S. cerevisiae* and *C. albicans* strains, which means that strains remained susceptible to fluconazole in the presence and absence of EDTA regardless of the presence of MOPS buffer. However, the presence of EDTA resulted a slight decrease in MIC values. For example, in the presence of MOPS, MIC of

fluconazole was 0.42 μg/ml, when EDTA was not present, which decreased to 0.21 μg/ml after addition of EDTA (Table 7.3).

The results of testing compounds in *S. cerevisiae* and *C. albicans in vitro* exhibited that blue light treated compounds behaved similarly with addition of EDTA and showed a drop in MICs. In general, for both fluconazole and the shortlisted compounds, the MICs in the absence of MOPS were not significantly different from those in the presence of MOPS (Figures 7.6 to 7.9).

It has been demonstrated that addition of 10 mM EDTA increases the susceptibility of both *S. cerevisiae* and *C. albicans* to fluconazole. A similar trend is seen when EDTA is used in combination with the blue light activated compounds, in the presence and absence of MOPS. The MIC of light activated Compound 1 in *S. cerevisiae* was 5.21 μg/ml in the presence of MOPS, which dropped to 2.6 μg/ml when EDTA was added. Similarly, Compound 43, showed a lower MIC in *C. albicans* in the presence of MOPS when EDTA was added (10.42 μg/ml) than without EDTA at a (25 μg/ml). As shown in Table 7.3, EDTA addition decreased the susceptibility of both species *S. cerevisiae* and *C. albicans* to fluconazole and treated compounds in either presence or absence of MOPS.

Table 7.3 Minimum inhibitory concentrations MICs$_{50}$ susceptibility results for *S. cerevisiae* and *C. albicans* in the presence and absence of 10 mM EDTA with and without MOPS (a final concentration of 0.165 M).

Compounds	*S. cerevisiae*				*C. albicans*			
	MICs with MOPS (µg/ml)		MICs without MOPS (µg/ml)		MICs with MOPS (µg/ml)		MICs without MOPS (µg/ml)	
	NO EDTA	EDTA	NO EDTA	EDTA	NO EDTA	EDTA	NO EDTA	EDTA
Fluconazole	0.42	0.21	0.42	0.33	0.42	0.33	0.42	0.33
Compound 1	5.21	2.6	5.21	4.16	10.42	4.16	10.42	5.21
Compound 2	10.42	4.16	10.42	8.33	16.67	5.21	16.67	8.33
Compound 11	16.67	16.67	16.67	8.33	20.83	16.67	20.83	16.67
Compound 36	25	10.42	25	16.67	20.83	16.67	20.83	16.67
Compound 43	20.83	16.67	20.83	16.67	25	10.42	16.67	8.33

7.2.4 Photoactivated antimicrobial compounds decreased significantly the viability of HeLa cell line

Most photoactivated compounds work via the release of ROS (Radicals via Type 1 reactions reactions and singlet oxygen via Type 2), which is able to kill cells as a result of oxidative stress (Baltazar *et al.*, 2015). *In vitro* studies have only allowed measurement of singlet oxygen production in a non-biological environment and radical species could not be measured, as discussed in Chapter 3. Therefore, an alternative method was required to determine if the antimicrobial effect of the compounds was a result of ROS release.

The cellular response of fungi to oxidative stress has been well characterised, especially in the yeast *S. cerevisiae*. As such, mutant strains of *S. cerevisiae*, deleted for key genes involved in the stress response, were utilised to help understand the mechanism of action of the shortlisted compounds. *S. cerevisiae* was selected as a model organism due to the ability to delete genes from the genome and the high level of homologue to *C. albicans* pathways, especially in regard to stress (Pascual-Ahuir *et al.*, 2007).

The compounds were tested against *S. cerevisiae* strains deleted for Hog1, a key component of the stress activated MAPK pathway, and Msn2/4p, transcription factors that are downstream targets of the oxidative stress response. Deletion of the genes encoding these proteins results in sensitivity of cells to oxidative stress. Therefore, this phenotype was used to investigate the effect of the blue light treated compounds against *HOG1* and *MSN2/4* genomic deletion strains compared to the wildtype MIC values. The strains were tested using the EUCAST antifungal susceptibility method, following 20-minute blue light activation of the compounds (EUCAST 7.3: Arendrup *et al.*, 2015a). The experiment was conducted twice in duplicate. Two-way ANOVA analysis was conducted to determine significance of results. The data presented in Figure 7.10 compares the MICs for wildtype *S. cerevisiae* and the deletion strains, *hog1Δ* and *msn2/4Δ*, when exposed to each of the light activated shortlisted compounds. Increased sensitivity of the deletion strains to the compounds when compared to the wildtype control would suggest that the associated signalling pathways are being activated.
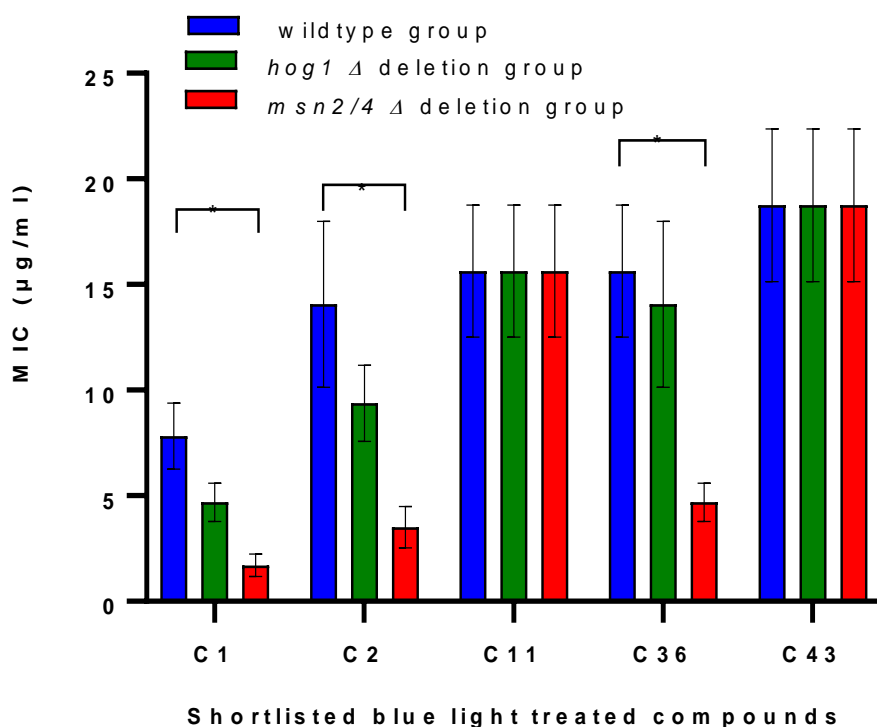
Figure 7.10 Comparison of the MICs of shortlisted compounds according to EUCAST method against wildtype, *hog1Δ* deletion and *msn2/4Δ* deletion strains of *S. cerevisiae* after 20 min blue light exposure. The experiment was conducted in duplicate, n=2. Values are the means ±SEM. Two-way ANOVA analysis of results was conducted.

Three control bioassays with hydrogen peroxide, blue light alone and untreated compounds against wildtype, *hog1Δ* deletion and *msn2/4Δ* deletion strains of *S. cerevisiae* were carried out. The level of growth inhibition for the control, hydrogen peroxide H_2O_2, against *msn2/4Δ* was significantly higher than wildtype strain (at 37% versus 19%) without reaching MIC. While *hog1Δ* deletion did not show a significant difference when compared with wildtype (data not shown). No growth inhibition was observed for the wildtype or deletion strains following exposure to blue light alone.

Following blue light activation of Compounds 11 and 43, no significant change in the MIC was observed between the wildtype control and the deletion strains. The MIC for the light treated Compounds 1, 2 and 36 showed no significant reduction in the *hog1Δ* deletion when compared to wildtype, 7.81 µg/ml versus 4.69 µg/ml, 14.06 µg/ml versus 9.375 µg/ml and 15.63 µg/ml versus 14.06 µg/ml, respectively

(Figure 7.10). However, a significant decrease in MIC was seen in the *msn2/4Δ* deletion when compared to wildtype *S. cerevisiae* for Compound 1 (7.81 µg/ml versus 1.7 µg/ml), Compound 2 (14.06 µg/ml versus 3.515 µg/ml) and Compound 36 (15.63 µg/ml versus 4.688 µg/ml) (Figure 7.10).

7.2.5 Only Compounds 1, 2 and 43 show an antifungal activity against *C. albicans* biofilms

It has previously been reported that the five shortlisted compounds have photoantifungal activity against *C. albicans* following activation by blue light (Table 7.1). EUCAST guidelines utilise free planktonic cells for the *in vitro* susceptibility test. However, *C. albicans* infections can be associated with biofilm formation, which is difficult to fully eradicate using normal therapy approaches. As the EUCAST method does not provide an accurate *in vitro–in vivo* correlation, *C. albicans* biofilms were prepared in flat bottom 96-well microtiter plates (Ramage *et al.,* 2001). Concentrations of fluconazole (0 to 64 µg/ml), amphotericin B (0 to 16 µg/ml) and the five shortlisted compounds (0 to 25 µg/ml) were added to the biofilm cells. These concentrations were chosen as they were within the MICs ranges previously obtained in Chapters 3 and 4. Following exposure to blue light for 20 min the plates were incubated for 48 h at 35°C.

To evaluate the effects of the control drugs and the blue light activated compounds against biofilm sessile cells, a colorimetric method using the XTT reduction assay was performed. The metabolic activity of biofilm cells was determined in a microtiter plate reader at 490 nm and the MICs of fluconazole, amphotericin B and tested compounds were defined as the first drug concentrations leading to 50% reduction of *C. albicans* metabolic activity.

The metabolic activity calculated was: (OD_{490nm} sample/ OD_{490nm} drug-free control)* 100%.

The graphs show the means ±SEM (standard error of the mean) of the percent metabolic activity for the concentrations series of fluconazole, amphotericin B and blue light treated compounds against *C. albicans* biofilm cells (Figures 7.11 to 7.17). Fluconazole was used as a control in *C. albicans* planktonic cells and amphotericin B for sessile cells.
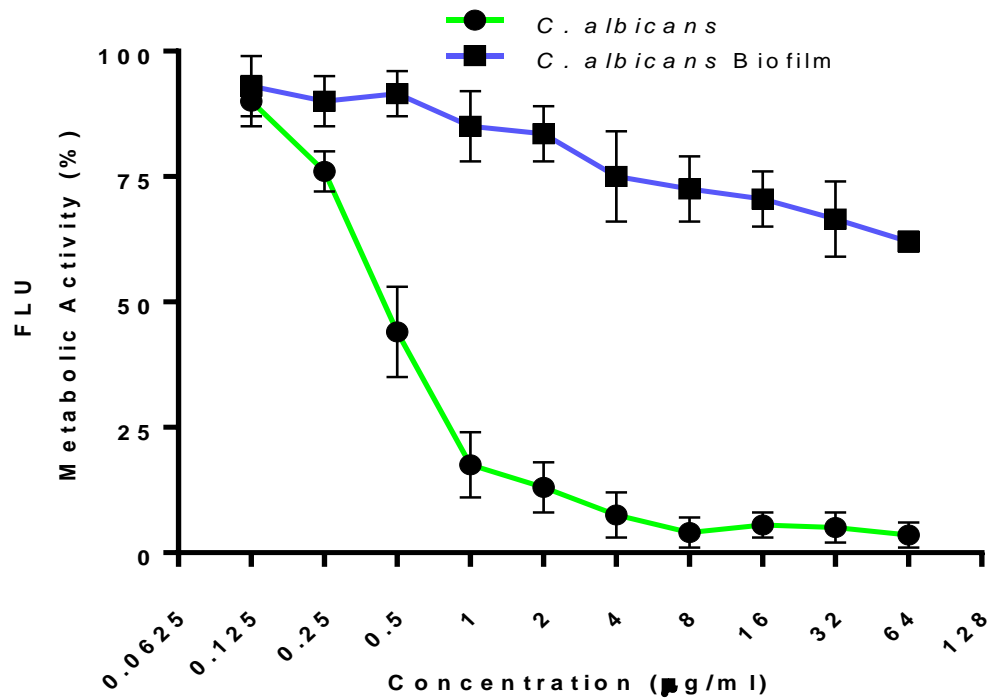
Figure 7.11 Effect of fluconazole on the metabolic activity of *C. albicans* and *C. albicans* biofilms. Comparison of the MICs of fluconazole against *C. albicans* and *C. albicans* biofilm. The metabolic activity calculated was: $(OD_{490nm}$ sample/ OD_{490nm} drug-free control)* 100%. Minimum inhibitory concentrations were determined to be the first concentration showing $\geq$ 50% reduction of *C. albicans* and *C. albicans* biofilm metabolic activity. Data shown as means of duplicates ±SEM.
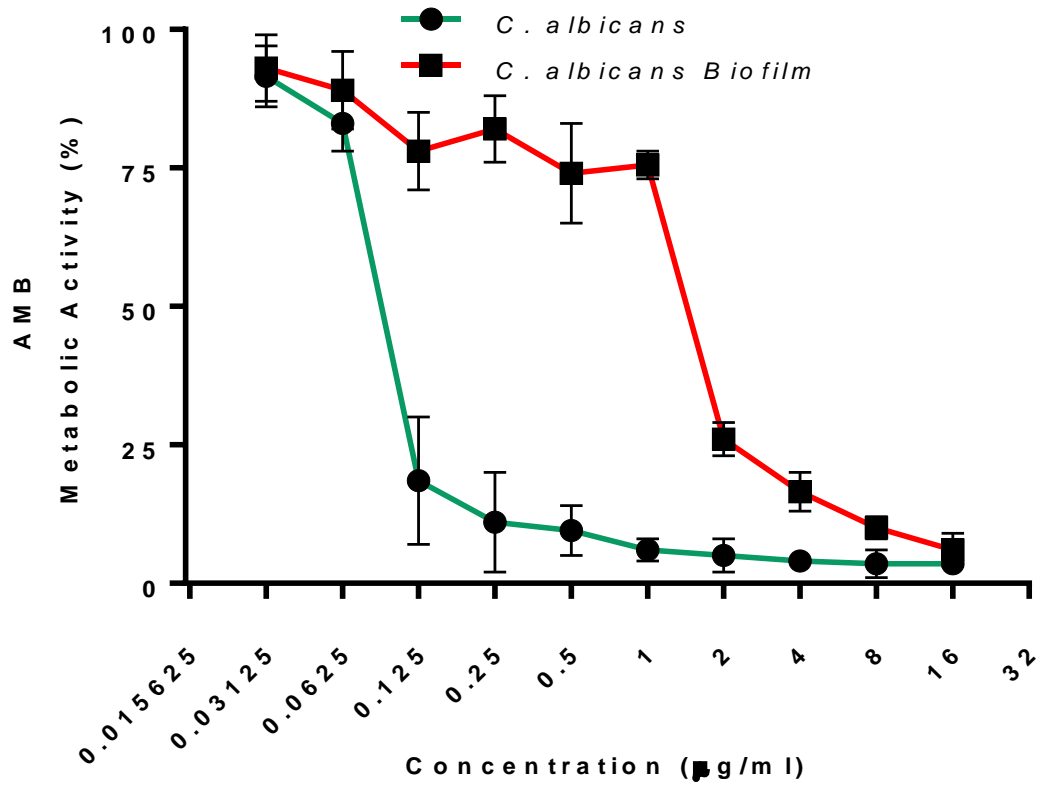
Figure 7.12 Effect of amphotericin B on the metabolic activity of *C. albicans* and *C. albicans* biofilms. Comparison of the MICs of amphotericin B against *C. albicans* and *C. albicans* biofilm. The metabolic activity calculated was: (OD$_{490nm}$ sample/ OD$_{490nm}$ drug-free control)* 100%. Minimum inhibitory concentrations were determined to be the first concentration showing ≥ 50% reduction of *C. albicans* and *C. albicans* biofilm metabolic activity. Data shown as means of duplicates ±SEM.
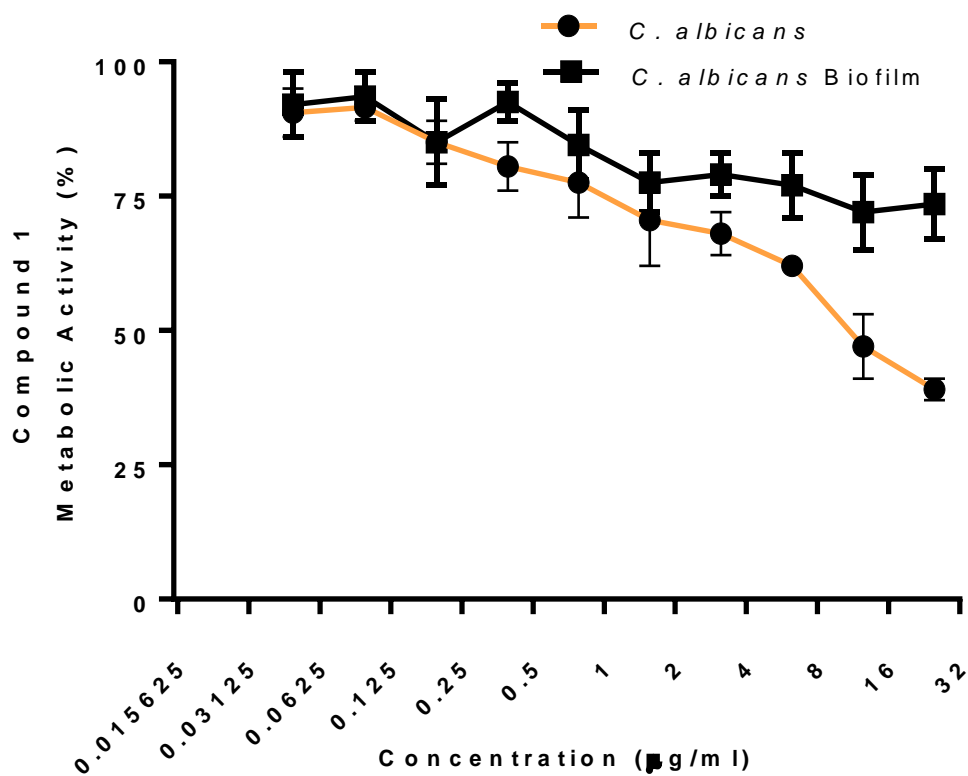
Figure 7.13 Effect of 20 min blue light treated Compound 1 on the metabolic activity of *C. albicans* and *C. albicans* biofilms. The metabolic activity calculated was: (OD_{490nm} sample/ OD_{490nm} drug-free control)* 100%. Minimum inhibitory concentrations were determined to be the first concentration showing ≥ 50% reduction of *C. albicans* biofilm metabolic activity. Data shown as means of duplicates ±SEM.
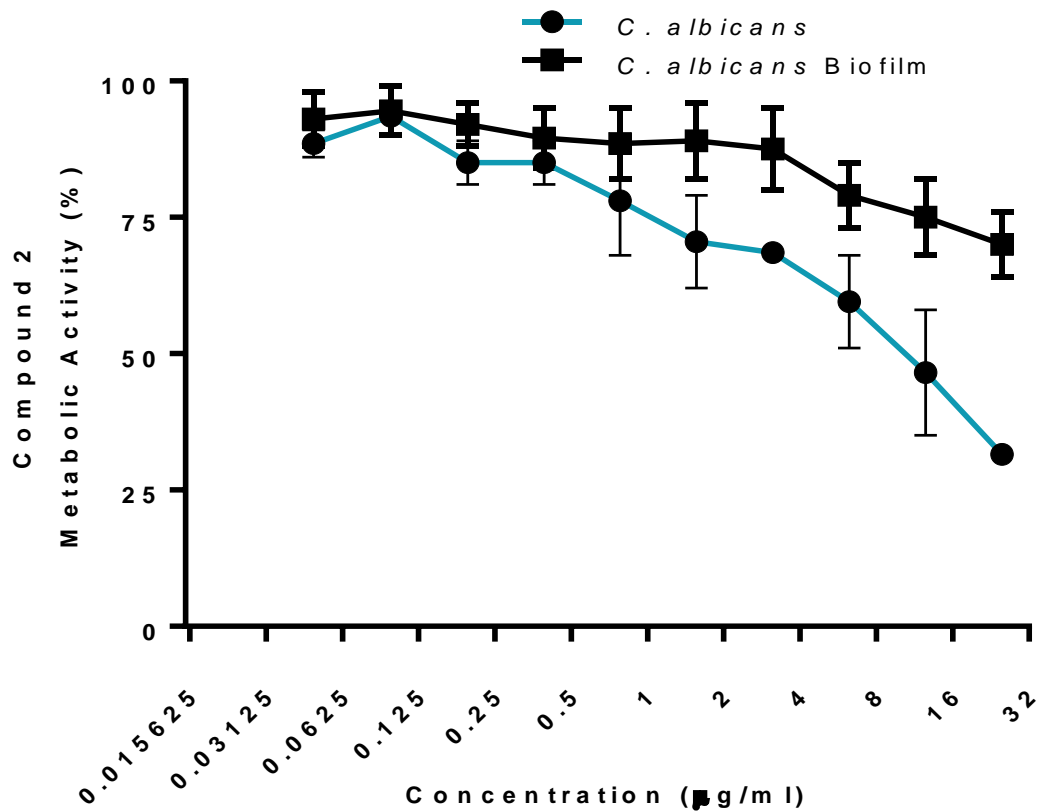
Figure 7.14 Effect of 20 min blue light treated Compound 2 on the metabolic activity of *C. albicans* and *C. albicans* biofilms. The metabolic activity calculated was: (OD_{490nm} sample/ OD_{490nm} drug-free control)* 100%. Minimum inhibitory concentrations were determined to be the first concentration showing $\geq$ 50% reduction of *C. albicans* biofilm metabolic activity. Data shown as means of duplicates ±SEM.
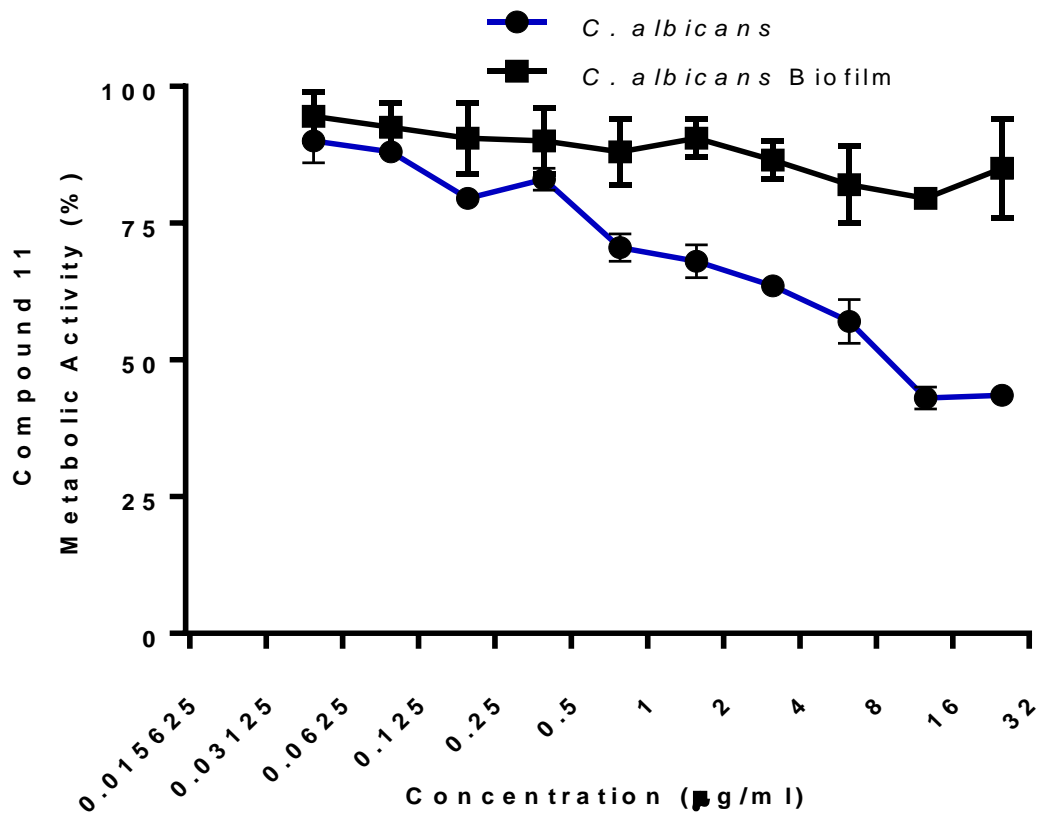
Figure 7.15 Effect of 20 min blue light treated Compound 11 on the metabolic activity of *C. albicans* and *C. albicans* biofilms. The metabolic activity calculated was: (OD_{490nm} sample/ OD_{490nm} drug-free control)* 100%. Minimum inhibitory concentrations were determined to be the first concentration showing ≥ 50% reduction of *C. albicans* biofilm metabolic activity. Data shown as means of duplicates ±SEM.
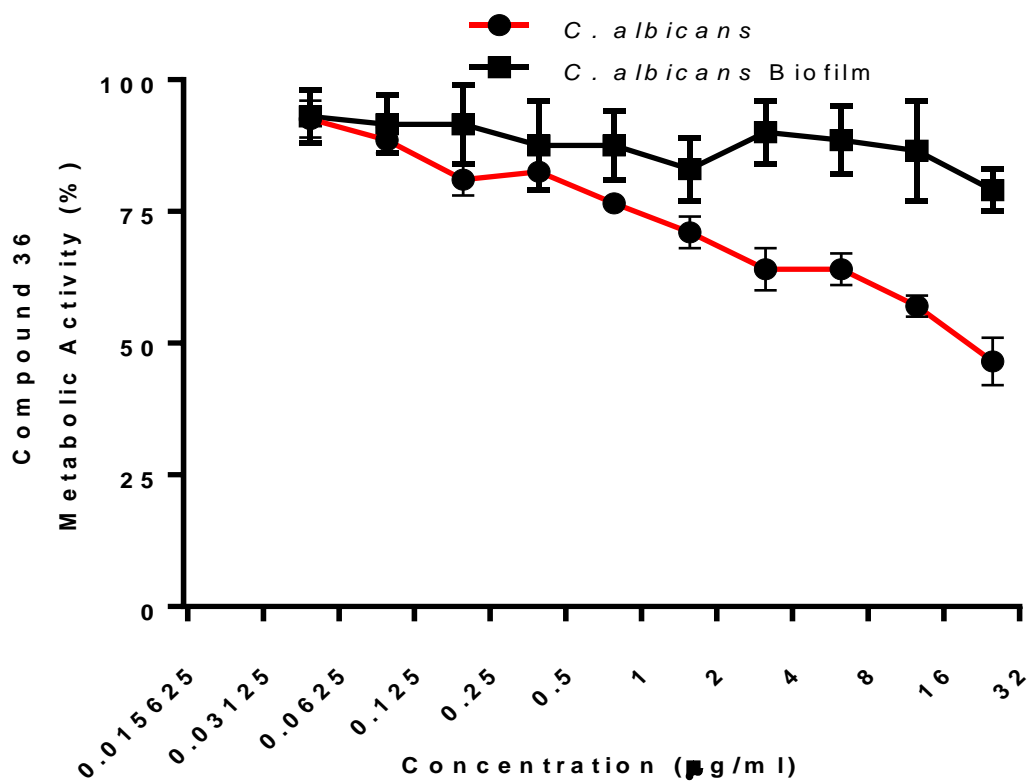
Figure 7.16 Effect of 20 min blue light treated Compound 36 on the metabolic activity of *C. albicans* and *C. albicans* biofilms. The metabolic activity calculated was: (OD_{490nm} sample/ OD_{490nm} drug-free control)* 100%. Minimum inhibitory concentrations were determined to be the first concentration showing ≥ 50% reduction of *C. albicans* biofilm metabolic activity. Data shown as means of duplicates ±SEM.
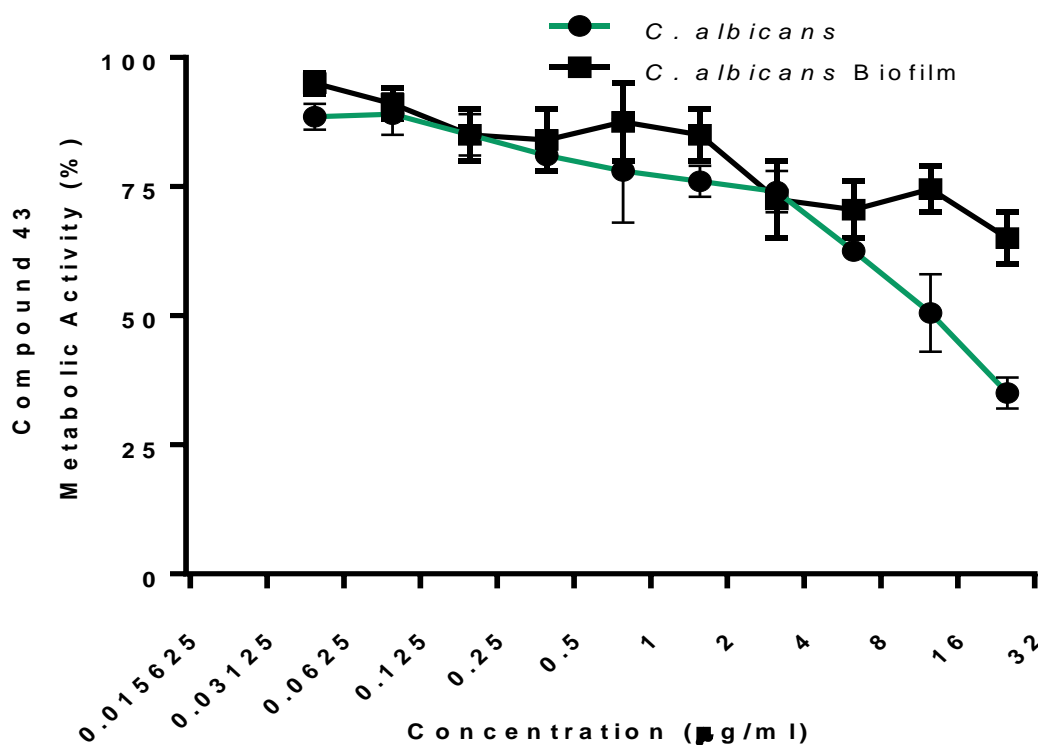
Figure 7.17 Effect of 20 min blue light treated Compound 43 on the metabolic activity of *C. albicans* and *C. albicans* biofilms. The metabolic activity calculated was: (OD_{490nm} sample/ OD_{490nm} drug-free control)* 100%. Minimum inhibitory concentrations were determined to be the first concentration showing ≥ 50% reduction of *C. albicans* biofilm metabolic activity. Data shown as means of duplicates ±SEM

As shown in Figure 7.11, fluconazole reduced the fungal metabolic activity in a concentration-dependent manner in planktonic *C. albicans.* Exposure of planktonic *C. albicans* suspensions to concentrations of 0.5 μg/ml decreased their metabolic activity by more than 50% (MIC of 0.5 μg/ml). When exposed to a *C. albicans* biofilm, fluconazole was less effective, reaching a total inactivation of metabolic viability of 38%.

Regarding amphotericin B, as shown in Figure 7.12, it significantly reduced the metabolic activity of planktonic *C. albicans* suspensions in a concentration-dependent way, with a determined MIC of 0.125 μg/ml. A higher concentration of 2 μg/ml was required to inhibit the *C. albicans* biofilms and this value was 16-fold higher than the MIC determined in planktonic *C. albicans* cells.

None of the light activated shortlisted compounds were able to decrease the metabolic activity of *C. albicans* biofilms to the threshold percentage of 50% (Figures 7.13 to 7.17). In all cases metabolism inactivation was noted, with only a significant decrease in metabolic activity seen with Compound 1 (26 %), Compound 2 (30 %) and Compound 36 (35%), at the maximum concentrations tested (Figures 7.13 to 7.17). While testing all the light activated compounds exhibited a significant decrease in the metabolic activity of planktonic *C. albicans* to the threshold percentage of 50% (Figures 7.13 to 7.17).

The compounds alone showed no significant effect on the metabolic activity of both planktonic *C. albicans* and *C. albicans* biofilms.

7.2.6 *S. cerevisiae* and *C. albicans* exhibited growth at drug concentration above the MIC (SMG), with no MIC change between 24 and 48 h

Antifungal MIC measurements determined by the EUCAST method can inform about the resistance or sensitivity of a microorganism to the drug and help in making treatment decisions. However, this does not necessarily predict the fungal response to the treatment within a clinical situation. To better correlate antifungal response *in vitro* with that seen in the clinic, the term perseverance was defined (Rosenberg *et al.*, 2018). Perseverance is the ability of fungal cells to grow at a drug concentration above the MIC and is measured as the degree of supra-MIC growth (SMG) in the broth microdilution assay. Perseverance may be considered a useful parameter for predicting clinical persistence and choosing appropriate antifungal therapies as it correlates with the success or failure of treatment in the clinic.

In general, the MICs of photoactivated compounds do not change when analysed on consecutive days (Giuliani *et al.*, 2010; Tavares *et al.*, 2010). To reinforce the idea that susceptibility/resistance is not time-dependent, the MICs of the shortlisted compounds were measured and then compared with the SMG. The MICs of blue light treated compounds were determined against *S. cerevisiae* and *C. albicans* following 24 and 48 h incubation to provide information about resistance. MIC values were measured using the EUCAST broth microdilution method and determined to be the first well giving growth inhibition of ≥ 50% of that of drug-free control. Fluconazole was used as a control drug and the experiment was conducted in triplicate.
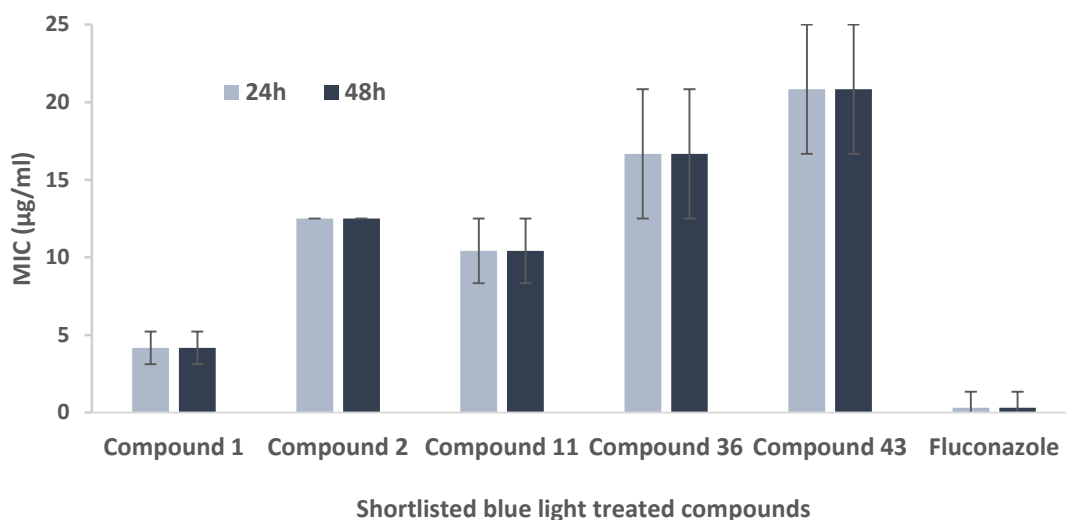
Figure 7.18 Effect of incubation time on MIC values measured in *S. cerevisiae* at 24 and 48 h. MICs values were determined using the EUCAST broth microdilution assay following 24 and 48 h incubation with the light activated compound. The MIC was determined to be the compound concentration at which 50% of the growth in the absence of compound is inhibited. The five shortlisted blue light treated compounds were used in a twofold serial dilution (0-25 µg/ml). Data shown as means of triplicates ±SEM. Two-way ANOVA analysis was used to determine significant results.
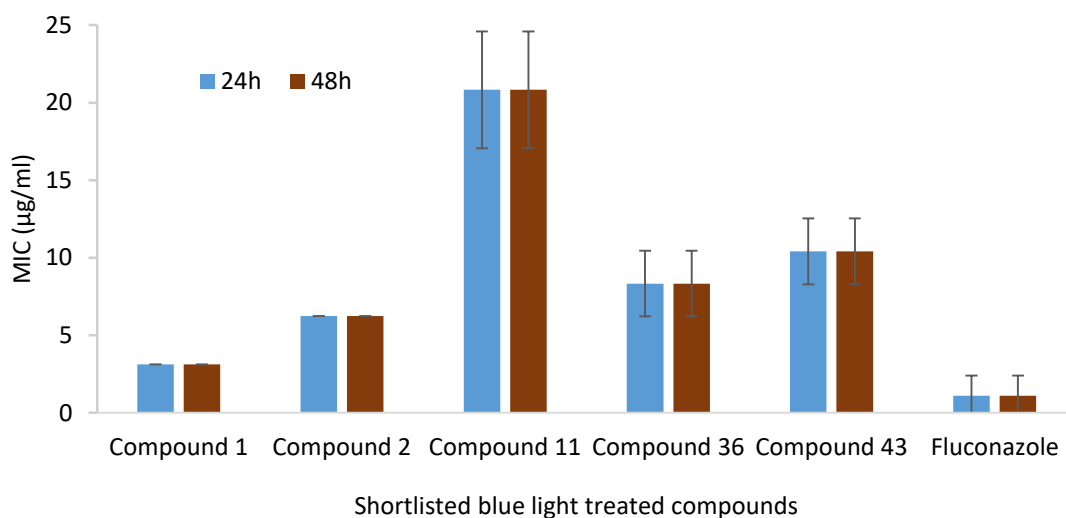
Figure 7.19 Effect of incubation time on MIC values measured in *C. albicans* at 24 and 48 h MICs values were measured at 24 and 48 h to be the compound concentration at which 50% of the growth in the absence of compound is inhibited. The five shortlisted blue light treated compounds were used in serial twofold dilutions (0-25 µg/ml). Data shown as means of triplicates ±SEM. Two-way ANOVA analysis was used to determine significant results.

Results shown in Figures 7. 18 and 7.19 demonstrate that, following blue light activation of the compounds, the MICs against *S. cerevisiae* and *C. albicans* did not change between 24 and 48 h. Two-way ANOVA analysis of results was carried out to dhow significant differene.

Supra-MIC growth (SMG) for tested compounds was quantified using the optical density method as the average growth per well obtained above the MIC at 24 and 48 h, normalised to the growth level seen in the drug-free control.
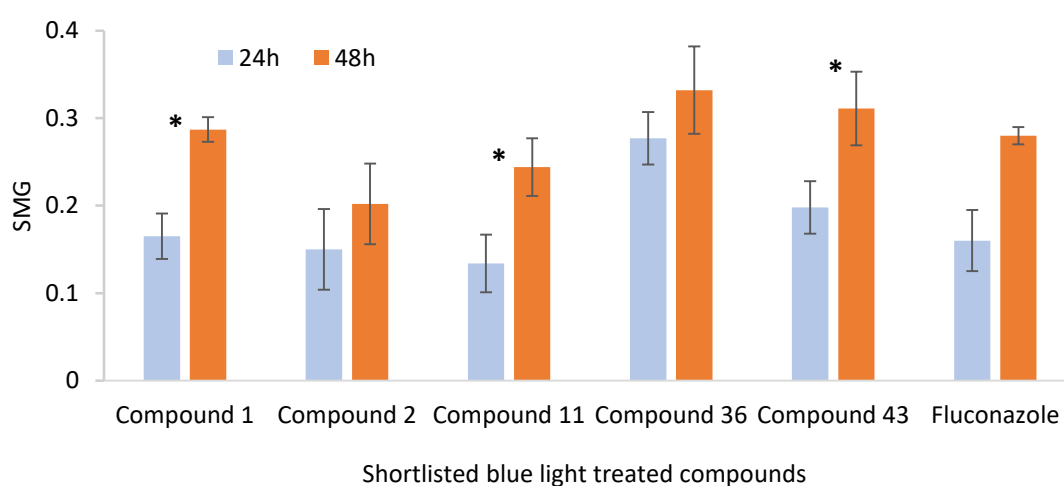
Figure 7.20 Effect of incubation time on SMG values measured in *S. cerevisiae* at 24 and 48 h. Supra-MIC Growth (SMG) values were measured at 24 and 48 h as the average growth per well above the MIC divided by the compound-free growth control. The five shortlisted blue light treated compounds were used in serial twofold dilutions (0-25 µg/ml). Data shown as means of triplicates ±SEM. ANOVA analysis of results shows significant difference between SMG at 24h and 48 h for Compounds 1, 11 and 43 *$p <$ 0.05.
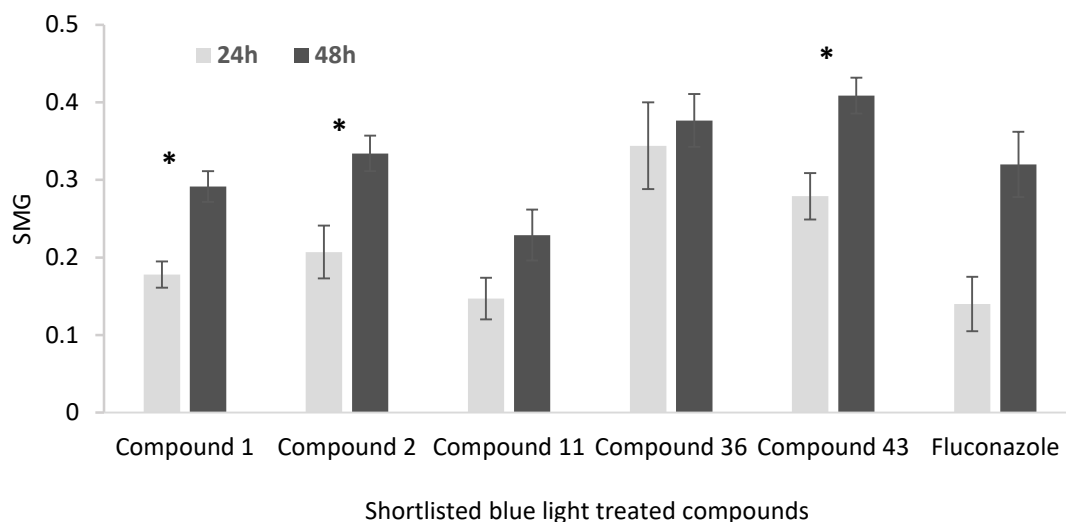
Figure 7.21 Effect of incubation time on SMG values measured in *C. albicans* at 24 and 48 h. Supra-MIC Growth (SMG) values were measured at 24 and 48 h as the average growth per well above the MIC divided by the compound-free growth control. The five shortlisted blue light treated compounds were used in serial twofold dilutions (0-25 µg/ml). Data shown as means of triplicates ±SEM. ANOVA analysis of results shows significant difference between SMG at 24h and 48 h for Compounds 1, 2 and 43 *p <0.05.

SMG values were measured at 24 and 48 h by measuring SMG in the broth microdilution assay (Figures 7.20 and 7.21). For all compounds tested, *S. cerevisiae* and *C. albicans* showed growth at concentrations above the MIC and there was a significant increase in the calculated SMG between 24 h and 48 h.

Both fungal species exhibited growth at a drug concentration above the MIC, while the MIC levels did not change between 24 and 48 h.

7.2.7 Effect of blue light and activated compounds on mammalian cells

7.2.7.1   Optimisation of the cell viability protocol

The candidate compounds have all demonstrated antimicrobial activity, however, their effect on mammalian cells has not been determined. As any new antimicrobial reagent would be required to have minimal affect in host cells, the shortlisted compounds were tested to determine their toxicity in mammalian cells. The assays were performed using HeLa cells, an immobilised human cell line derived from cervical cancer cells. To determine the best time range for evaluating the effects of the compounds, a growth curve was performed over a period of four days.

HeLa cells were seeded in 12-well plate at a density of 5,000 cells per well in EMEM. After 24, 48, 72 and 96 h incubation at 37˚C, three wells were trypsinised and the cell number determined by a manual cell count using a haemocytometer, and via trypan blue, to determine cell viability. This process was repeated three times in triplicate (Figure 7.22). The growth curve shows an increase in cell numbers over time, with a reduced growth rate at 96 h, indicating that compounds should be tested throughout 96 h post treatment.
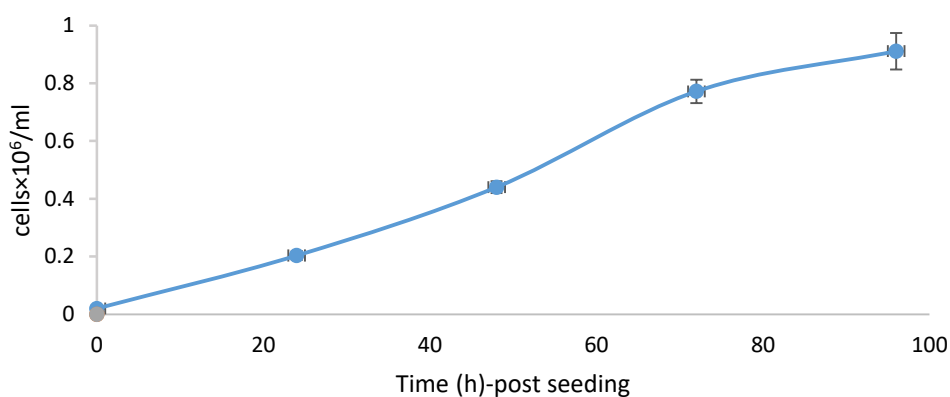
Figure 7.22 Growth curve for HeLa cells over a period of 24, 48, 72 and 96 h incubation. 5,000 cells/ml were seeded in EMEM and the cell number was determined by counting cells manually using haemocytometer. The experiments were conducted on three independent occasions in triplicate. Data shown as means ±SEM.

7.2.7.2 2,000 cells/well is the appropriate initial seeding density for the toxicity experiments

PrestoBlue® is a resazurin-based cell permeable viability indicator that is quickly reduced by metabolically active cells (living cells). Production of the fluorescent reduced form can be measured (Ex 535 nm / Em 612 nm), providing a quantitative measure of viability and cytotoxicity. To optimise the assay for determining cell viability following exposure to the compound, the optimal cell number had to be identified. This was determined by measuring the linearity of fluorescence versus cell number to find a suitable working cell density. Cells were seeded into a 96 well plate at a final concentration of 500, 1,000, 2,000, 2,500, 5,000 and 10,000 cells in EMEM complete medium and incubated for 24, 48, 72 and 96 h. PrestoBlue®, at ratio 1:10, was then added to the cells for one hour and the fluorescence measured using a Tecan GENius PRO plate reader (Ex 535 nm / Em 612 nm) (Figure 7.23). This process was repeated three times in triplicate. The graph obtained (Figure 7.22) illustrates the change in fluorescent intensity of the live cells over a four-day period
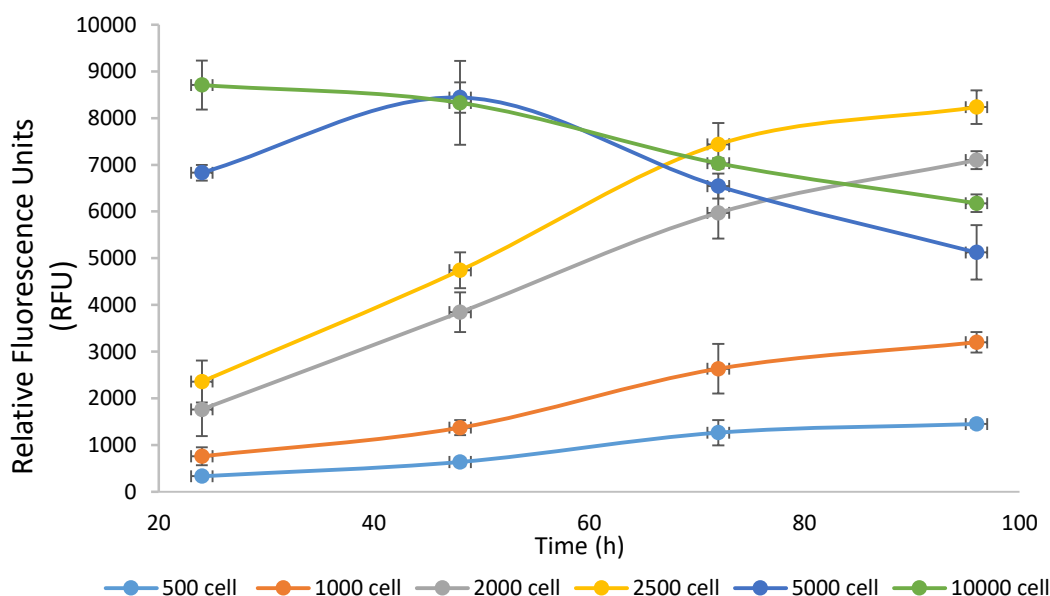
Figure 7.23 The relationship between fluorescence and increasing HeLa cell number. The linearity assay was performed for HeLa cells after 24, 48, 72 and 96 h of incubation at 37°C using the PrestoBlue® reagent. The initial seeding density was 500, 1,000, 2,000, 2,500, 5,000 and 10,000 cells in EMEM complete media. Fluorescence represents mean values generated from three independent experiments in triplicate. Data shown as means ±SEM.

Figure 7.23 indicates that an initial seeding density of between 5,000 and 10,000 cells/well, results in a consistent fluorescence signal across the time points, indicating saturation of the signal. When the initial cell seeding density is decreased to between 500 and 1,000 cells/well, there is a linear increase in the fluorescence signal over time, but the readings are relatively low (less than 3,000 RFU). However, when the initial cell seeding density is 2 500 cells/well, there is a linear relationship between fluorescence and time which is consistent until it starts to plateau at 80 h. A linear increase in signal without the saturation plateau is seen with 2,000 cells/well, indicating that this is the appropriate initial seeding density for the toxicity experiments.

7.2.7.3   Blue light alone has no effect on HeLa cells viability

All of the candidate compounds have antimicrobial activity following exposure to 20 min of blue light. Before investigating the effect of the activated compounds on the HeLa cells, experiments were undertaken to investigate the effect of blue light alone. The PrestoBlue® assay was used to provide a quantitative measure of cell viability in the presence and absence of blue light.

To characterise the effect of blue light illumination alone on HeLa cells, HeLa cells were seeded at 2,000 cells per well, then incubated for 24 h before being exposed to blue light for 20 min (Figure 7.24). 20 min was used as, in the antimicrobial studies; this was determined to be the optimal time for compound activation. The cell viability was then measured using the PrestoBlue® assay at 24 h, 48 h and 72 h post exposure, three times in triplicate. Data is shown as means ±SEM, and two-way ANOVA analysis was conducted to determine the significant results.
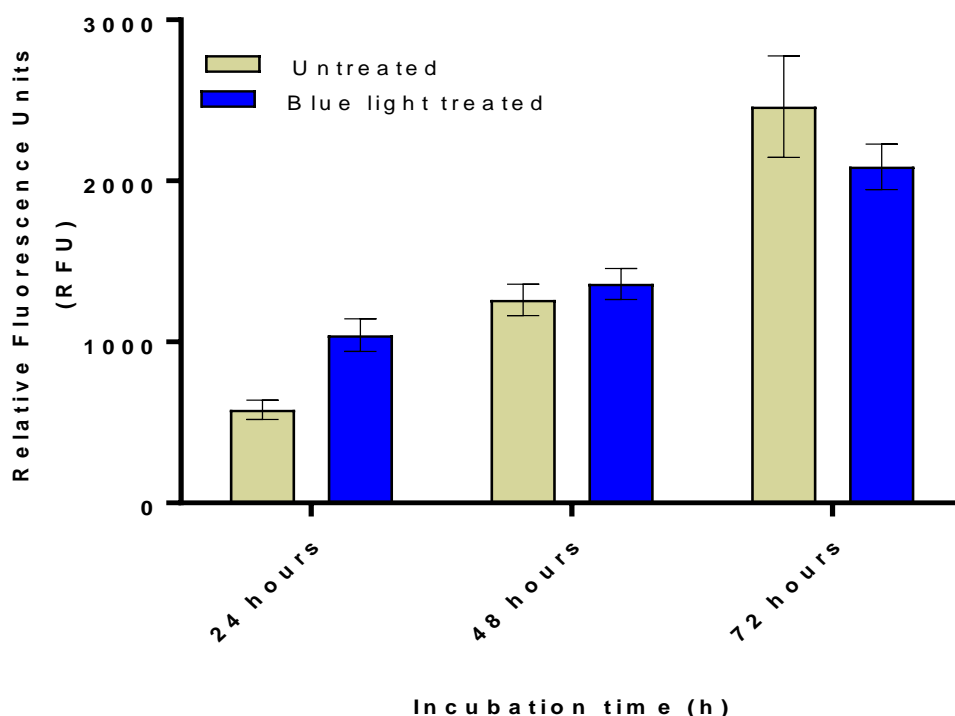
Figure 7.24 Cell viability in HeLa cells following 20 min exposure to blue light. The viability assay was performed for HeLa cells after 24, 48, and 72 h of incubation at 37˚C using the PrestoBlue® reagent. Cell viability was expressed by fluorescence values. The experiment was conducted in triplicate, n=3. Data shown as means ±SEM. ANOVA analysis of results shows no significant effect of blue light treatment in comparison with the control.

It can be noted that there was no significant difference in viability between the treated and non-treated samples after 24, 48 and 72 h (Figure 7.24).

7.2.7.4 All candidate compounds significantly reduced HeLa cells' viability

The five shortlisted compounds with antimicrobial activity (Table 7.1), were studied in HeLa cells to assess their toxicity at the MICs determined in microbial cells.

HeLa cells were seeded at 2,000 cells per well and incubated for 24 h before treatment with the blue light activated compounds. The concentrations used were the highest MICs obtained following the antimicrobial studies, 25 µg/ml and 32 µg/ml. The cell viability was measured using the PrestoBlue® assay at 24 h, 48 h and 72 h following treatment. As controls, HeLa cells were both left untreated

and treated with a vehicle control, 0.625% DMSO, which was the highest DMSO concentration used in antimicrobial testing. The experiment was conducted in triplicate, n=3. Two-way ANOVA analysis of results was conducted. Data is presented as relative fluorescence intensity (RFU) following exposure of the cells to different conditions.
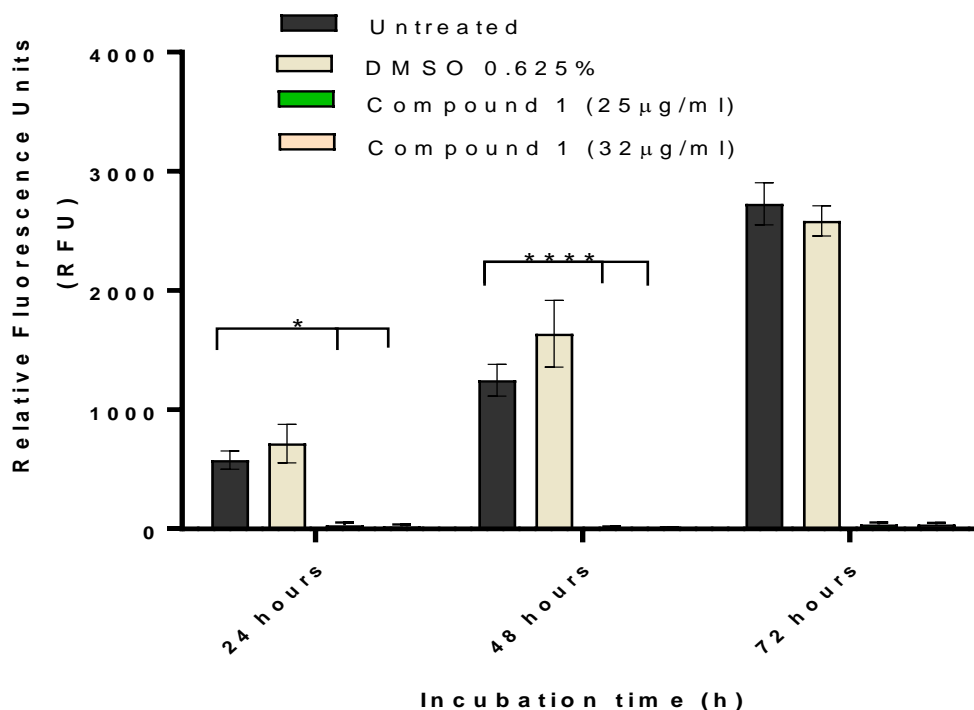
Figure 7.25 Cell viability of HeLa cells treated with blue light activated Compound 1. HeLa cells were seeded at an initial density of 2,000 cells. Following 24 h incubation cells were either untreated, treated with 0.625% DMSO or activated Compound 1. The viability assay was performed for HeLa cells after 24, 48, and 72 h of incubation at 37°C using the PrestoBlue® reagent. Cell viability was expressed by fluorescence values. The experiment was conducted in triplicate, n=3. Data shown as means ±SEM. ANOVA analysis of results shows no significant effect of the control cells treated with 0.625% DMSO and an overall significant effect of treatment with Compound 1 in comparison with untreated cells. *p <0.05 comparing viability of untreated and compound treated HeLa cells after 24 h of treatment, while ****p <0.0001 after 47 and 72 h of treatment.
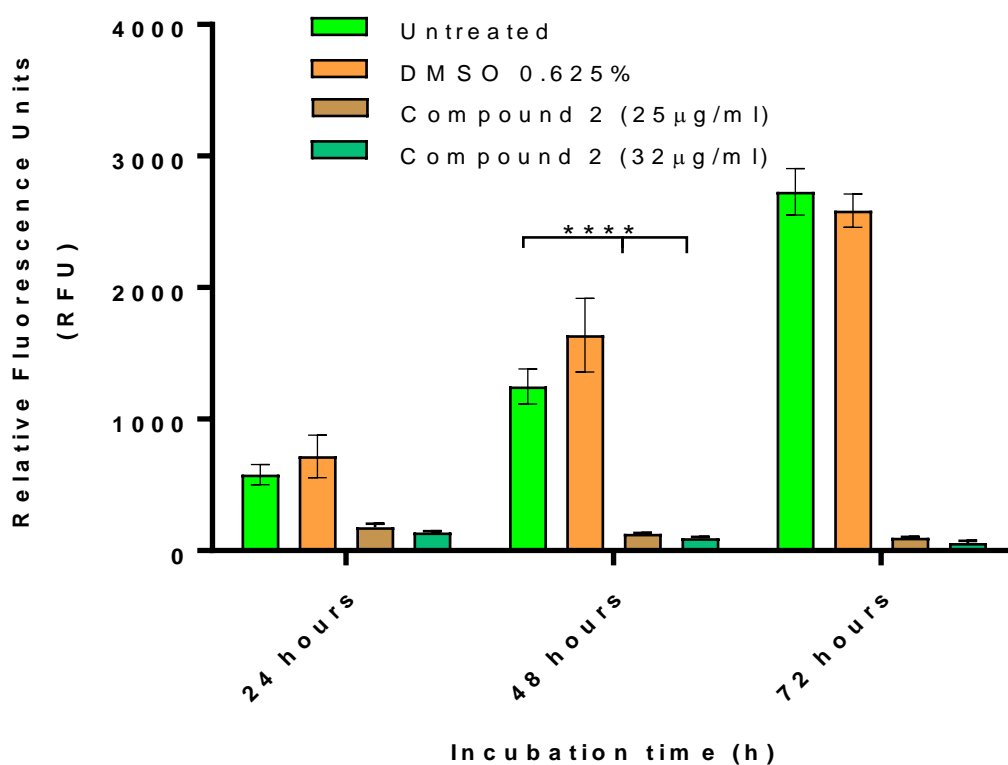
Figure 7.26 Cell viability, determined by PrestoBlue, in HeLa Cells treated with two varying concentrations (25, 32 µg/ml) of Compound 2, HeLa cells treated with 0.625% DMSO and untreated HeLa cells. The viability assay was performed for HeLa cells after 24, 48, and 72 h of incubation at 37˚C using the PrestoBlue® reagent. Cell viability was expressed by fluorescence values. The experiment was conducted in triplicate, n=3. Data shown as means ±SEM. ANOVA analysis of results, show no significant effect of the cells treated with 0.625% DMSO and two concentrations (25, 32) µg/ml of Compound 2 in comparison with untreated cells after 24 h of treatment. ****$p <$ 0.0001 comparing viability of untreated and compound treated HeLa cells after 48 and 72 h of treatment.
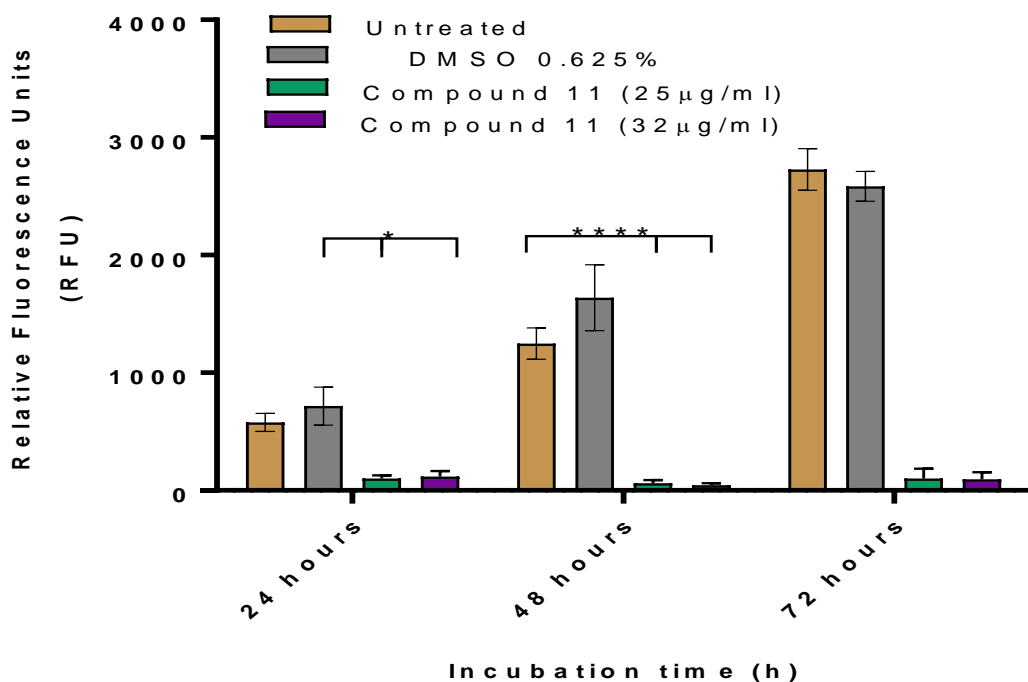
Figure 7.27 Cell viability, determined by PrestoBlue, in HeLa Cells treated with two varying concentrations (25, 32 µg/ml) of Compound 11, HeLa cells treated with 0.625% DMSO and untreated HeLa cells. The viability assay was performed for HeLa cells after 24, 48, and 72 h of incubation at 37˚C using the PrestoBlue® reagent. Cell viability was expressed by fluorescence values. The experiment was conducted in triplicate, n=3. Data shown as means ±SEM. ANOVA analysis of results, show no significant effect of the cells treated with 0.625% DMSO and two concentrations (25, 32) µg/ml of Compound 11 in comparison with untreated cells after 24 h of treatment. ****p<0.0001 comparing viability of untreated and compound treated HeLa cells after 48 and 72 h of treatment.
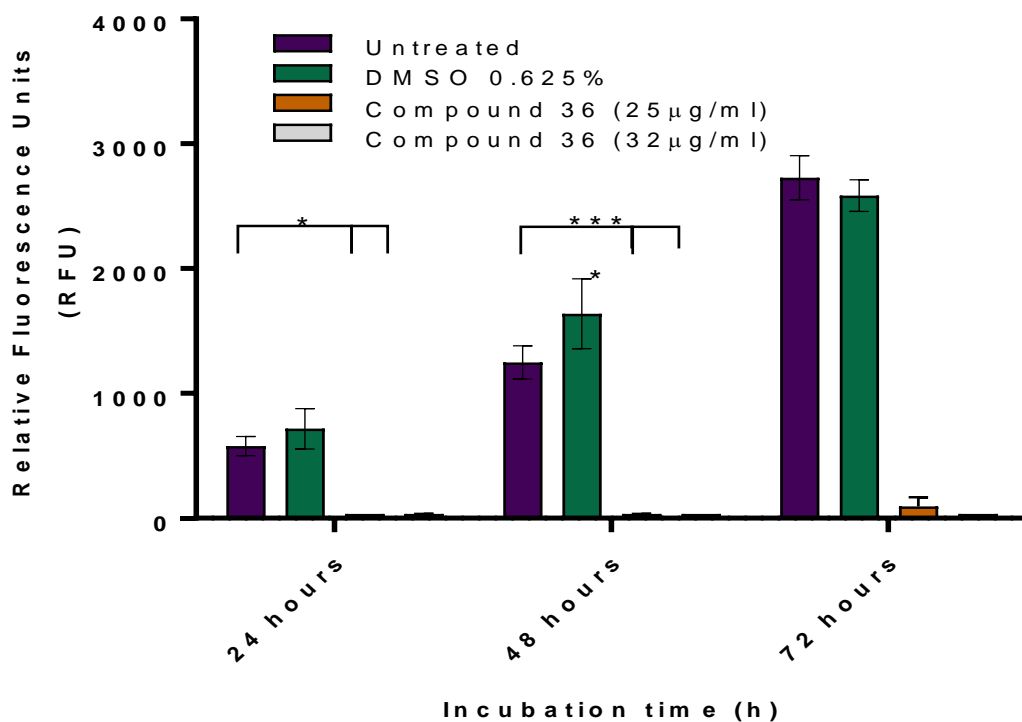
Figure 7.28 Cell viability, determined by PrestoBlue®, in HeLa Cells treated with Two varying concentrations (25, 32 µg/ml) of Compound 36, HeLa cells treated with 0.625% DMSO and untreated HeLa cells. The viability assay was performed for HeLa cells after 24, 48, and 72 h of incubation at 37˚C using the PrestoBlue® reagent. Cell viability was expressed by fluorescence values represent. The experiment was conducted in triplicate, n=3. Data shown as means ±SEM. ANOVA analysis of results, show no significant effect of the control cells treated with 0.625% DMSO and an overall significant effect of treatment with Compound 24 in comparison with untreated cells. *P<0.05 comparing viability of untreated and compound treated HeLa cells after 24 h of treatment, while ****p <0.0001 after 48 and 72 h of treatment.
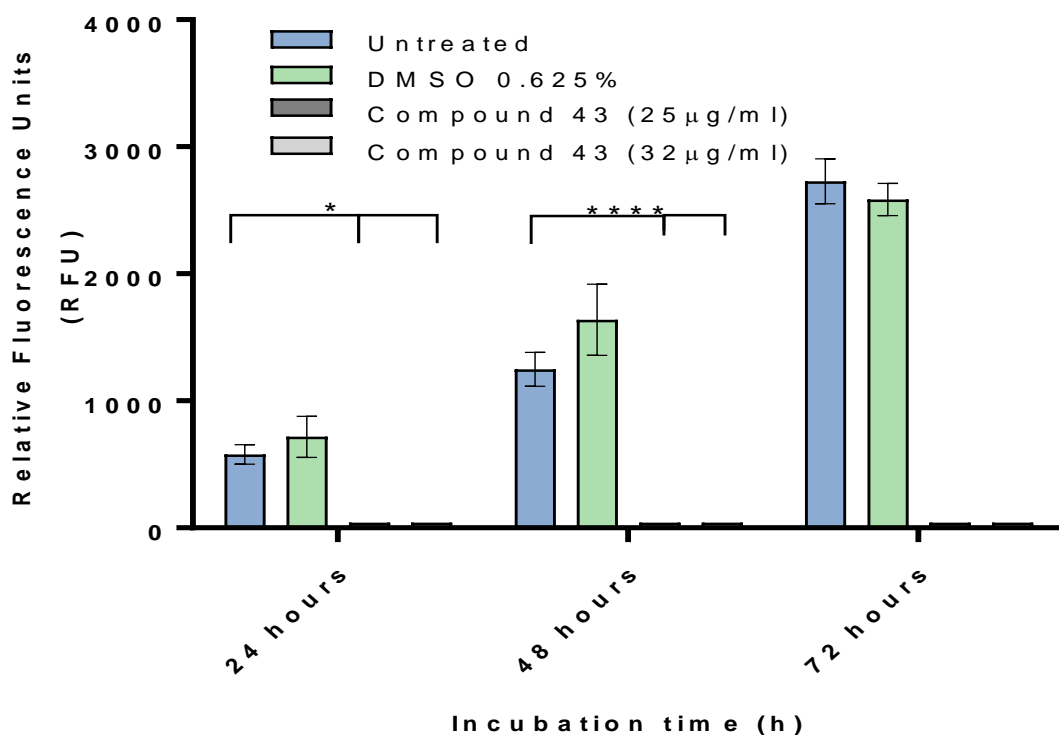
Figure 7.29 Cell viability, determined by PrestoBlue, in HeLa Cells treated with two varying concentrations (25, 32 µg/ml) of Compound 43, HeLa cells treated with 0.625% DMSO and untreated HeLa cells. The viability assay was performed for HeLa cells after 24, 48, and 72 h of incubation at 37°C using the PrestoBlue® reagent. Cell viability was expressed by fluorescence values. The experiment was conducted in triplicate, n=3. Data shown as means ±SEM. ANOVA analysis of results, show no significant effect of the control cells treated with 0.625% DMSO and an overall significant effect of treatment with Compound 31 in comparison with untreated cells. *p<0.05 comparing viability of untreated and compound treated HeLa cells after 24 h of treatment, while ****p<0.0001 after 48 and 72 h of treatment.

At the concentration tested (0.625%), DMSO showed no toxicity against HeLa cells as their viability had not changed significantly when compared to that of untreated cells (Figures 7.25 to 7.29) after 24, 48 and 72 h of incubation.

Following treatment with all five shortlisted compounds in the presence of blue light the fluorescence values dropped significantly after 24, 48 and 72 h incubation when compared to the controls. This demonstrates a significant reduction in the viability of HeLa cells, with little difference observed between the two test concentrations (Figures 7.25 to 7.29).

When testing the compounds alone in the absence of blue light fluorescence, values also reduced significantly when compared to untreated cells (data not shown).

7.3 Discussion

Based on their antimicrobial activity, five compounds were shortlisted for further testing including acridine based Compounds 1, 2 and 11 and acridine-isoalloxazine based Compounds 36 and 43. All of these compounds had MICs below 32 µg/ml against the tested bacterial and fungal species (Table 7.1). These compounds were further characterised to determine whether they had the potential for clinical use. Further, additional information on these shortlisted compounds could inform further formulation improvements.

7.3.1 All shortlisted compounds are static against the tested fungal and bacterial species

Antimicrobial agents are classified as either static, which inhibit microbial growth, or cidal, that actively kill microbes.

Analysis of the shortlisted compounds within this study have indicated that they are all static to both fungi and bacteria (Table 7.2). This contrasts with other studies using photoactive acridine compounds, specifically acridine orange, where a bactericidal effect against *S. aureus* and *E. coli* was observed (Wainwright *et al.*, 1997). The discrepancy between results is possibly due to the bactericidal activity of acridine orange in the absence of light, which was not observed in our tested compounds. Additionally, the effect of blue light alone (400 -450 nm) was not investigated within this study. Therefore, the bactericidal results seen following light activation may have resulted from a cumulative effect.

Other studies have also demonstrated that PDT has fungicidal effect against *Candida* species by using a viable cell counting method (Dovigo *et al.*, 2011; Zhang *et al.*, 2016). In contrast, the method utilised in this study relies on taking the sample from the first well with no visible growth, which may mean some viable cells are still present. The control drugs used in this study were shown to be static (fluconazole) and cidal (gentamicin), which agreed with Calderón *et al.,* 2007 and confirmed that the method is accurate.

ROS generally have a reversible effect, which depends on the level of ROS and the target (Magder, 2006, Dharmaraja, 2017). This suggests that the ROS released from the PDT compounds in this study are probably at low enough levels that the cell can adapt.

Various studies have found that cidal and static compounds have similar effectiveness when used to control clinical infections, with no differences observed in clinical responses or mortality (Nemeth *et al.*, 2015; Wald-Dickler *et al.*, 2017). This suggests that, although static to the microorganisms tested, these compounds may still be clinically effective. There are important factors affecting the response to antimicrobial therapy, including host defence systems, optimal dosing, pharmacokinetics and inadequate penetration of the infection site (Estes *et al.,* 1998).

7.3.2 Development of resistance of PDT

The growing emergence of antimicrobial treatment resistance is spreading worldwide, threatening the effectiveness of antimicrobials and increasing mortality rates, for example methicillin-resistant *Staphylococcus aureus* (MRSA) infections cause 11,285 deaths per year in the USA (Alanis, 2005, Hawkey, 2008). Microbial resistance usually occurs more rapidly with static agents than it does with cidal agents (Gould *et al.*, 2002). As the shortlisted compounds are static, there may be an increased chance of resistance developing. Data presented in this chapter indicates that, following three repeated exposures to suboptimal concentrations of the shortlisted compounds, no obvious resistance was detected in the microorganisms tested. This is consistent with data from other studies in fungi and bacteria following repeated exposure to the PDT agents (Giuliani *et al.*, 2010; Tavares *et al.*, 2010).

Microbes have developed many mechanisms to increase their resistance to antimicrobial agents. These mechanisms include a thickening of their outer wall, mutations within the target protein, encoding of new proteins which prevent the penetration of agents, and an increase in efflux transporters to remove compounds from the cell (Tavares *et al.*, 2010). However, evidence suggests that resistance to PDT agent does not develop due to the absence of a specific target (Dougherty *et al.*, 1998; Castano *et al.*, 2004). In PDT, both types of reaction

release highly toxic reactive oxygen species (ROS) such as free radicals and $^1O_2$, able to inflict damage in a multi-target process to cytoplasmic membrane, cell wall and DNA. Due to this property of PDT development of resistance to ROS is seldom observed (Giuliani *et al.*, 2010) . Additionally, cell wall structures and membranes are the main targets of photoactivated compounds, and for this reason, the target cells have no chance to develop resistance by stopping uptake or influx of the drugs as proper adhesion to these structures is usually sufficient to damage the target cell without the need for penetration inside the cells. However, the number of exposures was significantly higher than that of our study, which should be considered in future work.

7.3.3 Effect of pH and EDTA on in vitro susceptibility to photoactivated compounds

7.3.3.1   pH effect

The aim in this study is to investigate whether the external environment influences the efficacy of the tested PDT compounds in clinical situations, which may affect the optimal site of action for compounds. The medium conditions, including temperature and pH, result in phenotypic, metabolic and physical changes in fungi and bacteria (Carvalho *et al.*, 2009; Sherrington *et al.*, 2017). The site of action of a variety of fungi include the stomach, skin and vagina. Given that these sites vary greatly in pH, for example vaginal pH is 4-4.5 and the intestine pH ranges between 5.5 and 7, we studied the effect of pH on the *in vitro* activity of blue light shortlisted compounds and fluconazole against the fungi *S. cerevisiae* and *C. albicans* using EUCAST susceptibility testing in the presence of MOPS. The antifungal agent used to inactivate fungi grown in vagina of pH 4-4.5 should be effective at correspondingly acidic conditions.

Acidic environments alone, particularly at pH 4 to 5, have exhibited a growth inhibition effect on fungi due to the increased sensitivity of β-glucanase, which breaks down the fungal cell wall by affecting β-glucan, the major component of the fungal cell wall (Sherrington *et al.*, 2017; Mayer *et al.*, 2013; Weckwerth *et al.*, 2012). However, the pH change can be overcome by the adaptive response induced in fungi, as fungi have the ability to actively modify the pH of their environment by secreting natural acids or alkali (Vylkova *et al.*, 2011; Ramon *et*

al., 1999; Vylkova *et al.,* 2017). Additionally, pH changes may trigger hyphal formation in fungi, which is generally accepted to be more resistant than the yeast form (Ceccato-Antonini *et al.*, 2004; Ramon *et al.*, 1999). This concept supports the findings observed in this study and might cause *S. cerevisiae* and *C. albicans* to become more resistant (Figure 7.6 and 7.8).

In the present study, the MIC of fluconazole, Compound 1, Compound 2 and Compound 36 was mostly affected by a decrease in pH, in the presence of MOPs. These compounds showed at least a threefold increase in MIC against *S. cerevisiae* and a twofold increase in MIC against *C. albicans*, when the pH was decreased from 7 to 4. A similar trend was observed for Compounds 11 and 43, showing less than a twofold increase in MIC against *S. cerevisiae* and *C. albicans*, ranging between 16.67 and 25 µg/ml (Figure 7.6 and 7.8). In general, a decrease in pH resulted in a decrease in the susceptibility of *S. cerevisiae* and *C. albicans* to the photoactivated antimicrobial compounds. The presence of chlorine in the structures of Compounds 11 and 43 may indicate that they are less affected by the change in pH.

The antifungal agent, fluconazole, used in this study showed a decrease in susceptibility of *S. cerevisiae* and *C. albicans* when pH was dropped from 7 to 4 (Figures 7.6 and 7.8). This data supports the results of several reports conducted on different azole antifungals including fluconazole which exhibited a similar decreasing trend in the susceptibility of *C. albicans* when pH was reduced, as higher fluconazole concentration was necessary in an acidic environment (pH 4 to 5.5) than in neutral condition (pH 7) to achieve the same growth inhibition extent. This may suggest to result from the fact that changes in pH instigate marked changes in the cell wall, which may influence the susceptibility of *S. cerevisiae* and *C. albicans* to fluconazole, or a potential consideration is the protonation of fluconazole, demonstrating reduced efficacy against fungal cells (Danby *et al.*, 2012; Vasconcellos *et al.*, 2014). Further to this, it has been shown that acidic pH decreases the susceptibilities of the *Bacteroides fragilis* group to several antibiotics including ciprofloxacin, ampicillin-sulbactam and clindamycin (Falagas *et al.*, 1997). The effect of pH on *in vitro* susceptibilities of bacteria is suggested to be due the pH impact either on the permeability of bacteria to antibiotic or on the stability of antibiotics (Corkill *et al.*, 1994) .

Studying the effect of pH change on the efficacy of PDT agent, polyethylenimine-chlorin(e6) conjugates, showed that although pH decreased, the cellular uptake of the compound was not affected (Huang *et al.*, 2011). In the case of the less susceptibility of bacteria *S. aureus* and *E. coli* to the previous PDT agent, which was observed when pH decreased, it is suggested that the pH drop influenced the compound itself (Huang *et al.*, 2011) . This may potentially support the suggestion that PDT shortlisted compounds in this study are inactivated by pH drop.

The impact of pH on decreasing *in vitro* susceptibilities of fungal and bacterial cells to antimicrobials by increasing the MIC may be mediated through a variety of mechanisms. Firstly, as pH can influence the permeability of microbes to antimicrobials (Cuchural *et al.*, 1988) this suggests that the shortlisted compounds used in this study have been prevented, to some level, from the adhesion or penetration into the examined microbes which would reduce the ROS killing effect. Secondly, the stability and activity of enzymes which inactivate antimicrobials are influenced by pH. Finally, the stability and kinetics of the shortlisted compounds are suggested to be affected by pH change (Smith *et al.*, 1990). Additionally, pH effect may influence fungal growth and instigate conversion from the yeast to the hyphal form, which is more resistant to all antimicrobial compounds (Ramon *et al.*, 1999).

The EUCAST method to assess antimicrobial activity, involves the addition of a buffering agent, MOPS, to the media. Results presented in this chapter indicate that removal of MOPS from the media has no significant impact on the effectiveness of the compounds at the various pH levels tested.

It has been shown that *C. albicans* cells grown in unbuffered medium are able to modulate pH changes, thus, the effect of the antifungal is negated via the manipulation of extracellular pH (Kulkarny *et al.*, 2014; Vylkova, 2017).

Using two PDT agents methylene blue (MB) and toluidine blue (TB) as photosensitising drugs, phototoxicity effects observed were not related to the

specific pH values of the medium, they were attributed to the ability of the medium to permit changes in the pH values (Carvalho *et al.*, 2009). It has been found that in a saline buffered medium the phototoxicity effects with either MB or TB, significantly decreased compared to that of non-buffered saline, due to the ability of the saline medium to control the pH. MOPS was also the buffer used to resist pH changes, but the medium in our study was RPMI, which may potentially possess a reduced ability to control pH change.

7.3.3.2   EDTA effect

The aim in this study is to investigate the role of metal ions present in the external environment in the activity of the tested PDT compounds by using EDTA, an effective chelator of magnesium and calcium. EDTA was used in combination with antimicrobials to evaluate the resultant antimicrobial potency.

This study has investigated the EDTA effect on *in vitro* susceptibility of *S. cerevisiae* and *C. albicans* to fluconazole and blue light treated shortlisted compounds in the presence of MOPS buffer. Comparison of the MIC values for *S. cerevisiae* and *C. albicans* following treatment with the photoactive compounds in the presence of 10 mM EDTA, resulted in a significant decrease in the MIC when compared to control groups and EDTA alone (Table 7.5). The presence or absence of MOPS did not exhibit any significant impact on these results.

As 10 mM EDTA alone had no observable impact on the growth of the cells, it is suggested that the presence of the EDTA is affecting the susceptibility of the fungal cells to the photoactivated compounds. EDTA chelates the divalent cations Mg^{+2} and Ca^{+2} (George *et al.*, 2009), which are present in the cell wall of both fungi and bacteria. Removal of these ions can result in damage, making *S. cerevisiae* and *C. albicans* cells more permeable, and therefore susceptible, to the photoactivated compounds. Although this study showed that EDTA alone had no significant effect on *S. cerevisiae* and *C. albicans*, there are studies which demonstrate that EDTA does itself have an antimicrobial effect. However, an effect was only seen with a concentration of EDTA significantly higher than utilised in this study, 0.6 M compared to 10 mM (Şen *et al.*, 1997) .

It has been demonstrated that EDTA has potential antifungal activity against *C. albicans* using a broth microdilution method. This activity is attributed to its chelating property, as calcium ions play a critical role in the morphogenesis and pathogensis of *C. albicans*. Therefore, it may be expected that other chelating agents would also possess antifungal potential (Ates *et al.*, 2005, Li *et al.*, 2018).

EDTA concentration at 17%, which is 200-fold higher than the concentration used in our study, exhibited significant antifungal activity against *C. albicans* when using an agar diffusion test, which has been related to the severe collapse in cell wall by removing calcium, inhibiting enzyme reactions and limiting nutritional conditions with this mechanism (Şen *et al.*, 1997). When testing *C. albicans* biofilms EDTA alone was used at a concentration much higher than that used in our study at 25 mM against *C. albicans* biofilms At this concentration it was observed to demonstrate significant activity against *C. albicans* biofilms by employing the XTT assay to test viability of biofilms (Casalinuovo *et al.*, 2017).

Gram-negative bacteria occasionally exhibit resistance to PDT, consequently it was suggested to pre-treat them with EDTA, which can cause Gram-negative bacteria to lose up to 50% of their lipopolysaccharide and thus become more sensitive to PDT agents (Sperandio *et al.*, 2013). This approach was used by treatment of *S. epidermidis* biofilms with EDTA followed by TBO as a PDT agent. The treatment with 89 mM EDTA helped to disrupt biofilm structure and increase the permeability of TBO and this thus enhanced the photodynamic efficacy of TBO (Fu *et al.*, 2013). While the concentration of EDTA used in this study did not show any antimicrobial activity alone it is possible that increased susceptibility of the fungal cells to the compounds occurred in EDTA's presence, due to a synergistic effect (Table 7.5). The reason for this finding is potentially related to the ability of EDTA to make the outer wall of *S. cerevisiae* and *C. albicans* more permeable, and allow photoactivated shortlisted compounds to penetrate and accumulate inside. These compounds are then photoactivated, thus releasing ROS which kill the tested fungi.

7.3.4 Mechanism of action of the photoactivated antimicrobial compounds

The mechanism of action of photoantimicrobial therapy has been discussed extensively and demonstrated to result from the interaction of photons of visible light with photosensitising agents known as photosensitisers (Dougherty *et al.*, 1998). Following absorption of light photons of specific wavelengths, the photosensitisers produce free radicals and singlet oxygen via Type 1 and Type 2 reactions, respectively. These resultant species have the ability to attack cellular targets and kill the microbial cells (Baltazar *et al.*, 2015).

In this study, photochemistry data demonstrated that the shortlisted compounds released singlet oxygen following exposure to blue light (Table 3.3). As these findings did not correlate with photobiological data and radical species could not be measured, this study attempted to determine the mechanism of action of the compounds using *S. cerevisiae* deletion strains.

In *S. cerevisiae*, many stresses are signalled through the high osmolarity glycerol (HOG) MAPK pathway, including osmotic, metal and oxidative stress, pH and citric acid (Saito *et al.*, 2004; Pascual-Ahuir *et al.*, 2007; Bilsland *et al.*, 2004). One of the downstream targets of the HOG pathway are the transcription factors, Msn2/4p, which are also activated in response to oxidative stress. Specifically, Msn2/4p are responsible for activation of oxidative stress response by binding to the stress response element (STRE) within specific genes (Hasan *et al.*, 2002). For example, in response to hydrogen peroxide, they activate transcription of the antioxidant defence genes, *CTT1* and *SOD1* (Hasan *et al.*, 2002). As a result, deletion of the genes encoding these proteins results in sensitivity of cells to oxidative stress and specifically to hydrogen peroxide, a resultant radical species (Pascual-Ahuir *et al.*, 2007; Martinezpastor *et al.*, 1996). Therefore, if the antimicrobial activity of the shortlisted compounds is via this mechanism, we would expect to see a decrease in the MIC of the relevant deletion strains when compared to the wildtype control.

To confirm that the deletion strains exhibited sensitivity to ROS, hydrogen peroxide (H_2O_2) was used as a control. As expected, both deletion strains, *msn2/4Δ* and *hog1Δ,* were more sensitive than the wildtype (Figure 7.10). This is consistent with other research findings, which demonstrated that the encoded

proteins, Hog1p and Msn2/4p have a significant role in resistance to H_2O_2, with the effect being more profound for Msn2/4p (Hasan *et al.*, 2002; Bilsland *et al.*, 2004).

The MICs for the photoactivated Compounds 1, 2 and 36, showed a similar trend, with both mutant strains showing increased sensitivity. However, *msn2/4Δ* was significantly more sensitive than *hog1Δ* when compared to the wildtype (Hasan *et al.*, 2002).

Compared to other stresses, Hog1p phosphorylation and accumulation in the nucleus following oxidative stress is delayed, which indicates a lesser role for this protein in the oxidative response (Bilsland *et al.*, 2004) . Although the transcription factors Msn2/Msn4p are targets of the HOG pathway as part of the general stress response, they are also activated by oxidative stress via a number of other signalling pathways. This includes the negative regulators, Ras/protein kinase A pathway (PKA), which are down regulated following oxidative stress causing activation of Msn2/4 (Costa *et al.*, 2001) . These findings are consistent with results following hydrogen peroxide stress, the *msn2/4Δ* strains are more sensitive to Compounds 1, 2 and 36 when compared to *hog1Δ*, although the MIC is still reduced compared to the wildtype control. This suggests that Compounds 1, 2 and 36 are inhibiting cell growth via oxidative stress resulting mainly from H_2O_2, a direct precursor of hydroxyl radicals (Hasan *et al.*, 2002; Costa *et al.*, 2001). Testing the shortlisted compounds alone in the absence of light did not demonstrate any significant inhibitory effect against the examined strains. This current study and the aforementioned studies showed that the *msn2/4* transcription factors play an important role in the cellular response to these particular photoactivated chemicals.

For Compounds, 11 and 43 no significant differences in the MICs were observed between wildtype *S. cerevisiae* and the mutant strains. This indicates that these compounds must inhibit growth via an alternative mechanism. The lack of response in the *hog1Δ* suggests that these compounds are not causing any level of detectable general stress to the cell.

This data has been obtained in *S. cerevisiae,* however, is it possible that a similar mechanism of action occurs in bacteria. In regard to bacterial response to oxidative stress, it is coordinated mainly by two regulons, *SoxRS* and *OxyR,* which respond to oxidative stress induced by ROS including superoxide anion, hydrogen peroxide and singlet oxygen (Netto *et al.,* 2007, Lushchak, 2011). Bacteria show much less complicated pathways of response to oxidative stress than fungi (Lushchak *et al.,* 2011). It was supposed that regulatory proteins SoxS and OxyR are sensors responding to increased hydrogen peroxide level in bacteria. Both forms bind to DNA but with different binding specificity, activating the expression of *SoxRS* and *OxyR* genes and resulting in increased protein levels (Hidalgo *et al.*, 1997; Imlay, 2015). The sensing step involves the oxidation of sensor molecules. *E. coli* is the most widely model system studied to investigate the oxidative stress in bacteria (Imlay, 2015). To detect oxidative stress in bacteria *E. coli* mutants that lack *oxyR* have been shown more sensitive to hydrogen peroxide than wildtype strains. Additionally, mutants that lack either set of superoxide dismutases and catalases that degrade superoxide and hydrogen peroxide, cannot grow when reacted with ROS (Keyer *et al.*, 1996; Touati *et al.*, 1995) .

In general fungi are more resistant to oxidative stress than bacteria which is reflected in the results obtained in our study, showing slightly more susceptibility of bacteria than fungi to the PDT shortlisted compounds.

7.3.5 *In vitro* antifungal susceptibility testing of *C. albicans* biofilms

As described earlier within this chapter, the shortlisted compounds exhibited antifungal activity against planktonic *C. albicans* cells, when activated with a dose of 115 J/cm^2 470 nm blue light for 20 min (Table 7.1). *C. albicans* pathogens typically form biofilm structures in clinical situations, which exhibit increased resistance to antifungal agents. As a consequence, this study evaluated the photoantifungal activity of the shortlisted compounds against *C. albicans* biofilm cells, using a previously published method (Ramage *et al.*, 2001) .

One of the main features of biofilms is that they are more resistant to broad-spectrum antimicrobial drugs when compared to planktonic cells (Tsang *et al.*, 2007; Punithavathy *et al.*, 2012; Khan *et al.*, 2011). In *C. albicans*, this decreased susceptibility is thought to be due to reduced penetration through the biofilm layers. These layers, which contain extracellular polymer matrix, in combination with the presence of efflux pumps, contribute to the increased resistance of *C. albicans* biofilms to antifungal drugs (Punithavathy *et al.*, 2012).

This supports the findings in this present study, which demonstrated that all the tested compounds, including the controls, exhibited a reduced effect on the metabolic activity of *C. albicans* biofilms when compared to planktonic *C. albicans*. For both control antifungal drugs, fluconazole and amphotericin B, the results (Figures 7.11 and 7.12) agreed with the published literature (Casalinuovo *et al.*, 2017; Chamilos *et al.*, 2005; Pierce *et al.*, 2008).

Overall, the biofilms were more sensitive to amphotericin B than fluconazole, with 2 µg/ml of amphotericin B resulting in > 50% reduction in metabolic activity (Figure 7.12), while fluconazole showed no effect at any of the concentrations tested (Figure 7.11). The discrepancy in susceptibility of *C. albicans* biofilms to fluconazole and amphotericin B may be explained in two ways. Firstly, it is suggested that the cell viability of biofilms treated with fluconazole could be due to a selection of drug-resistant cells, or to the proliferation of pre-existing persister cells: specific gene expression patterns in biofilm mass after fluconazole treatment, may be implicated (Punithavathy *et al.*, 2012). Secondly, the unique activity of amphotericin B can be attributed to its different mechanism of action, by forming pores in cell membrane following binding to membrane ergosterol, causing direct loss of cytosol and hence loss of viability, while fluconazole acts by inhibition of ergosterol synthesis without fungal cell disintegration (Van de Sande *et al.*, 2010; Chamilos *et al.*, 2005).

All light activated shortlisted compounds screened in this study caused a decrease in the metabolic activity of the *C. albicans* biofilms. Only Compounds 1, 2 and 36, at a concentration of 25 µg/ml, showed a significant reduction in metabolic activity (approx. 30 %) when compared with the untreated control (Figure 7.13 to 7.17). Neither the compounds nor blue light alone reduced significantly the metabolism of *C. albicans* biofilms (Figures 7.13 to 7.17). Compounds 1, 2 and 36 had approximately similar activity to Compounds 11 and

43 against tested fungi and bacteria; however, Compounds 11 and 36 did not significantly affect *C. albicans* biofilms. This indicates that the initial ranking of activity did not correlate with the results for biofilm data.

The results of Compounds 1, 2 and 36 are consistent with data from a number of different PDT agents (methylene blue and toluidine blue), which showed activity against *C. albicans* biofilms (De Melo *et al.*, 2013; Shi *et al.*, 2016). Notably higher inactivation was achieved on the metabolism of planktonic *C. albicans*, when compared to biofilm data (Hu *et al.*, 2018; Hosseini *et al.*, 2016). This supports the findings for Compounds 1, 2 and 36, which affected planktonic *C. albicans* significantly more than *C. albicans* biofilm when using the same XTT viability method.

The antimicrobial effect of aPDT is dependent both on cellular localisation of the photosensitiser and on the diffusion of ROS (radicals and $^1O_2$) which should be sufficient to inactivate biofilm structure (Hosseini *et al.*, 2016; Hu *et al.*, 2018).

Although Compounds 11 and 43 demonstrated relatively similar efficacy to Compounds 1, 2 and 36 in initial antimicrobial testing, their effect on biofilms was different. The reduced effect of Compounds 11 and 43 on the *C. albicans* biofilms is suggested to be due to the limited penetration of the compounds during the PDT process into biofilm structure, which leads to reduced photoantifungal activity. Additionally, ROS species (the damaging factors in PDT) cannot travel very far before disappearing (Vatansever *et al.*, 2013), thus this may suggest that Compounds 11 and 43 did not localise close to the target. One important point is that Compounds 1, 2 and 36 are working via the activation of *msn2/4* in oxidative stress while Compounds 11 and 43 have been suggested to work via another mechanism. This may suggest that the unknown mechanism of Compounds 11 and 43 was affected negatively when testing biofilms.

PDT can be used to treat bacterial biofilms as it has been demonstrated that methylene blue can be an effective PDT agent against *S. aureus* biofilms by inhibiting their growth (Briggs *et al.*, 2018). Different sensitivity of microbial biofilms was observed to PDT (Briggs *et al.*, 2018).

7.3.6 Measurement of supra-MIC growth (SMG), an indication of perseverance

In the case of treatment of *Candida* infections, a new drug response parameter termed perseverance, defined as supra-MIC growth (SMG), has been identified. This correlates with clinical outcomes in patients treated with antifungal agents and reflects the possible persistence of *C. albicans* in clinical settings (Rosenberg *et al.*, 2018). Perseverance relative to the minimum inhibitory concentration (MIC) was measured, using the standard EUCAST assay over two consecutive days, to provide information about both resistance and perseverance.

Perseverance (SMG) is correlated with a subpopulation of cells (represented by OD) that grows at concentrations above the MIC. The SMG values of fluconazole in this study were slightly lower than that measured in the study conducted by Rosenberg *et al.,* 2018. Blue light alone did not show any significant growth inhibition and did not have any impact on SMG.

For all shortlisted compounds (1, 2, 11, 36 and 43) and fluconazole, the SMG values increased significantly between 24 and 48 h.

Although the SMG increased for all the compounds tested, the MIC values determined against *C. albicans* did not change (Tables 7.18 and 7.19). It is suggested that perseverance is dependent upon pathways that do not affect the MIC and therefore can predict the possibility of failure or success of treatment in the clinic. This is reflected in our results, which showed that SMG increased significantly while the MIC of the shortlisted compounds did not change between 24 and 48 h. The reason behind this is unclear as the mechanisms behind the development of SMG have not yet been determined (Rosenberg *et al.,* 2017).

It has been reported that strains with higher SMG levels may relate to the failure of antifungal compounds to clear an infection despite an isolate being compound susceptible (Rosenberg *et al.,* 2018). This supports the suggestion that the significant increase in SMG values between 24 and 48 h in this study can predict that the studied *C. albicans* strain is more likely to give rise to persistent and/or recurrent infections.

Previous experiments, using mouse models and infection outcomes, have suggested that there was no relationship between the SMG phenomena and virulence (Rex *et al.*, 2002; Bennett *et al.*, 2003). However, it is believed that this discrepancy is due to the analysis of the immediate response rather than the clinical persistence or recurrence over long periods (Rosenberg *et al.,* 2017).

7.3.7 Effect of candidate compounds on mammalian cells

As any new antimicrobial agent would be required to have minimal affect in host cells, the shortlisted compounds were tested to determine their effect on mammalian cells. HeLa cells, an immobilised human cell line derived from cervical cancer cells, were chosen for testing as they reproduce rapidly, easily and cheaply (Suchland *et al.*, 2003; Limban *et al.*, 2008). Despite being cancerous, HeLa cells still have several characteristics in common with normal cells, as they produce proteins, express and regulate genes, and are susceptible to infections, which allows them to be used widely in antimicrobial testing (Hammerschlag, 1994, Wasson *et al.*, 2012).

The cellular growth curve for HeLa cell line was established to define the growth characteristics and determine the best time range for evaluating the effects of biological compounds. To provide a quantitative measurement of viability and toxicity, PrestoBlue® was chosen as it is faster and more sensitive than other assays such as 3-[4,5-dimethylthiazol-2-yl]-2,5-diphenyl tetrazonium bromide (MTT) cell viability assay (Boncler *et al.*, 2014). The greatest variable in viability assays is cell number, thus linearity of fluorescence versus cell number was studied to identify the optimal cell number. This was determined to be an initial seeding density of 2,000 cells/well, which was used for all future experiments.

The principle of PDT depends on the activation of the photosensitisers through an appropriate light source, in this case blue light. To determine whether the blue light alone effects HeLa cells, cell viability was determined following a 20-minute blue light exposure (470 nm, 115 J/cm^2). Treatment of HeLa cells with blue light demonstrated no significant effect on viability measured after 24, 48 and 72 h (Figure 7.21). This finding was in agreement with a previous study that used the same blue light wavelength but at a lower final irradiance dose of 3.7 J/cm^2 than

used in this experiment (Yang *et al.*, 2017). This result is further confirmed by data in human primary retinal epithelial cells and fibroblast cells, exposed to a similar wavelength and irradiance dose (Lee *et al.*, 2014; Mayer *et al.*, 2013).

However, this contrasts with human promyelocytic leukaemia cell lines (HL60) where blue light has been shown to reduce their viability significantly (Zhuang *et al.*, 2018). However, although a similar blue light wavelength was used to this study (470 nm versus 456 nm), the irradiation period was much longer (10 to 56 h) (Zhuang *et al.,* 2018). It is well established that shorter blue light wavelengths (405-415 nm) significantly decrease the viability of mammalian cells, including immortalised osteoblasts (OST 5) and normal human skin fibroblast (Ramakrishnan *et al.*, 2016; Mamalis *et al.*, 2015; Lee *et al.*, 2014). The suggested mechanism of action for these shorter wavelength (405 nm) involves the photo-excitation of endogenous porphyrins, which in turn produce ROS (Vandersee *et al.*, 2015; Yoshida *et al.*, 2015). ROS are reactive species causing oxidative damage to cell components including proteins, lipids and nucleic acids (Lubart *et al.*, 2011; Ramakrishnan *et al.*, 2016). Therefore, the use of a longer wavelength (approx. 470 nm) and limited irradiation (110 J/cm^2) in this study may indicate why there is no significant reduction in cell viability with blue light alone (Lee *et al.*, 2014; Mayer *et al.*, 2013).

As the shortlisted compounds were initially resuspended in DMSO the effect of the vehicle alone was assessed as a control. The highest DMSO concentration used in the antimicrobial testing was 0.625%, thus this was used in the control studies. No significant reduction in cell viability was detected in the vehicle control when compared to that of untreated HeLa cells (Figures 7.21, 7.22, 7.23, 7.24 and 7.25) at 24, 48 and 72 h. Our findings support several studies conducted also on HeLa cells, which found that DMSO only exhibits a cytotoxic effect at concentrations above 2% (Trivedi *et al.*, 1990; Forman *et al.*, 1999) . This is also consistent with findings in other mammalian cell lines including a haematopoietic progenitor cells (HPCs) and human adipose-derived adult stem cells (ASCs) (Timm *et al.*, 2013; Galmes *et al.,* 2002).

The ideal photosensitiser should not exhibit any significant effect on the host cell. However, in this study, the treatment of HeLa cells with two concentrations of the

shortlisted light activated compounds significantly decreased their viability (Figures 7.25 to 7.29). Additionally, compounds alone demonstrated a significant reduction in viability of HeLa cells. Our photoactivated findings are inconsistent with data from a blue light activated acridine-based compound, acridine orange (AO), where no significant reduction in cell viability of human immortalised uroepithelial cells (SV-Huc-1) was reported (Lin *et al.,* 2017). This difference in effect may be due to compound concentrations and the level of light activation used in these studies. The acridine orange was tested at a much lower concentration, 1µg/ml, compared to this study where compounds were tested at a concentration of 32 µg/ml. Further, despite using a similar activation wavelength, the irradiance dose (6 versus 115 J/cm^2) and duration (30 s versus 20 min) were higher in this current study. Additionally, blue light with similar wavelength to our study did not affect also the cell viability of human immortalised uroepithelial cells (SV-Huc-1) (Lin *et al.*, 2017).

Treatment with compounds alone was shown to elicit toxicity without blue light illumination. This suggests that the compounds are toxic to HeLa cells via a non-light activated mechanism, suggesting it is not via ROS production. Acridine-based compounds act at the level of DNA-coiling enzymes (topoisomerases) and the damage is caused by the stabilisation of the enzyme-DNA cleavage complex (Wainwright, 2015). Thus, its mechanism of action explains why HeLa cell line showed reduced viability at 24, 48 and 72 h following treatment with 25 and 32 µg/ml acridine-based compounds.

It has been reported in previous studies that the structure-activity relationship in acridines is of great importance, as they have been shown to localise and act in different regions/organelles depending on a combination of lipophilicity and degree of ionisation (Wainwright, 2015; Lin *et al.*, 2017). The toxicity of the examined compounds in this study against HeLa cells supports the idea of possible DNA intercalation causing the obtained toxicity.

8. General discussion

8.1 Overview of discussion

The rise in opportunistic microbial infections in immunocompromised patients and the reduction in efficiency of currently available treatments has resulted in an unmet medical need. As a result, photodynamic therapy has become an increasingly important area of research. This project utilised a library of novel photoactivated compounds, developed around a number of key molecules including acridine, flavine and anthraquinones. These compounds were then investigated to determine their antimicrobial activity against a range of clinically important pathogenic fungi, including *Candida albicans, Saccharomyces cerevisiae* and *Aspergillus* spp, and medically important bacteria, including *Escherichia coli* and *Staphylococcus aureus*.

Compounds were ranked based on their antimicrobial activity and the top five compounds were further characterised to determine whether they had a clinical use. This included assessing development of resistance, their mechanism of action, their ability to treat biofilm and their toxicity against mammalian cells.

Ultimately, compounds identified in this study may lay the foundation for the development of a new group of PDT antimicrobial drugs, which will help in the fight against a number of medically important pathogens.

8.2 Development of novel PDT compounds for use as antimicrobials

Research published previously has demonstrated that acridine, flavin and anthraquinone-based compounds may have potential photosensitising activity as they can release radical and singlet oxygen species via Type 1 and Type 2 reactions, respectively. Furthermore, PDT is emerging as an area of interest in the discovery of novel antimicrobial therapeutic approaches. Therefore, a set of novel synthesised compounds based around these core parental molecules were characterised under blue light exposure, which has been identified to be the corresponding visible light range for best excitation.

The key target criteria for PDT sensitisers is the production of toxic reactive oxygen species (ROS), either $^1O_2$ or free radicals. These molecular species are able to interact with multiple biological targets within the cell, effectively killing unwanted microbes. The ability to produce satisfactory levels of $^1O_2$ correlates with increasing the triplet excited state lifetime of a PS that can be obtained by increasing intersystem crossing (ISC) efficiency (Mehraban *et al.*, 2015; Azenha *et al.*, 2002; Pereira *et al.*, 2011). To enhance ISC of the synthesised compounds, enabling more $^1O_2$ production, hydroxyl and halogen atoms including Cl, I, F and Br were incorporated into the structures. This approach is supported by the findings of $^1O_2$ measurement in this current study, which demonstrated that the most efficient $^1O_2$ producers were the compounds substituted with halogens and hydroxyl groups.

8.3 Clinical use of novel PDT compounds as antimicrobials

With the development of new compounds which potentially have antimicrobial activity, it is important to have an accurate method to assess their therapeutic use. This study utilised the EUCAST microdilution broth assay to assess the susceptibility of microbial cells to the developed novel PDT compounds. This method is widely used within the field because it allows a quantitative measurement of MIC for antimicrobial compounds and reproducibility. However, this method is not without its limitations, including its high cost and difficulties in setting it up.

There are a number of alternative methods used to determine the effectiveness of antimicrobial agents. Currently, the solid media-based disk diffusion method utilised for the photoantimicrobial screening does not provide quantitative MIC values and should be read visually. However, the disk diffusion method allows susceptibility testing to be conducted for microorganisms that may not be able to grow in the microbroth dilution method, while the disk diffusion method is more accurate as it assesses accurate growth inhibition by measuring only viable cell count.

Based on the EUCAST method, of the fifty-nine photoactive compounds tested (Chapters 3, 4, 5 and 6), only thirteen acridine-based compounds and ten acridine-isoalloxazine compounds showed activity against both fungi and

bacteria. Interestingly, these compounds showed no significant growth inhibition in the absence of blue light, although acridines, such as acridine orange, enter the *S. cerevisiae* cell and accumulate in lysosomes or mitochondria or bind to DNA (Iwamoto *et al.*, 1987; Lin *et al.*, 2017). This suggests that these compounds are unable to enter the cell and thus unable to affect it at an intracellular level. As such, the antimicrobial activity of these compounds appears to result from the photoactivation of the compounds.

Following photoantimicrobial screening of all tested compounds three acridine-based compounds (1, 2 and 11), as well as two acridine-isoalloxazine based compounds (36 and 43), were shortlisted for further characterisation to determine whether they could move forward for clinical use (Figure 7.1). Upon examination of the data of these shortlisted compounds it can be observed that these compounds can be used as broad-spectrum antimicrobial agents against bacteria and fungi as the MIC values obtained were similar.

A key fungal pathogen is *Aspergillus fumigatus*. Although this study exhibited photoantifungal activity for a selection of compounds against *S. cerevisiae* and *C. albicans*, the effects of photoactivation of tested compounds on *A. fumigatus* were shown to be insignificant. The reasons for the absence of effect can be ascribed to the fact that the high concentrations of mannitol present in the conidia of *A. fumigatus* can act as an antioxidant to scavenge ROS released during photosensitising activity of tested compounds and thus prevent oxidative damage. This concept is supported by evidence that *A. fumigatus* accumulates terhalose and mannitol in its spores to survive under a variety of stress conditions and also use mannitol as a ROS scavenger (Ruijter *et al.*, 2003; Smirnoff *et al.*, 1989; Jennings *et al.*, 1998).

A fundamental difference in susceptibility to PDT agents between fungi and bacteria has been demonstrated and can be explained by their physiology and morphology (Jori *et al.*, 2006; Vatansever *et al.*, 2013). Photodynamic therapy against microorganisms is considered to be affected by the mechanism of the production of radicals and singlet oxygen that react against several cell target molecules including membrane lipids, cytoplasmic enzymes and nucleic acids (Castano *et al.*, 2004; Liu *et al.*, 2015) . The great difference in size and surface

area between the bacterial and fungal cells means that the amount of ROS needed to kill fungi is much greater than the amount necessary to kill the bacterial cell (Zeina *et al.*, 2001; Demidova *et al.*, 2004). This is supportive of the suggestion that the difference in susceptibility observed in this study may reflect differences in cell size as *S. cerevisiae* and *C. albicans* species are approximately 25-50 times larger than the bacterial species, *S. aureus* and *E. coli*, and may therefore require more ROS to inactivate them.

One of the key clinical issues associated with currently utilised antimicrobials is the development of resistance. All the shortlisted compounds were shown to be static not cidal, which may increase the possibility of cells developing resistance (Gould *et al.*, 2002). However, evidence suggests that microbial resistance does not develop to PDT agents because of having multi-target impact on cell wall, cytoplasmic membrane and DNA (Giuliani *et al.*, 2010). This was assessed within this study, with no resistance observed following repeated exposures to the shortlisted compounds. Although this agrees with data in the literature, the number of exposures in this study was significantly lower. Previously mentioned studies regarding the development of resistance have been conducted in *in vitro*. The major limitation of this study is that antimicrobial compounds act in conditions so remote from those that exist in infected patients and so the purely antimicrobial properties may be profoundly influenced by pharmacologic considerations, by the underlying condition of the patient, and by patient's immunologic status (Greenwood, 1981; Dufour *et al.*, 2015). It is suggested that the *in vivo* environment may encourage the development of resistance, which might not be reflected in *in vitro* testing as it has been shown that tracking *in vivo* resistance evolution using whole-genome sequencing (WGS) revealed that resistant subpopulations could emerge which is most likely to occur in the case of high-burden infections (Van Hal *et al.*, 2013; Howden *et al.*, 2011).

The possibility of failure or success of fungal treatment in the clinic has been suggested to correlate with the perseverance parameter (SMG) (Rosenberg *at al.* 2017). The increasing trend of SMG values between 24 and 48 h in *S. cerevisiae* and *C. albicans* (Figures 7.17 and 7.18) may relate to the possible failure of antifungals to clear fungal infections clinically, despite the tested fungi being shown to be susceptible to the compound.

The PDT shortlisted compounds may be of clinical importance for patients with microbial infections if their effect on mammalian cells is minimal. It has been demonstrated in Chapter 7 that treatment with these acridine-based compounds was observed to elicit toxicity with and without blue light irradiation using PrestoBlue® assay. The toxicity of the tested compounds in this study against HeLa cells supports the idea of possible DNA intercalation causing the obtained toxicity. Treatment of human immortalised uroepithelial cells (SV-Huc-1) with acridine orange did not show a significant reduction in cell viability (Lin *et al.*, 2017). The difference in effect is probably due to using lower compound concentrations and different levels of light activation.

Microbial biofilms often have high degree of complexity and are often challenging to treat due to their high resistance to traditional antimicrobial treatments. As described in Chapter 7, the photoantifungal activity of shortlisted compounds was studied against *C. albicans* biofilm and planktonic cells using the colorimetric metabolic XTT assay, which evaluates the viability of cells. It has been demonstrated in Chapter 7 that Compounds 1, 2 and 36, at a concentration of 25 µg/ml, showed a significant drop in metabolic activity when exposed to blue light against *C. albicans* biofilms, however they exhibited a higher reduction in metabolic activity in planktonic *C. albicans*. The findings in this study support several studies using different PDT agents, which inactivated the viability of *C. albicans* biofilms and showed more susceptibility to these agents in planktonic *C. albicans* than *C. albicans* biofilms (Diogo *et al.*, 2017; Shi *et al.*, 2016; De Melo *et al.*, 2013). The remaining shortlisted Compounds, 11 and 24, could inactivate the viability of planktonic *C. albicans*, however minimal effect was observed on the *C. albicans* biofilms. The antimicrobial effect of PDT is reliant on both cellular localisation of the compounds and on the diffusion of ROS that should be sufficient to reduce the viability of biofilm cells (Diogo *et al.*, 2017; Hu *et al.,* 2018). This highlighted the possibility that Compounds 11 and 43 could not penetrate well inside the biofilm cells, however, they were able to penetrate into the planktonic *C. albicans* cells and inactivate their metabolism. Although the effect of shortlisted compounds was not investigated in this current study against bacterial biofilms, various studies conducted on PDT agents have shown antibacterial activity against *S. aureus* biofilms (Pereira *et al.*, 2011). This may

suggest that the PDT shortlisted compounds could have *in vitro* antimicrobial activity against bacterial biofilms.

The acridine-based shortlisted compounds cannot be used clinically based on mammalian toxicity data obtained in this study. However, other PDT agents such as porphyrin related photosensitisers could be used widely clinically due to their antimicrobial effect with no toxicity against mammalian cells.

8.4   Characterisation of novel PDT compounds

To determine the mechanism of action of these compounds both *in vitro* and *in vivo* tools were utilised. Initially, screening using several *in vitro* spectrophotometric assays determined that $^1O_2$ measurements were not consistent with antimicrobial data. Furthermore, free radicals, another key molecule produced by PDT agents, could not be measured.

The mechanism of action of Compounds 1, 2 and 36 was identified using *S. cerevisiae* deletion strains, as demonstrated in Chapter 7, confirmed that the *msn2/4* transcription factors play a significant role in the cellular response to the particular photoactivated Compounds (1, 2 and 36). The data in the current study is supported by the evidence that deletion of the genes encoding these *Msn2/4* proteins results in susceptibility of cells to oxidative stress and specifically to hydrogen peroxide, a resultant radical species (Pascual-Ahuir *et al.*, 2007; Hasan *et al.*, 2002; Martinez Pastor *et al.*, 1996). Therefore, it is suggested that *in vitro* photochemical data for $^1O_2$ in this study aligns with the mechanism of action of Compounds 1, 2 and 36, which means that oxidative stress through *msn2/4* may be the meachanism of action of these compounds. For Compounds 11 and 43 the mechanism of action may not be due to ROS and possibly they have alternative mechanisms of action as *msn2/4* is not involved in the mechanism of action of these compounds.

A major drawback of the *in vitro* spectrophotometric assay is its lack of biological relevance and poor alignment with the mechanism of action of compounds. The ROS including hydroxyl radical ·OH and singlet oxygen $^1O_2$ *in vitro* may not be easy to detect, because of their extremely short lifetimes. Additionally, the

reaction mechanisms in biological screening depend on different considerations. Firstly, the localisation of PS is critical as ROS are highly reactive and cannot travel far from their site of production before degrading. Secondly, penetration of the PS into the cell is also important, as the data did not confirm whether these compounds enter the cell or not. Thirdly, the amount of species released during PDT depends on the solvent and media used (Pérez-Jiménez *et al.*, 2006) .

An alternative detection method is the addition of ·OH and $^1O_2$ quenchers or scavengers *in vivo* to the illuminated microbial suspension containing the PSs during PDT may be more helpful in identifying the role of each species by monitoring the extent of microbial inactivation (Tavares *et al.*, 2010). However, inherent difficulties with the commonly-used quencher methods include the ability of quenchers to react with any oxidising agent, as well as the possibility of the two agents involved in PDT (·OH and $^1O_2$) to indiscriminately oxidise many of these quenchers. Further to this, the introduction of fluorescence probes to measure and characterise the identity of different ROS produced during PDT *in vitro* has become recently popular, Fluorescence probes, 3'-(p-hydroxyphenyl)-fluorescein (HPF) and singlet oxygen sensor green reagent (SOSG) were used to determine ·OH and $^1O_2$, respectively. However, it is generally accepted that these probes (HPF and SOSG) are not very specific for ·OH and $^1O_2$ and also the approach is not biologically relevant (Price *et al.*, 2010) .

The *in vitro* chemical methods used in this project were not biologically relevant and were not easy to characterise PDT agents. The chemical data obtained does not match with antimicrobial activity, thus testing them biologically suggests that some of them work by PDT mechanism while others do not.

8.5   Optimisation of PDT compounds for clinical use

The data within this study found that Gram-negative *E. coli* were more resistant to tested photoactivated compounds than Gram-positive *S. aureus* by showing higher MIC values. In the case of Gram-negative bacteria, photoinactivation is difficult as they are relatively impermeable to neutral or anionic compounds due to their highly negatively charged surface. Therefore, it is desirable for clinical applications of these shortlisted compounds to introduce positive charge which make them more active against Gram-positive and negative bacteria as well as

fungi. Additionally, using disrupting agents such as polymixin nonapeptide in combination with the compounds can be an alternative to allow the penetration of the compound that can then cause killing damage to the cell when it is exposed to light.

To obtain an effective irradiance dose it is suggested to use low power with long exposure time, which increases significantly the antimicrobial activity, when compared to high power with short illumination time (Murdoch *et al.*, 2012). Furthermore, it is generally accepted that synergistic combinations of two or more agents can overcome possible toxicity and side effects associated with high doses of single drugs and increase the effect compared with using the individual drug in the equivalent dose (Yasukawa *et al.*, 2012; Fila *et al.*, 2017). Utilising shorter blue light wavelength with a higher irradiance dose achieves the best potential antimicrobial blue light efficacy (Murdoch *et al.*, 2012). This suggests that combination of shorter antimicrobial blue light with the shortlisted compounds increased their activity. However, using shorter blue light may damage the DNA.

Since these acridine-based shortlisted compounds have been absorbed in the blue light region, the best activating light is expected to be blue light. However, red light is more advantageous for the PS applications due to the better tissue penetration of red light than other light wavelengths.

The toxicity prevents the use of these shortlisted compounds clinically. In order to make them less toxic and direct them to the intended location in the body, a nanoparticle drug delivery system could be a good option. The shortlisted compounds could be loaded onto polymer based nanoparticles which offer selectivity for microbial infections without affecting the host tissue (Sakima *et al.*, 2018). However, this approach might be expensive and time consuming.

The purpose of this study was to develop photoactivated antimicrobial compounds; however, they did not show encouraging results. To make the compounds more effective, first of all we need to know whether they enter the cell or not. The shortlisted compounds are expected to enter the cell and could have two effects, by entering the cell and be activated or by having another unclear mechanism. Acridine-based compounds are expected to have the most efficacy due to having multiple mechanisms of action.

9. Conclusions

The *in vitro* photochemistry methods used in this project have no biological relevance. Ultimately, unless we test the compounds in biological systems we will not have acceptable indication about the therapeutic potential.

Among the photosensitisers tested in this thesis, five acridine-based compounds are the most active compounds biologically against the fungi *S. cerevisiae* and *C. albicans* and the bacteria *S. aureus* and *E. coli*, with no activity against *A. fumigatus*. The anti-biofilm effect observed in this study may serve as a strong base for further formulation development to form a promising approach in treatment of chronic biofilm infections.

The present study has also confirmed that fungi and bacteria photosensitised by the shortlisted compounds do not develop resistance mechanisms against the photodynamic process following three repeated exposures.

Through the investigation of the mechanism of action using deleted *S. cerevisiae* strains, a remarkable role for msn2/4 in oxidative cellular response has been determined for Compounds 1, 2 and 36. It has been further demonstrated that msn2/4 has not been activated in response to the Compounds 11 and 43 and thus other mechanisms could be involved.

Since the observations that testing acridine-based shortlisted compounds inactivated significantly the viability of HeLa cells, utility of these compounds would not be justified at present.

10. References:

Abana, C. M., Brannon, J. R., Ebbott, R. A., Dunigan, T. L., Guckes, K. R., et al. 2017. Characterization of blue light irradiation effects on pathogenic and nonpathogenic Escherichia coli. *Microbiology Open,* 6**,** e00466.

Abrahamse, H. & Hamblin, M. R. 2016. New photosensitizers for photodynamic therapy. *Biochemical Journal,* 473**,** 347-364.

Admassie, M. 2018. Current review on molecular and phenotypic mechanism of bacterial resistance to antibiotic. *Science Journal of Clinical Medicine,* 7**,** 13.

Agarwal, S., Singh, S. S., Verma, S. & Kumar, S. 2000. Antifungal activity of anthraquinone derivatives from Rheum emodi. *Journal of Ethnopharmacology,* 72**,** 43-46.

Ahgilan, A., Sabaratnam, V. & Periasamy, V. 2016. Antimicrobial properties of vitamin B2. *International Journal of Food Properties,* 19**,** 1173-1181.

Alanis, A. J. 2005. Resistance to antibiotics: are we in the post-antibiotic era? *Archives of Medical Research,* 36**,** 697-705.

Albert, A. 1951. The acridines. Their preparation, physical, chemical and biological properties and uses. London: Edward Arnold & Co.

Allison, R., Cuenca, R., Downie, G., Camnitz, P., Brodish, B., et al. 2005. Clinical photodynamic therapy of head and neck cancers—a review of applications and outcomes. *Photodiagnosis and Photodynamic Therapy,* 2**,** 205-222.

Allison, R. R., Bagnato, V. S. & Sibata, C. H. 2010. Future of oncologic photodynamic therapy. *Future Oncology,* 6**,** 929-940.

Alves, E., Costa, L., Carvalho, C. M., Tomé, J. P., Faustino, M. A., et al. 2009. Charge effect on the photoinactivation of Gram-negative and Gram-positive bacteria by cationic meso-substituted porphyrins. *BMC Microbiology,* 9**,** 70.

Anderson, J. B., Sirjusingh, C. & Ricker, N. 2004. Haploidy, diploidy and evolution of antifungal drug resistance in Saccharomyces cerevisiae. *Genetics,* 168**,** 1915-1923.

Andriole, V. T. 1999. Current and future antifungal therapy: new targets for antifungal agents. *Journal of Antimicrobial Chemotherapy,* 44**,** 151-162.

Antunez, C., Blanca-Lopez, N., Torres, M. J., Mayorga, C., Perez-Inestrosa, E., et al. 2006. Immediate allergic reactions to cephalosporins: Evaluation of cross-reactivity with a panel of penicillins and cephalosporins. *Journal of Allergy and Clinical Immunology,* 117**,** 404-410.

Apak, R., Güçlü, K., Demirata, B., Özyürek, M., Çelik, S., et al. 2007. Comparative evaluation of various total antioxidant capacity assays applied to phenolic compounds with the CUPRAC assay. *Molecules,* 12**,** 1496-1547.

Arendrup, M., Guinea, J., Mouton, J., Howard, S. & Subcommittee on Antifungal Susceptibility Testing of the ESCMID European Committee for Antimicrobial Susceptibility Testing, 2015a. EUCAST definitive document E. DEF 7.3. Method for the determination of broth dilution minimum inhibitory concentrations of antifungal agents for yeasts. Vaxjo, Sweden: EUCAST.

Arendrup, M., Guinea, J., Mouton, J., Howard, S. & Subcommittee on Antifungal Susceptibility Testing of the ESCMID European Committee for Antimicrobial Susceptibility Testing, 2015b. EUCAST definitive document E. DEF 9.3. Method for the determination of broth dilution minimum inhibitory concentrations of antifungal agents for conidia firming moulds. Vaxjo, Sweden: EUCAST.

Ates, M., Akdeniz, B. G. & Sen, B. H. 2005. The effect of calcium chelating or binding agents on aureus albicans. *Oral Surgery, Oral Medicine, Oral Pathology, Oral Radiology, and Endodontology,* 100**,** 626-630.

Augusto, O. & Vaz, S. M. 2007. EPR spin-trapping of protein radicals to investigate biological oxidative mechanisms. *Amino Acids,* 32**,** 535-542.

Ayo, R., Amupitan, J. & Zhao, Y. 2007. Cytotoxicity and antimicrobial studies of 1, 6, 8-trihydroxy-3-methyl-anthraquinone (emodin) isolated from the leaves of Cassia nigricans Vahl. *African Journal of Biotechnology,* 6.

Azenha, E. l. G., Serra, A. C., Pineiro, M., Pereira, M. M., Melo, J. S., et al. 2002. Heavy-atom effects on metalloporphyrins and polyhalogenated porphyrins. *Chemical Physics,* 280**,** 177-190.

Babanzadeh, S. & Mehdipour-Ataei, S. 2018. Synthesis of novel photoactive aromatic polyamides based on anthraquinone chromophore: Characterization and properties. *Advances in Polymer Technology.* 37: 3475-3481.

Baier, J., Maisch, T., Maier, M., Engel, E., Landthaler, M., et al. 2006. Singlet oxygen generation by UVA light exposure of endogenous photosensitizers. *Biophysical Journal,* 91**,** 1452-1459.

Balouiri, M., Sadiki, M. & Ibnsouda, S. K. 2016. Methods for in vitro evaluating antimicrobial activity: A review. *Journal of Pharmaceutical Analysis,* 6**,** 71-79.

Baltazar, L. M., Ray, A., Santos, D. A., Cisalpino, P. S., Friedman, A. J., et al. 2015. Antimicrobial photodynamic therapy: an effective alternative approach to control fungal infections. *Frontiers in Microbiology,* 6, 202.

Bannerman, D. D., Paape, M. J., Lee, J. W., Zhao, X., Hope, J. C., et al. 2004. Escherichia coli and Staphylococcus aureus elicit differential innate immune responses following intramammary infection. *Clinical and Diagnostic Laboratory Immunology,* 11**,** 463-472.

Bennett, R. J. & Johnson, A. D. 2003. Completion of a parasexual cycle in Candida albicans by induced chromosome loss in tetraploid strains. *The EMBO Journal,* 22**,** 2505-2515.

Bertoloni, G., Lauro, F. M., Cortella, G. & Merchat, M. 2000. Photosensitizing activity of hematoporphyrin on Staphylococcus aureus cells. *Biochimica et Biophysica Acta (BBA)-General Subjects,* 1475**,** 169-174.

Bilsland, E., Molin, C., Swaminathan, S., Ramne, A. & Sunnerhagen, P. 2004. Rck1 and Rck2 MAPKAP kinases and the HOG pathway are required for oxidative stress resistance. *Molecular Microbiology,* 53**,** 1743-1756.

Biscaro Pedrolli, D., Jankowitsch, F., Schwarz, J., Langer, S., Nakanishi, S., et al. 2013. Riboflavin analogs as antiinfectives: occurrence, mode of action, metabolism and resistance. *Current Pharmaceutical Design,* 19**,** 2552-2560.

Blair, J. M., Webber, M. A., Baylay, A. J., Ogbolu, D. O. & Piddock, L. J. 2015. Molecular mechanisms of antibiotic resistance. *Nature Reviews Microbiology,* 13**,** 42.

Blondeau, J. M. 2004. Fluoroquinolones: mechanism of action, classification, and development of resistance. *Survey of Ophthalmology,* 49 Suppl 2**,** S73-78.

Boncler, M., Różalski, M., Krajewska, U., Podsędek, A. & Watala, C. 2014. Comparison of PrestoBlue and MTT assays of cellular viability in the assessment of anti-proliferative effects of plant extracts on human endothelial cells. *Journal of Pharmacological and Toxicological Methods,* 69**,** 9-16.

Bowman, S. M. & Free, S. J. 2006. The structure and synthesis of the fungal cell wall. *Bioessays,* 28**,** 799-808.

Brachmann, C. B., Davies, A., Cost, G. J., Caputo, E., Li, J., et al. 1998. Designer deletion strains derived from Saccharomyces cerevisiae S288C: a useful set of strains and plasmids for PCR-mediated gene disruption and other applications. *Yeast,* 14**,** 115-132.

Brand-Williams, W., Cuvelier, M.-E. & Berset, C. 1995. Use of a free radical method to evaluate antioxidant activity. *Food Science and Technology-Lebensmittel-Wissenschaft & Technologie,* 28**,** 25-30.

Briggs, T., Blunn, G., Hislop, S., Ramalhete, R., Bagley, C., et al. 2018. Antimicrobial photodynamic therapy—a promising treatment for prosthetic joint infections. *Lasers in Medical Science,* 33**,** 523-532.

Bumah, V. V., Aboualizadeh, E., Masson-Meyers, D. S., Eells, J. T., Enwemeka, C. S., et al. 2017. Spectrally resolved infrared microscopy and chemometric tools to reveal the interaction between blue light (470 nm) and methicillin-resistant Staphylococcus aureus. *Journal of Photochemistry and Photobiology B: Biology,* 167**,** 150-157.

Calderón, C. B. & Sabundayo, B. P. 2007. Antimicrobial classifications. *Antimicrobial Susceptibility Testing Protocols,* 7, 60-88.

Carrillo-Munoz, A. J., Giusiano, G., Ezkurra, P. A. & Quindos, G. 2006. Antifungal agents: mode of action in yeast cells. *Revista Española de Quimioterapia,* 19**,** 130-139.

Carvalho, G. G., Felipe, M. P. & Costa, M. S. 2009. The photodynamic effect of methylene blue and toluidine blue on Candida albicans is dependent on medium conditions. *The Journal of Microbiology,* 47**,** 619.

Casalinuovo, I., Sorge, R., Bonelli, G. & Di Francesco, P. 2017. Evaluation of the antifungal effect of EDTA, a metal chelator agent, on Candida albicans biofilm. *European Review for Medical and Pharmacological Sciences,* 21**,** 1413-1420.

Castano, A. P., Demidova, T. N. & Hamblin, M. R. 2004. Mechanisms in photodynamic therapy: part one—photosensitizers, photochemistry and cellular localization. *Photodiagnosis and Photodynamic Therapy,* 1**,** 279-293.

Catherinot, E., Lanternier, F., Bougnoux, M.-E., Lecuit, M., Couderc, L.-J. & Lortholary, O. 2010. Pneumocystis jirovecii pneumonia. *Infectious Disease Clinics,* 24**,** 107-138.

Ceccato-Antonini, S. R. & Sudbery, P. E. 2004. Filamentous growth in Saccharomyces cerevisiae. *Brazilian Journal of Microbiology,* 35**,** 173-181.

Chabrier-Rosello, Y., Foster, T. H., Perez-Nazario, N., Mitra, S. & Haidaris, C. G. 2005. Sensitivity of Candida albicans germ tubes and biofilms to photofrin-mediated phototoxicity. *Antimicrobial Agents and Chemotherapy,* 49**,** 4288-4295.

Chamilos, G. & Kontoyiannis, D. 2005. Update on antifungal drug resistance mechanisms of Aspergillus fumigatus. *Drug Resistance Updates,* 8**,** 344-358.

Chien, S.-C., Wu, Y.-C., Chen, Z.-W. & Yang, W.-C. 2015. Naturally occurring anthraquinones: chemistry and therapeutic potential in autoimmune diabetes. *Evidence-Based Complementary and Alternative Medicine,* 2015: 2-12.

Choi, C. W., Kim, S. C., Hwang, S. S., Choi, B. K., Ahn, H. J., et al. 2002. Antioxidant activity and free radical scavenging capacity between Korean

medicinal plants and flavonoids by assay-guided comparison. *Plant Science,* 163**,** 1161-1168.

Chopra, I. & Roberts, M. 2001. Tetracycline antibiotics: mode of action, applications, molecular biology, and epidemiology of bacterial resistance. *Microbiology and Molecular Biology Reviews,* 65**,** 232-60 .

Chukwujekwu, J., Coombes, P., Mulholland, D. & Van Staden, J. 2006. Emodin, an antibacterial anthraquinone from the roots of Cassia occidentalis. *South African Journal of Botany,* 72**,** 295-297.

Cieplik, F., Deng, D., Crielaard, W., Buchalla, W., Hellwig, E., et al. 2018. Antimicrobial photodynamic therapy–what we know and what we don't. *Critical Reviews in Microbiology,* 44**,** 571-589.

Cieplik, F., Tabenski, L., Buchalla, W. & Maisch, T. 2014. Antimicrobial photodynamic therapy for inactivation of biofilms formed by oral key pathogens. *Frontiers in Microbiology,* 5**,** 405.

Cincotta, L., Foley, J. & Cincotta, A. 1987. Novel red absorbing benzo [a] phenoxazinium and benzo [a] phenothiazinium photosensitizers: in vitro evaluation. *Photochemistry and Photobiology,* 46**,** 751-758.

Cokol, M., Chua, H. N., Tasan, M., Mutlu, B., Weinstein, Z. B., et al. 2011. Systematic exploration of synergistic drug pairs. *Molecular Systems Biology,* 7**,** 544.

Comini, L., Montoya, S. N., Páez, P., Argüello, G. A., Albesa, I., et al. 2011. Antibacterial activity of anthraquinone derivatives from Heterophyllaea pustulata (Rubiaceae). *Journal of Photochemistry and Photobiology B: Biology,* 102**,** 108-114.

Corkill, J. E., Deveney, J., Pratt, J., Shears, P., Smyth, A., et al. 1994. Effect of pH and CO_2 on in vitro susceptibility of Pseudomonas cepacia to β-lactams. *Pediatric Research,* 35**,** 299.

Cosgrove, S. E., Sakoulas, G., Perencevich, E. N., Schwaber, M. J., Karchmer, A. W., et al. 2003. Comparison of mortality associated with methicillin-resistant and methicillin-susceptible Staphylococcus aureus bacteremia: a meta-analysis. *Clinical Infectious Diseases,* 36**,** 53-59.

Costa-Orlandi, C., Sardi, J., Pitangui, N., De Oliveira, H., Scorzoni, L., et al. 2017. Fungal biofilms and polymicrobial diseases. *Journal of Fungi,* 3**,** 22.

Costa, D. C., Gomes, M. C., Faustino, M. A., Neves, M. G., Cunha, Â., et al. 2012. Comparative photodynamic inactivation of antibiotic resistant bacteria by first and second generation cationic photosensitizers. *Photochemical & Photobiological Sciences,* 11**,** 1905-1913.

Costa, V. & Moradas-Ferreira, P. 2001. Oxidative stress and signal transduction in Saccharomyces cerevisiae: insights into ageing, apoptosis and diseases. *Molecular Aspects of Medicine,* 22**,** 217-246.

Cowen, L. E., Nantel, A., Whiteway, M. S., Thomas, D. Y., Tessier, D. C., et al. 2002. Population genomics of drug resistance in Candida albicans. *Proceedings of the National Academy of Sciences,* 99**,** 9284-9289.

Cuchural, G., Hurlbut, S., Malamy, M. & Tally, F. 1988. Permeability to β-lactams in Bacteroides fragilis. *Journal of Antimicrobial Chemotherapy,* 22**,** 785-790.

Dai, T. H., Fuchs, B. B., Coleman, J. J., Prates, R. A., Astrakas, C., et al. 2012. Concepts and principles of photodynamic therapy as an alternative antifungal discovery platform. *Frontiers in Microbiology,* 3, 1-16.

Danby, C. S., Boikov, D., Rautemaa-Richardson, R. & Sobel, J. D. 2012. Effect of pH on in vitro susceptibility of Candida glabrata and Candida albicans

to 11 antifungal agents and implications for clinical use. *Antimicrobial Agents and Chemotherapy,* 56**,** 1403-1406.

Dave, H. & Ledwani, L. 2012. A review on anthraquinones isolated from Cassia species and their applications. *Indian Journal of Natural Products and Resources,* 3, 291-319.

Davies, J. & Davies, D. 2010. Origins and evolution of antibiotic resistance. *Microbiology and Molecular Biology Reviews,* 74**,** 417-433.

Davies, M. J. 2016. Detection and characterisation of radicals using electron paramagnetic resonance (EPR) spin trapping and related methods. *Methods,* 109**,** 21-30.

De Melo, W. C., Avci, P., De Oliveira, M. N., Gupta, A., Vecchio, D., et al. 2013. Photodynamic inactivation of biofilm: taking a lightly colored approach to stubborn infection. *Expert Review of Anti-infective Therapy,* 11**,** 669-693.

Vasconcellos, A. A., Gonçalves, L. M., Cury, A. A. & Silva, W. J. 2014. Environmental pH influences Candida albicans biofilms regarding its structure, virulence and susceptibility to fluconazole. *Microbial Pathogenesis,* 69**,** 39-44.

Demain, A. L. & Elander, R. P. 1999. The beta-lactam antibiotics: past, present, and future. *Antonie Van Leeuwenhoek,* 75**,** 5-19.

Demidova, T. & Hamblin, M. 2004. Photodynamic therapy targeted to pathogens. *International Journal of Immunopathology and Pharmacology,* 17**,** 245-254.

Denning, D. W. & Bromley, M. J. 2015. How to bolster the antifungal pipeline. *Science,* 347**,** 1414-1416.

DeRosa, M. C. & Crutchley, R. J. 2002. Photosensitized singlet oxygen and its applications. *Coordination Chemistry Reviews,* 233**,** 351-371.

Desai, J. V., Mitchell, A. P. & Andes, D. R. 2014. Fungal biofilms, drug resistance, and recurrent infection. *Cold Spring Harbor Perspectives in Medicine,* 4**,** a019729.

Devasahayam, G., Scheld, W. M. & Hoffman, P. S. 2010. Newer antibacterial drugs for a new century. *Expert Opinion on Investigational Drugs,* 19**,** 215-234.

Dharmaraja, A. T. 2017. Role of reactive oxygen species (ROS) in therapeutics and drug resistance in cancer and bacteria. *Journal of Medicinal Chemistry,* 60**,** 3221-3240.

Diogo, P., Fernandes, C., Caramelo, F., Mota, M., Miranda, I. M., et al. 2017. Antimicrobial photodynamic therapy against endodontic Enterococcus faecalis and Candida albicans mono and mixed biofilms in the presence of photosensitizers: A comparative study with classical endodontic irrigants. *Frontiers in Microbiology,* 8**,** 498.

Donnelly, R. F., McCarron, P. A. & Tunney, M. M. 2008. Antifungal photodynamic therapy. *Microbiological Research,* 163**,** 1-12.

Dougherty, T. J., Gomer, C. J., Henderson, B. W., Jori, G., Kessel, D., et al. 1998. Photodynamic therapy. *JNCI: Journal of the National Cancer Institute,* 90**,** 889-905.

Dovigo, L. N., Pavarina, A. C., de Oliveira Mima, E. G., Giampaolo, E. T., Vergani, C. E., et al. 2011. Fungicidal effect of photodynamic therapy against fluconazole-resistant Candida albicans and Candida glabrata. *Mycoses,* 54**,** 123-130.

Dufour, N., Debarbieux, L., Fromentin, M. & Ricard, J.-D. 2015. Treatment of highly virulent extraintestinal pathogenic Escherichia coli pneumonia with bacteriophages. *Critical Care Medicine,* 43**,** e190-e198.

Echeverría, J., Opazo, J., Mendoza, L., Urzúa, A. & Wilkens, M. 2017. Structure-activity and lipophilicity relationships of selected antibacterial natural flavones and flavanones of Chilean flora. *Molecules,* 22**,** 608.

Edwards, A. M. 2006. *General properties of flavins*, The Royal Society of Chemistry: Cambridge, UK.

Emri, T., Szarvas, V., Orosz, E., Antal, K., Park, H., et al. 2015. Core oxidative stress response in Aspergillus nidulans. *BMC Genomics,* 16**,** 478.

Ergaieg, K., Chevanne, M., Cillard, J. & Seux, R. 2008. Involvement of both Type I and Type II mechanisms in Gram-positive and Gram-negative bacteria photosensitization by a meso-substituted cationic porphyrin. *Solar Energy,* 82**,** 1107-1117.

European Committee for Antimicrobial Susceptibility Testing (EUCAST) of the European Society for Clinical Microbiology and Infectious Diseases (ESCMID), 2003. EUCAST Discussion Document E. Dis 5.1: determination of minimum inhibitory concentrations (MICs) of antibacterial agents by broth dilution. *Clin. Microbiol. Infect.,* *9*, 1-7.

Falagas, M. E., McDermott, L. & Snydman, D. R. 1997. Effect of pH on in vitro antimicrobial susceptibility of the Bacteroides fragilis group. *Antimicrobial Agents and Chemotherapy,* 41**,** 2047-2049.

Fila, G., Kawiak, A. & Grinholc, M. S. 2017. Blue light treatment of Pseudomonas aeruginosa: Strong bactericidal activity, synergism with antibiotics and inactivation of virulence factors. *Virulence,* 8**,** 938-958.

Fisher, M. C., Hawkins, N. J., Sanglard, D. & Gurr, S. J. 2018. Worldwide emergence of resistance to antifungal drugs challenges human health and food security. *Science,* 360**,** 739-742.

Floegel, A., Kim, D.-O., Chung, S.-J., Koo, S. I. & Chun, O. K. 2011. Comparison of ABTS/DPPH assays to measure antioxidant capacity in popular antioxidant-rich US foods. *Journal of Food Composition and Analysis,* 24**,** 1043-1048.

Forman, S., Káš, J., Fini, F., Steinberg, M. & Ruml, T. 1999. The effect of different solvents on the ATP/ADP content and growth properties of HeLa cells. *Journal of Biochemical and Molecular Toxicology,* 13**,** 11-15.

Franchini, C., Muraglia, M., Corbo, F., Florio, M. A., Di Mola, A., et al. 2009. Synthesis and biological evaluation of 2-mercapto-1, 3-benzothiazole derivatives with potential antimicrobial activity. *Archiv der Pharmazie,* 342**,** 605-613.

Franz, R., Kelly, S. L., Lamb, D. C., Kelly, D. E., Ruhnke, M., et al. 1998. Multiple molecular mechanisms contribute to a stepwise development of fluconazole resistance in clinical Candida albicans strains. *Antimicrobial Agents and Chemotherapy,* 42**,** 3065-3072.

Friedberg, J. S., Skema, C., Baum, E. D., Burdick, J., Vinogradov, S. A., et al. 2001. In vitro effects of photodynamic therapy on Aspergillus fumigatus. *Journal of Antimicrobial Chemotherapy,* 48**,** 105-107.

Fu, X.-j., Fang, Y. & Yao, M. 2013. Antimicrobial photodynamic therapy for methicillin-resistant Staphylococcus aureus infection. *BioMed Research International,* 2013, 2-7.

Fuentefria, A. M., Pippi, B., Dalla Lana, D. F., Donato, K. K. & de Andrade, S. F. 2018. Antifungals discovery: an insight into new strategies to combat antifungal resistance. *Letters in Applied Microbiology,* 66**,** 2-13.

Fuller, K. K., Ringelberg, C. S., Loros, J. J. & Dunlap, J. C. 2013. The fungal pathogen Aspergillus fumigatus regulates growth, metabolism, and stress resistance in response to light. *MBio,* 4**,** 1-10.

Galbis-Martínez, M., Padmanabhan, S., Murillo, F. J. & Elías-Arnanz, M. 2012. CarF mediates signaling by singlet oxygen, generated via photoexcited protoporphyrin IX, in Myxococcus xanthus light-induced carotenogenesis. *Journal of Bacteriology,* 194**,** 1427-1436.

George, S., Hamblin, M. R. & Kishen, A. 2009. Uptake pathways of anionic and cationic photosensitizers into bacteria. *Photochemical & Photobiological Sciences,* 8**,** 788-795.

Georgopapadakou, N. H. & Tkacz, J. S. 1995. The fungal cell wall as a drug target. *Trends in Microbiology,* 3**,** 98-104.

Gessler, N., Egorova, A. & Belozerskaya, T. 2013. Fungal anthraquinones. *Applied Biochemistry and Microbiology,* 49**,** 85-99.

Gholivand, M., Kashanian, S., Peyman, H. & Roshanfekr, H. 2011. DNA-binding study of anthraquinone derivatives using chemometrics methods. *European Journal of Medicinal Chemistry,* 46**,** 2630-2638.

Gillum, A. M., Tsay, E. Y. & Kirsch, D. R. 1984. Isolation of the Candida albicans gene for orotidine-5′-phosphate decarboxylase by complementation of S. cerevisiae ura3 and E. coli pyrF mutations. *Molecular and General Genetics,* 198**,** 179-182.

Giuliani, F., Martinelli, M., Cocchi, A., Arbia, D., Fantetti, L., et al. 2010. In vitro resistance selection studies of RLP068/Cl, a new Zn (II) phthalocyanine suitable for antimicrobial photodynamic therapy. *Antimicrobial Agents and Chemotherapy,* 54**,** 637-642.

Gould, I. M. & MacKenzie, F. Antibiotic exposure as a risk factor for emergence of resistance: the influence of concentration. Symposium Series (Society for Applied Microbiology), 2002. 78S-84S.

Gow, N. A., Latge, J.-P. & Munro, C. A. 2017. The fungal cell wall: structure, biosynthesis, and function. *Microbiology Spectrum*, 5, 1-25.

Greenwood, D. 1981. In vitro veritas? Antimicrobial susceptibility tests and their clinical relevance. *The Journal of Infectious Diseases,* 144**,** 380-385.

Grinholc, M., Rodziewicz, A., Forys, K., Rapacka-Zdonczyk, A., Kawiak, A., et al.. 2015. Fine-tuning recA expression in Staphylococcus aureus for antimicrobial photoinactivation: importance of photo-induced DNA damage in the photoinactivation mechanism. *Applied Microbiology and Biotechnology,* 99**,** 9161-9176.

Gulshan, K. & Moye-Rowley, W. S. 2007. Multidrug resistance in fungi. *Eukaryotic Cell,* 6**,** 1933-1942.

Gupta, S., Maclean, M., Anderson, J., MacGregor, S., Meek, R., et al. 2015. Inactivation of micro-organisms isolated from infected lower limb arthroplasties using high-intensity narrow-spectrum (HINS) light. *The Bone & Joint Journal,* 97**,** 283-288.

Gutiérrez-Preciado, A., Torres, A. G., Merino, E., Bonomi, H. R., Goldbaum, F. A., et al. 2015. Extensive identification of bacterial riboflavin transporters and their distribution across bacterial species. *PLoS One,* 10**,** e0126124.

Gwynne, P. J. & Gallagher, M. P. 2018. Light as a broad-spectrum antimicrobial. *Frontiers in Microbiology,* 9**,** 119.

Ha, D. O., Jeong, M. K., Park, C. U., Park, M. H., Chang, P. S., et al. 2009. Effects of riboflavin photosensitization on the degradation of bisphenol A (BPA) in model and real-food systems. *Journal of Food Science,* 74**,** C380-C384.

Haas, R., Dörtbudak, O., Mensdorff-pouilly, N. & Mailath, G. 1997. Elimination of bacteria on different implant surfaces through photosensitization and soft laser. An in vitro study. *Clinical Oral Implants Research,* 8**,** 249-254.

Hacker, J., Blum-Oehler, G., Mühldorfer, I. & Tschäpe, H. 1997. Pathogenicity islands of virulent bacteria: structure, function and impact on microbial evolution. *Molecular Microbiology,* 23**,** 1089-1097.

Halstead, F. D., Thwaite, J. E., Burt, R., Laws, T. R., Raguse, M., et al. 2016. Antibacterial activity of blue light against nosocomial wound pathogens growing planktonically and as mature biofilms. *Applied and Environmental Microbiology,* 82**,** 4006-4016.

Hamblin, M. R. & Hasan, T. 2004. Photodynamic therapy: a new antimicrobial approach to infectious disease? *Photochemical & Photobiological Sciences,* 3**,** 436-450.

Hamblin, M. R., O'Donnell, D. A., Murthy, N., Rajagopalan, K., Michaud, N.,et al. 2002. Polycationic photosensitizer conjugates: effects of chain length and Gram classification on the photodynamic inactivation of bacteria. *Journal of Antimicrobial Chemotherapy,* 49**,** 941-951.

Hammerschlag, M. R. 1994. Antimicrobial susceptibility and therapy of infections caused by Chlamydia pneumoniae. *Antimicrobial Agents and Chemotherapy,* 38**,** 1873.

Hasan, R., Leroy, C., Isnard, A. D., Labarre, J., Boy-Marcotte, E., et al. 2002. The control of the yeast H2O2 response by the Msn2/4 transcription factors. *Molecular Microbiology,* 45**,** 233-241.

Hawkey, P. 2008. The growing burden of antimicrobial resistance. *Journal of Antimicrobial Chemotherapy,* 62**,** i1-i9.

Hawkins, C. L. 2004. EPR spin trapping of protein radicals. *Free Radical Biology and Medicine,* 36**,** 1072-1086.

Heatley, N. 1944. A method for the assay of penicillin. *Biochemical Journal,* 38**,** 61.

Heelis, P. 1982. The photophysical and photochemical properties of flavins (isoalloxazines). *Chemical Society Reviews,* 11**,** 15-39.

Heelis, P. 2018. The photochemistry of flavins. *Chemistry and biochemistry of flavoenzymes.* Boca Raton, Florida: CRC Press.

Heling, I. & Chandler, N. 1998. Antimicrobial effect of irrigant combinations within dentinal tubules. *International Endodontic Journal,* 31**,** 8-14.

Hemberger, S., Pedrolli, D. B., Stolz, J., Vogl, C., Lehmann, M., et al. 2011. RibM from Streptomyces davawensis is a riboflavin/roseoflavin transporter and may be useful for the optimization of riboflavin production strains. *BMC Biotechnology,* 11**,** 119.

Hermann, T. 2007. Aminoglycoside antibiotics: old drugs and new therapeutic approaches. *Cellular and Molecular Life Sciences,* 64**,** 1841-1852.

Hidalgo, E., Ding, H. & Demple, B. 1997. Redox signal transduction: mutations shifting [2Fe-2S] centers of the SoxR sensor-regulator to the oxidized form. *Cell,* 88**,** 121-129.

Hill, R., Healy, B., Holloway, L., Kuncic, Z., Thwaites, D., et al. 2014. Advances in kilovoltage x-ray beam dosimetry. *Physics in Medicine & Biology,* 59**,** R183.

Hoi, J. W. S., Lamarre, C., Beau, R., Meneau, I., Berepiki, A., et al. 2011. A novel family of dehydrin-like proteins is involved in stress response in the human fungal pathogen Aspergillus fumigatus. *Molecular Biology of the Cell,* 22**,** 1896-1906.

Holmes, A. R., Cannon, R. D. & Shepherd, M. G. 1991. Effect of calcium ion uptake on Candida albicans morphology. *FEMS Microbiology Letters,* 77**,** 187-193.

Holmes, A. R., Cardno, T. S., Strouse, J. J., Ivnitski-Steele, I., Keniya, M. V., et al. 2016. Targeting efflux pumps to overcome antifungal drug resistance. *Future Medicinal Chemistry,* 8**,** 1485-1501.

Hosseini, N., Yazdanpanah, S., Saki, M., Rezazadeh, F., Ghapanchi, J., et al. 2016. Susceptibility of Candida albicans and Candida dubliniensis to photodynamic therapy using four dyes as the photosensitizer. *Journal of Dentistry,* 17**,** 354.

Howden, B. P., Mcevoy, C. R., Allen, D. L., Chua, K., Gao, W., et al. 2011. Evolution of multidrug resistance during Staphylococcus aureus infection involves mutation of the essential two component regulator WalKR. *PLoS Pathogens,* 7**,** e1002359.

Hu, X., Huang, Y.-Y., Wang, Y., Wang, X. & Hamblin, M. R. 2018. Antimicrobial photodynamic therapy to control clinically relevant biofilm infections. *Frontiers in Microbiology,* 9, 1-15.

Huang, K. C., Mukhopadhyay, R., Wen, B., Gitai, Z. & Wingreen, N. S. 2008. Cell shape and cell-wall organization in Gram-negative bacteria. *Proceedings of the National Academy of Sciences,* 105**,** 19282-19287.

Huang, L., Zhiyentayev, T., Xuan, Y., Azhibek, D., Kharkwal, G. B., et al. 2011. Photodynamic inactivation of bacteria using polyethylenimine–chlorin (e6) conjugates: effect of polymer molecular weight, substitution ratio of chlorin (e6) and pH. *Lasers in Surgery and Medicine,* 43**,** 313-323.

Huang, R., Kim, H. J. & Min, D. B. 2006. Photosensitizing effect of riboflavin, lumiflavin, and lumichrome on the generation of volatiles in soy milk. *Journal of Agricultural and Food Chemistry,* 54**,** 2359-2364.

Hurley, J. C. 2005. Mortality due to vancomycin-resistant enterococcal bacteremia versus vancomycin-susceptible enterococcal bacteremia: An ecological analysis. *Clinical Infectious Diseases,* 41**,** 1541-1542.

Hwang, C. S., Rhie, G., Oh, J. H., Huh, W. K., Yim, H. S., et al. 2002. Copper- and zinc-containing superoxide dismutase (Cu/ZnSOD) is required for the protection of Candida albicans against oxidative stresses and the expression of its full virulence. *Microbiology,* 148**,** 3705-3713.

Imlay, J. A. 2015. Diagnosing oxidative stress in bacteria: not as easy as you might think. *Current Opinion in Microbiology,* 24**,** 124-131.

Inbaraj, J. J., Krishna, M. C., Gandhidasan, R. & Murugesan, R. 1999. Cytotoxicity, redox cycling and photodynamic action of two naturally occurring quinones. *Biochimica et Biophysica Acta (BBA)-General Subjects,* 1472**,** 462-470.

Ito, T. & Kobayashi, K. 1978. Mutagenesis in yeast cells by storage in tritiated water. *Radiation Research,* 76**,** 139-144.

Iwamoto, Y., Itoyama, T., Yasuda, K., Morita, T., Shimizu, T., et al. 1993. Photodynamic DNA strand breaking activities of acridine compounds. *Biological and Pharmaceutical Bulletin,* 16**,** 1244-1247.

Iwamoto, Y., Yoshioka, H. & Yanagihara, Y. 1987. Singlet oxygen-producing activity and photodynamic biological effects of acridine compounds. *Chemical and Pharmaceutical Bulletin,* 35**,** 2478-2483.

Jamal, M., Ahmad, W., Andleeb, S., Jalil, F., Imran, M., et al. 2018. Bacterial biofilm and associated infections. *Journal of the Chinese Medical Association,* 81**,** 7-11.

Jao, R. L. & Jackson, G. G. 1964. Gentamicin sulfate, new antibiotic against Gram-negative bacilli. Laboratory, pharmacological, and clinical evaluation. *JAMA,* 189**,** 817-822.

Jennings, D. B., Ehrenshaft, M., Pharr, D. M. & Williamson, J. D. 1998. Roles for mannitol and mannitol dehydrogenase in active oxygen-mediated plant defense. *Proceedings of the National Academy of Sciences,* 95**,** 15129-15133.

Jeong, H. G. & Choi, M. S. 2016. Design and Properties of Porphyrin-based Singlet Oxygen Generator. *Israel Journal of Chemistry,* 56**,** 110-118.

Jiang, X. & Dai, Z. 2018. Reactive oxygen species in photodynamic therapy. *Chinese Science Bulletin,* 63**,** 1783-1802.

Jin, J.-Y., Lee, S.-H. & Yoon, H.-J. 2010. A comparative study of wound healing following incision with a scalpel, diode laser or Er, Cr: YSGG laser in guinea pig oral mucosa: A histological and immunohistochemical analysis. *Acta Odontologica Scandinavica,* 68**,** 232-238.

Johns, S. C., Crouch, L. L., Grieve, S., Maloney, H. L., Peczkowski, G. R., et al. 2014. A rapid, chromatography-free route to substituted acridine–isoalloxazine conjugates under microwave irradiation. *Tetrahedron Letters,* 55**,** 3308-3311.

Jori, G., Fabris, C., Soncin, M., Ferro, S., Coppellotti, O., et al. 2006. Photodynamic therapy in the treatment of microbial infections: basic principles and perspective applications. *Lasers in Surgery and Medicine,* 38**,** 468-481.

Jukic, E., Blatzer, M., Posch, W., Steger, M., Binder, U., et al. 2017. Oxidative stress response tips the balance in Aspergillus terreus amphotericin B resistance. *Antimicrobial Agents and Chemotherapy,* 61**,** 1-11.

Juzeniene, A., Peng, Q. & Moan, J. 2007. Milestones in the development of photodynamic therapy and fluorescence diagnosis. *Photochemical & Photobiological Sciences,* 6**,** 1234-1245.

Kahlmeter, G., Brown, D., Goldstein, F., MacGowan, A., Mouton, J., et al. 2006. European Committee on Antimicrobial Susceptibility Testing (EUCAST) technical notes on antimicrobial susceptibility testing. *Clinical Microbiology and Infection,* 12**,** 501-503.

Kasai, S., Yamanaka, S., Wang, S. C. & Matsui, K. 1979. Anti-riboflavin activity of 8-O-alkyl derivatives of riboflavin in some Gram-positive bacteria. *Journal of Nutritional Science and Vitaminology,* 25**,** 289-298.

Kemegne, G. A., Mkounga, P., Ngang, J. J. E., Kamdem, S. L. S. & Nkengfack, A. E. 2017. Antimicrobial structure activity relationship of five anthraquinones of emodine type isolated from Vismia laurentii. *BMC Microbiology,* 17**,** 41.

Keshishyan, E., Zaporozhtseva, Z., Zenina, O. & Zrodnikov, V. 2015. Photodynamic inactivation of bacteria in vitro under the effect of blue light. *Bulletin of Experimental Biology and Medicine,* 158**,** 475.

Keyer, K. & Imlay, J. A. 1996. Superoxide accelerates DNA damage by elevating free-iron levels. *Proceedings of the National Academy of Sciences,* 93**,** 13635-13640.

Khan, M. S. A. & Ahmad, I. 2011. Antibiofilm activity of certain phytocompounds and their synergy with fluconazole against Candida albicans biofilms. *Journal of Antimicrobial Chemotherapy,* 67**,** 618-621.

Khan, S., Rayis, M., Rizvi, A., Alam, M. M., Rizvi, M., et al. 2019. ROS mediated antibacterial activity of photoilluminated riboflavin: A photodynamic mechanism against nosocomial infections. *Toxicology Reports,* 6**,** 136-142.

Khaydukov, E., Mironova, K., Semchishen, V., Generalova, A., Nechaev, A., et al. 2016. Riboflavin photoactivation by upconversion nanoparticles for cancer treatment. *Scientific Reports,* 6**,** 35103.

Klepser, M. E. 2001. New insights in medical mycology: Focus on fungal infections - introduction. *Pharmacotherapy,* 21**,** 109-110.

Knappe, W.-R. 1977. Photochemistry of (Iso) alloxazines, v mechanism of the photoreaction of flavin with 1, 4-cyclohexadiene and analogous compounds. *Zeitschrift für Naturforschung B,* 32**,** 434-437.

Koh, E. & Fluhr, R. 2016. Singlet oxygen detection in biological systems: Uses and limitations. *Plant Signaling & Behavior,* 11**,** e1192742.

Konopka, K. & Goslinski, T. 2007. Photodynamic therapy in dentistry. *Journal of Dental Research,* 86**,** 694-707.

Kotra, L. P., Haddad, J. & Mobashery, S. 2000. Aminoglycosides: perspectives on mechanisms of action and resistance and strategies to counter resistance. *Antimicrobial Agents and Chemotherapy,* 44**,** 3249-56.

Kübler, A. C. 2005. Photodynamic therapy. *Medical Laser Application,* 20**,** 37-45.

Kulkarny, V. V., Chavez-Dozal, A., Rane, H. S., Jahng, M., Bernardo, S. M., et al. 2014. Quinacrine inhibits Candida albicans growth and filamentation at neutral pH. *Antimicrobial Agents and Chemotherapy,* 58**,** 7501-7509.

Kumar, A., Ghate, V., Kim, M. J., Zhou, W., Khoo, G. H., et al. 2015. Kinetics of bacterial inactivation by 405 nm and 520 nm light emitting diodes and the role of endogenous coproporphyrin on bacterial susceptibility. *Journal of Photochemistry and Photobiology B: Biology,* 149**,** 37-44.

Kumar, V., Lockerble, O., Kell, S. D., Ruane, P. H., Platz, M. S., et al. 2004. Riboflavin and UV-light based pathogen reduction: extent and consequence of DNA damage at the molecular level. *Photochemistry and Photobiology,* 80**,** 15-21.

Kwiatkowski, S., Knap, B., Przystupski, D., Saczko, J., Kędzierska, E., et al. 2018. Photodynamic therapy–mechanisms, photosensitizers and combinations. *Biomedicine & Pharmacotherapy,* 106**,** 1098-1107.

Lange, R. P., Locher, H. H., Wyss, P. C. & Then, R. L. 2007. The targets of currently used antibacterial agents: Lessons for drug discovery. *Current Pharmaceutical Design,* 13**,** 3140-3154.

Lee, J. B., Kim, S. H., Lee, S. C., Kim, H. G., Ahn, H. G., et al. 2014. Blue light–induced oxidative stress in human corneal epithelial cells: protective effects of ethanol extracts of various medicinal plant mixtures. *Investigative Ophthalmology & Visual Science,* 55**,** 4119-4127.

Lewinska, A., Wnuk, M., Slota, E. & Bartosz, G. 2007. Total anti-oxidant capacity of cell culture media. *Clinical and Experimental Pharmacology and Physiology,* 34**,** 781-786.

Lewis, R. E., Lund, B. C., Klepser, M. E., Ernst, E. J. & Pfaller, M. A. 1998. Assessment of antifungal activities of fluconazole and amphotericin B administered alone and in combination against Candida albicans by using a dynamic in vitro mycotic infection model. *Antimicrobial Agents and Chemotherapy,* 42**,** 1382-1386.

Li, Y., Sun, L., Lu, C., Gong, Y., Li, M., et al. 2018. Promising antifungal targets against Candida albicans based on ion homeostasis. *Frontiers in Cellular and Infection Microbiology,* 8.

Liang, J. Y., Yuann, J. M. P., Hsie, Z. J., Huang, S. T. & Chen, C. C. 2017. Blue light induced free radicals from riboflavin in degradation of crystal violet by microbial viability evaluation. *Journal of Photochemistry and Photobiology B: Biology,* 174**,** 355-363.

Liang, Y., Lu, L. M., Chen, Y. & Lin, Y. K. 2016. Photodynamic therapy as an antifungal treatment. *Experimental and Therapeutic Medicine,* 12**,** 23-27.

Limban, C., Chifiriuc, M. C., Missir, A. V., Chiriţă, I. & Bleotu, C. 2008. Antimicrobial activity of some new thioureides derived from 2-(4-chlorophenoxymethyl) benzoic acid. *Molecules,* 13**,** 567-580.

Lin, Y. C., Lin, J. F., Tsai, T. F., Chen, H. E., Chou, K. Y., et al. 2017. Acridine orange exhibits photodamage in human bladder cancer cells under blue light exposure. *Scientific Reports,* 7**,** 14103.

Liu, Y., Qin, R., Zaat, S. A., Breukink, E. & Heger, M. 2015. Antibacterial photodynamic therapy: overview of a promising approach to fight antibiotic-resistant bacterial infections. *Journal of Clinical and Translational Research: JCTRES,* 1**,** 140-167.

Liu, Y., Wang, Y., Dong, G. Q., Zhang, Y. Q., Wu, S. C., et al. 2013. Novel benzothiazole derivatives with a broad antifungal spectrum: design, synthesis and structure-activity relationships. *Medchemcomm,* 4**,** 1551-1561.

Losi, A. 2007. Flavin-based blue-light photosensors: a photobiophysics update. *Photochemistry and Photobiology,* 83**,** 1283-1300.

Lu, C., Wang, H., Lv, W., Xu, P., Zhu, J., et al. 2011. Antibacterial properties of anthraquinones extracted from rhubarb against Aeromonas hydrophila. *Fisheries Science,* 77**,** 375.

Lu, M., Li, T., Wan, J., Li, X., Yuan, L., et al. 2017. Antifungal effects of phytocompounds on Candida species alone and in combination with fluconazole. *International Journal of Antimicrobial Agents,* 49**,** 125-136.

Lubart, R., Lipovski, A., Nitzan, Y. & Friedmann, H. 2011. A possible mechanism for the bactericidal effect of visible light. *Laser Therapy,* 20**,** 17-22.

Lushchak, V. I. 2011. Adaptive response to oxidative stress: Bacteria, fungi, plants and animals. *Comparative Biochemistry and Physiology Part C: Toxicology & Pharmacology,* 153**,** 175-190.

Lyon, J. P., Moreira, L. M., De Moraes, P. C. G., Dos Santos, F. V. & De Resende, M. A. 2011. Photodynamic therapy for pathogenic fungi. *Mycoses,* 54**,** E265-E271.

Macdonald, I. J. & Dougherty, T. J. 2001. Basic principles of photodynamic therapy. *Journal of Porphyrins and Phthalocyanines,* 5**,** 105-129.

Maclean, M., Macgregor, S. J., Anderson, J. G. & Woolsey, G. 2009. Inactivation of bacterial pathogens following exposure to light from a 405-nanometer light-emitting diode array. *Applied and Environmental Microbiology,* 75**,** 1932-1937.

Maclean, M., Murdoch, L. E., MacGregor, S. J. & Anderson, J. G. 2013. Sporicidal effects of high-intensity 405 nm visible light on endospore-forming bacteria. *Photochemistry and Photobiology,* 89**,** 120-126.

Maertens, J. A. 2004. History of the development of azole derivatives. *Clinical Microbiology and Infection,* 10 Suppl 1**,** 1-10.

Maertens, J. A. & Boogaerts, M. A. 2000. Fungal cell wall inhibitors: emphasis on clinical aspects. *Current Pharmaceutical Design,* 6**,** 225-239.

Magder, S. 2006. Reactive oxygen species: toxic molecules or spark of life? *Critical Care,* 10**,** 208.

Maisch, T. 2007. Anti-microbial photodynamic therapy: useful in the future? *Lasers in Medical Science,* 22**,** 83-91.

Makdoumi, K., Bäckman, A., Mortensen, J. & Craford, S. 2010. Evaluation of antibacterial efficacy of photo-activated riboflavin using ultraviolet light

(UVA). *Graefe's Archive for Clinical and Experimental Ophthalmology,* 248**,** 207-212.

Malachowa, N. & DeLeo, F. R. 2018. Staphylococcus aureus and polymicrobial skin and soft tissue infections. *The American Journal of the Medical Sciences,* 356**,** 503-504.

Malanovic, N. & Lohner, K. 2016. Gram-positive bacterial cell envelopes: The impact on the activity of antimicrobial peptides. *Biochimica et Biophysica Acta (BBA)-Biomembranes,* 1858**,** 936-946.

Malik, E. M. & Müller, C. E. 2016. Anthraquinones as pharmacological tools and drugs. *Medicinal Research Reviews,* 36**,** 705-748.

Malik, R., Manocha, A. & Suresh, D. 2010. Photodynamic therapy-a strategic review. *Indian Journal of Dental Research,* 21**,** 285.

Malik, Z., Hanania, J. & Nitzan, Y. 1990. New trends in photobiology bactericidal effects of photoactivated porphyrins—an alternative approach to antimicrobial drugs. *Journal of Photochemistry and Photobiology B: Biology,* 5**,** 281-293.

Malmir, M., Serrano, R. & Silva, O. Anthraquinones as potential antimicrobial agents-A review.

Mamalis, A., Garcha, M. & Jagdeo, J. 2015. Light emitting diode-generated blue light modulates fibrosis characteristics: Fibroblast proliferation, migration speed, and reactive oxygen species generation. *Lasers in Surgery and Medicine,* 47**,** 210-215.

Marioni, J., Bresolí-Obach, R., Agut, M., Comini, L. R., Cabrera, J. L., et al. 2017. On the mechanism of Candida tropicalis biofilm reduction by the combined action of naturally-occurring anthraquinones and blue light. *PloS One,* 12**,** e0181517.

Marr, K. A., Rustad, T. R., Rex, J. H. & White, T. C. 1999. The trailing end point phenotype in antifungal susceptibility testing is pH dependent. *Antimicrobial Agents and Chemotherapy,* 43**,** 1383-1386.

Martin, J. P. & Logsdon, N. 1987. The role of oxygen radicals in dye-mediated photodynamic effects in Escherichia coli B. *Journal of Biological Chemistry,* 262**,** 7213-7219.

Martinezpastor, M. T., Marchler, G., Schuller, C., MarchlerBauer, A., Ruis, H., et al. 1996. The Saccharomyces cerevisiae zinc finger proteins Msn2p and Msn4p are required for transcriptional induction through the stress-response element (STRE). *Embo Journal,* 15**,** 2227-2235.

Martins, S. A. R., Combs, J. C., Noguera, G., Camacho, W., Wittmann, P., et al. 2008. Antimicrobial efficacy of riboflavin/UVA combination (365 nm) in vitro for bacterial and fungal isolates: a potential new treatment for infectious keratitis. *Investigative Ophthalmology & Visual Science,* 49**,** 3402-3408.

Mathai, S., Smith, T. A. & Ghiggino, K. P. 2007. Singlet oxygen quantum yields of potential porphyrin-based photosensitisers for photodynamic therapy. *Photochemical & Photobiological Sciences,* 6**,** 995-1002.

Mayer, F. L., Wilson, D. & Hube, B. 2013. Candida albicans pathogenicity mechanisms. *Virulence,* 4**,** 119-128.

Mayrhofer, S., Domig, K. J., Mair, C., Zitz, U., Huys, G., et al. 2008. Comparison of broth microdilution, Etest, and agar disk diffusion methods for antimicrobial susceptibility testing of Lactobacillus acidophilus group members. *Applied and Environmental Microbiology,* 74**,** 3745-3748.

Mehraban, N. & Freeman, H. 2015. Developments in PDT sensitizers for increased selectivity and singlet oxygen production. *Materials,* 8**,** 4421-4456.

Meletiadis, J., Mouton, J. W., Meis, J. F., Bouman, B. A., Donnelly, J. P., et al. 2001. Colorimetric assay for antifungal susceptibility testing of Aspergillus species. *Journal of Clinical Microbiology,* 39**,** 3402-3408.

Miceli, M. H., Diaz, J. A. & Lee, S. A. 2011. Emerging opportunistic yeast infections. *Lancet Infectious Diseases,* 11**,** 142-151.

Miller, E. L. 2002. The penicillins: a review and update. *Journal of Midwifery & Womens Health,* 47**,** 426-434.

Miller, N. J. & Rice-Evans, C. A. 1997. Factors influencing the antioxidant activity determined by the ABTS•+ radical cation assay. *Free Radical Research,* 26**,** 195-199.

Mingeot-Leclercq, M. P., Glupczynski, Y. & Tulkens, P. M. 1999. Aminoglycosides: activity and resistance. *Antimicrobial Agents and Chemotherapy,* 43**,** 727-737.

Minnock, A., Vernon, D. I., Schofield, J., Griffiths, J., Parish, J. H., et al. 1996. Photoinactivation of bacteria. Use of a cationic water-soluble zinc phthalocyanine to photoinactivate both gram-negative and gram-positive bacteria. *Journal of Photochemistry and Photobiology B: Biology,* 32**,** 159-164.

Mishra, B. B., Kishore, N., Tiwari, V. K., Singh, D. D. & Tripathi, V. 2010. A novel antifungal anthraquinone from seeds of Aegle marmelos Correa (family Rutaceae). *Fitoterapia,* 81**,** 104-107.

Mitchell, D. G., Rosen, G. M., Tseitlin, M., Symmes, B., Eaton, S. S., et al. 2013. Use of rapid-scan EPR to improve detection sensitivity for spin-trapped radicals. *Biophysical Journal,* 105**,** 338-342.

Moan, J. & BERG, K. 1991. The photodegradation of porphyrins in cells can be used to estimate the lifetime of singlet oxygen. *Photochemistry and Photobiology,* 53**,** 549-553.

Mohanlall, V. & Odhav, B. 2013. Antibacterial, anti-inflammatory and antioxidant activities of anthraquinones from Ceratotheca triloba (Bernh) Hook F. *Journal of Medicinal Plant Research*, 7, 877-886.

Moorhead, S., Maclean, M., MacGregor, S. J. & Anderson, J. G. 2016. Comparative sensitivity of Trichophyton and Aspergillus conidia to inactivation by violet-blue light exposure. *Photomedicine and Laser Surgery,* 34**,** 36-41.

Munin, E., Giroldo, L. M., Alves, L. P. & Costa, M. S. 2007. Study of germ tube formation by Candida albicans after photodynamic antimicrobial chemotherapy (PACT). *Journal of Photochemistry and Photobiology B: Biology,* 88**,** 16-20.

Munita, J. M. & Arias, C. A. 2016. Mechanisms of antibiotic resistance. *Microbiology Spectrum,* 4.

Murdoch, L., McKenzie, K., Maclean, M., Macgregor, S. & Anderson, J. 2013. Lethal effects of high-intensity violet 405-nm light on Saccharomyces cerevisiae, Candida albicans, and on dormant and germinating spores of Aspergillus niger. *Fungal Biology,* 117**,** 519-527.

Murdoch, L. E., Maclean, M., Endarko, E., MacGregor, S. J. & Anderson, J. G. 2012. Bactericidal effects of 405 nm light exposure demonstrated by inactivation of Escherichia, Salmonella, Shigella, Listeria, and Mycobacterium species in liquid suspensions and on exposed surfaces. *The Scientific World Journal,* 2012, 1-7.

Natarajan, U., Randhawa, N., Brummer, E. & Stevens, D. 1998. Effect of granulocyte-macrophage colony-stimulating factor on candidacidal activity of neutrophils, monocytes or monocyte-derived macrophages and synergy with fluconazole. *Journal of Medical Microbiology,* 47**,** 359-363.

Nemeth, J., Oesch, G. & Kuster, S. P. 2015. Bacteriostatic versus bactericidal antibiotics for patients with serious bacterial infections: systematic review and meta-analysis. *Journal of Antimicrobial Chemotherapy,* 70**,** 382-395.

Netto, L. E. S., De Oliveira, M. A., Monteiro, G., Demasi, A. P. D., Cussiol, J. R. R., et al. 2007. Reactive cysteine in proteins: protein folding, antioxidant defense, redox signaling and more. *Comparative Biochemistry and Physiology Part C: Toxicology & Pharmacology,* 146**,** 180-193.

Nielsen, H. K., Garcia, J., Vaeth, M. & Schlafer, S. 2015. Comparison of riboflavin and toluidine blue O as photosensitizers for photoactivated disinfection on endodontic and periodontal pathogens in vitro. *PloS One,* 10**,** e0140720.

Nitzan, Y., Gutterman, M., Malik, Z. & Ehrenberg, B. 1992. Inactivation of gram-negative bacteria by photosensitized porphyrins. *Photochemistry and Photobiology,* 55**,** 89-96.

Nitzan, Y., Salmon-Divon, M., Shporen, E. & Malik, Z. 2004. ALA induced photodynamic effects on gram positive and negative bacteria. *Photochemical & Photobiological Sciences,* 3**,** 430-435.

Nixon, M., Jackson, B., Varghese, P., Jenkins, D. & Taylor, G. 2006. Methicillin-resistant Staphylococcus aureus on orthopaedic wards: incidence, spread, mortality, cost and control. *Journal of Bone and Joint Surgery Br,* 88**,** 812-817.

Odds, F. C., Brown, A. J. & Gow, N. A. 2003. Antifungal agents: mechanisms of action. *Trends in Microbiology,* 11**,** 272-279.

Ormond, A. & Freeman, H. 2013. Dye sensitizers for photodynamic therapy. *Materials,* 6**,** 817-840.

Orstavik, D. & Haapasalo, M. 1990. Disinfection by endodontic irrigants and dressings of experimentally infected dentinal tubules. *Dental Traumatology,* 6**,** 142-149.

Pappas, P. G., Rex, J. H., Sobel, J. D., Filler, S. G., Dismukes, W. E., et al. 2004. Guidelines for treatment of candidiasis. *Clinical Infectious Diseases,* 38**,** 161-189.

Paris, S., Wysong, D., Debeaupuis, J. P., Shibuya, K., Philippe, B., et al. 2003. Catalases of Aspergillus fumigatus. *Infection and Immunity,* 71**,** 3551-3562.

Pascual-Ahuir, A. & Proft, M. 2007. The Sch9 kinase is a chromatin-associated transcriptional activator of osmostress-responsive genes. *Embo Journal,* 26**,** 3098-3108.

Pedreño, Y., Gimeno-Alcañiz, J. V., Matallana, E. & Argüelles, J. C. 2002. Response to oxidative stress caused by H_2O_2 in Saccharomyces cerevisiae mutants deficient in trehalase genes. *Archives of Microbiology,* 177**,** 494-499.

Peleg, A. Y. & Hooper, D. C. 2010. Hospital-acquired infections due to gram-negative bacteria. *New England Journal of Medicine,* 362**,** 1804-1813.

Penzer, G. & Radda, G. 1967. The chemistry and biological function of isoalloxazines (flavines). *Quarterly Reviews, Chemical Society,* 21**,** 43-65.

Pereira, C. A., Romeiro, R. L., Costa, A. C., Machado, A. K., Junqueira, J. C., et al. 2011. Susceptibility of Candida albicans, Staphylococcus aureus, and Streptococcus mutans biofilms to photodynamic inactivation: an in vitro study. *Lasers in Medical Science,* 26**,** 341-348.

Pereira, M. M., Monteiro, C. J., Simões, A. V., Pinto, S. M., Abreu, A. R., et al. 2010. Synthesis and photophysical characterization of a library of photostable halogenated bacteriochlorins: an access to near infrared chemistry. *Tetrahedron,* 66**,** 9545-9551.

Pérez-Jiménez, J. & Saura-Calixto, F. 2006. Effect of solvent and certain food constituents on different antioxidant capacity assays. *Food Research International,* 39**,** 791-800.

Pérez-Torrado, R. & Querol, A. 2016. Opportunistic strains of Saccharomyces cerevisiae: a potential risk sold in food products. *Frontiers in Microbiology,* 6**,** 1522.

Perlin, D. S., Rautemaa-Richardson, R. & Alastruey-Izquierdo, A. 2017. The global problem of antifungal resistance: prevalence, mechanisms, and management. *The Lancet Infectious Diseases,* 17**,** e383-e392.

Petrikkos, G. & Skiada, A. 2007. Recent advances in antifungal chemotherapy. *International Journal of Antimicrobial Agents,* 30**,** 108-117.

Pfaller, M., Boyken, L., Hollis, R., Kroeger, J., Messer, S., et al. 2011. Comparison of the broth microdilution methods of the European Committee on Antimicrobial Susceptibility Testing and the Clinical and Laboratory Standards Institute for testing itraconazole, posaconazole, and voriconazole against Aspergillus isolates. *Journal of Clinical Microbiology,* 49**,** 1110-1112.

Pierce, C. G., Uppuluri, P., Tristan, A. R., Wormley, F. L., Mowat, E., et al. 2008. A simple and reproducible 96-well plate-based method for the formation of fungal biofilms and its application to antifungal susceptibility testing. *Nature Protocols,* 3**,** 1494.

Prasad, R. & Rawal, M. K. 2014. Efflux pump proteins in antifungal resistance. *Frontiers in Pharmacology,* 5**,** 202.

Price, M. & Kessel, D. H. 2010. On the use of fluorescence probes for detecting reactive oxygen and nitrogen species associated with photodynamic therapy. *Journal of Biomedical Optics,* 15**,** 051605.

Punithavathy, P., Nalina, K. & Menon, T. 2012. Antifungal susceptibility testing of Candida tropicalis biofilms against fluconazole using calorimetric indicator resazurin. *Indian Journal of Pathology and Microbiology,* 55**,** 72.

Pushpan, S., Venkatraman, S., Anand, V., Sankar, J., Parmeswaran, D., et al. 2002. Porphyrins in photodynamic therapy-a search for ideal photosensitizers. *Current Medicinal Chemistry-Anti-Cancer Agents,* 2**,** 187-207.

Rajendran, M., Gandhidasan, R. & Murugesan, R. 2004. Photosensitisation and photoinduced DNA cleavage by four naturally occurring anthraquinones. *Journal of Photochemistry and Photobiology A: Chemistry,* 168**,** 67-73.

Ramage, G., Walle, K. V., Wickes, B. L. & López-Ribot, J. L. 2001. Standardized method for in vitro antifungal susceptibility testing of Candida albicansbiofilms. *Antimicrobial Agents and Chemotherapy,* 45**,** 2475-2479.

Ramakrishnan, P., Maclean, M., Macgregor, S. J., Anderson, J. G. & Grant, M. H. 2016. Cytotoxic responses to 405 nm light exposure in mammalian and bacterial cells: involvement of reactive oxygen species. *Toxicology in Vitro,* 33**,** 54-62.

Ramon, A. M., Porta, A. & Fonzi, W. A. 1999. Effect of environmental pH on morphological development of Candida albicans is mediated via the PacC-related transcription factor encoded by PRR2. *Journal of Bacteriology,* 181**,** 7524-7530.

Ray, A. C. & Eakin, R. 1975. Studies on the biosynthesis of aspergillin by Aspergillus niger. *Applied and Environmental Microbiology,* 30**,** 909-915.

Re, R., Pellegrini, N., Proteggente, A., Pannala, A., Yang, M., et al. 1999. Antioxidant activity applying an improved ABTS radical cation decolorization assay. *Free Radical Biology and Medicine,* 26**,** 1231-1237.

Reboli, A. C., Rotstein, C., Pappas, P. G., Chapman, S. W., Kett, D. H., et al. 2007. Anidulafungin versus fluconazole for invasive candidiasis. *New England Journal of Medicine,* 356**,** 2472-2482.

Rella, A., Farnoud, A. M. & Del Poeta, M. 2016. Plasma membrane lipids and their role in fungal virulence. *Progress in Lipid Research,* 61**,** 63-72.

Reller, L. B., Weinstein, M., Jorgensen, J. H. & Ferraro, M. J. 2009. Antimicrobial susceptibility testing: a review of general principles and contemporary practices. *Clinical Infectious Diseases,* 49**,** 1749-1755.

Rex, J. H. & Pfaller, M. A. 2002. Has antifungal susceptibility testing come of age? *Clinical Infectious Diseases,* 35**,** 982-989.

Rhea, J., Hopp, D. C., Rabenstein, J., Smith, C., Lucas, S., et al. 2012. 5-Hydroxy ericamycin, a new anthraquinone with potent antimicrobial activity. *The Journal of Antibiotics,* 65**,** 623.

Rhodes, J. C. 2006. Aspergillus fumigatus: growth and virulence. *Medical Mycology,* 44**,** S77-S81.

Rios, A. C., Moutinho, C. G., Pinto, F. C., Del Fiol, F. S., Jozala, A., et al. 2016. Alternatives to overcoming bacterial resistances: state-of-the-art. *Microbiological Research,* 191**,** 51-80.

Rodriguez-Bano, J., Navarro, M. D., Romero, L., Muniain, M. A., De Cueto, M., et al. 2006. Bacteremia due to extended-spectrum beta-lactamase producing Escherichia coli in the CTX-M era: A new clinical challenge. *Clinical Infectious Diseases,* 43**,** 1407-1414.

Roelandts, R. 2002. The history of phototherapy: something new under the sun? *Journal of the American Academy of Dermatology,* 46**,** 926-930.

Roemer, T. & Krysan, D. J. 2014. Antifungal drug development: challenges, unmet clinical needs, and new approaches. *Cold Spring Harbor Perspectives in Medicine,* 4**,** a019703.

Roh, H. J., Kim, A., Kang, G. S. & Kim, D. H. 2016. Photoinactivation of major bacterial pathogens in aquaculture. *Fisheries and Aquatic Sciences,* 19**,** 28.

Rosa, L. P. & da Silva, F. C. 2014. Antimicrobial photodynamic therapy: a new therapeutic option to combat infections. *Journal of Medical Microbiology & Diagnosis,* 3**,** 1.

Rosenberg, A., Ene, I. V., Bibi, M., Zakin, S., Segal, E. S., et al. 2018. Antifungal tolerance is a subpopulation effect distinct from resistance and is associated with persistent candidemia. *Nature Communications,* 9**,** 2470.

Ruane, P. H., Edrich, R., Gampp, D., Keil, S. D., Leonard, R. L., et al. 2004. Photochemical inactivation of selected viruses and bacteria in platelet concentrates using riboflavin and light. *Transfusion,* 44**,** 877-885.

Ruijter, G. J., Bax, M., Patel, H., Flitter, S. J., Vondervoort, P. J., et al. 2003. Mannitol is required for stress tolerance in Aspergillus niger conidiospores. *Eukaryotic Cell,* 2**,** 690-698.

Ruiz-Herrera, J. 2016. *Fungal cell wall: structure, synthesis, and assembly*. Boca Raton, Florida: CRC press.

Russo, T. A. & Johnson, J. R. 2000. Proposal for a new inclusive designation for extraintestinal pathogenic isolates of Escherichia coli: ExPEC. *Journal of Infectious Diseases,* 181**,** 1753-1754.

Sabbahi, S., Alouini, Z., Jemli, M. & Boudabbous, A. 2008. The role of reactive oxygen species in Staphylococcus aureus photoinactivation by methylene blue. *Water Science and Technology,* 58**,** 1047-1054.

Saito, H. & Tatebayashi, K. 2004. Regulation of the osmoregulatory HOG MAPK cascade in yeast. *Journal of Biochemistry,* 136**,** 267-272.

Sakima, V., Barbugli, P., Cerri, P., Chorilli, M., Carmello, J., et al. 2018. Antimicrobial photodynamic therapy mediated by curcumin-loaded polymeric nanoparticles in a murine model of oral candidiasis. *Molecules,* 23**,** 2075.

Sant, D., Tupe, S., Ramana, C. & Deshpande, M. 2016. Fungal cell membrane— promising drug target for antifungal therapy. *Journal of Applied Microbiology,* 121**,** 1498-1510.

Sardi, J., Scorzoni, L., Bernardi, T., Fusco-Almeida, A. & Giannini, M. M. 2013. Candida species: current epidemiology, pathogenicity, biofilm formation, natural antifungal products and new therapeutic options. *Journal of Medical Microbiology,* 62**,** 10-24.

Sarkar, P., Yarlagadda, V., Ghosh, C. & Haldar, J. 2017. A review on cell wall synthesis inhibitors with an emphasis on glycopeptide antibiotics. *MedChemComm,* 8**,** 516-533.

Sauer, A., Letscher-Bru, V., Speeg-Schatz, C., Touboul, D., Colin, J., et al. 2010. In vitro efficacy of antifungal treatment using riboflavin/UV-A (365 nm) combination and amphotericin B. *Investigative Ophthalmology & Visual Science,* 51**,** 3950-3953.

Scheffers, D. J. & Pinho, M. G. 2005. Bacterial cell wall synthesis: new insights from localization studies. *Microbiology and Molecular Biology Reviews,* 69**,** 585-607.

Scheld, W. M. 2003. Maintaining fluoroquinolone class efficacy: review of influencing factors. *Emerg Infect Dis,* 9**,** 1-9.

Şen, B. H., Safavi, K. E. & Spångberg, L. S. 1997. Growth patterns of Candida albicans in relation to radicular dentin. *Oral Surgery, Oral Medicine, Oral Pathology, Oral Radiology, and Endodontology,* 84**,** 68-73.

Sherrington, S. L., Sorsby, E., Mahtey, N., Kumwenda, P., Lenardon, M. D., et al. 2017. Adaptation of Candida albicans to environmental pH induces cell wall remodelling and enhances innate immune recognition. *PLoS Pathogens,* 13**,** 1-24.

Shi, H., Li, J., Zhang, H., Zhang, J. & Sun, H. 2016. Effect of 5-aminolevulinic acid photodynamic therapy on Candida albicans biofilms: an in vitro study. *Photodiagnosis and Photodynamic Therapy,* 15**,** 40-45.

Shimamura, T., Sumikura, Y., Yamazaki, T., Tada, A., Kashiwagi, T., et al. 2014. Applicability of the DPPH assay for evaluating the antioxidant capacity of food additives–inter-laboratory evaluation study–. *Analytical Sciences,* 30**,** 717-721.

Sikkema, J., de Bont, J. A. & Poolman, B. 1995. Mechanisms of membrane toxicity of hydrocarbons. *Microbiol. Mol. Biol. Rev.,* 59**,** 201-222.

Sikorska, E., Sikorski, M., Steer, R., Wilkinson, F. & Worrall, D. 1998. Efficiency of singlet oxygen generation by alloxazines and isoalloxazines. *Journal of the Chemical Society, Faraday Transactions,* 94**,** 2347-2353.

Silhavy, T. J., Kahne, D. & Walker, S. 2010. The bacterial cell envelope. *Cold Spring Harbor Perspectives in Biology,* 2**,** a000414.

Smirnoff, N. & Cumbes, Q. J. 1989. Hydroxyl radical scavenging activity of compatible solutes. *Phytochemistry,* 28**,** 1057-1060.

Smith, G. B., Dezeny, G. C. & Douglas, A. W. 1990. Stability and kinetics of degradation of imipenem in aqueous solution. *Journal of Pharmaceutical Sciences,* 79**,** 732-740.

Sobel, J. D., Chaim, W., Nagappan, V. & Leaman, D. 2003. Treatment of vaginitis caused by Candida glabrata: use of topical boric acid and flucytosine. *American Journal of Obstetrics and Gynecology,* 189**,** 1297-1300.

Sperandio, F., Huang, Y.-Y. & R Hamblin, M. 2013. Antimicrobial photodynamic therapy to kill Gram-negative bacteria. *Recent Patents on Anti-infective Drug Discovery,* 8**,** 108-120.

Spettel, K., Barousch, W., Makristathis, A., Zeller, I., Nehr, M., et al. 2019. Analysis of antifungal resistance genes in Candida albicans and Candida glabrata using next generation sequencing. *PloS One,* 14**,** e0210397.

Steiner, R. 2006. New laser technology and future applications. *Medical Laser Application,* 21**,** 131-140.

Sucher, A. J., Chahine, E. B. & Balcer, H. E. 2009. Echinocandins: the newest class of antifungals. *Annals of Pharmacotherapy,* 43**,** 1647-1657.

Suchland, R., Geisler, W. & Stamm, W. E. 2003. Methodologies and cell lines used for antimicrobial susceptibility testing of Chlamydia spp. *Antimicrobial Agents and Chemotherapy,* 47**,** 636-642.

Tanzi, E. L., Lupton, J. R. & Alster, T. S. 2003. Lasers in dermatology: four decades of progress. *Journal of the American Academy of Dermatology,* 49**,** 1-34.

Tavares, A., Carvalho, C., Faustino, M. A., Neves, M. G., Tomé, J. P., et al. 2010. Antimicrobial photodynamic therapy: study of bacterial recovery viability and potential development of resistance after treatment. *Marine Drugs,* 8**,** 91-105.

Thaipong, K., Boonprakob, U., Crosby, K., Cisneros-Zevallos, L. & Byrne, D. H. 2006. Comparison of ABTS, DPPH, FRAP, and ORAC assays for estimating antioxidant activity from guava fruit extracts. *Journal of Food Composition and Analysis,* 19**,** 669-675.

Timm, M., Saaby, L., Moesby, L. & Hansen, E. W. 2013. Considerations regarding use of solvents in in vitro cell based assays. *Cytotechnology,* 65**,** 887-894.

Tommasi, R., Brown, D. G., Walkup, G. K., Manchester, J. I. & Miller, A. A. 2015. ESKAPEing the labyrinth of antibacterial discovery. *Nature Reviews Drug Discovery,* 14**,** 529.

Tong, S. Y., Davis, J. S., Eichenberger, E., Holland, T. L. & Fowler, V. G. 2015. Staphylococcus aureus infections: epidemiology, pathophysiology, clinical manifestations, and management. *Clinical Microbiology Reviews,* 28**,** 603-661.

Touati, D., Jacques, M., Tardat, B., Bouchard, L. & Despied, S. 1995. Lethal oxidative damage and mutagenesis are generated by iron in delta fur mutants of Escherichia coli: protective role of superoxide dismutase. *Journal of Bacteriology,* 177**,** 2305-2314.

Trivedi, A. B., Kitabatake, N. & Doi, E. 1990. Toxicity of dimethyl sulfoxide as a solvent in bioassay system with HeLa cells evaluated colorimetrically with 3-(4, 5-dimethyl thiazol-2-yl)-2, 5-diphenyl-tetrazolium bromide. *Agricultural and Biological Chemistry,* 54**,** 2961-2966.

Trzaska, W. J., Wrigley, H. E., Thwaite, J. E. & May, R. C. 2017. Species-specific antifungal activity of blue light. *Scientific Reports,* 7**,** 4605.

Tsang, C., Ng, H. & McMillan, A. 2007. Antifungal susceptibility of Candida albicans biofilms on titanium discs with different surface roughness. *Clinical Oral Investigations,* 11**,** 361-368.

Tseng, S., Teng, L., Chen, C., Lo, T. H., Hung, W., et al. 2009. Toluidine blue O photodynamic inactivation on multidrug-resistant pseudomonas aeruginosa. *Lasers in Surgery and Medicine,* 41**,** 391-397.

Uchimiya, M. & Stone, A. T. 2009. Reversible redox chemistry of quinones: Impact on biogeochemical cycles. *Chemosphere,* 77**,** 451-458.

Valduga, G., Bertoloni, G., Reddi, E. & Jori, G. 1993. Effect of extracellularly generated singlet oxygen on Gram-positive and Gram-negative bacteria. *Journal of Photochemistry and Photobiology B: Biology,* 21**,** 81-86.

Van Belkum, A. 2003. Molecular diagnostics in medical microbiology: yesterday, today and tomorrow. *Current Opinion in Pharmacology,* 3**,** 497-501.

Van de Sande, W. W., Tavakol, M., Van Vianen, W. & Bakker-Woudenberg, I. A. 2010. The effects of antifungal agents to conidial and hyphal forms of Aspergillus fumigatus. *Medical Mycology,* 48**,** 48-55.

Van Hal, S. J., Steen, J. A., Espedido, B. A., Grimmond, S. M., Cooper, M. A., et al. 2013. In vivo evolution of antimicrobial resistance in a series of Staphylococcus aureus patient isolates: the entire picture or a cautionary tale? *Journal of Antimicrobial Chemotherapy,* 69**,** 363-367.

Van Overveld, F. W., Haenen, G. R., Rhemrev, J., Vermeiden, J. P. & Bast, A. 2000. Tyrosine as important contributor to the antioxidant capacity of seminal plasma. *Chemico-Biological Interactions,* 127**,** 151-161.

Vandeputte, P., Ferrari, S. & Coste, A. T. 2012. Antifungal resistance and new strategies to control fungal infections. *International Journal of Microbiology,* 2012**,** 713687.

Vandersee, S., Beyer, M., Lademann, J. & Darvin, M. E. 2015. Blue-violet light irradiation dose dependently decreases carotenoids in human skin, which indicates the generation of free radicals. *Oxidative Medicine and Cellular Longevity,* 2015.

Vatansever, F., De Melo, W. C., Avci, P., Vecchio, D., Sadasivam, M., et al. 2013. Antimicrobial strategies centered around reactive oxygen species–bactericidal antibiotics, photodynamic therapy, and beyond. *FEMS Microbiology Reviews,* 37**,** 955-989.

Vermes, A., Guchelaar, H. J. & Dankert, J. 2000. Flucytosine: a review of its pharmacology, clinical indications, pharmacokinetics, toxicity and drug interactions. *Journal of Antimicrobial Chemotherapy,* 46**,** 171-179.

Vogl, C., Grill, S., Schilling, O., Stülke, J., Mack, M., et al. 2007. Characterization of riboflavin (vitamin B2) transport proteins from Bacillus subtilis and Corynebacterium glutamicum. *Journal of Bacteriology,* 189**,** 7367-7375.

Vollmer, W., Blanot, D. & De Pedro, M. A. 2008. Peptidoglycan structure and architecture. *FEMS Microbiology Reviews,* 32**,** 149-167.

Vylkova, S. 2017. Environmental pH modulation by pathogenic fungi as a strategy to conquer the host. *PLoS Pathogens,* 13**,** e1006149.

Vylkova, S., Carman, A. J., Danhof, H. A., Collette, J. R., Zhou, H., et al. 2011. The fungal pathogen Candida albicans autoinduces hyphal morphogenesis by raising extracellular pH. *MBio,* 2**,** 1-8.

Wainwright, M. 2001. Acridine—a neglected antibacterial chromophore. *Journal of Antimicrobial Chemotherapy,* 47**,** 1-13.

Wainwright, M. 2004. Photoantimicrobials-a PACT against resistance and infection. *Drugs Future,* 29**,** 85-93.

Wainwright, M. 2009. *Photosensitisers in biomedicine*. Hoboken, New Jersey: John Wiley & Sons.

Wainwright, M. 2015. Tricyclic cationic chromophores as models for new photoantimicrobials. *Journal of the Brazilian Chemical Society,* 26**,** 2390-2404.

Wainwright, M., O'Kane, C. & Rawthore, S. 2016. Phenothiazinium photosensitisers XI. improved toluidine blue photoantimicrobials. *Journal of Photochemistry and Photobiology B-Biology,* 160**,** 68-71.

Wainwright, M., Phoenix, D., Marland, J., Wareing, D. & Bolton, F. 1997. In-vitro photobactericidal activity of aminoacridines. *The Journal of Antimicrobial Chemotherapy,* 40**,** 587-589.

Wald-Dickler, N., Holtom, P. & Spellberg, B. 2017. Busting the myth of "static vs cidal": a systemic literature review. *Clinical Infectious Diseases,* 66**,** 1470-1474.

Walsh, C. & Wright, G. 2005. Introduction: antibiotic resistance. *Chem Rev,* 105**,** 391-394.

Wang, J., Zhao, H., Kong, W., Jin, C., Zhao, Y., et al. 2010. Microcalorimetric assay on the antimicrobial property of five hydroxyanthraquinone derivatives in rhubarb (Rheum palmatum L.) to Bifidobacterium adolescentis. *Phytomedicine,* 17**,** 684-689.

Wasson, C. J., Zourelias, J. L., Aardsma, N. A., Eells, J. T., Ganger, M. T., et al. 2012. Inhibitory effects of 405 nm irradiation on Chlamydia trachomatis growth and characterization of the ensuing inflammatory response in HeLa cells. *BMC Microbiology,* 12**,** 176.

Watanabe, S., Togashi, S. I., Takahashi, N. & Fukui, T. 2002. L-tryptophan as an antioxidant in human placenta extract. *Journal of Nutritional Science and Vitaminology,* 48**,** 36-39.

Weckwerth, P. H., Carnietto, C., Weckwerth, A. C., Duarte, M. A., Kuga, M. C., et al. 2012. In vitro susceptibility of oral Candida albicans strains to different pH levels and calcium hydroxide saturated aqueous solution. *Brazilian Dental Journal,* 23**,** 192-198.

Weishaupt, K. R., Gomer, C. J. & Dougherty, T. J. 1976. Identification of singlet oxygen as the cytotoxic agent in photo-inactivation of a murine tumor. *Cancer Research,* 36**,** 2326-2329.

White, T. C., Holleman, S., Dy, F., Mirels, L. F. & Stevens, D. A. 2002. Resistance mechanisms in clinical isolates of Candida albicans. *Antimicrobial Agents and Chemotherapy,* 46**,** 1704-1713.

Wu, H., Moser, C., Wang, H. Z., Hoiby, N. & Song, Z. J. 2015. Strategies for combating bacterial biofilm infections. *International Journal of Oral Science,* 7**,** 1.

Wu, Y. W., Ouyang, J., Xiao, X. H., Gao, W. Y. & Liu, Y. 2006. Antimicrobial properties and toxicity of anthraquinones by microcalorimetric bioassay. *Chinese Journal of Chemistry,* 24**,** 45-50.

Yang, M. J., Hung, Y. A., Wong, T. W., Lee, N. Y., Yuann, J. M., et al. 2018. Effects of blue-light-induced free radical formation from catechin hydrate on the inactivation of Acinetobacter baumannii, including a carbapenem-resistant strain. *Molecules,* 23**,** 1631.

Yang, M. Y., Chang, C. J. & Chen, L. Y. 2017. Blue light induced reactive oxygen species from flavin mononucleotide and flavin adenine dinucleotide on lethality of HeLa cells. *Journal of Photochemistry and Photobiology B: Biology,* 173**,** 325-332.

Yasukawa, H., Konno, N., Haneda, Y., Yamamori, B., Iseki, M., et al. 2012. Photomanipulation of antibiotic susceptibility and biofilm formation of Escherichia coli heterologously expressing photoactivated adenylyl cyclase. *The Journal of General and Applied Microbiology,* 58**,** 183-190.

Yin, R., Dai, T., Avci, P., Jorge, A. E., De Melo, W. C., et al. 2013. Light based anti-infectives: ultraviolet C irradiation, photodynamic therapy, blue light, and beyond. *Current Opinion in Pharmacology,* 13**,** 731-762.

Yoshida, A., Shiotsu-Ogura, Y., Wada-Takahashi, S., Takahashi, S. S., Toyama, T., et al. 2015. Blue light irradiation-induced oxidative stress in vivo via ROS generation in rat gingival tissue. *Journal of Photochemistry and Photobiology B: Biology,* 151**,** 48-53.

Zaman, S. B., Hussain, M. A., Nye, R., Mehta, V., Mamun, K. T., et al. 2017. A review on antibiotic resistance: alarm bells are ringing. *Cureus,* 9.

Zeina, B., Greenman, J., Purcell, W. & Das, B. 2001. Killing of cutaneous microbial species by photodynamic therapy. *British Journal of Dermatology,* 144**,** 274-278.

Zgurskaya, H. I., Lopez, C. A. & Gnanakaran, S. 2015. Permeability barrier of Gram-negative cell envelopes and approaches to bypass it. *ACS Infectious Diseases,* 1**,** 512-522.

Zhang, Y., Zhu, Y., Chen, J., Wang, Y., Sherwood, M. E., et al. 2016. Antimicrobial blue light inactivation of Candida albicans: in vitro and in vivo studies. *Virulence,* 7**,** 536-545.

Zhu, T. C., Finlay, J. C. & Hahn, S. M. 2005. Determination of the distribution of light, optical properties, drug concentration, and tissue oxygenation in-vivo in human prostate during motexafin lutetium-mediated photodynamic therapy. *Journal of Photochemistry and Photobiology B: Biology,* 79**,** 231-241.

Zhuang, J., Liu, Y., Yuan, Q., Liu, J., Liu, Y., et al. 2018. Blue light-induced apoptosis of human promyelocytic leukemia cells via the mitochondrial-mediated signaling pathway. *Oncology letters,* 15**,** 6291-6296.

Zotchev, S. B. 2003. Polyene macrolide antibiotics and their applications in human therapy. *Current Medicinal Chemistry,* 10**,** 211-223.